

**The Application of Ruthenium(II) and Iridium(I) Complexes to the Synthesis of Complex  
Organic Products**

by

**Richard J. Liberatore**

Bachelor of Sciences, The College of Charleston, 2009

Submitted to the Graduate Faculty of  
The Dietrich School of Arts and Sciences in partial fulfillment  
Of the requirements for the degree of  
Doctor of Philosophy

University of Pittsburgh

2018

UNIVERSITY OF PITTSBURGH  
DIETRICH SCHOOL OF ARTS AND SCIENCES

This dissertation was presented

by

Richard J. Liberatore

It was defended

October 6<sup>th</sup>, 2017

and approved by

Kabirul Islam, PhD, Assistant Professor, Department of Chemistry

W. Seth Horne, PhD, Associate Professor, Department of Chemistry

Lin Zhang, PhD, Professor, Department of Pharmacy and Chemical Biology

Dissertation Advisor: Scott G. Nelson, PhD, Professor, Department of Chemistry

Copyright © by Richard J. Liberatore

2018

# The Application of Ruthenium(II) and Iridium(I) Complexes to the Synthesis of Complex Organic Products

Richard J. Liberatore, PhD

University of Pittsburgh, 2018

The application of transition metals to the synthesis complex organic products has become an extremely important facet of chemistry in the last few decades. Such metal complexes exhibit remarkable activity in the construction of new carbon-carbon or carbon-heteroatom bonds in both catalytic and asymmetric fashion. The advance in organometallic chemistry has allowed chemists to access new structural scaffolds while also minimizing the use of stoichiometric reagents. The document herein details the application of iridium(I) and ruthenium(II) complexes to the synthesis of complex organic products. Iridium(I) compounds display good activity in the chemoselective isomerization of di(allyl) ethers and carbonates to access allyl vinyl compounds which are classic substrates for Claisen rearrangements. Ruthenium(II) catalysis can provide  $\alpha,\beta$ -substituted- $\gamma,\delta$ -unsaturated aldehydes and amides from allyl vinyl species such as allyl vinyl ethers, carbonates, silyl enol ethers and allyl acetates. Our methodology was utilized in the construction of the active core of a potential cancer therapeutic, actinoranone.

## CONTENTS

LIST OF TABLES .....	XIV
LIST OF FIGURES .....	XVI
LIST OF SCHEMES .....	XVIII
LIST OF ABBREVIATIONS.....	XIX
PREFACE.....	XXI
1.0 INTRODUCTION: HISTORY OF CURRENT ASYMMETRIC CATALYSIS OF [3,3]- SIGMATROPIC REARRANGEMENTS.....	1
1.1 EARLY STOICHIOMETRIC LEWIS ACID CATALYSIS .....	1
1.1.1 Achiral Stoichiometric Catalysis.....	2
1.1.2 Asymmetric Stoichiometric Catalysis .....	2
1.2 SUB-STOICHIOMETRIC CATALYSIS OF [3,3]-SIGMATROPIC REARRANGEMENTS .....	4
1.3 ERA OF PALLADIUM CATALYSIS IN [3,3]-SIGMATROPIC PROCESSES.....	7
1.3.1 Palladium(II) Catalysis of the Rearrangement of Allyl Esters, Imidates and Thioimidates.....	7
1.3.2 Palladium(II) Catalysis of the Cope and Claisen Rearrangements.....	8

1.3.3	Asymmetric Palladium(II) Catalysis .....	10
1.3.4	Palladium(0) Catalysis of Allyl Imidates .....	11
1.4	TRANSITION METAL CATALYZED ALLYLIC ALKYLATIONS: AN ALTERNATIVE TO THE CLAISEN REARRANGEMENT .....	12
1.4.1	Stoichiometric Palladium-Mediated Allylic Alkylations .....	12
1.4.2	Catalytic Palladium-Mediated Allylic Alkylations .....	13
1.4.3	Allylic Alkylation by Other Late Transition Metals: Accessing Alternative Regioisomers .....	14
1.5	ACCESSING [3,3]-CLAISEN PRODUCTS USING RUTHENIUM(II) COMPLEXES ...	15
1.5.1	Piano-stool Cp and Cp*Ru(II) Complexes .....	15
1.5.2	Asymmetric Ruthenium(II) Catalyzed Allylic Alkylations .....	16
1.5.3	Origin of Regioselectivity in Ruthenium(II) Catalyzed Allylic Alkylation.....	17
2.0	IRIDIUM(I) CATALYZED OLEFIN ISOMERIZATION AND APPLICATION TO RUTHENIUM(II) CATALYZED CLAISEN REARRANGEMENTS. ....	19
2.1	EXPLORATION OF IRIDIUM(I) CATALYZED OLEFIN ISOMERIZATION IN THE NELSON LABORATORY .....	19
2.2	OTHER ALLYL TO VINYL ETHER ISOMERIZATION STRATEGIES AND THEIR DISADVANTAGES.....	20
2.2.1	Strong Base Catalyzed Isomerization .....	20

2.2.2	Transition Metal Catalyzed Isomerizations of Allyl Ethers .....	21
2.2.3	Transition Metal Catalyzed Isomerizations and Rearrangement of Di(allyl) Ethers .	22
2.3	<b>DEVELOPMENT OF IRIDIUM CATALYZED ISOMERIZATION-CLAISEN REARRANGEMENT (ICR) CHEMISTRY .....</b>	<b>23</b>
2.3.1	Iridium Olefin Isomerization Reaction Modifications.....	23
2.3.2	Iridium Catalyzed Isomerization Mechanism.....	25
2.4	<b>IRIDIUM CATALYZED OLEFIN ISOMERIZATION FOR THE SYNTHESIS OF CARROLL-TYPE REARRANGEMENT SUBSTRATES.....</b>	<b>26</b>
2.4.1	Synthesis of Allyl Vinyl Carbonates .....	27
2.5	<b>RUTHENIUM-CATALYZED REARRANGEMENT OF ALLYL VINYL CARBONATES .....</b>	<b>28</b>
2.5.1	Reactivity of Allyl Vinyl Carbonate 111 to Transition Metal Catalysis.....	28
2.5.2	Initial Reaction Design .....	29
2.5.3	Effects of Lewis Acid and Ligand Modification .....	30
2.5.4	Substrate Scope of Ruthenium(II) Catalyzed Carbonate Rearrangements .....	32
2.5.6	Summary of Ruthenium Catalyzed Rearrangement of Allyl Vinyl Carbonates .....	34
2.6	<b>RUTHENIUM-CATALYZED REARRANGEMENT OF ALLYL VINYL ETHERS .....</b>	<b>35</b>
2.6.1	Advantages of Allyl Vinyl Ethers: Broader Substrate Scope.....	35
2.6.2	First Reactions of Allyl Vinyl Ether 111: Lewis Acid Activation .....	36

2.6.3	Ligand Modifications .....	37
2.7	<b>MECHANISTIC INVESTIGATION OF RUTHENIUM(II) CATALYZED REARRANGEMENT OF ALLYL VINYL ETHERS .....</b>	<b>39</b>
2.7.1	Outer or Inner-Sphere Mechanism: Origin of Selectivity.....	39
2.7.2	Cross-over Experiment.....	40
2.7.3	Possible Intramolecular Mechanism.....	41
2.7.4	Application of Pyridine-Amide Ligands.....	42
2.7.5	Optimization of Reaction Conditions .....	43
2.7.6	Exploration of Substrate Scope .....	45
2.7.7	Effects of Substrate Olefin Geometry.....	46
2.7.8	Effects of Substrate Aromaticity.....	47
2.7.9	Importance of Free Hydroxyl Group on the Ligand.....	48
2.7.10	Solid State Analysis .....	50
2.8	<b>PROPOSED MECHANISM OF RUTHENIUM(II) CATALYZED REARRANGEMENT OF ALLYL VINYL ETHERS .....</b>	<b>51</b>
2.8.1	Determination of Absolute Stereochemistry of the Pentenal Products .....	52
2.9	<b>SUMMARY OF RUTHENIUM-CATALYZED REARRANGEMENT OF ALLYL VINYL ETHERS .....</b>	<b>53</b>



3.0	DEVELOPMENT OF THE INTERMOLECULAR RUTHENIUM(II)-CATALYZED ASYMMETRIC ALLYLIC ALKYLATION .....	54
3.1	THE ENOLATE SOURCE IN TRANSITION METAL CATALYZED ENOLATE ADDITIONS .....	54
3.1.1	Silicon Protected Enolates in Mukaiyama Aldol Reactions .....	54
3.2	SILYL ENOL ETHERS AS NUCLEOPHILES IN NELSON GROUP RUTHENIUM(II) CATALYZED REACTIONS .....	55
3.2.1	Test Reactions of Silyl Enol Ethers with Allyl Acetates .....	55
3.2.2	Test Reactions of Silyl Enol Ethers with Allyl Carbonates and Ligand Screen .....	56
3.2.3	Allyl Acetates Revisited .....	58
3.3	STUDY OF THE PYRIDINE-IMIDAZOLINE LIGAND .....	59
3.3.1	Synthetic and Anticipated Effects of Pyridine-Imidazoline Modifications.....	59
3.3.2	Modification of the N-Alkyl Group .....	61
3.3.3	Modification of the Pyridine Ring.....	62
3.3.4	Modification of the Imidazoline Backbone.....	64
3.3.5	Effects of Pentamethylcyclopentadienyl (Cp*) .....	66
3.4	REACTION SCOPE .....	67
3.4.1	Reaction Scope of Ligand 201.....	68
3.4.2	Reaction Scope of Ligand 204 .....	70

3.4.3	Effects of Aliphatic Substrates.....	72
3.5	ABSOLUTE STEREOCHEMISTRY DETERMINATION OF AMIDE PRODUCTS....	74
3.6	MECHANISM OF RUTHENIUM(II) AAA AND CARBONATE REARRANGEMENTS .....	75
3.6.1	Origin of Enantioselectivity: Stereochemistry at C <sup>3</sup> .....	75
3.6.2	Diastereoselectivity: Stereochemistry at C <sup>2</sup> .....	77
3.6.3	Proposed Mechanism for the Ruthenium(II) Catalyzed AAA Reaction.....	80
3.7	SUMMARY OF RUTHENIUM CATALYZED AAA REACTIONS.....	81
4.0	EFFORTS TOWARDS THE TOTAL SYNTHESIS OF ACTINORANONE.....	83
4.1	ACTINORANONE: A NEW, MESOTERPENOID NATURAL PRODUCT .....	83
4.1.1	Actinoranone as a New Colorectal Cancer Therapeutic.....	83
4.2	SYNTHESIS OF THE WESTERN, NAPHTHALONE CORE.....	84
4.2.1	Retrosynthetic Analysis of Naphthalone Half.....	84
4.2.2	Application of Ruthenium(II) AAA Chemistry .....	85
4.2.3	Initial Attempt at a Wittig Homologation.....	86
4.2.4	Attempts at Homologation-Oxidation Wittig Approach .....	88
4.2.5	Attempts at Peterson Olefination-Oxidation Approach.....	89
4.2.6	Homologation-Oxidation with a Jovic-type Reaction .....	90

4.3	INITIAL EFFORTS TOWARDS THE SYNTHESIS OF TERPENOID HALF.....	91
4.3.1	First Retrosynthetic Analysis of Terpenoid Portion .....	91
4.3.2	First Synthetic Route: Synthesis of Tertiary Alcohol 252 .....	92
4.3.3	Cyclization by Acid-catalyzed Friedel-Craft of a Tertiary Alcohol.....	93
4.3.4	Formation of Ketone 267 by a Birch Reduction .....	94
4.3.5	Attempts to Use Iridium(I) Catalyzed Olefin Isomerization to Access Ketone.....	94
4.4	SECOND SYNTHETIC APPROACH: DOUBLE ALKYLATION OF A SUBSTITUTED CYCLOHEXENONE.....	95
4.4.1	Second Retrosynthetic Analysis of Naphthalone Half .....	96
4.4.2	Initial Attempts at a Conjugate Addition .....	96
4.4.3	Alternative Strategies to Sterically-Congested Conjugate Additions .....	97
4.4.4	Synthesis and Investigation of Keto Ester 288 .....	98
4.4.5	Attempts at in situ Enolate Alkylation .....	99
4.4.6	Trapping and Isolation of Aluminum Enolate.....	99
4.4.7	Studies of Silyl Enol Ether 282 .....	100
4.4.8	Studies of Vinyl Acetate 281.....	101
4.4.8	Improving Alkylation Selectivity with Increased Sterics .....	103
4.4.9	Planning the Au(I) Cyclization: Potential Regioselectivity Issues .....	104

4.4.10 Application of the Alkyne Zipper Reaction .....	105
4.4.11 A Cross-Coupling Approach .....	106
4.5 FUTURE EFFORTS.....	107
5.0 CONCLUSION.....	110
SUPPORTING INFORMATION.....	111
GENERAL INFORMATION:.....	111
GENERAL PROCEDURE FOR THE FORMATION OF DI(ALLYL) CARBONATES (GENERAL PROCEDURE A).....	111
GENERAL PROCEDURE FOR THE ISOMERIZATION OF DIALLYL CARBONATES (GENERAL PROCEDURE B) .....	116
GENERAL PROCEDURE FOR THE FORMATION OF DI(ALLYL) ETHERS (GENERAL PROCEDURE C).....	120
GENERAL PROCEDURE FOR THE ISOMERIZATION OF DI(ALLYL) ETHERS (GENERAL PROCEDURE D) .....	120
GENERAL PROCEDURE FOR SYNTHESIS OF DIMETHYLAMINOPYRIDINE AMIDE LIGANDS (GENERAL PROCEDURE F) .....	126
GENERAL PROCEDURE FOR RUTHENIUM CATALYZED ASYMMETRIC CLAISEN REARRANGEMENTS OF ALLYL VINYL CARBONATES (GENERAL PROCEDURE E).....	127

GENERAL PROCEDURE FOR THE RUTHENIUM CATALYZED ASYMMETRIC CLAISEN REARRANGEMENT OF ALLYL VINYL ETHERS (GENERAL PROCEDURE F) .....	128
GENERAL PROCEDURE FOR THE SYNTHESIS OF PYRROLE SILYL ENOL ETHERS (GENERAL PROCEDURE G).....	131
GENERAL PROCEDURE FOR THE SYNTHESIS OF IMIDAZOLYLPYRIDINE LIGANDS (GENERAL PROCEDURE H).....	133
GENERAL PROCEDURE FOR THE RUTHENIUM CATALYZED ASYMMETRIC ENOLATE ALLYLIC ALKYLATIONS (GENERAL PROCEDURE I) .....	140
APPENDIX A: CRYSTAL DATA FOR [CP*IR(126)CL]PF <sub>6</sub> .....	165
BIBLIOGRAPHY .....	201

## LIST OF TABLES

Table 1: Ligand and Lewis Acid Optimization of Ruthenium(II)-Catalyzed Carbonate Rearrangements .....	32
Table 2: Effects of Aryl Substituents on Reaction Dynamics .....	34
Table 3: Lewis Acid Screening for the Rearrangement of Allyl Vinyl Ethers .....	37
Table 4: Effects of Modification of the Ligand Oxazoline .....	38
Table 5: Effects of Modification of Ligand Pyridine .....	39
Table 6: Optimization of Amide Ligand Sterics .....	43
Table 7: Effects of Additives on the Allyl Vinyl Ether Rearrangements .....	44
Table 8: Substrate Scope of Ruthenium-Catalyzed Rearrangement of Allyl Vinyl Ethers .....	46
Table 9: Aliphatic Allyl Vinyl Rearrangement .....	48
Table 10: Effect of Ligand Type of Rearrangement of Carbonate 189 .....	58
Table 11: Effect of Increasing Acidity of Borate .....	59
Table 12: Anticipated Effects of Imidazoline Modifications .....	61
Table 13: Modification of the N-Alkyl Group .....	62
Table 14: Modification of Pyridine Ring .....	63
Table 15: Modification of Imidazoline Backbone .....	65
Table 16: Effects of Cp* .....	67
Table 17: Substrate Scope Using Ligand 201 .....	70
Table 18: Substrate Scope Using Ligand 204 .....	72
Table 19: AAA Reaction with Aliphatic Substrates .....	74
Table 20: Cyclization of Tertiary Alcohol 252 .....	94
Table 21: Attempts at Deprotection and Alkylation of Silyl Enol Ether 282 .....	101

Table 22: Deprotection and Alkylation of Acetate 281.....	103
Table 23: Crystal data and structure refinement for [Cp*Ir(126)Cl]PF <sub>6</sub> .....	165
Table 24: Atomic coordinates (x 10 <sup>4</sup> ) and equivalent isotropic displacement parameters (Å <sup>2</sup> x 10 <sup>3</sup> ) .....	167
Table 25: Bond lengths [Å] and angles [°] for [Cp*Ir(126)Cl]PF <sub>6</sub> .....	171
Table 26: Anisotropic displacement parameters (Å <sup>2</sup> x 10 <sup>3</sup> ) for Bond lengths [Å] and angles [°] for [Cp*Ir(126)Cl]PF <sub>6</sub> .....	193
Table 27: Hydrogen coordinates (x 10 <sup>4</sup> ) and isotropic displacement parameters (Å <sup>2</sup> x 10 <sup>3</sup> ).....	197

## LIST OF FIGURES

Figure 1: Product Inhibition in Catalysis of Claisen Rearrangements.....	1
Figure 2: Cyclization-Rearrangement Mechanism .....	8
Figure 3: Allylic Alkylations as Analogues of Claisen Rearrangements .....	13
Figure 4: Asymmetric Bonding in Ruthenium Allyl Complexes.....	18
Figure 5: General Mechanism for Transition Metal Olefin Isomerization .....	21
Figure 6: Diastereoselectivity in Olefin Isomerization .....	22
Figure 7: Allyl Shifts in Di(allyl) Ethers.....	24
Figure 8: Mechanism of Allyl to Vinyl Ether Isomerization by Ir(I)-Catalysis.....	25
Figure 9: Mechanism of E to Z Olefin Isomerization in Iridium-Catalyzed Isomerization Reactions .....	26
Figure 10: Lack of Reactivity of Substituted Allyl Carbonates in Iridium(I)-Catalyzed Isomerizations .....	28
Figure 11: Test Conditions for Ruthenium-Catalyzed Rearrangement of Allyl Vinyl Carbonates.....	29
Figure 12: Ruthenium Model Ligands .....	31
Figure 13: Outer and Inner Sphere Pathways.....	40
Figure 14: Oxazoline Cross-Over Experiment.....	41
Figure 15: Hydrogen-bonding in Ruthenium Catalysis .....	42
Figure 16: Product Inhibition by Pentenal Product.....	45
Figure 17: Olefin Geometry Experiment .....	47
Figure 18: Indanol Ligand Cross-Over Experiment.....	49
Figure 19: Borylation of Indanol Ligand.....	49
Figure 20: Crystal Structure of [Cp*Ir(126)Cl]PF <sub>6</sub> .....	50



Figure 21: Interconversion of Diastereomers.....	51
Figure 22: Proposed Mechanism for Ruthenium Catalyzed Rearrangement of Allyl Vinyl Ethers ....	52
Figure 23: Transition State and Origin of Diastereoselectivity .....	53
Figure 24: Intercoversion of Diastereomers 210 and 211 .....	76
Figure 25: Interconversion Between exo and endo Allyl Orientation .....	76
Figure 26: Enantioselectivity at C <sup>3</sup> Allyl Carbon .....	77
Figure 27: Transition States of Enolate Addition to C3 Carbon.....	78
Figure 28: Diastereoselectivity of Mukaiyama Aldol Reactions as Model of AAA Reaction.....	79
Figure 29: Origin of Diastereoselectivity at C <sup>2</sup> .....	80
Figure 30: Proposed Mechanism of Intermolecular Allylic Alkylation.....	81
Figure 31: Proposed Structure of Actinoranone .....	83
Figure 32: Proposed Convergent Synthesis of Actinoranone .....	84
Figure 33: Strategies for Trapping of Aluminum Enolate .....	100
Figure 34: Mechanism of Alkyne Zipper Isomerization .....	106

## LIST OF SCHEMES

Scheme 1: Iridium(I)-Catalyzed Isomerization-Claisen Rearrangements (ICR) .....	20
Scheme 2: Allyl Vinyl Ethers and Carbonates as Claisen Rearrangement Substrates.....	27
Scheme 3: Synthesis of Allyl Vinyl Carbonate.....	28
Scheme 4: Synthesis of Substituted Allyl Vinyl Carbonates .....	33
Scheme 5: Synthesis of Amide Ligands .....	43
Scheme 6: Determination of Absolute Stereochemistry of AAA Amide Products.....	75
Scheme 7: Retrosynthesis of Tetrahydronaphthalone Half 225 .....	85
Scheme 8: Attempted Homologation of 228.....	87
Scheme 9: Mechanism of Dihydronaphthalene 236 Formation .....	88
Scheme 10: Wittig-Oxidation.....	89
Scheme 11: Peterson Olefination-Oxidation.....	89
Scheme 12: Mechanism of Jovic-type Homologation.....	90
Scheme 13: Retrosynthetic Analysis of Terpenoid Half 236.....	92
Scheme 14: Halogenation of Acid Precursor 250 .....	93
Scheme 15: Birch Reduction of Tetrahydronaphthalone 253.....	94
Scheme 16: Revised Retrosynthetic Analysis of Terpenoid Half 224.....	96
Scheme 17: Double Alkylation of 276b via Acetate Trapping of Aluminum Enolate .....	104
Scheme 18: Gold(I) Catalyzed Cyclization of Alkynes 296 and 299 .....	105
Scheme 19: Synthesis of Suzuki Coupling Partner 303.....	107
Scheme 20: Synthesis of 267 from $\beta$ -ionone .....	108
Scheme 21: Synthesis of Enantiomeric 309 from (+)-Scalerylolide.....	109

## LIST OF ABBREVIATIONS

BArF .....	Tetrakis(3,5-trifluoromethylphenyl)borate
b:l.....	branched:linear ratio
bipy.....	2,2'-bipyridine
BINOL.....	1,1'-bi-2-naphthol
BOX.....	bis(oxazoline)
BSA .....	bis(trimethylsilyl)acetamide
Bt.....	benzotriazole
COD .....	cyclooctadiene
coe.....	cyclooctene
cot.....	1,3,5-cyclooctatriene
dba.....	dibenzilideneacetone
DiBAL-H.....	Diisobutylaluminum hydride
dpm .....	dipivaloylmethane
dppb.....	bis-1,4-(diphenylphosphino)butane
DCE.....	1,2-dichloroethane
DCM.....	dichloromethane
DME.....	Dimethoxyethane
DMF .....	dimethylformamide
DMSO .....	dimethylsulfoxide
dr .....	diastereomeric ratio
ee .....	enantiomeric excess
fod.....	6,6,7,7,8,8,8-heptafluoro-2,2-dimethyloctane-3,5-dione

GC-MS .....gas chromatography – mass spectroscopy

ICR ..... isomerization-Claisen rearrangement

IMes ..... 1,3-bis(2,4,6-trimethylphenyl)-imidazolium

LA..... Lewis acid

LDA..... lithium di(isopropyl)amide

MIB.....3-exo-morpholinoisoborneo

MS..... molecular sieves

NBS..... N-bromosuccinimide

NHC..... N-heterocycliccarbene

NR.....no reaction

PPA..... polyphosphoric acid

RT.....room temperature

salen .....salicylic acid amine

sol .....solvent/solvento

TBAF..... tetrabutylammonium fluoride

TC..... thiophene-2-carboxylate

Tf..... triflate

THF ..... tetrahydrofuran

TMS ..... trimethylsilyl

TS ..... transition state

Ts..... tosylat

## PREFACE

This document would not be possible without the support of many people throughout my graduate school experience. I would like to thank my parents, Mark and Karen Liberatore and all my family for all the encouragement and support in pursuit of my goals as a scientist. I would like to thank Dr. Scott Nelson for accepting me into his research group and providing me with years of guidance and knowledge throughout my years at the University of Pittsburgh. I also owe gratitude to all the past members of the Nelson research group for years of advice and consultation, especially that of Dr. Michael Nardone and Dr. Maryll Geherty. Lastly, I want to thank the Department of Chemistry at the University of Pittsburgh for providing me with ample support throughout my years at the University.<sup>3</sup>

## 1.0 INTRODUCTION: HISTORY OF CURRENT ASYMMETRIC CATALYSIS OF [3,3]-SIGMATROPIC REARRANGEMENTS

The Claisen rearrangement of allyl vinyl ethers and related [3,3]-sigmatropic rearrangements are valuable tools in organic synthesis.<sup>1</sup> The prevalence of such transformations resides in a well-defined transition state resulting in stereospecific, diastereoselective reactions. The diastereoselective nature of Claisen reactions has led to the development of new variations in regards to substrate scope and conditions since the process leads to structurally-complex substrates. One method for promoting [3,3]-sigmatropic reactions is through thermal initiation; yet harsh reaction conditions can cause decomposition or promote undesired side reactions. Many research teams through recent history have demonstrated that milder reaction conditions, achieved through catalysis, increase functional group tolerance and provide access to alternate diastereomeric configurations and enantioenriched products.

### 1.1 EARLY STOICHIOMETRIC LEWIS ACID CATALYSIS

[3,3]-sigmatropic rearrangements commonly utilize Lewis acid catalysis by taking advantage of the Lewis basic heteroatom present in allyl vinyl ethers or similar functionality. Lewis acid-heteroatom coordination weakens the C-O  $\sigma$ -bond and accelerates bond scission. Typically, the approach requires greater than one equivalent of catalyst due to product inhibition.<sup>2</sup> The greater basicity of carbonyl product **2** renders them better ligands for the Lewis-acidic catalyst complexes than ether precursor **1** (Figure 1).

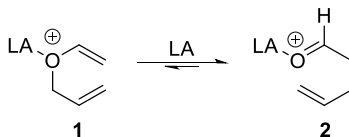
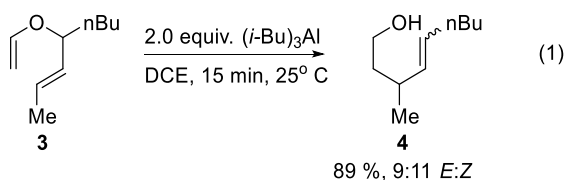


Figure 1: Product Inhibition in Catalysis of Claisen Rearrangements

### 1.1.1 Achiral Stoichiometric Catalysis

The tris(halo)boron complexes  $\text{BF}_3$  and  $\text{BCl}_3$  were first used to promote the rearrangement of aryl vinyl ethers.<sup>3-4</sup> When performed at  $0^\circ\text{C}$ , the examined rearrangements had rate accelerations of up to  $10^{10}$  over the thermal counterpart displaying the potential of the catalyst. However, the substrate scope is limited to aryl substrates and requires excess boron. Aluminum complexes are demonstrated to facilitate aryl vinyl ether, as well as simple allyl vinyl ether, rearrangements.<sup>5-7</sup> Tris(alkyl)aluminum species exhibit remarkable activity. For example, ether **3** undergoes catalytic rearrangement to give alcohol **4** in 89% yield with a moderate preference for *Z* olefin geometry, resulting from *in situ* reduction, in 15 min at ambient conditions (Eq 1). However, the achiral nature of the process, and need for 2 equivalents of aluminum complex, limits the utility of the reaction to more complex, chiral structures.

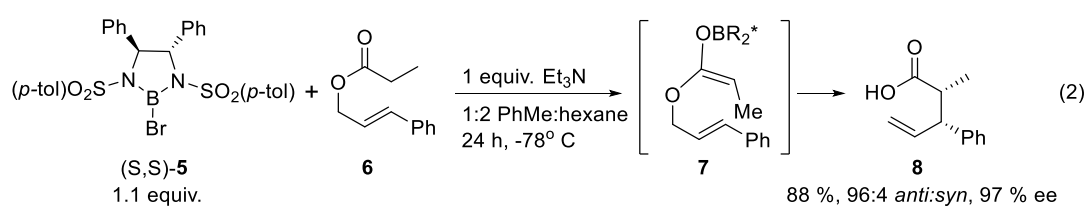


### 1.1.2 Asymmetric Stoichiometric Catalysis

Aluminum- and boron-mediated [3,3]-sigmatropic rearrangements have been developed into a limited number of asymmetric Claisen variants. Ireland-Claisen rearrangements mediated by boron complex **5** provide one noteworthy example of enantioselective Claisen rearrangements that utilize stoichiometric quantities of the chiral controller.<sup>8-9</sup> Thus, the boron Lewis acid is used, first, to generate boron enolate **7** that undergoes an *in situ* [3,3]-rearrangement to afford the characteristic 2,3-disubstituted pentenal product with excellent relative and absolute stereocontrol (give specific numbers here). The enolization reaction conditions can be exploited to generate either *E* or *Z* boron enolates, thereby affording access to either *syn* or *anti* Claisen adducts, each with high

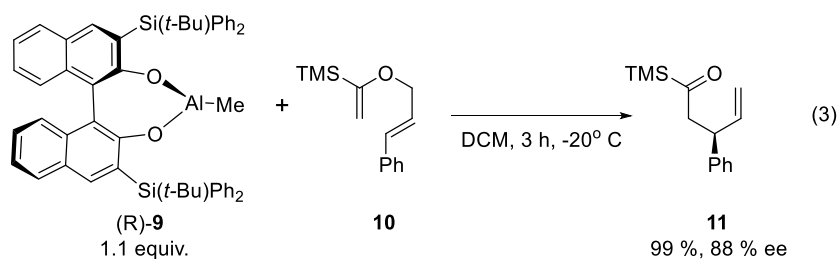
enantioselectivity. While this variant of the Ireland-Claisen rearrangement provides a versatile solution to realizing enantioselective sigmatropic rearrangements, the requirement for stoichiometric quantities of the enantioenriched boron Lewis acid highlights the advantages that might be realized from a catalytic asymmetric reaction variant.

Both reactions require a full equivalent of boron, as well as pendent functionality on the substrate, in order to ensure a chiral transition state. The Ireland-Claisen variant uses the boron complex (S,S)-**5** with easily accessible allyl ester **6** providing enantioenriched acid **8** in 97 % ee. The solvent and amine additive determine diastereoselectivity by influencing the enolate geometry. The use of Et<sub>3</sub>N and PhMe/hexane displays a strong preference for formation of the Z-boroenolate **7** producing *anti* diastereomer **8** in 88 % yield (Eq 2).

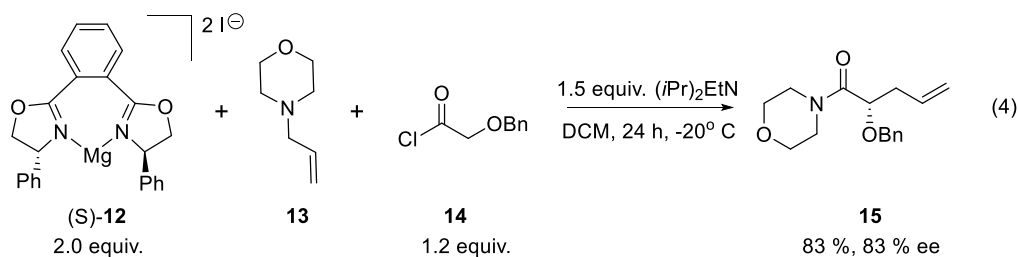


Another notable example of enantioselective Lewis acid-mediated [3,3]-sigmatropic rearrangements comes from Al(III)-mediated Claisen rearrangements. In these reactions, aluminum-based Lewis acid **9** derived from 2,2'-binaphthol (2,2'-BINOL) mediated the rearrangement of vinyl cinnamyl ether **10** to furnish ketone **11** with 88 % ee in 99 % yield (Eq 3).<sup>10-11</sup> While this approach to enantioselective Claisen variants eliminates the need for covalently attached chiral controllers, the reactions are useful for only a limited subset of substrates and still require a stoichiometric amount of the enantioenriched Lewis acid.





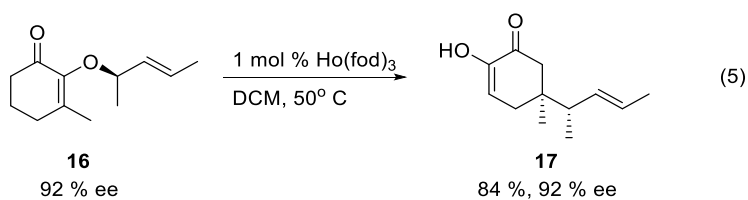
A magnesium-mediated Claisen-Bellus reaction represents the last prominent example of chiral, stoichiometric catalysis.<sup>12</sup> The quaternary ammonium intermediate resulting from the addition of N-allyl morpholine **13** to acid chloride **14** successfully transforms into amide **15** in the present of complex **12** derived from bis(oxazoline) (BOX) structural motifs (Eq 4). The reaction is stereospecific and the obtained amide product **15** exhibits notable enantioselectivity up to 83 % ee in 83 % yield. However, as with boron and aluminum-catalyzed reactions, up to three equivalents of the magnesium-ligand complex was necessary for to obtain useful optical purity. Thus, the need for a large amount of catalyst makes the reaction expensive and replacing the catalyst with a stoichiometric variant would represent an atom-economical improvement.



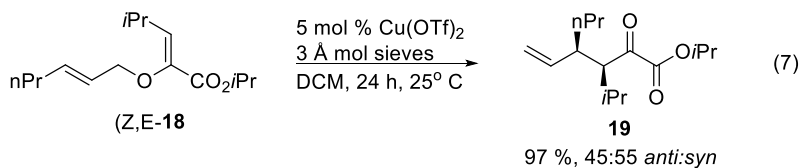
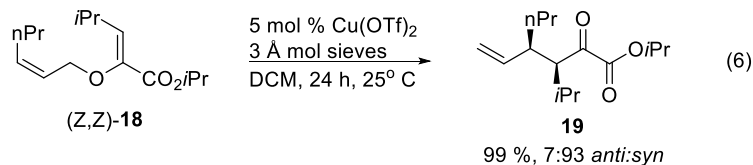
## 1.2 SUB-STOICHIOMETRIC CATALYSIS OF [3,3]-SIGMATROPIC REARRANGEMENTS

The sub-stoichiometric catalysis of Claisen rearrangements has been realized in the past twenty years using a variety of methods and reagents to provide more efficient approaches compared to stoichiometric catalysis outlined previously. Chromium, manganese, iron porphyrin and iron salen

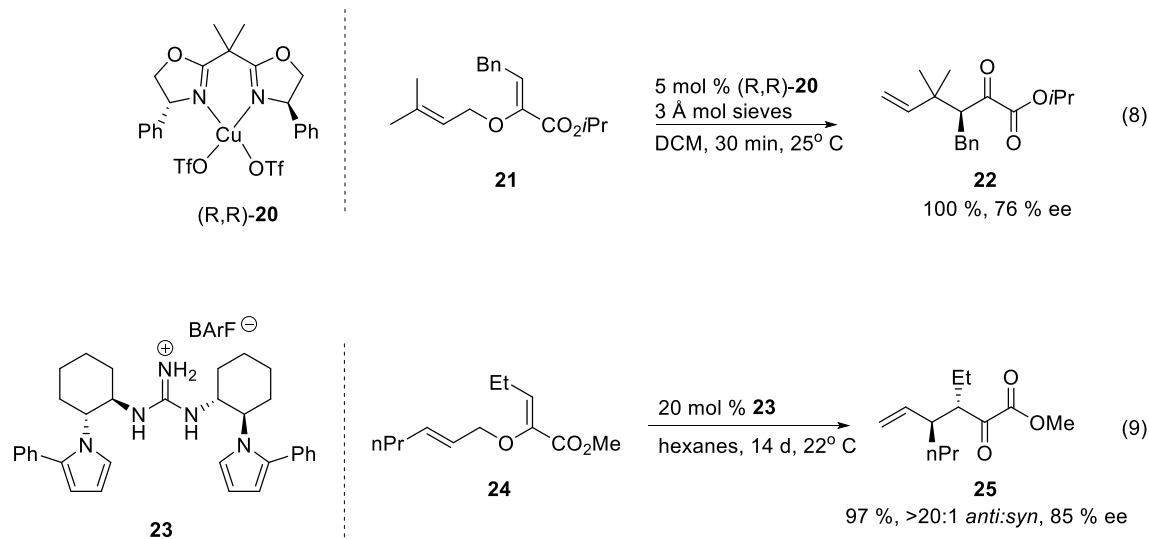
complexes have exhibited moderate reactivity in promoting rearrangements of simple allyl vinyl ethers albeit with limited diastereoselectivity compared to the non-catalyzed thermal reactions.<sup>13</sup> Metal triflates perform well on a number of allyl vinyl structural motifs. Bismuth triflate is a representative catalyst for the rearrangement of aryl vinyl ethers systems, demonstrating activity at 5 mol % catalyst loading at 80° C.<sup>14</sup> Additionally, the lanthanide-complexes Eu(fod)<sub>3</sub> and Ho(fod)<sub>3</sub> are extremely efficient at 1 mol% loading in the stereospecific transformation of enantiomeric enriched allyl vinyl ethers. Reacting chiral cyclic ether **16** to Ho(fod)<sub>3</sub> furnishes the diketone **17** as a single diastereomer and complete conservation of chirality (Eq 5).<sup>15-16</sup> These reactions represent a strong improvement to sub-stoichiometric loading of catalyst but still lack asymmetric induction.



The Gosteli-Claisen rearrangement of 2-alkoxycarbonyl allyl vinyl ethers display excellent activity towards M(OTf)<sub>x</sub> type salts.<sup>2</sup> The best candidates, Yb(OTf)<sub>3</sub> and Cu(OTf)<sub>3</sub>, demonstrate good activity under 10 mol % catalyst loading while minimizing the formation of the [1,3]-rearranged side products.<sup>17</sup> The best results for are obtained using a *Z,Z* allyl vinyl ethers. (*Z,Z*)-**18** rearranges smoothly to provide ester **19** in 99 % yield and 93:7 preference for the *syn* isomer through a chair-like transition state (Eq 6). However, reactions of the (*Z,E*)-**19** isomer is highly dependent on pendant substituents and lack the control observed using *Z,Z* isomer (Eq 7). The chair transition state obtained using *Z,E* esters is sterically disfavored, often resulting in poor diastereoselectivity of *ca.* 1:1 *syn:anti* **19** and significant formation of the linear [1,3] isomer.



Asymmetric transformations using sub-stoichiometric catalyst loadings are reported, however, examples are uncommon. Gosteli-Claisen reactions with Cu(OTf)<sub>2</sub>-BOX complex **20** to provide enantioenriched products from ether **21** to produce ester **22** with 76 % ee in 100 % yield (Eq 8). Still, the reaction is sensitive to variations in substrate substitution patterns.<sup>18-19</sup> Related, 2-alkoxycarbonyls can undergo organocatalyst is successful despite requiring prolonged reaction times. The 2-alkoxycarbonyl systems rearrange through the use of chiral, hydrogen-bonding, guanadinium salt derivative **23** producing an ordered chair transition state in the same manner as Cu(OTf)<sub>2</sub>.<sup>20</sup> The rearrangement of ether **24** requires 14 days to furnish the keto ester **25** with respectable enantioselectivity of 76 % ee and 100 % yield, and excellent diastereoselectivity over 20:1 *anti:syn* (Eq 9). The limited examples of sub-stoichiometric asymmetric catalysis was a inspiration for the work in this document.



### 1.3 ERA OF PALLADIUM CATALYSIS IN [3,3]-SIGMATROPIC PROCESSES

#### 1.3.1 Palladium(II) Catalysis of the Rearrangement of Allyl Esters, Imidates and Thioimidates

Throughout the last half-century, there have been numerous studies on palladium catalyzed [3,3]-rearrangements. Heteroatom rich substrates such as allylic esters, imidates, and thioimidates represent early successes at employing palladium(II) salts to mediate a [3,3] sigmatropic rearrangement as these species are analogous to allyl vinyl ethers utilized in Claisen rearrangements.<sup>21-23</sup> The soft metal center coordinates to the alkene and activates it towards nucleophilic attack by the carbonyl oxygen or similar basic heteroatom and undergoes a cyclization-rearrangement mechanism. The driving force of the reaction and resulting product distribution is determined by the relative stability of the product, *i.e.* the formation of lower energy conjugated species, or by release of steric strain (Figure 2: Cyclization-Rearrangement Mechanism). The rearrangement of secondary ester **26** to **27** in 93 % yield requiring only 10 mol % PdCl<sub>2</sub>(CH<sub>3</sub>CN)<sub>2</sub>. The reactions proceed quickly at ambient temperatures with transfer of chirality and excellent functional group tolerance exhibiting the potential utility of the transformation (Eq 10).<sup>24</sup>

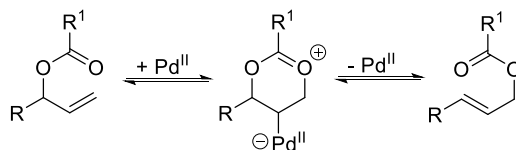
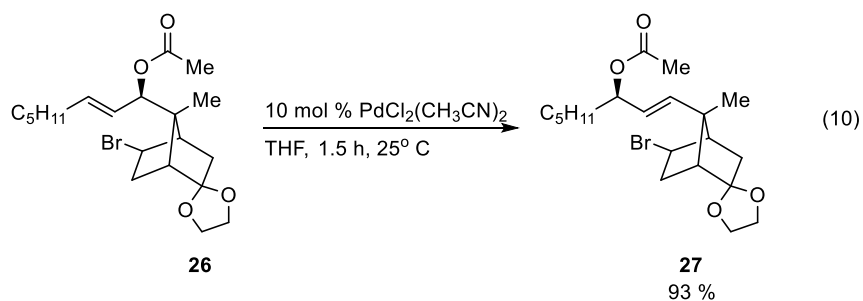
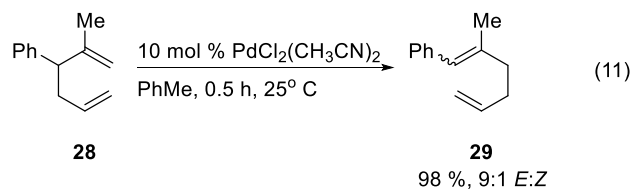


**Figure 2: Cyclization-Rearrangement Mechanism**

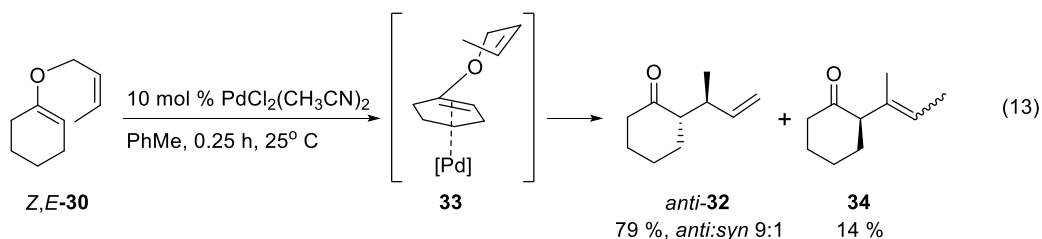
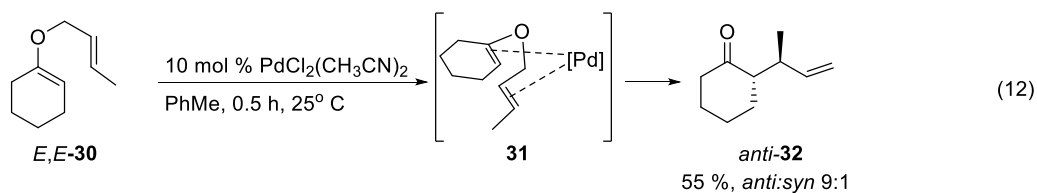


### 1.3.2 Palladium(II) Catalysis of the Cope and Claisen Rearrangements

Palladium-catalyzed [3,3]-rearrangements become problematic upon examining the catalysis of Cope and Claisen reaction systems. Aliphatic 3-phenyl-1,5-hexadiene **28** are thermal Cope rearrangement substrates but in the presence of palladium(II)-complexes, the dienes often form insoluble or unreactive metal-olefin complexes at ambient temperatures which makes the reaction limited in utility to specific substitution patterns. Hence, if one olefin is sufficiently blocked at the 2- or 5-position, such as diene **28**, the palladium(II)-complex will preferentially coordinate to the least substituted double bond and then the cyclization-rearrangement mechanism proceeds to yield styrene **29** (Eq 11).<sup>25-26</sup> The rates in benzene at room temperature are estimated to approach values  $10^{10}$  greater than the thermal Cope process. These reactions demonstrated the powerful early applications of platinum group metal catalysis in [3,3]-sigmatropic rearrangements; however, the reactions are not stereoselective and are limited in substrate scope.

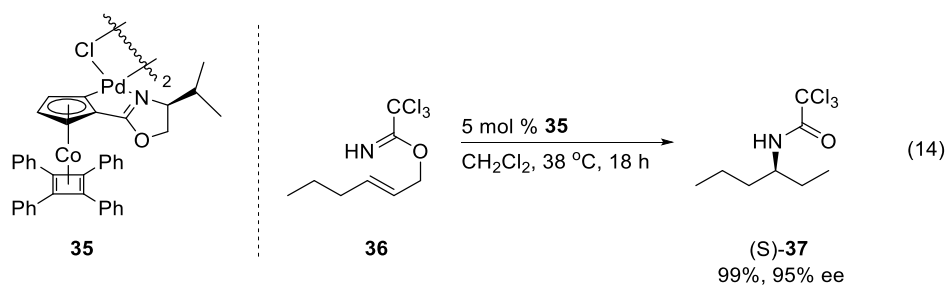


The palladium(II)-catalyzed Claisen rearrangement of allyl vinyl ethers suffer from similar structure constrains as observed in Cope reactions. The more electron-rich vinyl ether can irreversibly binds to the palladium-complex rendering the reaction inert when left unsubstituted as the olefin can bind too strongly to the metal center.<sup>27-28</sup> Remarkably, in contrast to the Cope rearrangement of 1,5-hexadienes, the boat transition state dominates in the palladium(II)-catalyzed reaction and leads to the formation of  $\gamma,\delta$ -unsaturated ketones, albeit with the opposite diastereoselectivity of the thermal Claisen counterpart which could be valuable if a synthetic project required this distinct orientation.<sup>29</sup> Furthermore, the boat transition state is sterically suppressed when using allyl vinyl *Z,E* or *E,Z* olefin geometry. The steric crowding reneges the palladium complex to simple coordination to vinyl ether olefin and a chair transition state is observed. This observation demonstrates the dramatic effects substrate geometry can have on a reaction mechanism and demonstrates a weakness in this reaction methodology as the reaction lacks consistent stereospecificity. The mechanistic distinction is observed in the rearrangement of cyclohexanone derived crotyl ethers. The allyl vinyl *E,E*-**30** proceeds through the boat transition state **31** to furnish ketone *anti*-**32** as the *anti*-diastereomer wherein the thermal rearrangement provides the *syn*-diastereomer (Eq 12). Conversely *Z,E*-**30** is sterically unable to form the boat and thus proceeds through chair **33** to also provide *anti*-**32** as well as isomerized product **34**, the same product produced *via* the thermal rearrangement of *Z,E*-**30** (Eq 13). Overall the competing mechanisms for the palladium(II) mediated reactions could result in unpredictable product distributions in more complicated substrates and thus engendered the need for more predictable methods.



### 1.3.3 Asymmetric Palladium(II) Catalysis

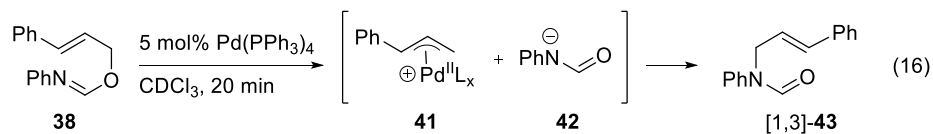
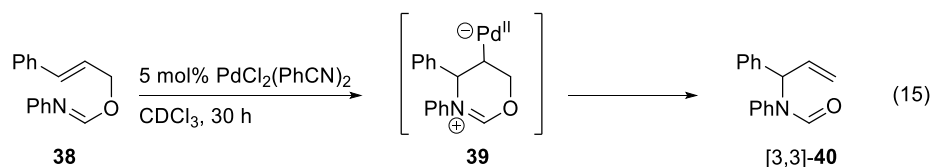
While palladium(II)-complexes demonstrate remarkable activity in catalyzing [3,3]-sigmatropic rearrangements through the cyclization-rearrangement mechanism, enantioselective variants are rare yet are important for modern synthetic needs. The rearrangement of allyl imidates to amides by cationic palladium(II)-complexes remains a prime example with some substrates reaching 60% ee.<sup>30-31</sup> Allyl imidates are often limited to electron-deficient substituents on the imine carbon. The deficiency suppresses nitrogen to palladium coordination which results in counterproductive C-O cleavage. The dimeric, cyclometallated palladium(II)-complexes **35** improves enantioselectivities to synthetically useful levels and recent examples provide enantioenriched amides **37** from achiral imidates **36** at room temperature (Eq 14).<sup>32-33</sup>



### 1.3.4 Palladium(0) Catalysis of Allyl Imidates

Palladium(0) affects the rearrangements of allylic imidates to provide an isomeric product related to compound **37** acquired via palladium(II) catalysis.<sup>34</sup> These substrates are analogues of allyl vinyl ethers seen in Claisen rearrangements. The mechanistic differentiation to the cyclization-rearrangement mechanism attributed to palladium(II)-complexes is illustrated by the reaction of cinnamyl-derived imidate **38**. Under palladium(II) conditions the formal [3,3]-rearranged product **40** is realized as the sole product through the cyclization-rearrangement intermediate **39** (Eq 15). However, under palladium(0) conditions, the reaction yields the [1,3]-rearranged product **43** (Eq 16). The product results from the combination of the amide anion **42** and the electrophilic palladium(II)  $\pi$ -allyl complex **41**. Palladium(0) generates the  $\pi$ -allyl complex *in situ* via oxidative insertion into the labile C-O bond of the imidate. In general, the rearrangement of allyl vinyl imidates demonstrated how formal [3,3] rearrangements of allyl vinyl substrates could be a novel method for accessing enantioenriched Claisen products from simple, achiral starting materials.





Until the discovery of palladium(0) catalysis all the reactions discussed thus far are Lewis-acid based catalysis in which the fundamental [3,3] rearrangement mechanism is conserved. Since the catalyst functions as an acid there is often a need for large catalyst loadings and enantioselective versions can be very expensive. As alluded to, the investigation into palladium(0) catalysis opened up a new route to accessing alternative isomers of Claassen-type precursors. Since the mechanism does not proceed through the cyclization-rearrangement pathway there is a greater potential for asymmetric induction as the metal is not as far away from the bond-forming steps. The next section focuses on the development of allylic alkylations and how they represent a new approach to Claisen products.

## 1.4 TRANSITION METAL CATALYZED ALLYLIC ALKYLATIONS: AN ALTERNATIVE TO THE CLAISEN REARRANGEMENT

### 1.4.1 Stoichiometric Palladium-Mediated Allylic Alkylations

The allylic alkylation mechanism provides an alternative approach to accessing Claisen-type products.<sup>35-36</sup> Initial reactions of this type were first performed by the stoichiometric combinations of palladium(II) allyl dimer **44** and malonate **45** to generate  $\gamma,\delta$ -unsaturated esters **46** and **47** (Eq 17). The  $\gamma,\delta$ -unsaturated carbonyl motif **47** is the same as that obtained from a theoretical [3,3]-sigmatropic

rearrangements of vinyl ether **48** (Figure 3). Thus allylic alkylations can serve as new pathways to access Claisen-type products.

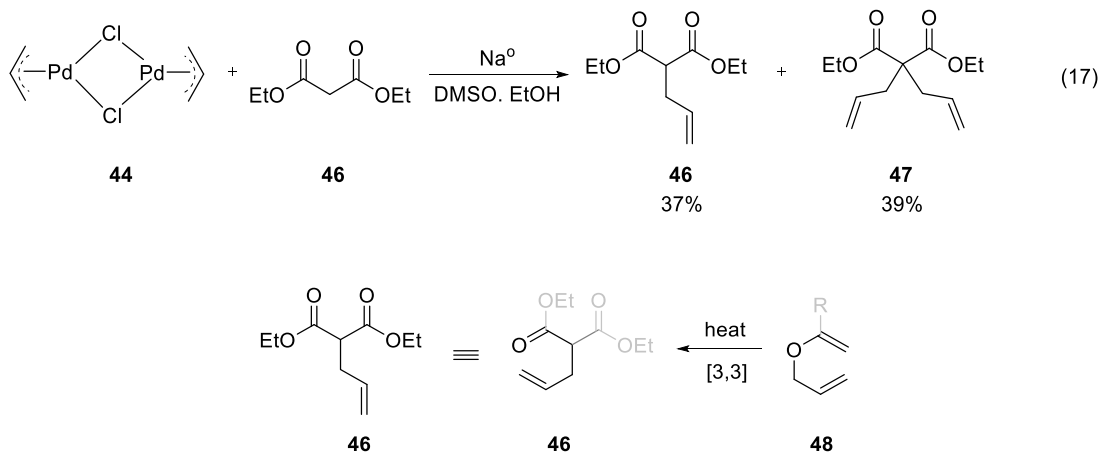
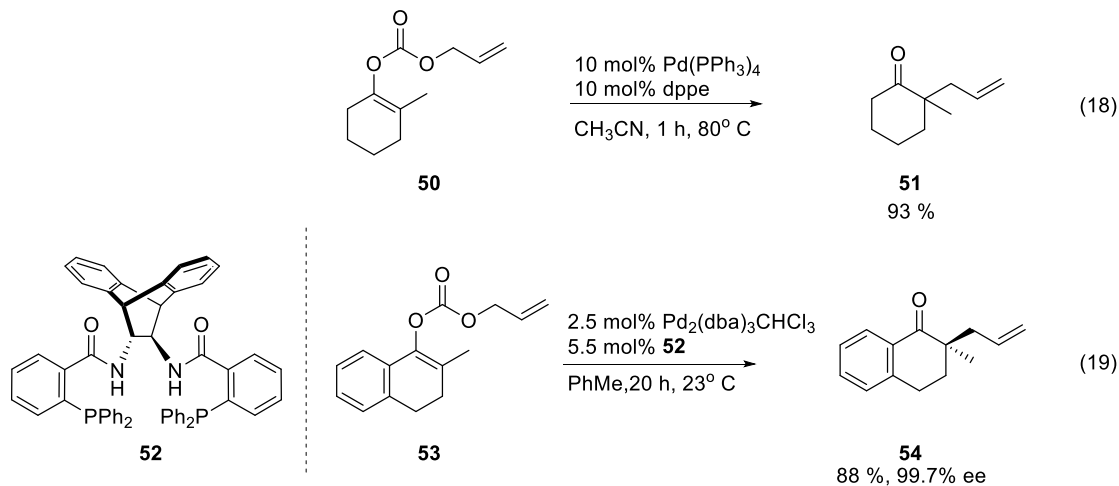


**Figure 3: Allylic Alkylations as Analogues of Claisen Rearrangements**

#### 1.4.2 Catalytic Palladium-Mediated Allylic Alkylations

Catalytic versions of allylic alkylations were realized by the treatment of allyl vinyl carbonates with palladium(0) phosphine complexes in catalyzed Carroll rearrangements. In an example reaction, the palladium oxidatively inserts into the labile C-O of carbonate **5m0** bond to generate CO<sub>2</sub>, an enolate, and a palladium(II) allyl complex. The enolate then recombines with the allyl fragment to regenerate a palladium(0) complex and  $\gamma,\delta$ -unsaturated ketone **51** in 93 % yield (Eq 18).<sup>37</sup> Further investigations led to asymmetric variant utilizing bis(phosphine) **52** and allyl vinyl carbonate **53** to generate the ketone **54** in 86 % yield with 99.7 % ee (Eq 19).<sup>38</sup>

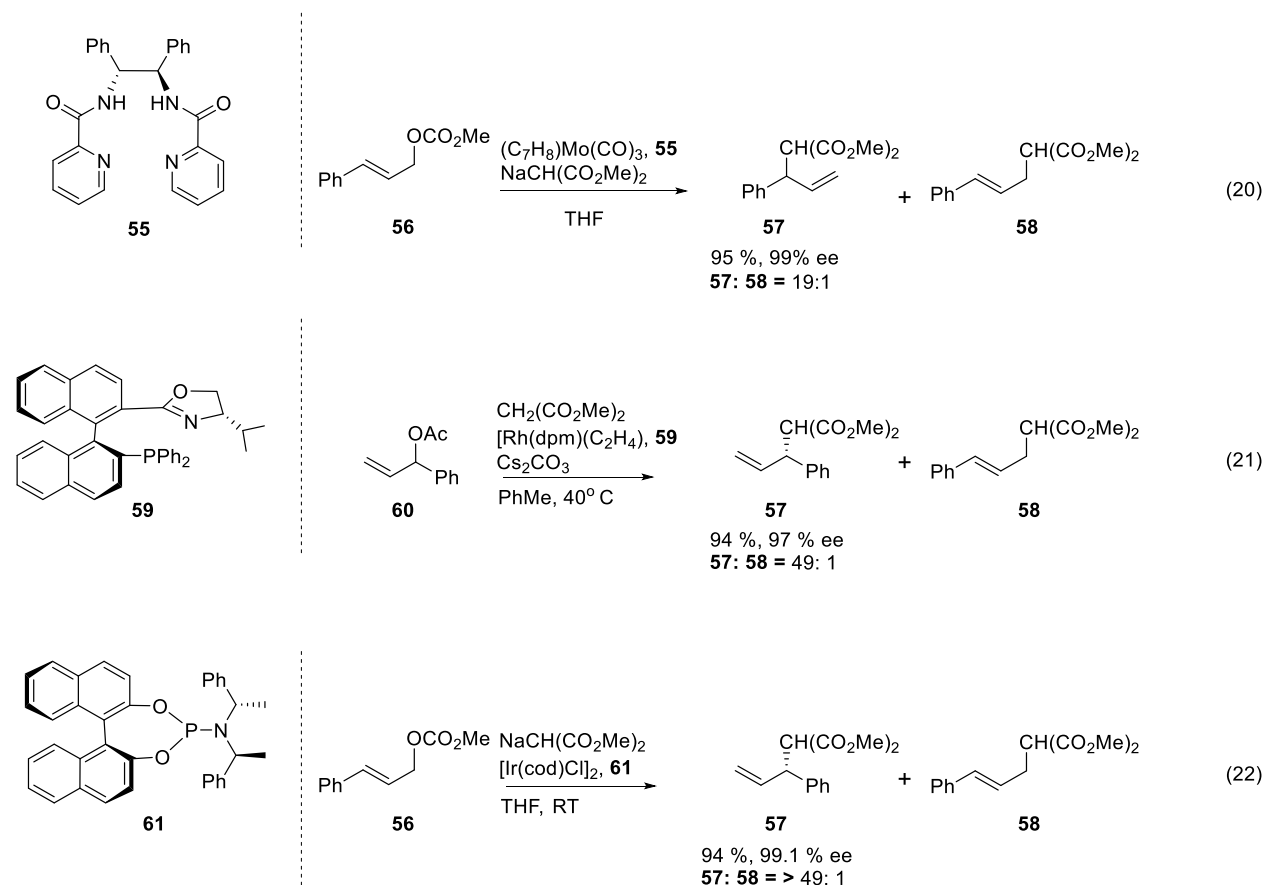


### 1.4.3 Allylic Alkylation by Other Late Transition Metals: Accessing Alternative Regioisomers

As illustrated previously, palladium(0)-catalyzed allylic alkylation reactions demonstrate regiochemical preference towards the [1,3] isomer by favoring nucleophilic attack on the least substituted terminus of the intermediate  $e\pi$ -allyl complex. The preference in regiochemistry represents loss of potential towards stereochemical complexity seen by the construction of a chiral center in [3,3] Claisen products. Nonetheless, other low valent and late transition metals are active in allylic alkylation reactions of metal  $\pi$ -allyl complexes and carbon-based nucleophiles. In contrast to palladium(0), these metals display alternate regiochemical preferences towards the branched alkylation products.<sup>39</sup>

Carbonyl complexes of molybdenum(0) and tungsten(0) display preference towards branched regioselectivity in the reaction of allyl acetate with malonate-type nucleophiles.<sup>40-42</sup> These products possess Molybdenum-mediated reactions produce enantioenriched alkylated products from simple cinnamyl carbonate **56** and operate in the same fashion as palladium(0) complexes providing malonates **57** and **58** with strong 19:1 regiochemical preference for the branched isomer **57** in 95% with 99% ee (Eq 20). Later transition metal complexes also exhibit the same regiochemical preference. Rhodium(I) and iridium(I) complexes perform alkylation reactions using chiral phosphines such as **59** and **60** starting from simple allylic donors to generate enantioenriched malonates **57** and **58** again with

strong 49:1 preference for the branched isomer **57** (Eq 21 and 22).<sup>43-48</sup> In addition, ruthenium(II) complexes facilitate the same transformation and one goal of our research group was to develop the metal into a tool for accessing enantioenriched products.

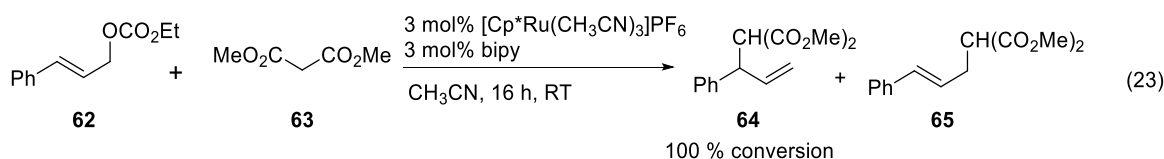


## 1.5 ACCESSING [3,3]-CLAISEN PRODUCTS USING RUTHENIUM(II) COMPLEXES

### 1.5.1 Piano-stool Cp and Cp\*Ru(II) Complexes

As the focus of our group was the development of allylic alkylations as surrogates for traditional Claisen rearrangements, we were especially interested in catalyst complexes that would mediate C–C bond construction at the more substituted allylic site. In this context, Ru(II)-complexes exhibit a strong tendency for delivering branched reaction products resulting from nucleophilic addition of malonate **63** to the more substituted site of the allyl complex derived from carbonate **62**. For example,

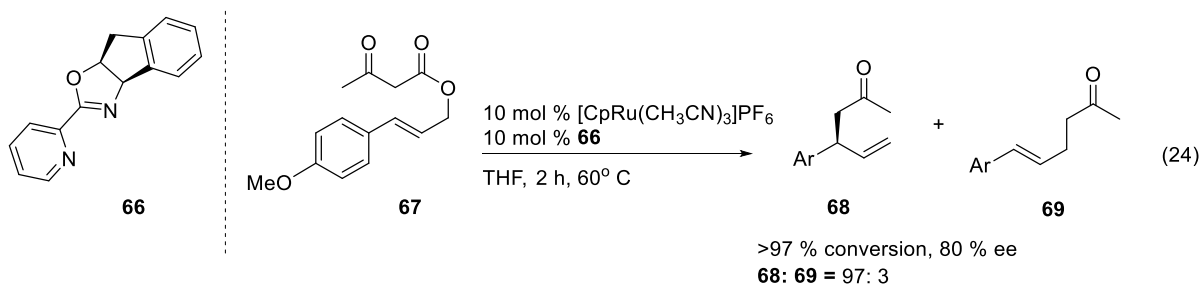
Ru(cod)(cot) complex catalyzes the addition of malonate anion to allylic chlorides to predominately afford the branched alkylation product **64** in preference to the linear product **65** preferred under Pd(0) catalysis (give specific numbers).<sup>49-50</sup> Similarly, [Cp\*Ru(CH<sub>3</sub>CN)<sub>3</sub>]PF<sub>6</sub>, was found to provide alkylated products with excellent selectivity for the branched reactions over 6:1 branched:linear in part due to the strong stabilization effects provided by the pentamethylcyclopentadienyl ligand.<sup>51</sup> Moreover, when the [Cp\*Ru(CH<sub>3</sub>CN)<sub>3</sub>]PF<sub>6</sub> was modified with bidentate 2,2'-bipyridine as a ligand, the branched:linear selectivity was further improved along with a commensurate improvement in catalyst activity up to 25:1 branched:linear featuring a chiral center (Eq 23).<sup>52-54</sup>



### 1.5.2 Asymmetric Ruthenium(II) Catalyzed Allylic Alkylations

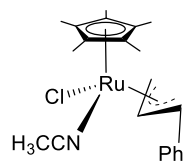
Enantioselective versions of the Ru(II)-catalyzed allylic alkylations reactions were obtained by replacing the achiral 2,2'-bipyridine ligand with enantioenriched bidentate ligands. For example, the Ru(II) complex obtained by reacting [Cp\*Ru(CH<sub>3</sub>CN)<sub>3</sub>]PF<sub>6</sub> with the enantioenriched pyridine oxazoline ligand **66** afforded enantioenriched products. The first ruthenium systems were extremely effective in the asymmetric allylation using phenol nucleophiles.<sup>55-56</sup> However, Carroll-type alkylation reactions using malonate-type nucleophiles display only moderate and varied degrees of enantioselectivity around 80% ee.<sup>56-58</sup> Modifying the system to use the less electron-rich [CpRu(CH<sub>3</sub>CN)<sub>3</sub>]PF<sub>6</sub> precursor and chiral pyridine-oxazoline ligands led to a balanced, yet active, catalyst system providing alkylated products in good yields and better enantioselectivities at the cost of increased catalyst loading (Eq 24). The optically active compounds are the same as those produced from racemic Claisen rearrangements. These results established the potential for using Ru(II)-

catalyzed enolate alkylations for an entry to 2,3-disubstituted pentenones that are formal equivalents of Claisen rearrangement reaction products.

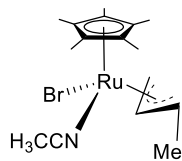
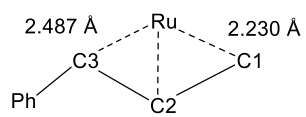


### 1.5.3 Origin of Regioselectivity in Ruthenium(II) Catalyzed Allylic Alkylation

Ruthenium and other transition metals demonstrate a greater preference for forming the more substituted [3,3]-product than transformations utilizing palladium. Understanding the regiochemical bias observed in ruthenium-catalyzed allylic alkylations is important as the preferment provides access to Claisen-type products. One reason for the observation comes from data analysis using X-ray crystal analysis and structural calculations which shows remarkable differences in Ru-C bond distances between the ruthenium atom and the terminal ( $C_1$ ) and interior ( $C_3$ ) carbons in ruthenium(II)  $\eta^3$ -allyl complexes **70** derived from cinnamyl allyl donors (Figure 4a).<sup>59-60</sup> However, aliphatic based allyl ligands bound to ruthenium complex **71** do not display such large differences in bond lengths (Figure 4b). The bond lengthening has been theorized to result from diminished  $\pi$ -backbonding from the metal center which is likely exacerbated by the presence of aryl groups. In this light, increasing the electron density on the metal center further decreases the magnitude of  $\pi$ -backbonding and increasing regioselectivity, hence elongation witnessed in aliphatic examples.<sup>60</sup> Understanding the origin of the regioselectivity will be important in our study in rationalizing potential trends in results using different substrates.



70



71

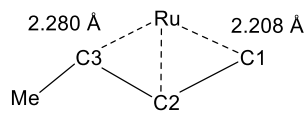


Figure 4: Asymmetric Bonding in Ruthenium Allyl Complexes

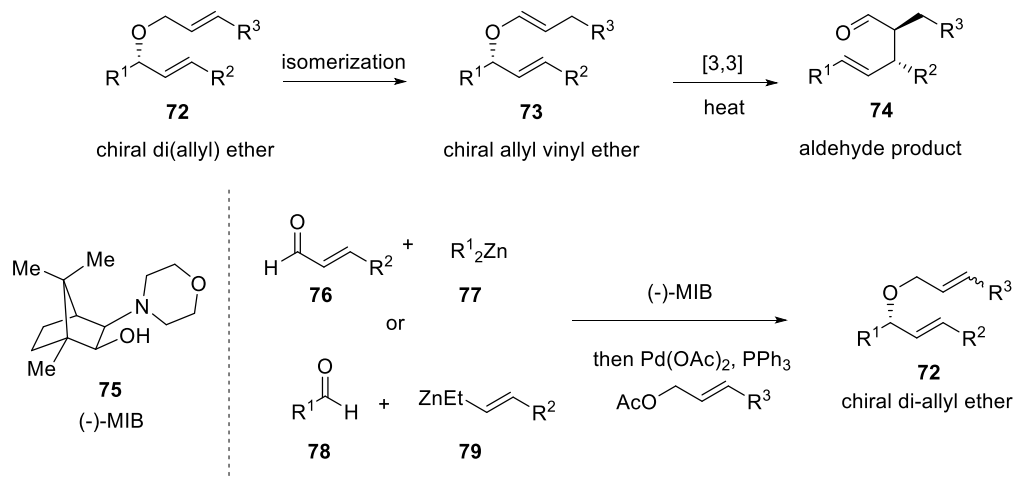
## 2.0 IRIDIUM(I) CATALYZED OLEFIN ISOMERIZATION AND APPLICATION TO RUTHENIUM(II) CATALYZED CLAISEN REARRANGEMENTS.

### 2.1 EXPLORATION OF IRIDIUM(I) CATALYZED OLEFIN ISOMERIZATION IN THE NELSON LABORATORY

Developing work on ruthenium(II)-catalyzed Claisen reactions required a source of starting materials to increase the substrate scope. Early work in the Nelson laboratory explored the use of iridium(I)-complexes to develop an asymmetric isomerization-Claisen rearrangement (ICR) strategy. The method was later used to produce the first substrates for the Ru(II)-catalyzed formal [3,3]-sigmatropic rearrangements and represented a cornerstone for our research. The ICR reaction was designed to take advantage of the strong diastereomeric control thermal Claisen rearrangements; by using a chiral substrate one can efficiently transfer the chirality of the starting material to the rearranged product.<sup>61</sup> If asymmetric di(allyl) ether **72** is successfully transformed *via* selective isomerization into allyl vinyl ether **73** then a convenient route towards valuable  $\gamma,\delta$ -unsaturated aldehyde **74** would be achieved through the Claisen rearrangement (Scheme 1). Fortunately, previous members of the Nelson group developed a route to optically pure di(allyl) ethers by addition of dialkylzinc complexes to aldehydes in the presence of borneol derived ligand MIB.<sup>62-63</sup> However, the necessary ethers are limited by the availability of alkyl zinc reagents. A better strategy would be to utilize a broader substrate scope of achiral di(allyl) vinyl ethers and then selectively isomerize one double bond to create the Claisen precursor.



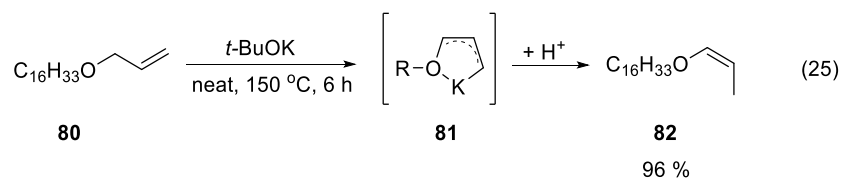
## Scheme 1: Iridium(I)-Catalyzed Isomerization-Claisen Rearrangements (ICR)



## 2.2 OTHER ALLYL TO VINYL ETHER ISOMERIZATION STRATEGIES AND THEIR DISADVANTAGES

### 2.2.1 Strong Base Catalyzed Isomerization

Multiple methodologies for the isomerization of allyl ethers to vinyl ethers have been developed however they suffer from limited effectiveness. Strong bases, such as a potassium *tert*-butoxide, at elevated temperatures isomerize simple allyl ethers like **80** through a cyclic transition state **81** to provide *cis*-vinyl **82** resulting from the intermediate ether-potassium chelate (Eq 25).<sup>64</sup> However, because of harsh, non-selective conditions the transformation is rare in tandem isomerization-sigmatropic rearrangement reactions.<sup>65</sup> To provide substrates for our Ru(II)-catalyzed processes we needed to find a simple method for accessing the required starting materials. In addition, the necessary isomerization would need to be selective to produce an allyl vinyl ether. This method would likely produce di(vinyl) products.



## 2.2.2 Transition Metal Catalyzed Isomerizations of Allyl Ethers

Isomerization processes are thought to progress through initial oxidative insertion of the metal complex into the allylic C-H bond of allyl ether **83** to form a  $\eta_1$   $\pi$ -allyl complex **85**. The intermediate equilibrates with the conjugated terminal  $\eta^1$   $\pi$ -allyl complex **87** through an  $\eta^3$ -allyl species **86** to afford vinyl ether **88** (Figure 5). Of interest are ruthenium(II), nickel(II), and iridium(I) compounds which have demonstrated to be successful isomerization catalysts albeit with varying degrees of geometric selectivity (Figure 6). For our needs, we would require a high degree of geometric purity.  $\text{H}_2\text{Ru}(\text{PPh}_3)_3$  is capable of isomerizing allyl vinyl ethers to provide a 1:1 ratio of *E* and *Z* geometric isomers.<sup>66</sup> Nickel systems such as  $\text{NiCl}_2(\text{dppb})/\text{LiBHEt}_3$  are capable, yet give predominantly the *Z* isomer.<sup>67</sup> In contrast,  $[\text{Ir}(\text{PR}_3)(\text{sol})_2]\text{PF}_6$  type complexes produce vinyl ethers in high yields furnishing the *E* isomer.<sup>68</sup> Geometric purity of in isomerization of enantiopure allyl vinyl ethers is paramount in ensuring the production of optically-active Claisen products. In addition, these methods are for single allyl ethers and may not be selective on di(allyl) systems.

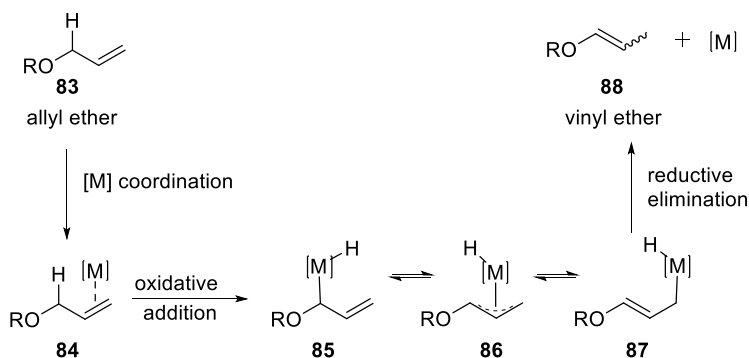
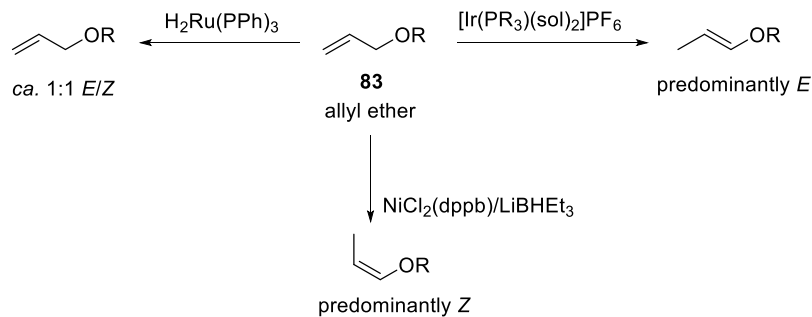


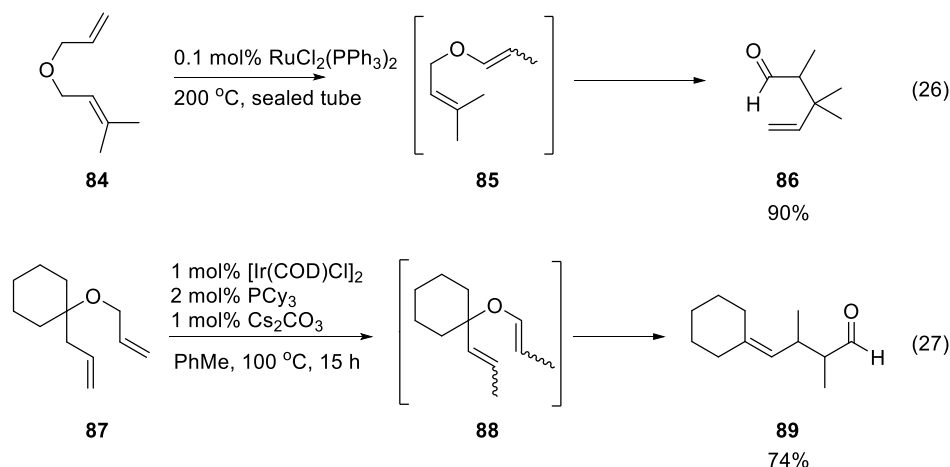
Figure 5: General Mechanism for Transition Metal Olefin Isomerization



**Figure 6: Diastereoselectivity in Olefin Isomerization**

### 2.2.3 Transition Metal Catalyzed Isomerizations and Rearrangement of Di(allyl) Ethers

Ruthenium and iridium systems are successfully employed in tandem isomerization-Claisen reactions of di(allyl) ethers, but are limited in substrate scope. The  $\text{Cl}_2\text{Ru}(\text{PPh}_3)_2$ ,  $\text{Rh}_3(\text{CO})_{12}/\text{IMes}$ , and  $[\text{Ir}(\text{COD})\text{Cl}]_2/\text{PCy}_3$  systems all react in this manner.<sup>22, 69-70</sup> To ensure the selectivity for the allyl vinyl ether, sterically demanding di-substituted alkenes are used to ensure mono isomerization (Eq 26). Alternatively, an  $\alpha$ -disubstituted ether completely blocks any formation of di(vinyl) product (Eq 27). Even with these modifications, reactions still require high temperatures and lack diastereoselectivity.



## 2.3 DEVELOPMENT OF IRIIDIUM CATALYZED ISOMERIZATION-CLAISEN REARRANGEMENT (ICR) CHEMISTRY

Our group sought to improve the iridium(I)-catalyzed isomerization process to effectively transform asymmetric di(allyl) ethers to the allyl vinyl Claisen precursors with strict geometric control.<sup>71</sup> The system is based on previous studies using  $[\text{Ir}(\text{PR}_3)_2(\text{sol})_2]\text{PF}_6$  systems because of reported bias towards *E* olefin geometry.<sup>68</sup> The complexes are usually generated by the treatment of commercially available  $[\text{Ir}(\text{COD})\text{Cl}]_2$  dimer with  $\text{PR}_3$  and a halide extractor such as  $\text{AgPF}_6$  to generate cationic  $(\text{PR}_3)_2\text{Ir}(\text{COD})$  salts. The iridium-based complexes also require treatment with reducing agents such as hydrogen, hydrides or boranes to remove the strongly bound COD moiety.

### 2.3.1 Iridium Olefin Isomerization Reaction Modifications

A method was required to increase the reactivity of the iridium complex without the need for cumbersome reducing agents. Exchanging two cyclooctenes (COE) for the chelating COD provided a convenient way to access a coordinately unsaturated iridium(I) species by elimination of the chelate effect.<sup>72</sup> Treatment di(allyl) ether **90** with  $[\text{Ir}(\text{PCy}_3)_3]\text{SbF}_6$  gave highly regioselective isomerization for the least substituted allyl group to provide the allyl vinyl ether **91** resulting in Claisen product **92**. However, employing silver salts or less basic triphenylphosphine ligands results in competing the allyl

shifts side reaction to form **93** and thus produce isomeric mixtures containing allyl vinyl ether **94**, giving undesired isomeric pentenal product **95** (Figure 7). To prevent the undesired pathway, a milder halide abstractor, NaBPh<sub>4</sub>, is used in the presence of small amount of acetone co-solvent to increase the solubility of the salt. Thus a method was realized that could perform the regioselective isomerization effectively to produce allyl vinyl ethers for subsequent ruthenium(II) catalyzed rearrangements.

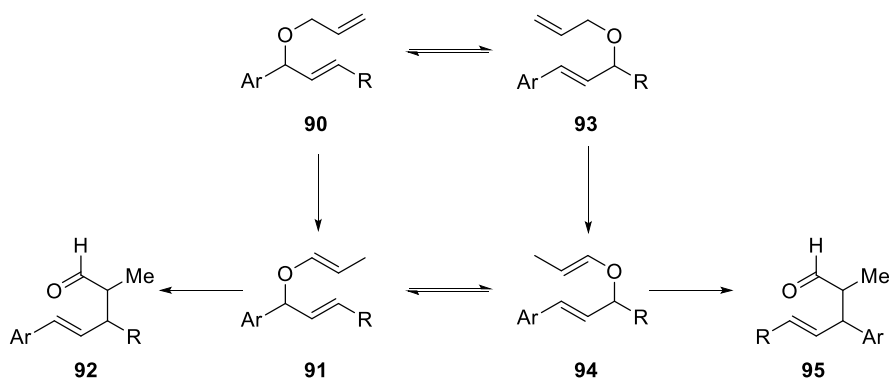
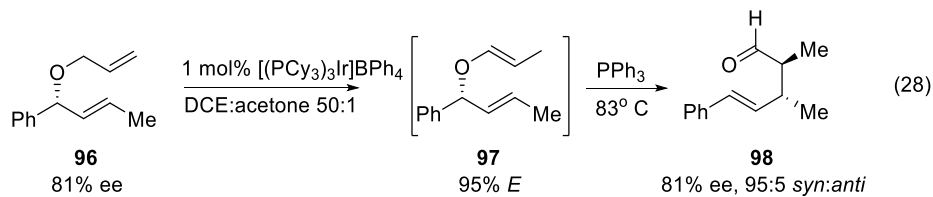


**Figure 7: Allyl Shifts in Di(allyl) Ethers**

The resultant Ir(PCy<sub>3</sub>)<sub>3</sub>]BPh<sub>4</sub> complex is good because it facilitates the room temperature isomerization of chiral ether **96** at room temperature with 95% *E*-selectivity to allyl vinyl substrate **97**. After addition of excess PPh<sub>3</sub> to sequester the iridium complex, thermal Claisen conditions provide the pentenal **98** with complete transfer of chirality (Eq 28). Our group utilized the ICR (iridium(I)-catalyzed rearrangement) in the total synthesis of (+)-calopin.<sup>73</sup> Thus this method represents a useful way to access enantiomerically-enriched pentenals.



### 2.3.2 Iridium Catalyzed Isomerization Mechanism

The diastereoselectivity of the iridium(I) isomerization of simple allyl ether **99** to **100** derives from sterically less demanding structure **101** resulting from initial complexation of the olefin to the iridium (Figure 8). Complex **101** then undergoes C-H insertion generating  $\eta^1$ -allyl complex **102**. Subsequent isomerization through  $\eta^3$ -complex **103** provides the lower energy, conjugated  $\eta^1$ -allyl complex **104** which upon reductive elimination furnishes enol ether *E*-**100**. Direct formation of *Z*-**100** is disfavored because of steric repulsion present in olefin complex **105** which would ultimately progress through allyl species **106** and **107**.

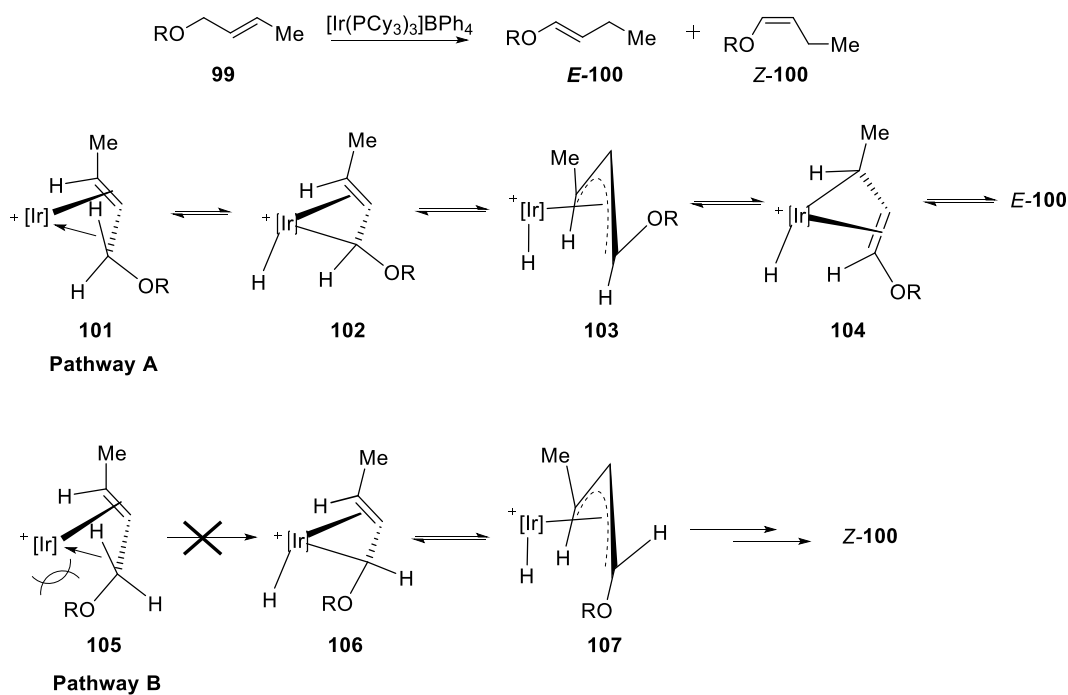
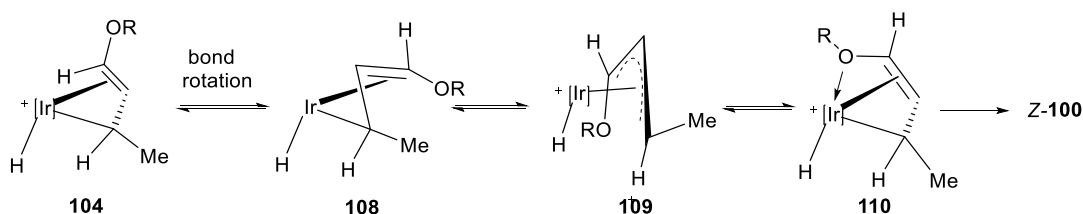


Figure 8: Mechanism of Allyl to Vinyl Ether Isomerization by Ir(I)-Catalysis

However, the formation of *Z*-**100** is observed in the reaction. The alternate diastereomer likely forms from Csp<sup>2</sup>-C(H)OR bond rotation of the η<sup>1</sup>-allyl intermediate **109** derived from structure **104** proceeding through alternate η<sup>3</sup>-allyl **110** and η<sup>1</sup>-allyl intermediate **111** which is stabilized by a dative bond with the ether oxygen (Figure 9). The desired *E*-**100** is susceptible to this reverse reaction (and thus *E* to *Z* isomerization) and show isomerization of the cinnamyl portion of the di(allyl) ethers, leading to undesired di(vinyl) products. Undesired pathways can be suppressed by careful reaction monitoring of the reaction. 2.199 2.291



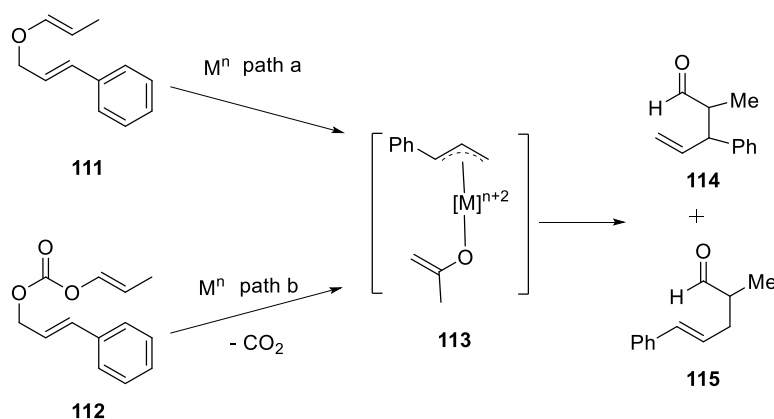
**Figure 9: Mechanism of *E* to *Z* Olefin Isomerization in Iridium-Catalyzed Isomerization Reactions**

## 2.4 IRIDIUM CATALYZED OLEFIN ISOMERIZATION FOR THE SYNTHESIS OF CARROLL-TYPE REARRANGEMENT SUBSTRATES

The success of regioselective iridium(I)-catalyzed of di(allyl) ethers to allyl vinyl ethers led our group to explore the usefulness of these Claisen precursors in ruthenium-catalyzed reactions as analogues to allyl β-ketoester substrates of Carroll rearrangements. The Carroll rearrangement is comparable the Claisen rearrangement as it ultimately produces the pentenal Claisen product from a metal-catalyzed decarboxylative allylation process. We sought to produce achiral allyl vinyl ethers or carbonates and then employ a chiral metal catalyst to affect the formal [3,3]-sigmatropic rearrangement (Scheme 2, path a). The metal would insert into the C-O bond of ether **111** or carbonate **112** to generate an allyl

complex **113**. Recombination forms rearranged products **114** and **115**. However, we thought that C-O bond in the vinyl ethers may be too strong to undergo oxidative insertion. Thus, we reasoned a more reactive motif, such as a carbonate, would work better, and the loss of CO<sub>2</sub> would promote faster reactivity (Scheme 2, path b). We chose ruthenium as our metal of choice due to the prevalence of the enolate to form branched products like **114** and for the record of successful asymmetric induction by chiral ligands.

### Scheme 2: Allyl Vinyl Ethers and Carbonates as Claisen Rearrangement Substrates



#### 2.4.1 Synthesis of Allyl Vinyl Carbonates

Fortunately, our conditions for iridium-catalyzed isomerization were found to be effective in the isomerization of di(allyl) carbonates. Addition of cinnamyl alcohol **115** to allyl chloroformate **116** and subjecting the resultant di(allyl) carbonate **118** to optimized iridium isomerization conditions (0.5 mol% [Ir(COE)<sub>2</sub>Cl]<sub>2</sub>, 2 mol% NaBPh<sub>4</sub>, 3 mol% PCy<sub>3</sub>) provided the allyl vinyl carbonate **112** (Scheme 3). The process results in 78% isolated yields with complete selectivity for the E isomer. In contrast to the use di(allyl) ethers, only the mono(vinyl) carbonate is observed and the reaction is slower and does not go to completion. However, the process requires substantially longer reaction times. The slower performance of the isomerization of carbonate motif **120** is attributed to the formation of a stable 5-member chelate **120** with the carbonyl-oxygen which attenuates the necessary allyl shift to



give the desired vinyl carbonate **121** (Figure 10a). Regrettably, any substitution on the allyl group shuts down the isomerization pathway when using carbonates. Crotyl carbonate **122** displays no isomerization to **124** when subjected to isomerization conditions over long periods of time (Figure 10b). The observed lack of activity arises from increased steric demand introduced by the methyl group and the stabilization derived from the carbonyl chelate **123**.

### Scheme 3: Synthesis of Allyl Vinyl Carbonate

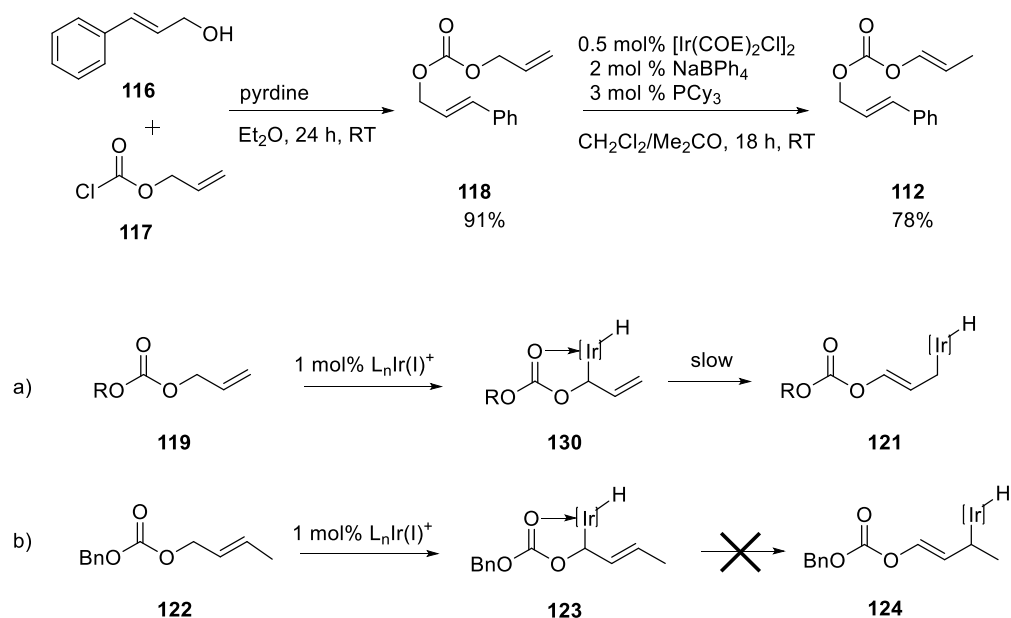


Figure 10: Lack of Reactivity of Substituted Allyl Carbonates in Iridium(I)-Catalyzed Isomerizations

## 2.5 RUTHENIUM-CATALYZED REARRANGEMENT OF ALLYL VINYL CARBONATES

### 2.5.1 Reactivity of Allyl Vinyl Carbonate 111 to Transition Metal Catalysis

Carbonate **111**, a model substrate, was initially screened using known palladium and ruthenium allylic alkylation conditions in order to evaluate the activity and regiochemical outcome of the transformation

under different conditions (Figure 11).<sup>38</sup> Interestingly, the use of the Trost ligand **125** and Pd<sub>2</sub>(dba)<sub>3</sub> gave no rearranged product in spite of the conditions working on similar allyl β-ketoester substrates. Employing Pd(PPh<sub>3</sub>)<sub>4</sub> in refluxing THF provided complete conversion, but unsurprisingly, provided the linear product **125** as the sole regioisomer. The use of the piano stool [CpRu(CH<sub>3</sub>CN)<sub>3</sub>]PF<sub>6</sub> and bipyridine demonstrated good activity as well as a preference for the branched product **114** by 6 to 1. We chose not to examine a Cp\*-based catalyst due to lack of enantiocontrol seen in previous works.<sup>57</sup> The preliminary results indicate that allyl vinyl carbonates perform as expected under Ru(II)-catalysis like β-keto esters examined in previous studies discussed previously.

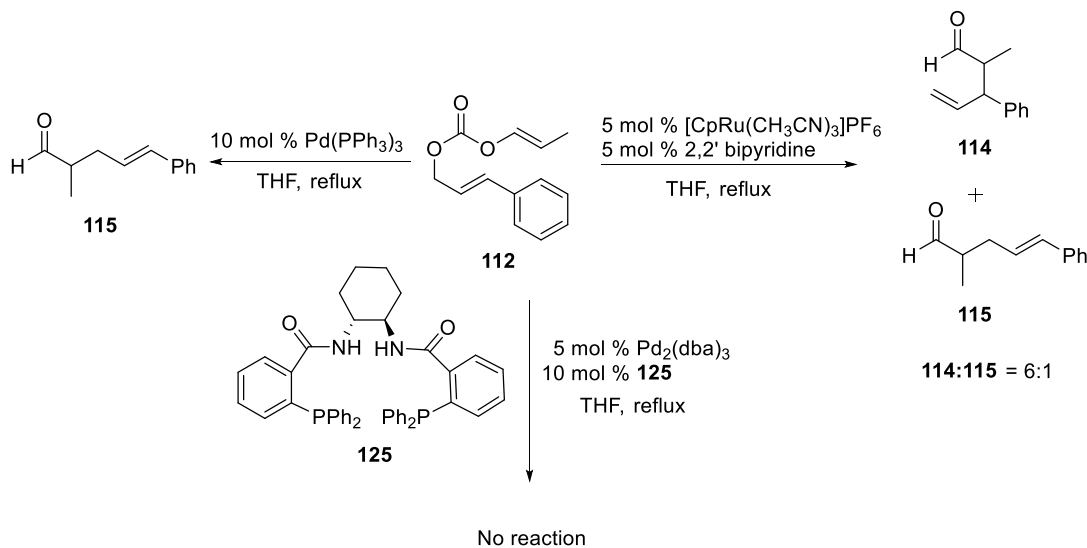


**Figure 11: Test Conditions for Ruthenium-Catalyzed Rearrangement of Allyl Vinyl Carbonates**

### 2.5.2 Initial Reaction Design

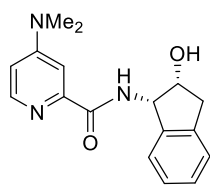
The satisfactory conversion and regioselectivity using Ru(II) complexes with allyl vinyl carbonates warranted further exploration. Our group performed many simple optimization experiments on the initial ruthenium(II) system varying solvents, ligands, and Lewis acid additives (Eq 29). Polar, aprotic

solvents, such as THF and acetonitrile, were found to enhance the regioselectivity towards the branched product. Changing the bipyridine ligand to the electron-rich pyridine oxazoline system **66** provided good regiochemical control and allowed the introduction of asymmetry.<sup>56</sup> Conversion improved at room temperature with the addition of co-catalytic boric acid to assist in C-O bond labialization by coordination to the carbonyl oxygen..

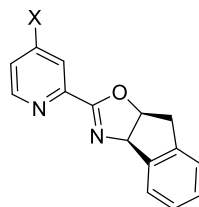
The reaction lacked significant diastereoselectivity, displaying only moderate selectivity for *anti*-**114** isomer by 1.7 to 1. However, the preference for the formation of the *anti*-diastereomer warranted continuing investigation into the process, as this stereoisomer is the opposite that obtained from thermal-Claisen reactions. Hence the reaction motif offers a compliment ICR chemistry which ultimately produces the *syn* diastereomer from the formal Claisen rearrangement mechanism.

### 2.5.3 Effects of Lewis Acid and Ligand Modification

Modifications to the ligand and Lewis acid were performed to increase selectivity. The indanol ligand **126** and pyridine oxazolines **66** and **127** were screened because of the success bipyrdine-type ligands, possibility for asymmetric induction, and ease of synthetic access (Figure 12). For Lewis acids, results demonstrated that B(OPh)<sub>3</sub> is superior to B(OMe)<sub>3</sub> in promoting conversion of the allyl vinyl carbonates as demonstrated by an increase from 61% to 100% conversion. For the ligands, the more electron-rich 4-dimethylaminopyridinyl oxazoline **127** provided the best regio- and diastereoselectivities while retaining respectable enantioselectivity (Table 1). The success of 4-amino substitutions in ligands in increasing the selectivity of metal-catalyzed reactions is documented in several studies which observed that increasing electron density on the metal boosts reactivity by accelerating oxidative addition and promoting enhanced branched to linear ratios.<sup>51, 57</sup> Therefore, increasing the speed of oxidative addition correlates to better selectivity.



126

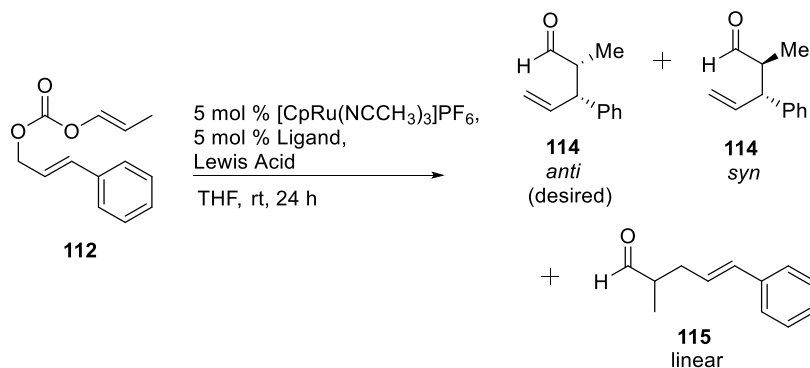


66: X = H  
127: X = NMe<sub>2</sub>

Figure 12: Ruthenium Model Ligands

Table 1: Ligand and Lewis Acid Optimization of Ruthenium(II)-Catalyzed Carbonate

### Rearrangements



Entry	ligand	Lewis acid	acid loading	114:115 <sup>a</sup>	anti:syn (114) <sup>a</sup>	conversion <sup>a</sup>	Comments
1	<b>126</b>	B(OPh) <sub>3</sub>	5 mol %	2.0: 1	1.4: 1	100 %	
2	<b>126</b>	B(OMe) <sub>3</sub>	5 mol %	3.6: 1	1.4 :1	67 %	
3	<b>126</b>	B(OMe) <sub>3</sub>	10 mol %	2.5: 1	1.3: 1	77 %	
4	<b>66</b>	B(OMe) <sub>3</sub>	5 mol %	5.4:1	1.7: 1	100 %	
5	<b>66</b>	B(OPh) <sub>3</sub>	5 mol %	11.6: 1	1.9: 1	100 %	
6	<b>127</b>	B(OMe) <sub>3</sub>	5 mol %	1.3:1	2.9: 1	30 %	
7	<b>127</b>	B(OPh) <sub>3</sub>	5 mol %	15.1 : 1	2.7: 1	100 %	81 % ee

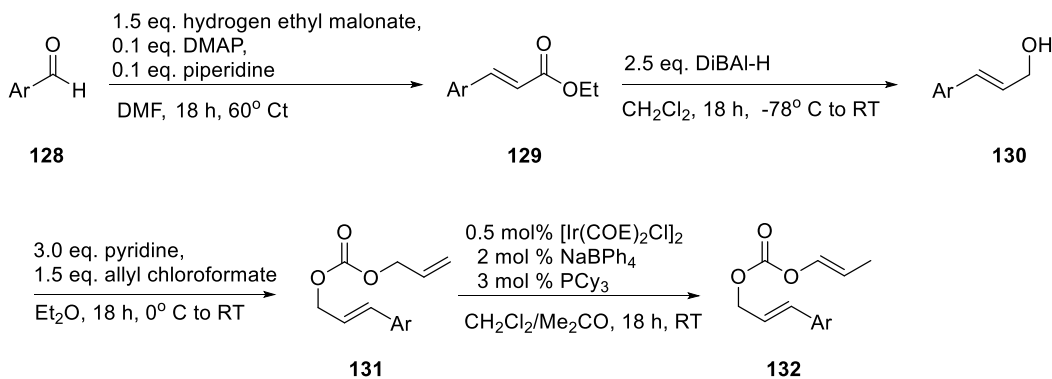
<sup>a</sup> Determined by <sup>1</sup>H-NMR of the crude product mixture.

### 2.5.4 Substrate Scope of Ruthenium(II) Catalyzed Carbonate Rearrangements

The improved conditions for the rearrangement of carbonates were applied to several synthetically-accessible carbonates featuring different aryl substituents to assess the effects of various substitution patterns affecting the electronic and steric parameters of the substrates (Scheme 4). The examined substrates are easily accessible from commercial available aryl aldehydes **128** by a convenient Aldol-type addition of hydrogen ethyl malonate to generate *E*-cinnamyl esters **129**.<sup>74</sup> Reduction with DiBAL-H gives cinnamyl alcohols **130** which is converted to di(allyl) carbonates **131** by treatment with allyl chloroformate under basic conditions (64 – 91% yield). Finally, treatment with the iridium

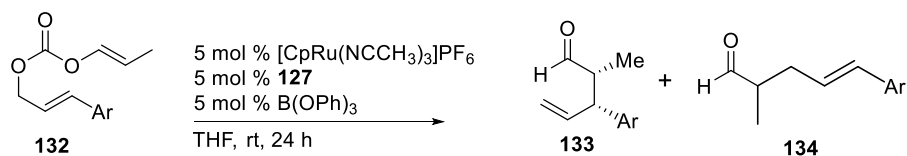
isomerization conditions gives the allyl vinyl carbonate **132** however in low yields (20 – 78%) where the unsubstituted phenyl substrate as the best case.

#### Scheme 4: Synthesis of Substituted Allyl Vinyl Carbonates



The cinnamyl substrates were subjected to ruthenium(II) rearrangement conditions to address the effects of substituents. In general, regiochemistry was excellent, rarely dropping below 10:1 (b:l) (Table 2). Enantioselectivity remained modest; however, further ligand modifications could improve the enantioselectivity by increasing the steric bulk of the chiral portions of the ligand. Diastereoselectivity remained poor with the *anti*-diastereomer being favored by *ca.* 2:1 over the *syn*-diastereomer produced in thermal [3,3]-Claisen rearrangements. Substitution at the *ortho*-position of the aryl group almost completely erodes diastereoselectivity (Table 2, Entry b). The absolute, R,R stereochemistry at the C<sup>2</sup> and C<sup>3</sup> produced by the transformation is identical to that of the aldehydes produced in concurrent studies of our ruthenium-catalyzed allyl vinyl ether rearrangements (*vide infra*).<sup>75-76</sup> In general, the methodology tolerates most functional groups, but strongly electron-withdrawing cinnamyl varieties display poor conversions.

**Table 2: Effects of Aryl Substituents on Reaction Dynamics**



Entry	Aryl	% yield <sup>a</sup>	<b>133:134</b> <sup>b</sup>	<i>anti:syn</i> ( <b>133</b> ) <sup>b</sup>	ee (%) <sup>c</sup>
a	Ph	79	14: 1	2.3: 1	82
b	<i>o</i> -OMePh	94	12.3: 1	1.1: 1	98
c	<i>m</i> -OMePh	100	17.3: 1	2,1: 1	71
d	<i>p</i> -OMePh	74	47.8: 1	2.4: 1	79
e	<i>m</i> -ClPh	42	9.1: 1	2.7: 1	89
f	<i>p</i> -BrPh	77	16.0: 1	3.0: 1	90
g	1-naphtyl	94	33.4: 1	1.8: 1	76

<sup>a</sup> Isolated yield after flash chromatography, <sup>b</sup> Determined by <sup>1</sup>H-NMR of the crude product mixture, <sup>c</sup> Determined by Chiral GC.

### 2.5.6 Summary of Ruthenium Catalyzed Rearrangement of Allyl Vinyl Carbonates

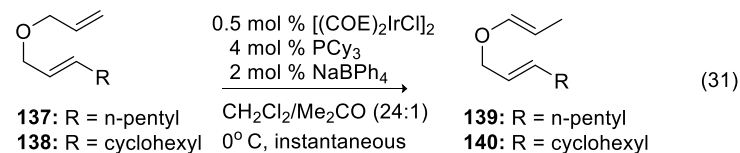
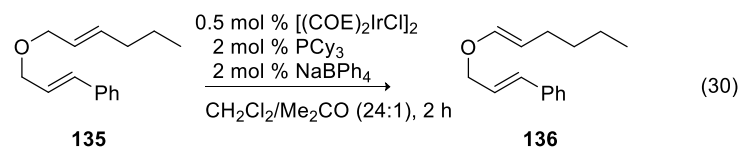
In conclusion, we developed methodology in the catalysis in the rearrangement of allyl vinyl carbonates to pentenal products. The reaction proceeds with excellent selectivity for the [3.3] product, and displays good enantioselectivity. However, the transformation exhibits limited preference for the *anti*-diastereomer which limits the usefulness of the process. Further investigation into improving the diastereoselectivity would normally follow. Yet, the substrate scope is restricted to cinnamyl and methyl substituents due to limited effectiveness of iridium-isomerization conditions on substituted di(allyl) carbonates further limiting the synthetic utility. A similar substrate motif may provide a wider range of substrate scope and better selectivities which may provide a more efficient route to produce the *anti*-diastereomer. Thus, we turned our attention to allyl vinyl ethers which we found to be easier to access however were less reactive overall.

## 2.6 RUTHENIUM-CATALYZED REARRANGEMENT OF ALLYL VINYL ETHERS

### 2.6.1 Advantages of Allyl Vinyl Ethers: Broader Substrate Scope

The disadvantages and limited scope of the ruthenium-catalyzed rearrangement of carbonates necessitated the development of an alternative methodology which overcomes the mediocre diastereoselectivity and limited substrate scope. Substrates were restricted to the use of unsubstituted allyl carbonates. Allyl vinyl ethers possess the same general structure as allyl vinyl carbonates and would follow the same pattern following oxidative addition albeit without the loss of CO<sub>2</sub>. To our advantage, iridium isomerization also works with a wider range of allyl vinyl ether substrates than di(allyl) carbonates. Substituted allyl cinnamyl substrates, such as 2-hexenyl cinnamyl ether **135** are selectively isomerized with excellent *E*-selectivity by simple reduction in phosphine loading and therefore increasing the proportion of iridium complexes with a free binding site increasing the catalyst activity (Eq 30). The aliphatic allyl vinyl ethers synthesis complements this approach. Increasing the phosphine loading and reducing the temperature and reaction time provides geometrically pure *n*-pentyl or cyclohexyl allyl vinyl ethers **139** and **140** from **137** and **138** albeit in low yields. The reaction must be quenched quickly to prevent the formation of di(vinyl) product. Unreacted starting material is also recovered (Eq 31). The availability of such reagents would allow for a greater variety of rearranged products not accessible from Ru-catalyzed carbonate rearrangements.

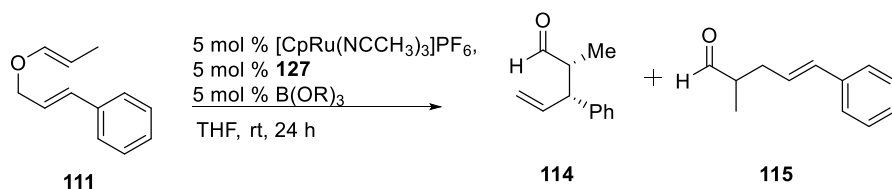




## 2.6.2 First Reactions of Allyl Vinyl Ether **111**: Lewis Acid Activation

Initial experiments to facilitate rearrangement of our standard substrate vinyl cinnamyl ether **111** and the pyridine-oxazoline ligand **127**, which was proven promising in the carbonate rearrangements, produced poor results with the ether rearrangements. The ethers limited reactivity toward oxidative insertion demonstrated that the C-O bond stronger than anticipated and not easily cleaved by the ruthenium. Therefore, several Lewis acids were introduced to bind to the ether oxygen and weaken the allyl C-O bond as seen with the carbonate reaction. A model reaction of the rearrangement of **111** was screened with several Lewis acids (Table 3). The relatively soft  $\text{ZnCl}_2$ ,  $\text{CuCl}$ ,  $\text{NiCl}_2$ , and  $\text{Ti}(\text{O}^i\text{Pr})_4$  acids saw no conversion. Stronger Lewis acids such as  $\text{Cu}(\text{OTf})_2$ ,  $\text{Sn}(\text{OTf})_2$ ,  $\text{AgPF}_6$ , and  $\text{Al}(\text{OTf})_3$  proved too reactive and gave mixtures of branched **114** and linear **115** in addition to unidentifiable side products. However, the tris(alkoxy) borates used for the carbonate reactions were effective in promoting the rearrangement while maintaining selectivity. Simple  $\text{B}(\text{OMe})_3$  provided a measurable conversion at only 5% yield. More acidic borates increase conversion rates to 63% in the model reaction. The attenuated reactivity with ethers is likely due to the greater difficulty oxidatively inserting into the C-O allyl ether bond. Additional experimentation was necessary to improve the reaction, to achieve benchmark results obtained using allyl vinyl carbonates

**Table 3: Lewis Acid Screening for the Rearrangement of Allyl Vinyl Ethers**



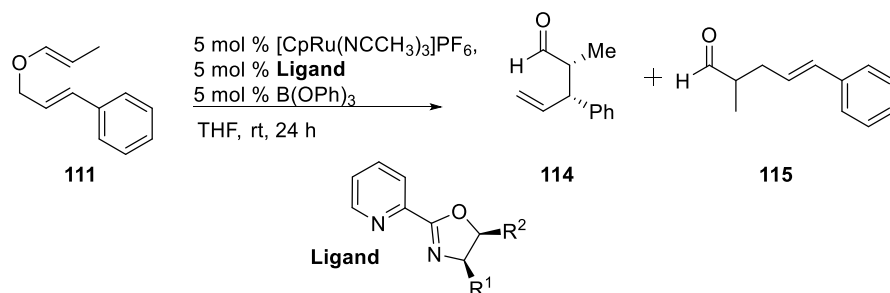
Lewis acid	conversion (%) <sup>a</sup>	<b>114:115</b> <sup>126</sup>	<i>anti:syn</i> ( <b>114</b> ) <sup>a</sup>	ee (%) <sup>c</sup>
B(OMe) <sub>3</sub>	5	N.D.	-	-
B(OCH <sub>2</sub> CF <sub>3</sub> ) <sub>3</sub>	10	N.D.	-	-
B(OPh) <sub>3</sub>	63	5: 1	2: 1	81

<sup>a</sup> Determined by <sup>1</sup>H-NMR of the crude product mixture <sup>b</sup> N.D. = not determined <sup>c</sup> Determined by Chiral GC.

### 2.6.3 Ligand Modifications

We subsequently modified the pyridine oxazoline ligand structure to increase conversion and selectivity. Modifying the electron-density is thought to influence activity and selectivity while modification of the oxazoline backbone provided information about the effect of ligand sterics on selectivity (Table 4). Overall there is little variation in regio- and diastereoselectivity. Increasing the steric bulk of the side groups slows reactivity and reduces enantioselectivity. The phenyl **141** displays an improvement to 78% conversion, but has worse enantioselectivity (53% ee). Benzyl **142** improves regioselectivity to 7:1 (b:l), but exhibits worse conversion and overall stereoselectivity. Iso-propyl **143** exhibits no benefit, and substitution with *tert*-butyl **144** completely inhibits reactivity. Now, the indanol-derived **66** provided the optimal balance and greatest enantioselectivity.

**Table 4: Effects of Modification of the Ligand Oxazoline**

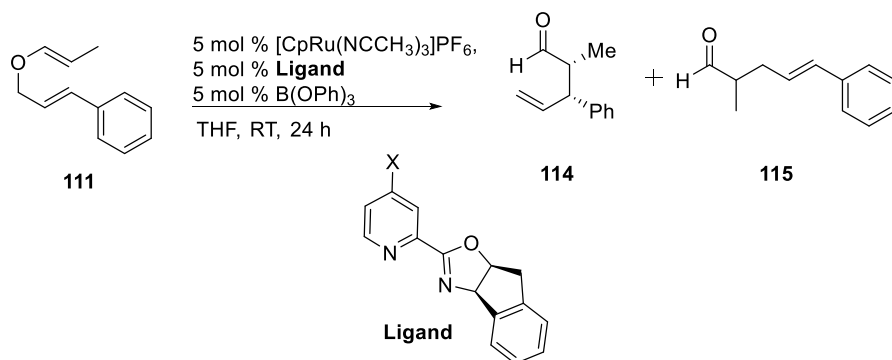


Entry	$\text{R}^1$	$\text{R}^2$	conversion(%) <sup>a</sup>	<b>114:115</b> <sup>a</sup>	<i>anti:syn</i> ( <b>114</b> ) <sup>a</sup>	ee (%) <sup>b</sup>
1	indanyl ( <b>66</b> )		63	5: 1	2: 1	81
2	Ph ( <b>141</b> )	H	78	4.5: 1	2: 1	53
3	Bn ( <b>142</b> )	H	40	7: 1	1.7: 1	72
3	<sup>i</sup> Pr ( <b>143</b> )	H	62	5: 1	1.6: 1	71
3	<sup>t</sup> Bu ( <b>144</b> )	H	0	-	-	-

<sup>a</sup> Determined by <sup>1</sup>H-NMR of the crude product mixture <sup>b</sup> Determined by Chiral GC.

We now endeavored to explore how ligand modification would affect the parameters of the reaction. The electron-density on the ruthenium center has been demonstrated to affect the activity and regioselectivity of ruthenium allylic alkylation chemistry.<sup>59-60,77</sup> The indanyl pyridine-oxazoline was modified at the 4-pyridyl position to increase the basicity of  $\text{N}_{\text{pyridine}}$ . The ligands were tested using the current optimal conditions (5 mol %  $\text{CpRu}(\text{CH}_3\text{CN})_3]\text{PF}_6$ , 5 mol %  $\text{B}(\text{OPh})_3$ , THF, RT, 24 h) in the rearrangement of **111** (Table 5). Compared to unsubstituted **66**, each ligand provided inferior conversion and diastereoselectivity. Nonetheless, the regioselectivity improved as electron-density increased. The dimethylamino **127** gives 12:1 **114:116** with moderate conversion (44%) and diastereoselectivity (1.6:1 *anti:syn*). Clearly, increasing the  $\text{N}_{\text{pyridine}}$  Lewis basicity translates to increased preference for the branched isomer **114**.

**Table 5: Effects of Modification of Ligand Pyridine**



Entry	X	conversion(%) <sup>a</sup>	114:115 <sup>a</sup>	syn:anti (114) <sup>a</sup>
1	Me ( <b>145</b> )	12.9	6.5: 1	2.25: 1
2	OMe ( <b>146</b> )	29	9: 1	2: 1
3	NMe <sub>2</sub> ( <b>127</b> )	44	12: 1	1.6: 1

<sup>a</sup> Determined by <sup>1</sup>H-NMR of the crude product mixture .

## 2.7 MECHANISTIC INVESTIGATION OF RUTHENIUM(II) CATALYZED REARRANGEMENT OF ALLYL VINYL ETHERS

### 2.7.1 Outer or Inner-Sphere Mechanism: Origin of Selectivity

At this juncture, the ligands were found to modify conversion, regio- and enantioselectivity of the rearrangement. Yet, the diastereoselectivity of the reaction, while varying slightly, remained low rarely exceeding 2:1 *anti:syn* indicating the metal coordination sphere was not substantially influencing the nucleophilic addition of the enolate to the allyl fragment. A possible explanation would that the enolate was dissociating before adding to the allyl complex; therefore, it was necessary to investigate the addition of the enolate. The addition could be taking place in an outer sphere or inner sphere type process (Figure 13). In an outer sphere pathway, the enolate dissociates from the metal (Figure 13a). However, in an inner sphere mechanism, the enolate remains bond the metal (Figure 13b). The outer sphere, dissociative pathway could explain the lack of diastereomeric control observed in the

rearrangement since the enolate would not be held as close to the metal and therefore not as affected by the ligand allowing the approaching enolate greater degrees of freedom for the nucleophilic attack. If the enolate were held as a ligand it would experience greater impact from the steric crowding of the other ligands.

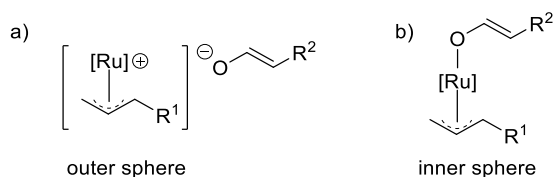


**Figure 13: Outer and Inner Sphere Pathways**

### 2.7.2 Cross-over Experiment

The nature of the mechanism was evaluated with a cross-over experiment. The two ether substrates, **147** and **148**, were subjected to standard test conditions (5 mol %  $[\text{CpRu}(\text{NCCH}_3)_3]\text{PF}_6$ , 5 mol % **66**, 5 mol %  $\text{B}(\text{OPh})_3$ ) of the ruthenium(II)-catalyzed rearrangement of allyl vinyl ethers (Figure 14). In an intramolecular reaction, only **149** and **150** would be produced, as the enolate would only combine with the allyl moiety from which it was liberated. In the intermolecular reaction counterpart, the enolate dissociates from the metal center, and a mixture of all four products would be expected. From this analysis, the crossover experiment indicates an intermolecular, outer-sphere process is in action as equimolar amounts of **149**, **150**, **151**, and **152** was obtained.

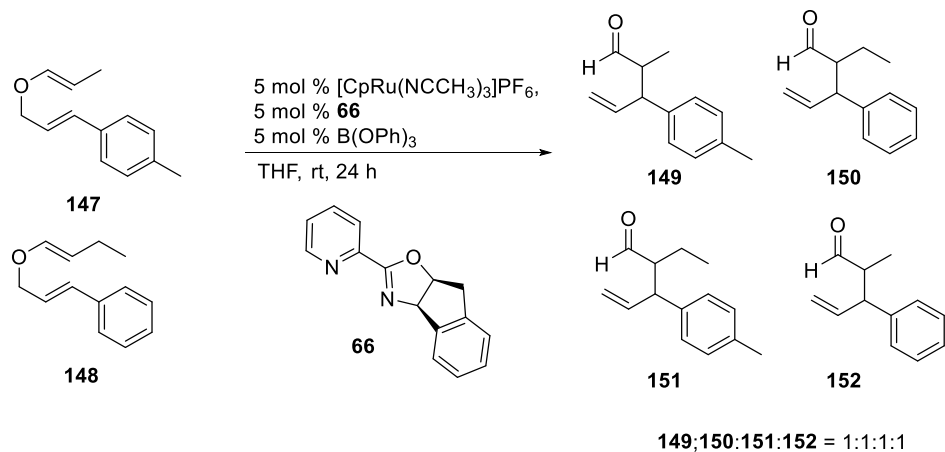


**Figure 14: Oxazoline Cross-Over Experiment**

### 2.7.3 Possible Intramolecular Mechanism

The results of the cross-over experiment suggested that an intermolecular process was occurring. We speculated that shifting the mechanism to an intermolecular process could improve diastereoselectivity. Evidence in recent publications suggest that intramolecular hydrogen bonding takes place in the ruthenium(II)-catalyzed transesterification of allyl ethers.<sup>78</sup> The study uses quinaldic acid as a ligand, which forms hydrogen-bonding interactions with the approaching allyl ether, and allows for an intramolecular process to take place (Figure 15a). It would be advantageous to the ruthenium-catalyzed rearrangement of allyl vinyl ethers if we utilize a similar technique. If our ligand coordinated to the incoming enolate then the enolate would be restricted in how it would approach the allyl complex hopefully resulting in an increase in diastereoselectivity. Furthermore, a carboxylate moiety will provide utility in catalysis as it can be modified to incorporate asymmetric pendent groups to induce chirality during the carbon-bond forming step. We could make a model ligand by hydrolysis of pyridine oxazoline ligand such as **66** yields to yield quinaldic acid analogue capable of hydrogen bonding in similar manner (Figure 15b).

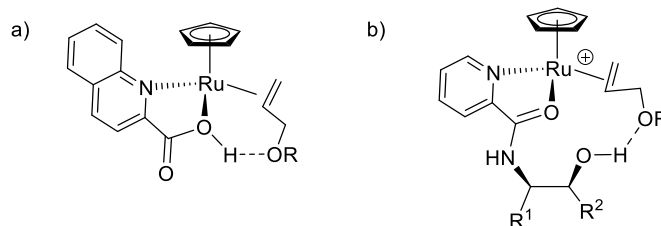


**Figure 15: Hydrogen-bonding in Ruthenium Catalysis**

#### 2.7.4 Application of Pyridine-Amide Ligands

The pyridine amide ligands are accessible from hitherto employed oxazoline ligands and allow for the same degree of customization. The condensation of 4-chloropicolinonitrile **153** and aminoalcohol **154** in the presence of zinc(II) chloride yields oxazoline **155**. Treating 4-chloro **155** with aqueous dimethylamine affects both the aromatic substitution and hydrolysis to supply amide ligand **126** (Scheme 5). Initially, several 4-dimethylamino ligands were examined. Electron-rich ligands increase the distortion of ruthenium pi-allyl systems increasing reaction regioselectivity (Table 6). Utilizing a 4-dimethylamino pyridine increases donation from the nitrogen to the ruthenium center. We were pleased to find a remarkable increase in diastereoselectivity in all cases from *ca.* 2:1 for oxazoline ligands to 10:1 *anti:syn* (**114**). Increasing ligand sterics correlated to increases in both diastereo- and enantioselectivity. The largest group, isopropyl-substituted **156**, increased selectivity for branched **124** the greatest yet the system began to experience degradation of stereochemistry. As witnessed with oxazoline ligands, indanyl-substituted **126** provided the optimal results (Table 6, Entry 1). Despite increased stereoselectivity, regioselectivity and was worse than the values achieved with oxazoline ligands. The amide substituent of the ligand would be held away from of the metal center and hold less influence on the orientation of the bonding of the allyl fragment causing a decrease in regioselectivity.

## Scheme 5: Synthesis of Amide Ligands

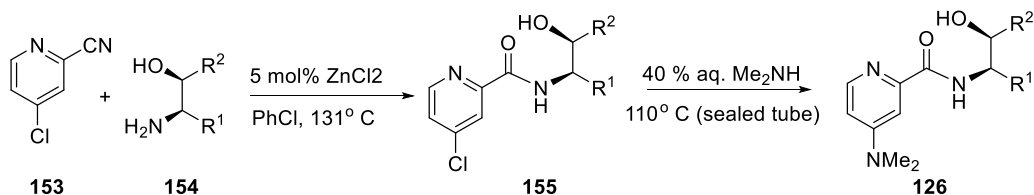
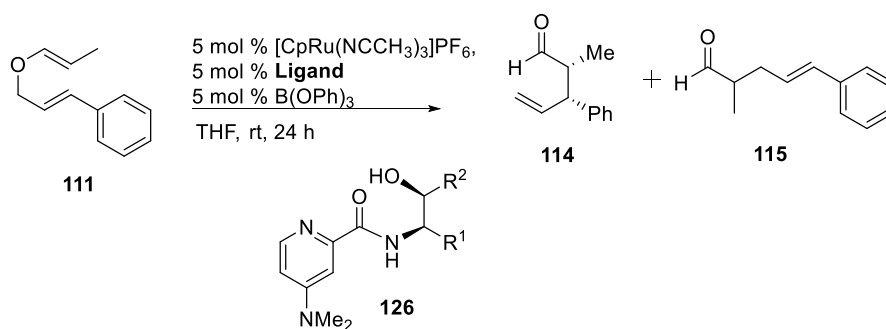


Table 6: Optimization of Amide Ligand Sterics



Entry	R <sup>1</sup>	R <sup>2</sup>	conversion(%) <sup>a</sup>	114:115 <sup>a</sup>	<i>anti:syn</i> (114) <sup>a</sup>	ee (%) <sup>b</sup>
1	indanyl ( <b>130</b> )	H	63	4:1	10:1	89
2	<sup>i</sup> Pr ( <b>156</b> )	H	42	6.7:1	6.7:1	76
3	Ph ( <b>157</b> )	H	39	3.2:1	5:1	55
3	Bn ( <b>158</b> )	H	42	4:1	3:1	22

<sup>a</sup> Determined by <sup>1</sup>H-NMR of the crude product mixture <sup>b</sup> Determined by Chiral GC.

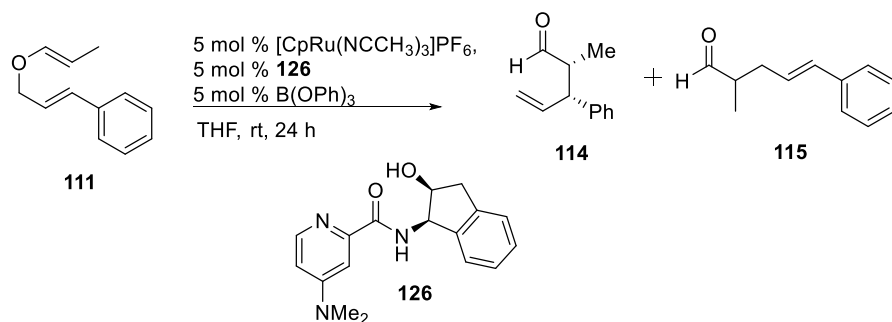
### 2.7.5 Optimization of Reaction Conditions

Pyridine amide ligands demonstrated a high degree of stereocontrol, however, the lack of conversion remained a major issue. Water deactivation of the ruthenium complex offers one possible explanation as the ligand may contain trace water due to the hydrogen bonding ability. The addition of 100% w/w 4Å molecular sieves to optimal conditions (5 mol % [CpRu(NCCH<sub>3</sub>)<sub>3</sub>]PF<sub>6</sub>, 5 mol % **66**, 5 mol % B(OPh)<sub>3</sub>, THF, RT, 24 h) produced a remarkable improvement to 93% conversion (Table 7, Entry 1). Interestingly, the additive increased regio- and diastereoselectivity to 16:1 *anti:syn*(**114**) and 4.6:1 (b:l)



(from 10:1 *anti:syn*(**114**), 4:1 b:l). Given the increase in effectiveness, the molecular sieves may perform an additional function besides water exclusion.

**Table 7: Effects of Additives on the Allyl Vinyl Ether Rearrangements**



Entry	Additive	Effect
1	4Å MS	93% conversion
2	1 equiv. <b>114</b>	34% conversion
3	20 mol% DMF/ 4Å MS	76% conversion
4	20 mol% acetone/ 4Å MS	82% conversion
5	20 mol% $\text{CH}_3\text{CN}$ / 4Å MS	100% conversion, <i>anti:syn</i> ( <b>114</b> ) = 20:1

We postulated that product inhibition was responsible for the lack of completion conversion by the basic aldehyde group of the pentenal products (Figure 16). Adding 100 mol % of pentenal product **114** to a fresh reaction resulted in decreased conversion (Table 7, Entry 2). Therefore, the product did not dissociate from the catalyst at a fast enough rate resulting in catalyst decomposition before being able to reenter the catalytic cycle. Thus, the catalyst experienced a low turnover number. We reasoned that a polar, coordinating co-solvent would help by displacing the product from the metal and allow fresh allyl vinyl ether substrate to react. Under standard reaction conditions (5 mol %  $\text{CpRu}(\text{CH}_3\text{CN})_3]\text{PF}_6$ , 5 mol %  $\text{B}(\text{OPh})_3$ , THF, RT, 24 h) and with 4Å molecular sieves, three common solvents were employed at 20 mol % loading. Unfortunately, carbonyl bearing acetone and dimethylformamide (DMF) reduced conversion, acting as inhibitors themselves (Table 7, Entries 3,

4). However, acetonitrile struck a balance and such could produce the pentenal **126** in 100 % conversion (Table 7, Entry 5).

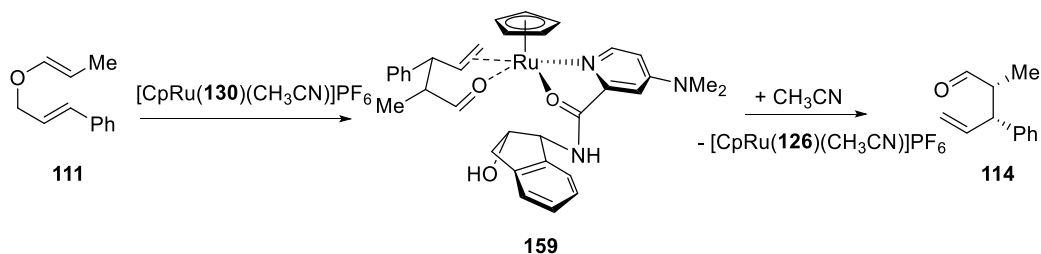
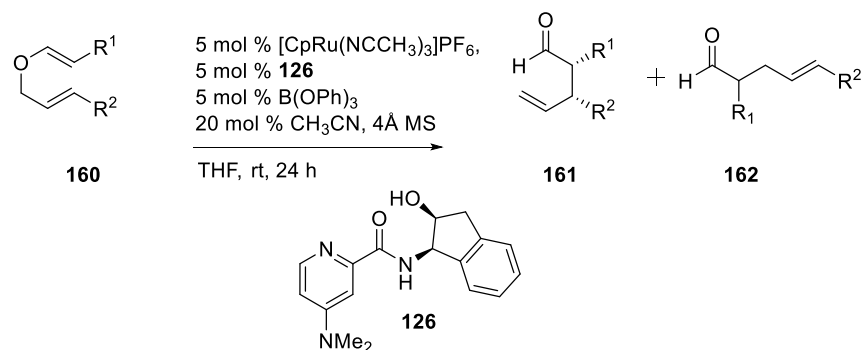


**Figure 16: Product Inhibition by Pentenal Product**

### 2.7.6 Exploration of Substrate Scope

The reaction's substrate scope was evaluated. Many C<sup>1</sup>-alkyl C<sup>6</sup>-aryl allyl vinyl ethers **160** were prepared and examined using the optimal conditions (Table 8). Conversion, yields and enantioselectivity in all instances were excellent. Diastereoselectivity for *anti*-**161** was superb, exceeding 10:1 *anti:syn*(**161**) in all instances except in one case (Table 8, Entry b). Regiochemistry correlates to ligand electronics. Substrates bearing electron-donating groups, especially on the 4-position of the phenyl ring, demonstrated the greatest degree of regioselectivity (**161:162**) for the branched product **161** (Table 8, Entries c, d, f, g). Conversely, electron-withdrawing groups erode selectivity (Table 8, Entries e, h). A 2-substituted aromatic group also diminished regioselectivity through steric interactions. Increasing electron-density on the allyl group decreased the magnitude of back-bonding from the ruthenium metal. The weaker the back-bonding, the longer the Ru-C<sup>3</sup> bond is, further promoting the difference in regiochemistry.

**Table 8: Substrate Scope of Ruthenium-Catalyzed Rearrangement of Allyl Vinyl Ethers**



Entry	R <sup>1</sup>	R <sup>2</sup>	conversion(%) <sup>a</sup>	<b>161</b> : <b>162</b> <sup>a</sup>	<i>anti:syn</i> ( <b>161</b> ) <sup>a</sup>	ee(%) <sup>b</sup>	yield <sup>c</sup>
a	Me	Ph	100	5.3:1	20:1	93	91
b	Et	Ph	100	3.6:1	6.3:1	99	89
c	Me	<sup>p</sup> C <sub>4</sub> H <sub>4</sub> CH <sub>3</sub>	98	7.6:1	17:1	92	90
d	Me	<sup>p</sup> C <sub>4</sub> H <sub>4</sub> OCH <sub>3</sub>	95	14:1	18:1	91	86
e	Me	<sup>p</sup> C <sub>4</sub> H <sub>4</sub> Br	97	4.7:1	25:1	92	92
f	Me	<sup>o</sup> C <sub>4</sub> H <sub>4</sub> OCH <sub>3</sub>	95	4.4:1	11.1:1	78	89
g	Me	<sup>m</sup> C <sub>4</sub> H <sub>4</sub> OCH <sub>3</sub>	93	6.5:1	25:1	93	80
h	Me	<sup>m</sup> C <sub>4</sub> H <sub>4</sub> Cl	100	4.6:1	16.6:1	96	78
i	Me	2-furyl	98	10:1	20:1	96	63
j	Me	1-naphthyl	97	3:1	10:1	96	90
k	Me	2-naphthyl	100	7:1	16:1	84	94

<sup>a</sup> Determined by <sup>1</sup>H-NMR of the crude product mixture <sup>b</sup> Determined by Chiral GC <sup>c</sup> Isolated yield after flash chromatography <sup>d</sup> Reaction time was 48 h

### 2.7.7 Effects of Substrate Olefin Geometry

Until this point, the allyl vinyl ethers' olefin geometries were solely *E,E* allyl vinyl ethers. The effect of olefin geometry was examined by the exposure of *Z*-vinyl ether **163** and *Z*-allyl **164** to standard reaction conditions (5 mol % CpRu(CH<sub>3</sub>CN)<sub>3</sub>]PF<sub>6</sub>, B(OPh)<sub>3</sub> and **126**, 20 mol % CH<sub>3</sub>CN, 4 Å MS, THF, RT, 24 h) ( Figure 17). Rationally, inversion of either olefin leads to the preference of the alternative

*syn*-diastereomer, mirroring the product obtained from a thermal Claisen of *E,E* ethers. Enantioselectivity is high (93% ee), but diastereo- and regioselectivity are considerably diminished versus the *E,E* isomers.

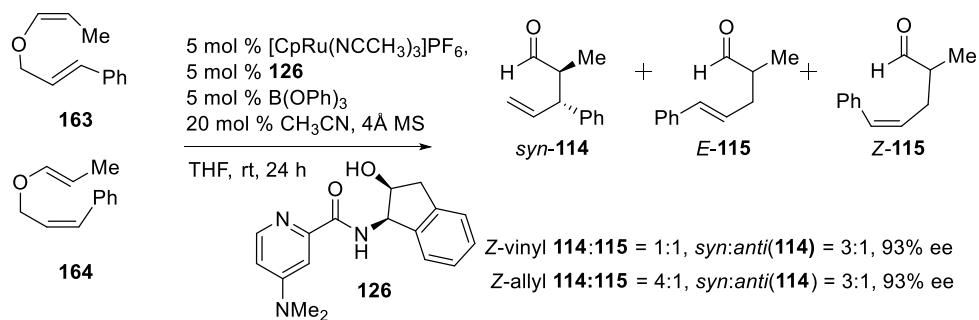
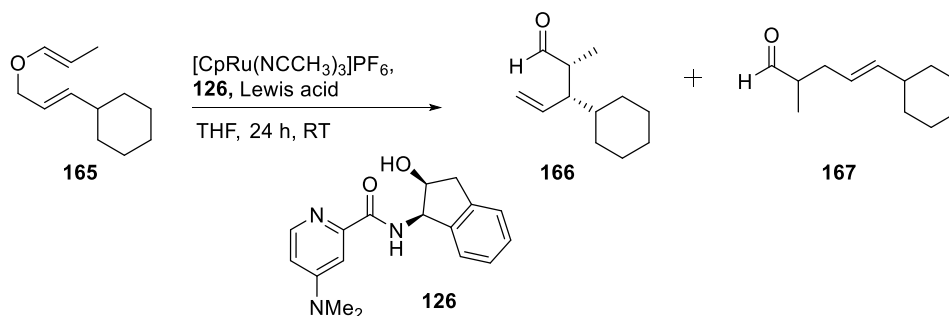


**Figure 17: Olefin Geometry Experiment**

### 2.7.8 Effects of Substrate Aromaticity

The effects of substrate aromaticity on the yield and selectivity of the ruthenium-catalyzed rearrangement of allyl vinyl ethers was examined (Table 9). Subjecting cyclohexyl variant **171** to standard reaction (5 mol % CpRu(CH<sub>3</sub>CN)<sub>3</sub>]PF<sub>6</sub>, THF, RT, 24 h) conditions unexpectedly gave no reaction. Increasing the catalyst loading to 10 mol % and using a stronger borate (B(OP<sup>i</sup>C<sub>6</sub>H<sub>4</sub>F)<sub>3</sub>) caused the substrate to react albeit with lackluster results. The yield was poor (44%) and the reaction was selective only for the linear regioisomer. The preference for the linear product supports studies indicating lack of asymmetry in aliphatic ruthenium(II)-allyl complexes mentioned previously.<sup>59-60</sup>

**Table 9: Aliphatic Allyl Vinyl Rearrangement**



Entry	Conditions	Results
1	5 mol% CpRu and <b>126</b> 5 mol% $\text{B}(\text{OPh})_3$ 24 h	No Reaction
2	10 mol% CpRu and <b>126</b> 10 mol% $\text{B}(\text{O}^i\text{C}_4\text{H}_4\text{F})_3$ 48 h	Only <b>167</b> observed 44% yield (22% ee)

### 2.7.9 Importance of Free Hydroxyl Group on the Ligand

We then investigated the dramatic improvement in results attributed to the amide ligand. The increase in diastereoselectivity results from hydrogen bonding between the enolate and the alcohol establishing an intramolecular mechanism. To study this phenomenon, the previous crossover experiment was reproduced (Figure 18). In this case, the optimal amide ligand was compared to methoxy-capped **168**. We sought to define to what extent the hydrogen bonding influenced reaction selectivity. Methoxy **168** ligand produced results like oxazoline **66**, resulting in a mixture of **149**, **150**, **151** and **152**. However, ligand **126** produced just **149** and **150** indicating that the hydroxyl group is critical in ensuring an intramolecular process.

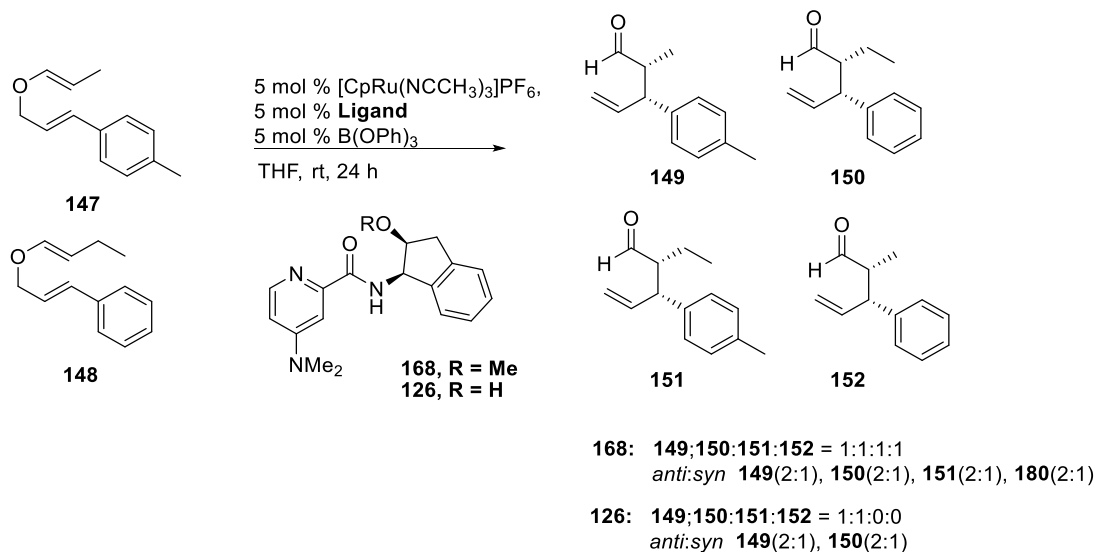


**Figure 18: Indanol Ligand Cross-Over Experiment**

Clearly, previous results indicate the indanol hydroxyl functionality serves an important function in the reaction mechanism. One hypothesis is the ligand alcohol on the ruthenium complex **169** initially forms boroester **170** with the triphenylborate. Molecular sieves are known to catalyze transesterifications as they greatly accelerate the *in situ* formation of a tetrakis(alkoxy)titanium(IV) complexes from alcohols and titanium(IV) chloride.<sup>79</sup> Then the borate of **170** can serve as a Lewis acid activator of the allyl vinyl ether and subsequent directing group for delivery of the resulting boroenolate.

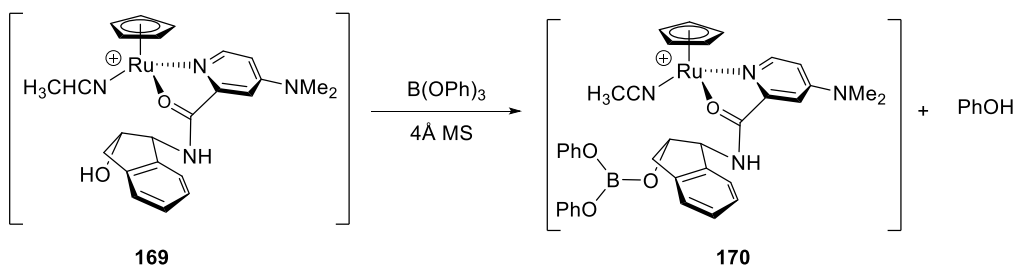


**Figure 19: Borylation of Indanol Ligand**

### 2.7.10 Solid State Analysis

A crystal structure of the active catalyst would substantiate many of our claims. Unfortunately, we were unable to obtain a crystal structure of the active catalyst  $[\text{CpRu}(\mathbf{126})(\text{NCCH}_3)][\text{PF}_6]$ . However, attempts to crystallize ruthenium(II)-complexes in the glovebox failed to produce an adequate structure. However, we obtained solid state data of a more robust, analogous pentamethylcyclopentadienyl ( $\text{Cp}^*$ ) iridium(III)-complex. We also attempted to create a  $\text{CpIr(III)}$  version however the substances lacked sufficient crystallinity. Treating  $[\text{Cp}^*\text{IrCl}_2]_2$  with  $\mathbf{126}$  and  $\text{NH}_4\text{PF}_6$  in methanol provides the piano tool complex  $[\text{Cp}^*\text{Ir}(\mathbf{126})\text{Cl}]\text{PF}_6$ . X-ray diffraction data indicates the solid crystallizes as two diastereomers  $\mathbf{171}$  and  $\mathbf{172}$  (Figure 20). The indanol ligand bonds to the ruthenium center through  $\text{N}_{\text{pyridine}}$  and carbonyl oxygen as anticipated. The presence of diastereomers shows that there is little energetic difference between the two binding modes. Secondly, only one isomer,  $\mathbf{172}$  has the indanol hydroxyl group oriented in such a manner to deliver the bound enolate to a Ru-allyl fragment.

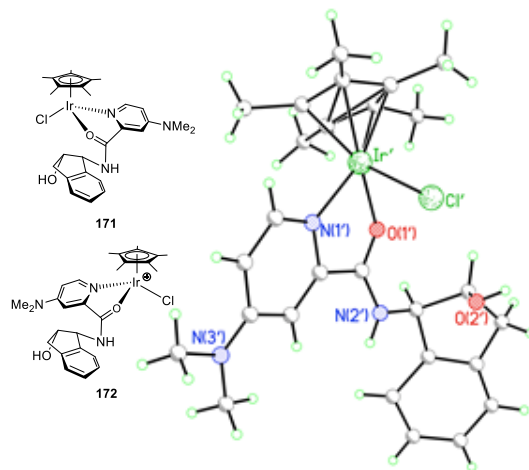


Figure 20: Crystal Structure of  $[\text{Cp}^*\text{Ir}(\mathbf{126})\text{Cl}]\text{PF}_6$

## 2.8 PROPOSED MECHANISM OF RUTHENIUM(II) CATALYZED REARRANGEMENT OF ALLYL VINYL ETHERS

The data collected thus far allowed us to construct a reasonable reaction mechanism for the ruthenium(II)-catalyzed rearrangement of allyl vinyl ethers. We propose the active catalyst forms *in situ* by mixing **126** and  $[\text{CpRu}(\text{NCCH}_3)_3]\text{PF}_6$  in THF forming the diastereomers **173** and **174** which interconvert *via* solvent action (Figure 21). The catalytic cycle begins with borylation of the indanol hydroxyl group forming active catalyst **175** (Figure 22). Interaction with substrate **163** results in formation of ruthenium-olefin complex **176**. Lewis acid activation of the vinyl ether facilitates oxidative addition to occur yielding  $\pi$ -allyl complex *endo*-**177**. The *exo*-isomer is disfavored due to steric interaction of the allyl C<sup>2</sup>-H bond and the Cp ring. The enolate conveniently bonds to the ligand as the borate ester. Only the illustrated diastereomer **174** can deliver the enolate to the C<sup>3</sup> of the allyl group and result in complex **178** which giving *anti*-**164** pentenal product. Liberation of **164** with  $\text{CH}_3\text{CN}$  regenerates the active catalyst complex **175**.

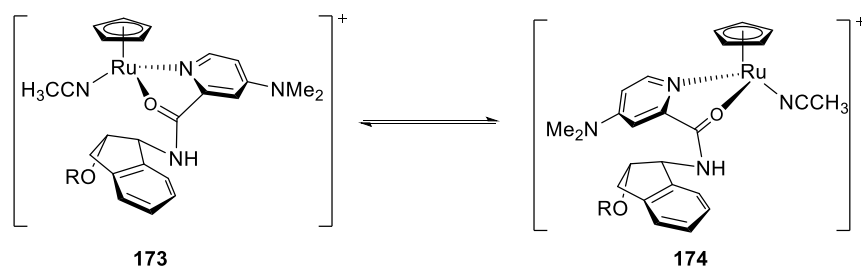
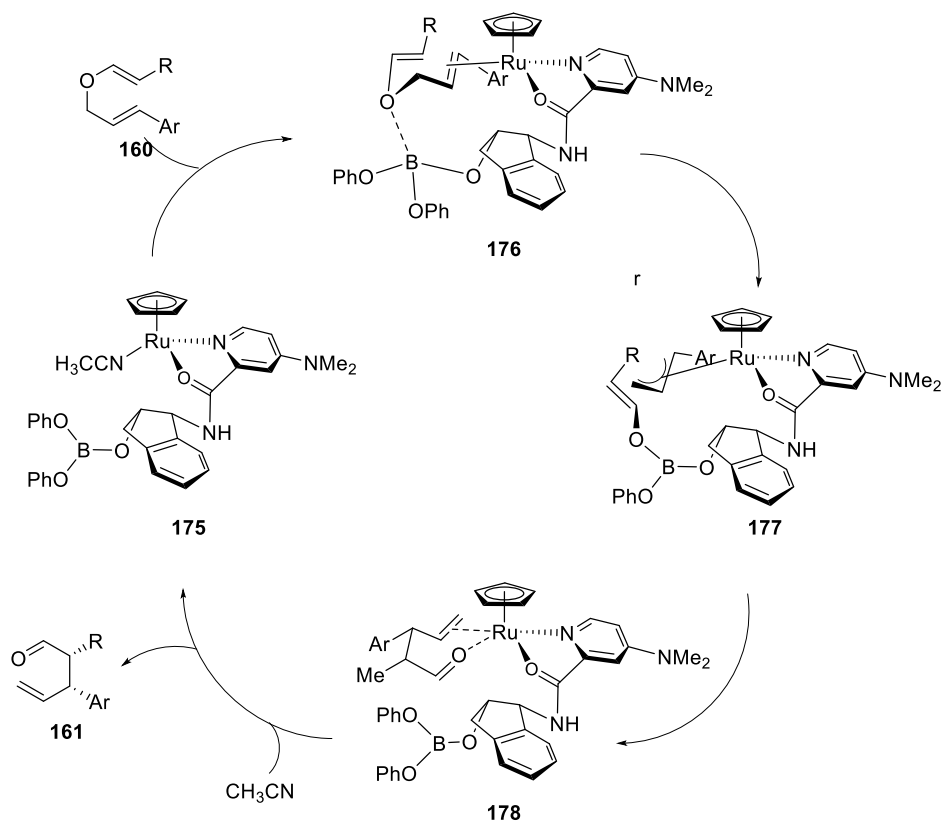


Figure 21: Interconversion of Diastereomers





**Figure 22: Proposed Mechanism for Ruthenium Catalyzed Rearrangement of Allyl Vinyl Ethers**

### 2.8.1 Determination of Absolute Stereochemistry of the Pentenal Products

The absolute stereochemistry of the resultant (R,R)-pentenals was determined by converting the aldehydes into amides of (R)-1-phenylethylamine and resolving the crystal structures.<sup>75-76</sup> The R-stereochemistry at the C<sup>3</sup> carbon supports attack of the enolate on the *endo*-oriented allyl group in structure **189** (Figure 23). The R-stereochemistry results from structural constraints imposed by the intramolecular addition of the boroenolate. The attack of the enolate is restricted to occur from the *si*-face of the boroenolate illustrated by Newman projection **191** resulting in (R,R)-pental **126**.

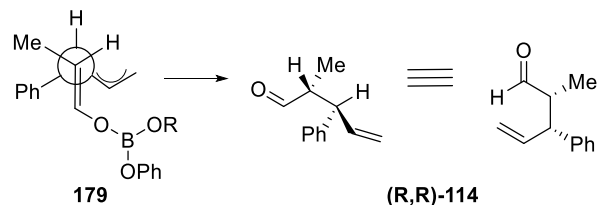


**Figure 23: Transition State and Origin of Diastereoselectivity**

## 2.9 SUMMARY OF RUTHENIUM-CATALYZED REARRANGEMENT OF ALLYL VINYL ETHERS

Thus, our group has developed a highly regio- and stereoselective ruthenium(II)/boron(III) catalytic system for the formal Claisen rearrangements of allyl vinyl ethers. The reaction produces the *anti*-diastereomer in excellent selectivity providing a compliment to the thermal process. However, both aliphatic and *Z*-olefin substrates work poorly. The indanol ligand hydroxyl group is responsible for the strong enantio- and diastereoselectivity of the reaction. The intramolecular nature of the process results in only a single orientation of the ligand a reactive species for the alkylation event.

### 3.0 DEVELOPMENT OF THE INTERMOLECULAR RUTHENIUM(II)- CATALYZED ASYMMETRIC ALLYLIC ALKYLATION

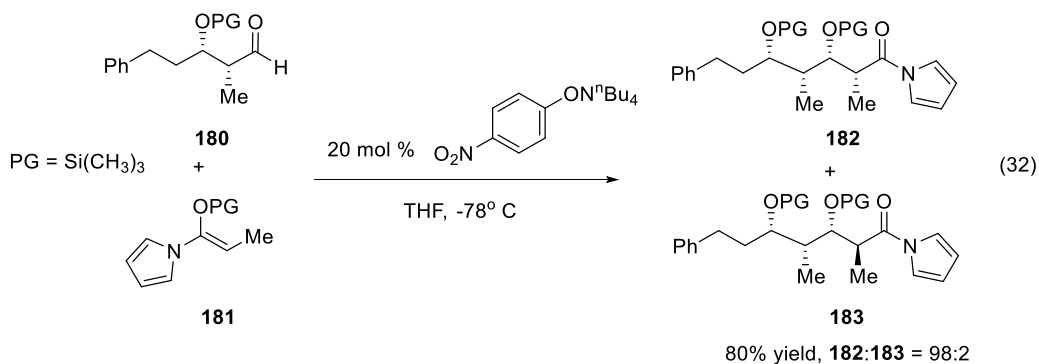
#### 3.1 THE ENOLATE SOURCE IN TRANSITION METAL CATALYZED ENOLATE ADDITIONS

The restricted substrate scope of our iridium(I)-isomerization techniques limited the expansion of the ruthenium(II)-catalyzed rearrangement of allyl vinyl carbonates and ethers. An intermolecular mechanism separating the allyl donor and enolate expands the substrate scope. As illustrated previously, enolate nucleophiles react in ruthenium(II)-catalyzed allylic alkylations. However, generating the reactive enolate can be complicated. Malonates are typical reactants, either as a reactive salt or in conjunction with a base. Ultimately, malonates are incapable of providing stereochemically enriched products yet, simple enolates also react as nucleophiles in allylic alkylations. However, until now the reactive enolates in our chemistry emerge *in situ* from a single molecule starting material that is difficult to modify synthetically. Decarboxylative Carroll rearrangements of allyl  $\beta$ -keto carbonates, and our own rearrangements of allyl vinyl species fall into this category.

##### 3.1.1 Silicon Protected Enolates in Mukaiyama Aldol Reactions

Our goal was to find an intermolecular replacement for the enolate liberated in both the ruthenium(II)-catalyzed rearrangements of allyl vinyl ethers in carbonates. The benefit of such a source would be that we could add the enolate and allyl source separately and would potentially be easier to access synthetically as well as more versatile in substrate scope. Silyl enol enolates present an alternative, stable source of nucleophilic carbon. Trimethylsilyl enol ethers perform well as nucleophiles in Mukaiyama aldol reactions developed in our research laboratory and in other works.<sup>80,81</sup> Specifically, TMS enol ethers derived from N-pyrrole amides demonstrate remarkable reactivity and

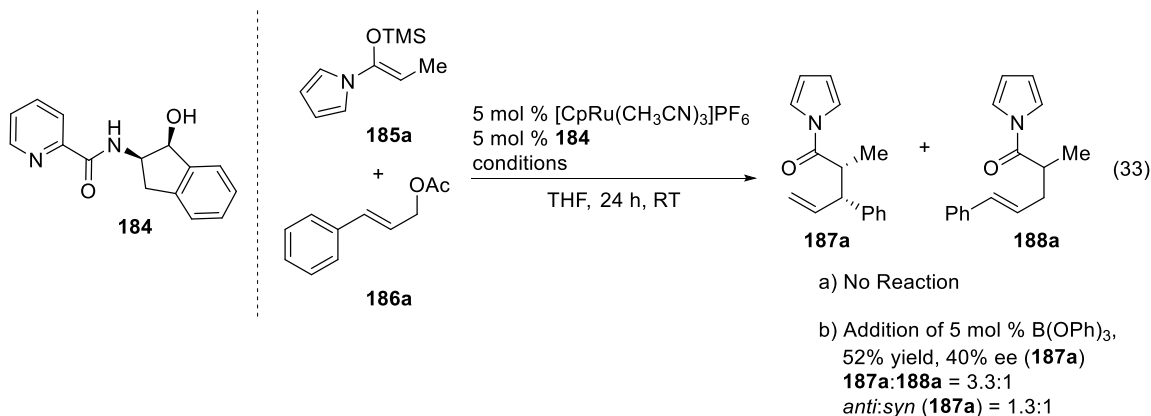
diastereoselectivity in contrast to TMS-protected ketone-derived enol ethers or O,S-ketene acetals (Eq 32).



### 3.2 SILYL ENOL ETHERS AS NUCLEOPHILES IN NELSON GROUP RUTHENIUM(II) CATALYZED REACTIONS

#### 3.2.1 Test Reactions of Silyl Enol Ethers with Allyl Acetates

We tested simple N-acyl pyrrole enol ether **185a** as a nucleophile and allyl acetate **186a** using conditions from our ruthenium(II)-catalyzed rearrangement of allyl vinyl ethers. Our initial results indicate that **185a** and **186a** fail to react in the presence of 5 mol % [CpRu(**184**)(NCCCH<sub>3</sub>)]PF<sub>6</sub> (Eq 33). Fortunately adding 5 mol % B(OPh)<sub>3</sub> facilitated the oxidative addition of the acetate to the ruthenium resulting in amide **187a** in 52% yield with modest selectivity. The liberated acetate from the oxidative addition is likely responsible for the deprotection of the silyl enol ether, mirroring previous palladium-catalyzed alkylations. However, the necessity of the boric acid indicated that a more labile leaving group may produce better results. Additionally, the poor diastereoselectivity observed using indanol ligand **184** suggest the hydroxyl functionality was not as beneficial in the intermolecular reaction.

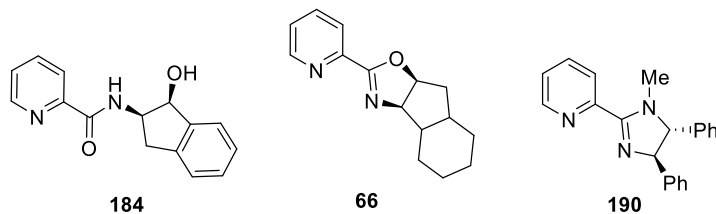
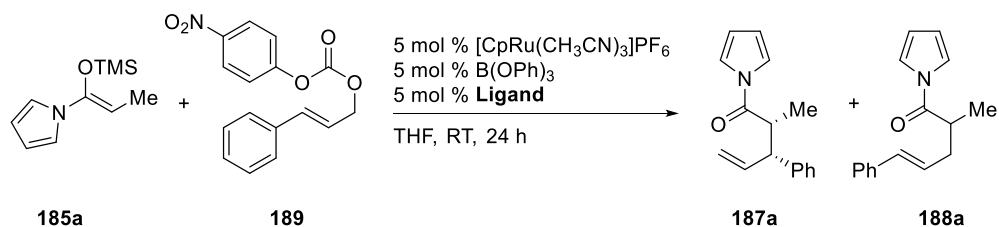


### 3.2.2 Test Reactions of Silyl Enol Ethers with Allyl Carbonates and Ligand Screen

We attributed the lack of reactivity of acetate **186a** to the acetate being a poor leaving group compared to a carbonate in the presence of triphenylborate. Thus, we replaced the starting material with *p*-nitrophenyl carbonate **189** resulting in a more reactive substrate since the phenoxide is a much better leaving group with the expulsion of CO<sub>2</sub>. The carbonate material displays increased yield (85 – 95%) in the reaction with TMS enol ether **185a** in the case of all ligand types (Table 10). The regioselectivity of indanol ligand **184** is mediocre and surprisingly shows no stereoselectivity. Oxazoline **66** improves regioselectivity to a respectable 10:1 *b:l*, enantioselectivity to 68%, yet only weak diastereoselectivity (*anti:syn*(**187a**) = 1.3:1). Imidazoline ligand **190**, an analogue of oxazolines, increased diastereoselectivity to 3:1 and enantioselectivity to 88% while maintaining regiochemistry and yield. We attributed the improvement to increased electron density on the metal center which results in a lesser back-bonding from the metal complex lengthening the C<sup>3</sup>-Ru bond. Simple starting material substitution to phenyl carbonate **202** lacking the nitro group dramatically affects the reaction. Unlike acetate and *p*-nitrophenoxide, unsubstituted phenoxide is more produces a more nucleophilic byproduct which adds to the  $\eta^3$ -allyl complex (rather than the silane) resulting in arylether **192** (Eq 34). Increasing the strength and loading of the boric acid to 30 mol % B(O<sup>*i*</sup>C<sub>6</sub>H<sub>4</sub>F)<sub>3</sub> is sufficient to sequester liberated phenoxide as the tetra(aryl) borate anion. Using B(O<sup>*i*</sup>C<sub>6</sub>H<sub>4</sub>F)<sub>3</sub>, branched amide

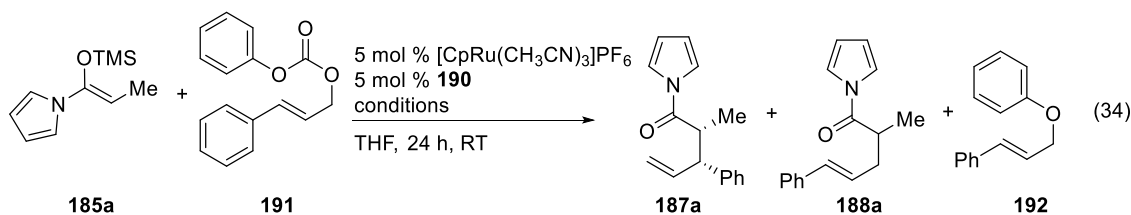
**187a** is formed in 82 % yield. Phenyl carbonate **191** provided greater selectivity than *p*-nitrophenyl carbonate. Regioselectivity climbed to 13:1 *b:l*; diastereoselectivity doubled to 6:1 *anti:syn* and enantioselectivity increased to 94%. Clearly, the leaving group dramatically affects selectivity in allylic alkylations.

**Table 10: Effect of Ligand Type of Rearrangement of Carbonate 189**



Entry	Ligand	% yield	<b>187a:188a</b> <sup>a</sup>	<i>anti:syn</i> ( <b>187a</b> ) <sup>a</sup>	ee (%) <sup>b</sup>
1	<b>184</b>	86	3.4:1	1:1	0
2	<b>66</b>	95	10:1	1.3:1	68
3	<b>190</b>	85	10:1	3:1	88

<sup>a</sup> Determined by <sup>1</sup>H-NMR of the crude product mixture    <sup>b</sup> Determined by Chiral GC.



a) Addition of 5 mol % B(OPh)<sub>3</sub>  
Only **192** formed

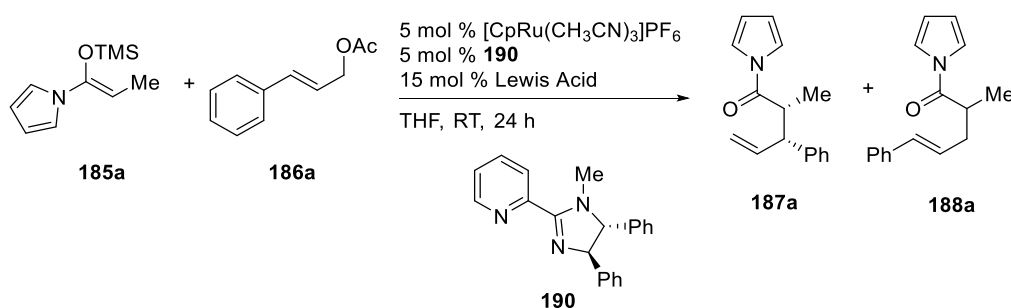
b) Addition of 30 mol % B(OP<sup>i</sup>C<sub>6</sub>H<sub>4</sub>F)<sub>3</sub>,  
82% yield, 94% ee (**187a**)  
**187a:188a** = 13:1  
*anti:syn* (**187a**) = 6:1

### 3.2.3 Allyl Acetates Revisited

The success of imidazoline ligands and stronger borates warranted reinvestigation into acetate **186a** as the allyl donor. Results thus far results indicated weaker leaving groups increase selectivity and furthermore, the acetate ion lacks the nucleophilicity possessed by alkoxides which have been

demonstrated to compete with enolate for nucleophilic additions. Acetate **186a** undergoes oxidative insertion in the presence of 5 mol % [CpRu(**190**)(NCCH<sub>3</sub>)]PF<sub>6</sub> and 15 mol % B(O<sup>*i*</sup>C<sub>6</sub>H<sub>4</sub>F)<sub>3</sub> to generate **187a** in 86% yield (Table 11, Entry 1). Additionally, regio- and stereochemistry are excellent. Regiochemistry remains high at 13:1 *b/l* and diastereoselectivity increases to 7:1 *anti:syn*. Enantioselectivity decreases only slightly to 92 %. Interestingly, increasing the strength of the Lewis acid results in worse diastereoselectivity (Table 11, Entries 2, 3). Evidently, B(O<sup>*i*</sup>C<sub>6</sub>H<sub>4</sub>F)<sub>3</sub> provides the ideal balance for the alkylation of cinnamyl acetates as greater diastereoselectivity is more desirable than regioselectivity as the regioisomers are easier to separate.

**Table 11: Effect of Increasing Acidity of Borate**



Entry	Lewis Acid	% yield	<b>187a</b> : <b>188a</b> <sup>a</sup>	<i>anti:syn</i> ( <b>187a</b> ) <sup>a</sup>	ee (%) <sup>b</sup>
1	B(O <sup><i>i</i></sup> C <sub>6</sub> H <sub>4</sub> F) <sub>3</sub>	86	13:1	7:1	92
2	B(O <sup><i>p</i></sup> C <sub>6</sub> H <sub>4</sub> CF <sub>3</sub> ) <sub>3</sub>	-	-	4:1	-
3	B(O <sup><i>p</i></sup> C <sub>6</sub> H <sub>4</sub> NO <sub>2</sub> ) <sub>3</sub>	-	-	2.3:1	-

<sup>a</sup> Determined by <sup>1</sup>H-NMR of the crude product mixture <sup>b</sup> Determined by Chiral GC.

### 3.3 STUDY OF THE PYRIDINE-IMIDAZOLINE LIGAND

#### 3.3.1 Synthetic and Anticipated Effects of Pyridine-Imidazoline Modifications

At the current juncture, we envisioned ligand modifications would further improve the dynamics of the allylic alkylation reaction. The imidazoline motif presents an easily-modified ligand framework. Treatment of pyridine-2-carboxaldehyde **193** and diamine **194** with NBS yields an imidazoline which



upon  $S_N2$  alkylation of  $N_{amine}$  results in ligand **195** (Eq 35).<sup>82</sup> We examined 4 specific regions of the ligand motif to determine that impact of such substitutions on the parameters of the allylic substitution reactions (Table 12). The “A” position increases steric crowding near the  $N_{pyridine}$  and influences regio- and diastereoselectivity. Substituents at the “B” position provide influence the electron density at the  $N_{pyridine}$  through resonance. Based on previous observations, increasing electron density on  $N_{pyridine}$  leads to increased regioselectivity. Similarly, the “C” substituent on  $N_{amine}$  contributes to the electron density and binding strength of  $N_{imidazoline}$  and corresponds to increased regioselectivity. Lastly, the “D” substituents influence the sterics about the allyl group and most importantly render the reaction asymmetric.

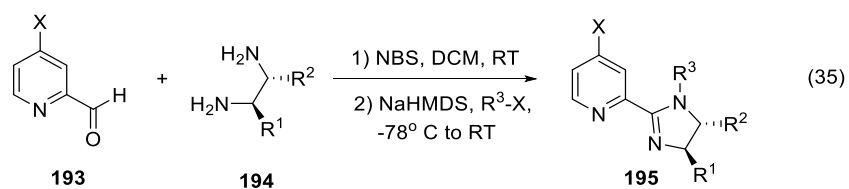
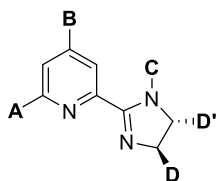


**Table 12: Anticipated Effects of Imidazoline Modifications**

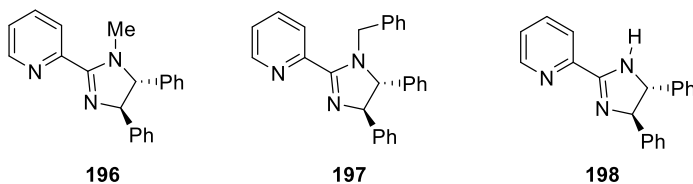
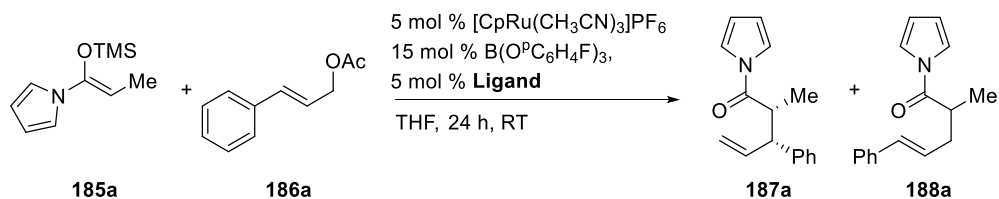


Substituent	Influence on Catalyst	Predicted Effect
<b>A</b>	Influences sterics of N <sub>pyridine</sub>	Altered regio- and diastereoselectivity
<b>B</b>	Increases electron density on N <sub>pyridine</sub>	Increased regioselectivity
<b>C</b>	Affects electron density on N <sub>imidazoline</sub>	Increased regioselectivity
<b>D</b>	Influences steric environment and electron density of N <sub>imidazoline</sub>	Increased stereoselectivity, especially enantioselectivity

### 3.3.2 Modification of the N-Alkyl Group

Simple S<sub>N</sub>2 reactions allow modification of the N<sub>amine</sub> alkyl group “C”. We compared the reaction of TMS enol ether **185a** and cinnamyl acetate **186a** under optimal conditions (5 mol % CpRu(CH<sub>3</sub>CN)<sub>3</sub>]PF<sub>6</sub>, 15 mol % B(O<sup>*t*</sup>C<sub>6</sub>H<sub>4</sub>F)<sub>3</sub>, THF, RT, 24 h) using 5 mol % **196**, **197**, or **198**. Free imidazoline **198** performed the worst with only 50 % yield (Table 13, Entry 3). Moreover, regio- and stereoselectivity were substantially decreased. The reactive free amine permitted multiple unproductive side reactions. N-methyl **196** and N-benzyl **197** worked better, but **196** was a superior choice (Table 13, Entries 1, 2). The added sterics of the benzyl moiety likely disrupts the binding of the ligand to ruthenium, resulting in decreased performance.

**Table 13: Modification of the N-Alkyl Group**



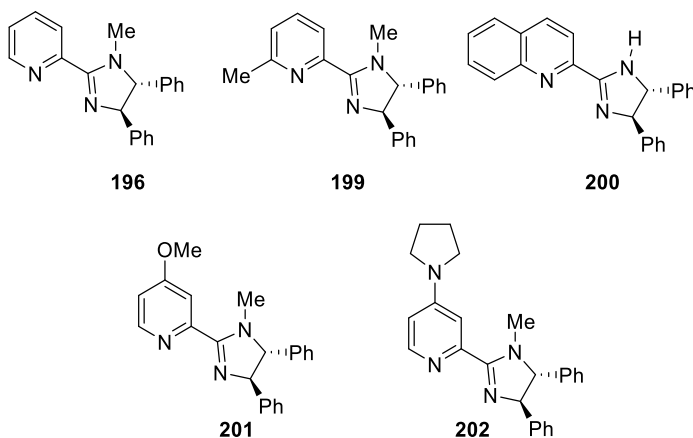
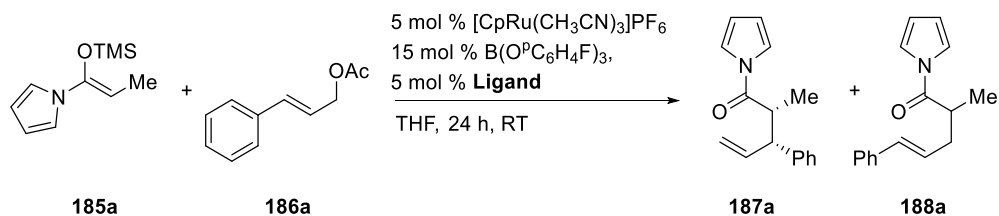
Entry	Ligand	% yield	<b>187a:188a</b> <sup>a</sup>	<i>anti:syn</i> ( <b>187a</b> ) <sup>a</sup>	ee (%) <sup>b</sup>
1	<b>196</b>	86	13:1	7:1	92
2	<b>197</b>	67	11:1	5:1	88
3	<b>198</b>	50	6.4:1	5:1	81

<sup>a</sup> Determined by <sup>1</sup>H-NMR of the crude product mixture <sup>b</sup> Determined by Chiral GC.

### 3.3.3 Modification of the Pyridine Ring

Using substituted pyridine-2-carboxaldehydes in imidazoline synthesis provides a convenient route to ligand modification. Worsening the Lewis basicity of the pyridine worsens the performance of the catalytic reaction (Table 14, Entries 2, 3). 6-methyl substituted **199** only gave 19 % yield of the product with slightly reduced selectivity. Although 6-methyl pyridine is more basic to simple acids, the added sterics actually reduce basicity to larger Lewis acids such as boranes.<sup>83</sup> The quinoline derivative **200** performs marginally better (50% yield) yet further erodes regio- and stereoselectivity. Quinoline has markedly reduced basicity compared to standard pyridine. The lessened degree of binding of N<sub>pyridine</sub> to the Ru and makes the ruthenium center less reactive and selective.

**Table 14: Modification of Pyridine Ring**



Entry	Ligand	% yield	<b>187a</b> : <b>188a</b> <sup>a</sup>	<i>anti:syn</i> ( <b>187a</b> ) <sup>a</sup>	ee (%) <sup>b</sup>
1	<b>196</b>	86	13:1	7:1	92
2	<b>199</b>	19	13:1	5:1	88
3	<b>200</b>	50	10:1	2.5:1	88
4	<b>201</b>	82	13:1	7:1	90
5	<b>202</b>	88	18:1	9:1	91

<sup>a</sup> Determined by <sup>1</sup>H-NMR of the crude product mixture <sup>b</sup> Determined by Chiral GC.

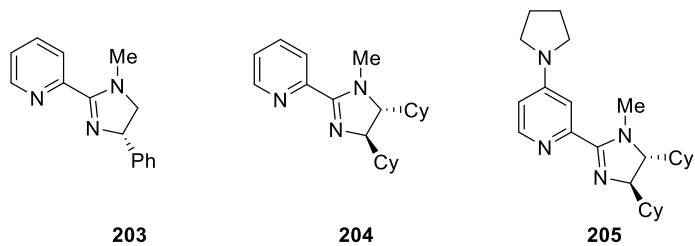
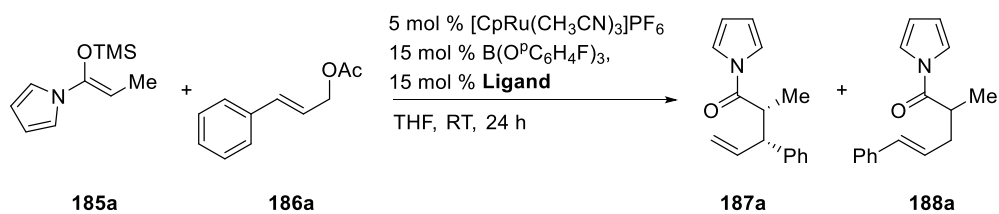
Conversely, modification of the 4-position of the pyridine improves reaction performance. Ligand synthesis starting with 4-chloropyridine-2-carboxaldehyde motif permits subsequent nucleophilic aromatic substitution of the chlorine. Donating groups at this position enhance the electron-donating ability of the N<sub>pyridine</sub>. 4-methoxy **201** performs nearly identically to control **196**, showing only slight decreases in yield and enantioselectivity (Table 14, Entry 4). However, 4-pyrrolidine **202** dramatically increases regio- and diastereoselectivity of the transformation, and provides nearly indistinguishable yield and enantioselectivity as the control (Table 14, Entry 5). Noticeably, the increasing

nucleophilicity of the nitrogen-substituent translates to better selectivity in the catalyst. We encountered the same effect during our work in ruthenium-catalyzed carbonate and ether rearrangement chemistry. The added donation helps distort the intermediate  $\pi$ -allyl complex and elongating the Ru-C<sup>3</sup> bond.

### 3.3.4 Modification of the Imidazoline Backbone

The asymmetric backbone strongly impacts of the results of ruthenium(II)-catalyzed allylic alkylations. Results collected thus far demonstrate the *anti*-diphenyl **196** is a strong ligand candidate. However, it is possible that the C<sup>5</sup>-phenyl group, distal to the binding N<sub>imidazoline</sub>, does not affect the reaction dynamics. The reaction of **185a** and **186a** and using ligand **203** under optimal conditions, which lacks the second phenyl group, furnishes amide products with an excellent yield of 93% (Table 15, Entry 1). Yet, all selectivities are severely reduced. Regioselectivity falls to 3:1 **187a:188a**, diastereoselectivity plummets to 1.5:1 *anti:syn*(**187a**), and enantioselectivity descends to 53%. Evidently, the distal phenyl group plays a pivotal role in enforcing reaction selectivity. Conceivably, the added steric encumbrance suppresses the alternate binding modes of the ligand – possibly coordination by the N<sub>amine</sub>.

**Table 15: Modification of Imidazoline Backbone**



Entry	Ligand	% yield	<b>187a</b> : <b>188a</b> <sup>a</sup>	<i>anti:syn</i> ( <b>187a</b> ) <sup>a</sup>	ee (%) <sup>b</sup>
1	<b>203</b>	94	3:1	1.5:1	53
2	<b>204</b>	89	20:1	5.4:1	97
3	<b>205</b>	91	42:1	4.7:1	95

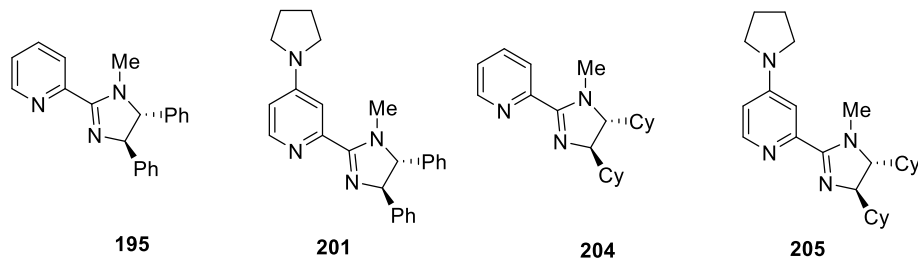
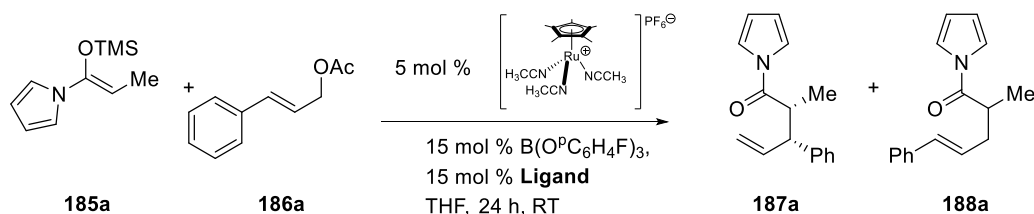
<sup>a</sup> Determined by <sup>1</sup>H-NMR of the crude product mixture <sup>b</sup> Determined by Chiral GC.

Having determined the necessity of substitution at the imidazoline C<sup>4</sup> and C<sup>5</sup> carbons, we assessed the effect of added steric bulk. Under established conditions (5 mol % CpRu(CH<sub>3</sub>CN)<sub>3</sub>]PF<sub>6</sub>, 15 mol % B(OPh)<sub>3</sub>, THF, RT, 24 h) dicyclohexyl analog **215** facilitates the reaction in respectable 89% yield (Table 15, Entry 2). Remarkably, the regio- and enantioselectivity improve to 20:1 **187a**:**188a** and 97% (from 13:1 and 92% using **196**). Diastereoselectivity, however, drops to 5.4:1 *anti:syn*(**187a**) (from 7:1). Introduction of a pyrrolidine on the pyridine further increases regioselectivity of the dicyclohexyl motif. Using ligand **204** provides the amide products in 91% yield and an astonishing 40:1 branched:linear ratio (Table 15, Entry 3). Despite the gains, diastereo- and enantioselectivity drop to 4.7:1 and 95%. Our results thus far indicate two strong ligand candidates for the intermolecular allylic alkylation reactions. The pyrrolidine-substituted diphenyl **205** produces amide **187a** in the best diastereomeric ratios (9:1 *anti:syn*). Alternatively, the unsubstituted dicyclohexyl **204** displays increased regioselectivity (20:1 branched:linear) and superior enantioselectivity (97%).

### 3.3.5 Effects of Pentamethylcyclopentadienyl (Cp\*)

A final test examined the effects of switching to Cp\*Ru(CH<sub>3</sub>CN)<sub>3</sub>]PF<sub>6</sub> as a precatalyst. We initially avoided the sterically encumbering ligand based on reports indicating it can erode activity and selectivity. The Cp\* complex performed extremely poorly using the best imidazoline ligand candidates (Table 16). Fascinatingly, pyrrolidine-substituted **201** and **204** displayed no conversion in the reaction, despite being the best candidates for the CpRu precatalyst. Evidently, the increased electron density on the ruthenium makes the intermediate pi-allyl complex more stable and less electrophilic (Table 16, Entries 2, 4). Unsubstituted **196** and **204** enabled moderate conversion. Diphenyl **196** gave 81% yield and decent regioselectivity of 7:1 **187a**:**188a**. Strangely, the reaction is diastereoselective for the *syn* isomer at 1:3 *anti*:*syn*. Enantioselectivity is phenomenal at 98%, but oddly for the opposite enantiomer encountered using CpRu. The change in enantioselectivity demonstrates how the large sterics of the Cp\* moiety affect the binding of the ligand of allyl groups. Lastly, the cyclohexyl **204** provided only 40% yield, and barely any diastereoselectivity at 1:1.5 *anti*:*syn*(**187a**). Evidently, CpRu-derived complexes are the ideal catalysts to provide the branched, *anti*, amide products in good yields.

**Table 16: Effects of Cp\***



Entry	Ligand	% yield	<b>187a</b> : <b>188a</b> <sup>a</sup>	<i>anti:syn</i> ( <b>187a</b> ) <sup>a</sup>	ee (%) <sup>b</sup>	yield(%) <sup>c</sup>
1	<b>196</b>	81	7:1	1:3	98	
2	<b>201</b>	N.R.	-	-	-	
3	<b>204</b>	40	21:1	1:1.5	N.D. <sup>c</sup>	
4	<b>205</b>	N.R.	-	-	-	

<sup>a</sup> Determined by <sup>1</sup>H-NMR of the crude product mixture, <sup>b</sup> Determined by Chiral GC, <sup>c</sup> N.D. = not determined

### 3.4 REACTION SCOPE

At the current point in our investigation, we were satisfied with current reaction parameters. Our test reaction using **185a** and **186a** demonstrate useful selectivities using the best ligand candidates **201** and **204**. However, **201** provides higher diastereoselectivity, while **204** promotes higher regio- and enantioselectivity. We further examined the scope of our reaction on a series of substituted TMS enol ethers and cinnamyl acetates by comparing both ligand motifs using optimized reaction conditions (5 mol % CpRu(CH<sub>3</sub>CN)<sub>3</sub>]PF<sub>6</sub>, 5 mol% ligand, 15 mol % B(OPC<sub>6</sub>H<sub>4</sub>F)<sub>3</sub>, THF, RT, 24 h).



### 3.4.1 Reaction Scope of Ligand 201

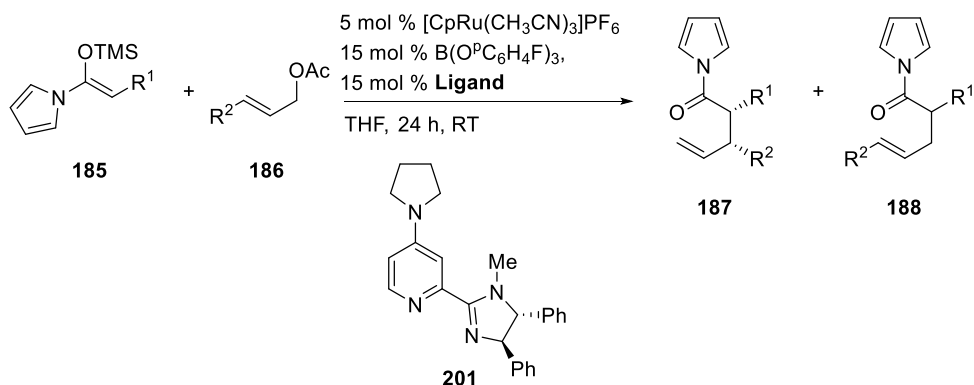
Generally, pyrrolidated, diphenyl ligand **201** afforded good yields and selectivity with multiple substituents present on substrates. However, simple **185a** and **186a** still supplied the overall best results (Table 17, Entry a). Interestingly, unsubstituted **185b** demonstrated decreased regio- and enantioselectivity indicating that sterics of the enol ether substituents play a crucial role in enforcing selectivity (Table 17, Entry b). Conversely, replacing R<sup>1</sup> with an n-propyl group in **185c** required a full equivalent of boric acid to achieve useful yields. Despite the sluggish reaction, the regio- and stereoselectivity only suffered a moderate decrease (Table 17, Entry c). Increasing the sterics of the enol ether by incorporating an isopropyl substituent in **185d** resulted in no product formation despite our best efforts. The nucleophile is too sterically hindered to react (Table 17, Entry d). The benzyl ether derivative **185e** exhibits decent yields and stereoselectivity (Table 17, Entry e). Yet, selectivity and yield are substantially diminished compared to methyl **185a**. The benzyl group is less sterically hindered than a methyl, and electronically distinct. Chlorinated **185f** reacts very slowly producing only *ca* 26% yield of a mixture of  $\alpha$ -chloro amide **185e** and its acetylated S<sub>N</sub>2 derivative (Table 17, Entry f). Despite incredible regioselectivity (32:1 *b:l*) the reaction almost completely lacked regioselectivity and the electron-withdrawing chloro substituent enables epimerization of the stereogenic center producing only 34% ee of **187f**.

Modifying the aromatic group of the acetate demonstrates the effect of electronics on the catalytic cycle. The electron-rich *p*-methoxyphenyl **186g** significantly increases regioselectivity of the reaction to 33:1 *b:l* with little degradation of other parameters (Table 17, Entry g). We witnessed similar effects in our previous ruthenium-catalyzed reaction designs. We attribute the increase in selectivity to decreased backbonding from the ruthenium to the allyl group, which lengthens the C<sup>3</sup>-Ru bond. However, *o*-methoxyphenyl **186h** exhibits considerably diminished regio- and diastereoselectivity. Clearly, groups at the 2-phenyl position inhibit reactivity through added steric bulk (Table 17, Entry

h). Furyl-derived **186i** produces amide derivatives with nearly identical selectivities as the control demonstrating good tolerance for electron-rich, reactive aromatic rings (Table 17, Entry i). Unsurprisingly, nitro **186j** suffers from poor yields and diastereoselectivity (Table 17, Entry j). Still, the reaction possesses respectable diastereoselectivity and enantioselectivity.

Overall, it seems the aromatic group identity correlates to regioselectivity. In most of cases, diastereo- and enantioselectivity were decent (4 to 8:1 *anti:syn* and 88-91%). Bulky enol ethers and electron-poor acetates were demonstrated to be the weakest substrate candidates. Halogenated enol ether substrates were poor choices because of lack of reactivity and secondary substitution pathways eroding enantioselectivity.

**Table 17: Substrate Scope Using Ligand 201**



Entry	R <sup>1</sup>	R <sup>2</sup>	yield(%) <sup>a</sup>	<b>187</b> : <b>188</b> <sup>b</sup>	<i>anti</i> : <i>syn</i> ( <b>187</b> ) <sup>b</sup>	ee <b>187</b> (%) <sup>c</sup> <i>anti</i> , <i>syn</i>
a	Me	Ph	88	18:1	9:1	95, 79
b	H	Ph	82	14:1	-	68
c <sup>d</sup>	n-propyl	Ph	82	13:1	7:1	89, 59
d	<i>i</i> -propyl	Ph	N.R.	-	-	-
e	OBn	Ph	80	11:1	4:1	90, 53
f	Cl,	Ph	21	32:1	1.3:1	34, -
	OAc (product)		5	32:1	1.3:1	N.D. <sup>e</sup>
g	Me	<sup>p</sup> C <sub>6</sub> H <sub>4</sub> OMe	92	>33:1	8:1	91, 67
h	Me	<sup>o</sup> C <sub>6</sub> H <sub>4</sub> OMe	81	8:1	4:1	89, 45
i	Me	2-furyl	89	17:1	8:1	89, 54
j	Me	<sup>p</sup> C <sub>6</sub> H <sub>4</sub> NO <sub>2</sub>	53	4:1	5:1	88, 47

<sup>a</sup> Isolated yield after flash chromatography, <sup>b</sup> Determined by <sup>1</sup>H-NMR of the crude product mixture, <sup>c</sup> Determined by chiral GC, <sup>d</sup> 1.0 equiv. B(OPh)<sub>3</sub>, <sup>e</sup> N.D. = not determined

### 3.4.2 Reaction Scope of Ligand 204

As anticipated, the cyclohexyl ligand **204** produced amide **187** with superior regio- and enantioselectivity compared with diphenyl ligand **201**. Still, diastereoselectivity was significantly reduced in all circumstances. In contrast to previous results, unsubstituted enol ether **185b** demonstrated higher regioselectivity than methyl **185a** in this case while maintaining decent yield and

excellent 95% ee (Table 18, Entry b). N-propyl **185c** still requires additional acid, but the reaction experienced an increase in regio- and enantioselectivity and only dropping to 6:1 *anti:syn* (Table 18, Entry c). Predictably, isopropyl **185d** did not react using ligand **204** mirroring previous results (Table 18, Entry d). Unlike results using ligand **204**, benzyl ether **185e** improved to be nearly complete regioselectivity compared to methyl **185a**. Even so, yield and diastereoselectivity were moderately reduced demonstrating the unpredictability of C<sup>2</sup>-alkoxy enol ethers.

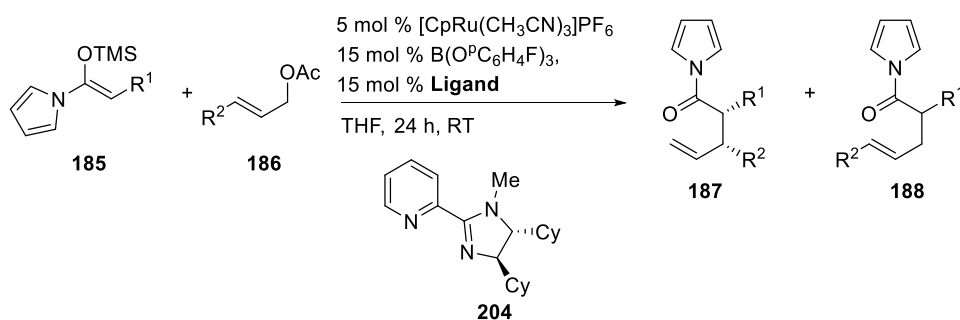
The chloro **185f** showed somewhat enhanced reactivity with ligand **204** producing a mixture of chlorinating and acetate products in overall 48% yield (Table 18, Entry f). Extraordinarily, the chloro product exhibited a 1:3 *anti:syn* diastereomeric ratio in favor of the *syn* product in contrast to diphenyl ligand **201** results. Interestingly the acetate derivative formed in a 2:1 *anti:syn* relationship. It is possible the [CpRu(**204**)(CH<sub>3</sub>CN)]PF<sub>6</sub> complex is active enough to facilitate an allyl shift of branched **187f** resulting in preferential formation of OAc-substituted *syn*-**187f**. Although mediocre, the results demonstrated that alternative substitution motifs can function in the reaction, yet may require specific reaction tunings to suppress unwanted side reactions.

The anisole derivatives **186h** and **186g** provided amide products in moderate yields however both provide near-complete regioselectivity (Table 18, Entries g, h). Unexpectedly, *o*-OMe **186h** did not suffer from the drop in regioselectivity observed using diphenyl ligand **201**. Of the two, *p*-OMe **186g** proceeded with the best diastereoselectivity (4:1 *anti:syn*) yet *o*-OMe **186h** provides the greatest enantioselectivity (98%). Furan-derived **186i** reacted in improved yields, regio- and enantioselectivity, suffering only a moderate decrease in diastereoselectivity. Finally, nitro **186j** reacted in 88% yield, dwarfing the 53% obtained using ligand **201** (Table 18, Entry i).

Based on our results, we concluded that the dicyclohexyl **204** ligand was the better overall ligand candidate than the diphenyl **201** in many cases. The increased regio- and enantioselectivities outweigh the benefit of increased diastereoselectivity. In addition, cyclohexyl **204** results in a more reactive

catalyst as evident by the reactions of chloro **197f** and nitro **198j**. Furthermore, **204** demonstrated superior enantioselectivity in the *syn* products as a bonus.

**Table 18: Substrate Scope Using Ligand 204**



Entry	R <sup>1</sup>	R <sup>2</sup>	yield(%) <sup>a</sup>	<b>187:188</b> <sup>b</sup>	<i>anti:syn</i> ( <b>187</b> ) <sup>b</sup>	ee <b>187</b> (%) <sup>c</sup> <i>anti,syn</i>
a	Me	Ph	89	20:1	5.4:1	97, 91
b	H	Ph	82	25:1	-	95
c <sup>d</sup>	n-propyl	Ph	82	19:1	6:1	96, 97
d	<i>i</i> -propyl	Ph	N.R.	-	-	-
e	OBn	Ph	75	>33:1	4:1	96, 89
f	Cl,	Ph	38	32:1	1:3	97, N.D. <sup>e</sup>
	OAc (product)		10	16:1	2:1	99, 97
g	Me	<sup>p</sup> C <sub>6</sub> H <sub>4</sub> OMe	79	>33:1	5:1	94, 89
h	Me	<sup>o</sup> C <sub>6</sub> H <sub>4</sub> OMe	79	>33:1	3.3:1	98, 85
i	Me	2-furyl	99	20:1	4.3:1	95, 93
j	Me	<sup>p</sup> C <sub>6</sub> H <sub>4</sub> NO <sub>2</sub>	88	5:1	4:1	94, 94

<sup>a</sup> Isolated yield after flash chromatography, <sup>b</sup> Determined by <sup>1</sup>H-NMR of the crude product mixture, <sup>c</sup> Determined by chiral GC, <sup>d</sup> 1.0 equiv. B(OPh)<sub>3</sub>, <sup>e</sup> N.D. = not determined

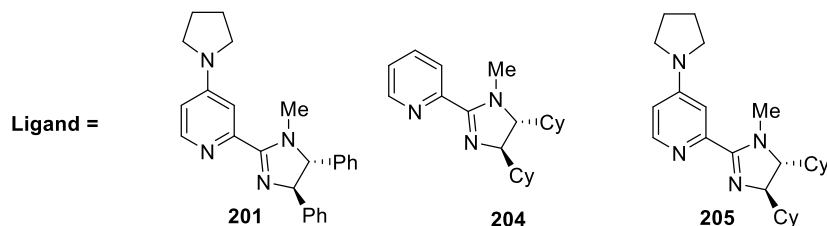
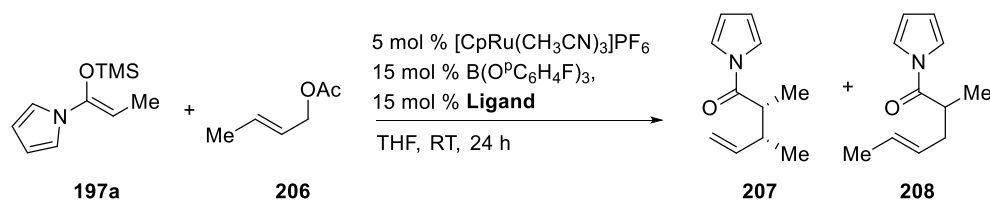
### 3.4.3 Effects of Aliphatic Substrates

Our efforts to use aliphatic allylic substrates in previous reactions were limited. The iridium(I)-catalyzed isomerization chemistry is applicable to few aliphatic substrate motifs. Additionally, the accessible materials react sluggishly and with poor selectivity. The intermolecular nature of the silyl

enol enolate addition chemistry avoids the need for chemoselective olefin isomerization allowing for a wider range of structural motifs.

Under our optimized conditions (5 mol %,  $\text{CpRu}(\text{CH}_3\text{CN})_3\text{PF}_6$ , 5 mol % ligand, 15 mol %  $\text{B}(\text{O}^i\text{C}_6\text{H}_4\text{F})_3$ , THF, RT, 24 h) crotyl acetate **206** and enolate **185a** reacted slowly regardless of ligand choice (36 – 37% yield (Table 19). It seems the aromatic group in cinnamyl substrates strongly accelerates the oxidative addition of the acetate group. Interestingly, diphenyl ligand **201** provides better regioselectivity, 4:1 **207:208**, but worse diastereoselectivity, 4:1 *anti:syn*, compared to dicyclohexyl **204** with 1.4:1 **207:208** and 7:1 *anti:syn*(**207**) (Table 19, Entries 1, 2). The reverse trend is evident in the reaction of aromatic substrates. The electron-rich pyrrolidine-substituted dicyclohexyl **205** began to approach synthetically useful selectivities despite being an unreactive ligand using aromatic cinnamyl systems. Nonetheless the overall yield hovers at 37% and diastereoselectivity drops to 4:1 *anti:syn* (Table 19, Entry 3). Remarkably, using **205** raised enantioselectivity to 80% (from 67% using **204**). In contrast, the substitution of pyrrolidine to the pyridine ring degraded the enantioselectivity in aromatic substrates (Table 15, Entry 3). The results indicate that the intermolecular alkylation reaction demonstrates promise as a viable method for accessing amides such as **207**. Yet, significant modifications are necessary to overcome the differing electronics of the aliphatic systems.

**Table 19: AAA Reaction with Aliphatic Substrates**



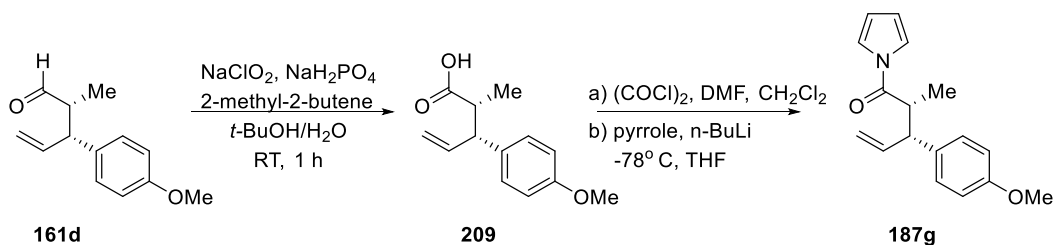
Entry	Ligand	yield (%) <sup>a</sup>	<b>207:208</b> <sup>b</sup>	<i>anti:syn</i> ( <b>207</b> ) <sup>b</sup>	ee <b>207</b> (%) <sup>c</sup>
1	<b>201</b>	36	4:1	4:1	N.D. <sup>d</sup>
2	<b>204</b>	37	1.4:1	7:1	67
3	<b>205</b>	37	6:1	4:1	80

<sup>a</sup> Isolated yield after column chromatography <sup>b</sup> Determined by <sup>1</sup>H-NMR of the crude product mixture, <sup>c</sup> Determined by Chiral GC, <sup>d</sup> N.D. = not determined

### 3.5 ABSOLUTE STEREOCHEMISTRY DETERMINATION OF AMIDE PRODUCTS

The absolute stereochemistry of amide products were determined by derivatization of known aldehyde **164d** to amide **199g** (Scheme 6).<sup>75</sup> The stereochemistry of amide **199g** produced from asymmetric alkylation was found to be the identical R,R isomer formed in the rearrangement of allyl vinyl ether and carbonates. The identical stereochemical orientation in each process suggests that allylic addition occurs to the same face of the allyl moiety in each of our ruthenium-catalyzed transformations.

## Scheme 6: Determination of Absolute Stereochemistry of AAA Amide Products



### 3.6 MECHANISM OF RUTHENIUM(II) AAA AND CARBONATE REARRANGEMENTS

#### 3.6.1 Origin of Enantioselectivity: Stereochemistry at C<sup>3</sup>

Both ruthenium-catalyzed AAA reactions and carbonate rearrangements proceed through similar intermolecular, outer-sphere type addition mechanisms to ultimately produce products with identical orientations. The stereochemistry of the reaction results from discrimination between binding modes of the imidazoline or oxazoline ligand to the ruthenium (Figure 24). The equilibrium between the imidazoline diastereomers **210** and **211** would be in favor of **211**. The disfavor for diastereomer **210** results from unfavorable steric interactions between proximal cyclohexyl carbon and the cyclopentadiene moiety on the ruthenium center. Structure **211**, however, has the proximal cyclohexyl pointed away from the ring. Similarly, for the rearrangement of allyl vinyl carbonates, the oxazoline ligand **66** would favor an analogous active catalyst **212** orienting the indane away from the cyclopentadiene ring. In contrast, the diastereomers **171** and **172** produced from the indanol ligand **126** used in intramolecular rearrangement of allyl vinyl ethers are energetically similar and are produced in equal amounts.



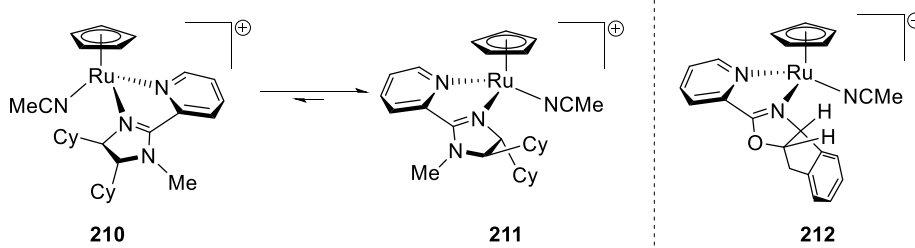


**Figure 24: Intercoversion of Diastereomers 210 and 211**

The oxidative addition of cinnamyl acetate (or carbonate) to ruthenium complex **211** results in allyl complex **213** (Figure 25). As discussed previously, we would expect the allyl moiety to bind as *endo*-**213** with the C<sup>2</sup>-H of the allyl fragment oriented away from the cyclopentadienyl ring as *exo*-**213** would presumably be sterically disfavored. Recall in the rearrangement of allyl vinyl ethers, only one diastereomer of the catalyst permits addition of the allyl fragment through TS **213** (Figure 26a). The orientation ultimately results in R stereochemistry on the C<sup>3</sup> carbon. However, the same model predicts the opposite stereochemistry when applied to the ruthenium-catalyzed AAA and carbonate reactions. Enolate attack on the bound allyl group of *endo*-**224** would proceed through TS **215**, adding to the opposite allyl face and eventually giving an S orientation (Figure 26b). Since the R stereochemistry is isolated as the actual isomer, there must be problems in the proposed model. The sterically demanding oxazoline and imidazoline ligand motifs must favor formation of the *exo*-allyl isomer. The allyl C<sup>2</sup>-H must detest the steric strain introduced by pendant phenyl, cyclohexyl or indane groups more so than the cyclopentadienyl ring.

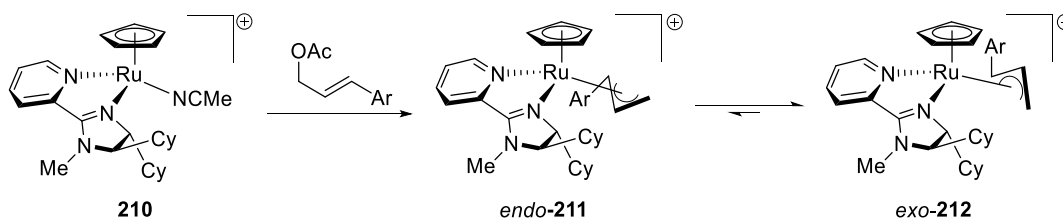


**Figure 25: Interconversion Between *exo* and *endo* Allyl Orientation**

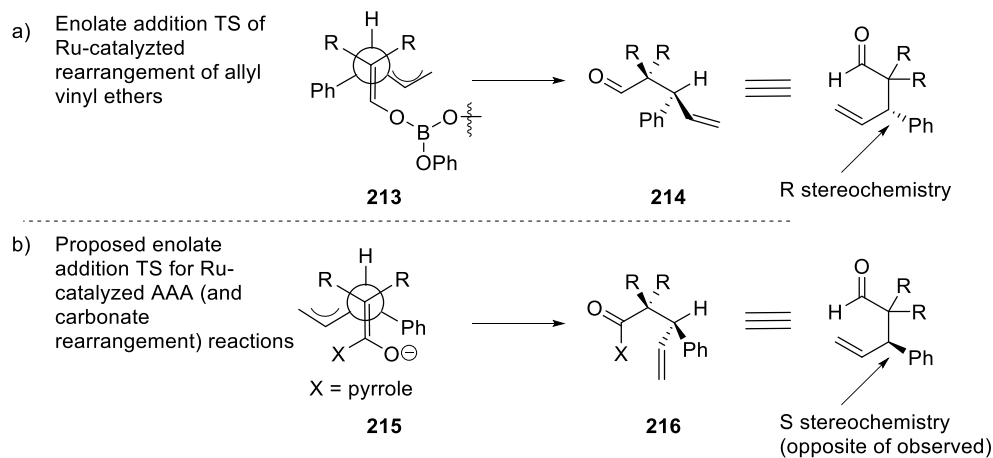


**Figure 26: Enantioselectivity at C<sup>3</sup> Allyl Carbon**

Additionally, the observation of the opposite enantiomer formed using Cp\*-derived catalysts supports the claim. A Cp\* is significantly larger than a Cp and helps to explain the lackluster results in general using Cp\*Ru/ligand systems. A bidentate ligand such as an oxazoline or imidazoline combined with a Cp\* presents an extremely crowded ruthenium center and can effectively switch the preferred binding mode of the allyl group as well as distort diastereomeric ratios. Moreover, the adding electron-density decreased the electrophilicity of the allyl group, further slowing the nucleophilic, enolate addition.

### 3.6.2 Diastereoselectivity: Stereochemistry at C<sup>2</sup>

Satisfied with an explanation of stereochemistry at the C<sup>3</sup> carbon, we could investigate diastereoselectivity at C<sup>2</sup>. The diastereoselectivity can be attributed to forces in an open transition state. Attack of the enolate can occur from the *re* or *si* face in *anti*-periplanar or *syn*-clinal mode producing 6 distinct transition states (Figure 27). Our results indicated a strong preference the *anti*-**187a** isomer.

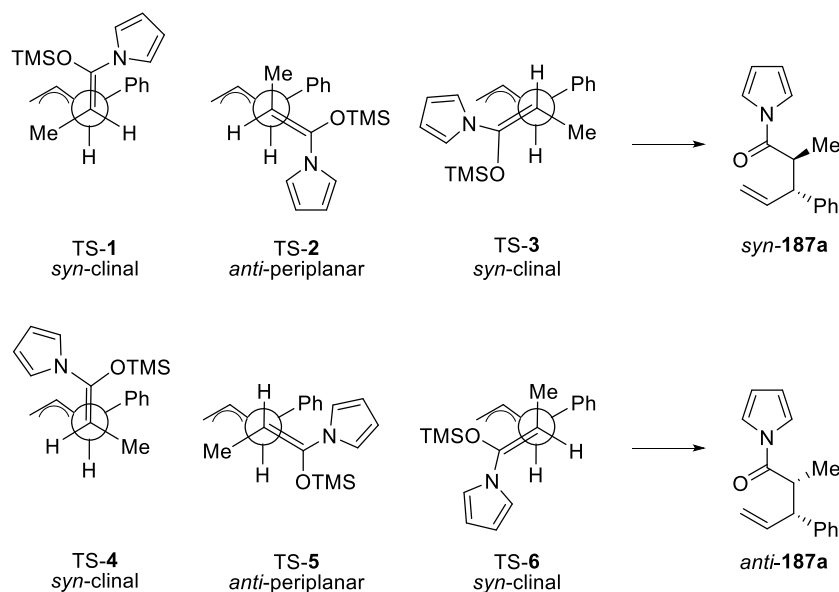
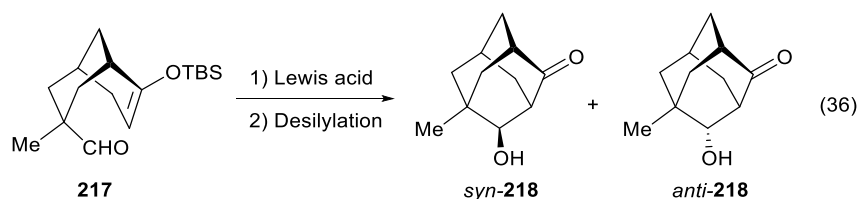


**Figure 27: Transition States of Enolate Addition to C3 Carbon**

While studies of our exact system are lacking, there are several studies on the diastereoselectivity of analogous Mukaiyama aldol additions of silyl enol ethers to aldehydes. A study by Denmark using a rigid, bicyclo[3.3.1]nonane enol ether **217** sought to examine the competition between *syn*-clinal and *anti*-periplanar transition states (Eq 36).<sup>84</sup> The *syn*-**218** isomer results from solely from a *syn*-clinal TS and the *anti*-**218** isomer from the *anti*-periplanar TS; the bicyclo structure limits the possibility of additional orientations. In most of trials, *anti*-**218** is favored by 3:1 up to 9:1 indicating a strong preference for the *anti*-periplanar pathway.



The Lewis acid-catalyzed addition of the TMS enol ether of pinacalone **219** to benzaldehyde **220** produces an analogous set of transition states to our reaction. Several studies have examined the transition states to rationalize the diastereoselectivity.<sup>85-86</sup> For example, in TS-**1a** the activated ketone

is the allyl moiety and the pyrrole is the *tert*-butyl in TS-1 (Figure 28). Heathcock rules out the gauche, *syn*-clinal transition states TS-1, TS-4, and TS-6 due to steric encumbrance. He also infers the carbonyl-bound Lewis acid (the allyl group in our model) is sterically-hindering enough to suppress the *anti*' TS-3.<sup>85</sup> Interestingly, he supports *anti*-periplanar, gauche TS-2 over the seemingly less-crowded TS-5. He attributes the preference to strong, steric interaction of the *tert*-butyl (pyrrole in our system) with the phenyl. Wiest and Helquist used computation gas-phase models to support Heathcock's observations.<sup>86</sup> The calculations advocated that TS-2 is more sterically-disfavored than first suggested and thus the staggered TS-5 remains the dominant transition state. In addition, they suggested the preference for an *anti*-periplanar transition state arises from minimizing dipole-dipole interactions in the  $\beta$ -hydroxyketone products. Hence, in our process, preference for an *anti*-periplanar process in our ruthenium chemistry could arise from destabilizing interactions between the amide carbonyl and ruthenium center.

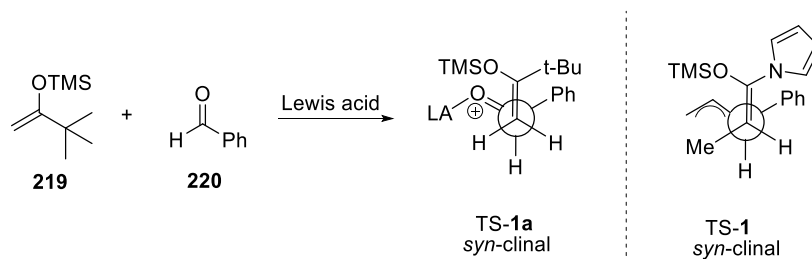


**Figure 28: Diastereoselectivity of Mukaiyama Aldol Reactions as Model of AAA Reaction**

In summary, the diastereoselectivity of the ruthenium-catalyzed AAA reaction arises from the preference of the alkylation event to occur *via* an *anti*-periplanar process. Hence, a simple, steric assessment of both possible *anti*-periplanar transition states, TS-2 and TS-5, reveal an obvious choice (Figure 29). The TS-2 structure has 3 distinct gauche interactions while TS-5 displays only 2 such interactions. Thus, *anti*-**187a** is formed at a much greater rate than *syn*-**187a**. However, it is crucial to

note that the system is sensitive to the inclusion of additional bulky substituents and thus modifications to the process may erode selectivity.

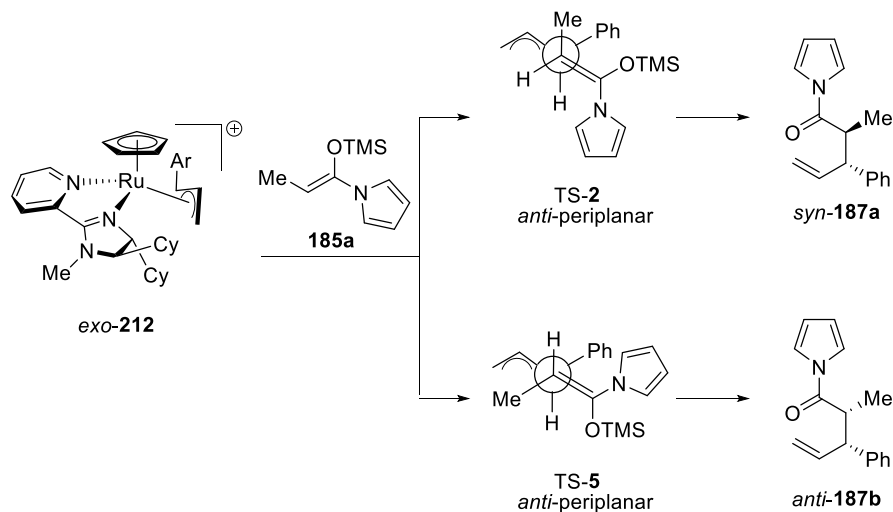


**Figure 29: Origin of Diastereoselectivity at C<sup>2</sup>**

### 3.6.3 Proposed Mechanism for the Ruthenium(II) Catalyzed AAA Reaction

The mechanism of the ruthenium-catalyzed AAA reaction follows a similar path as the rearrangement of allyl vinyl ethers (Figure 30). Complexation of ligand **201** and ruthenium precursor yields the diastereomer, complex **210**. Cinnamyl acetate **186** forms a complex with the ruthenium and boric acid to yield the ruthenium-olefin complex **221**. Subsequent oxidative addition produces the *exo*  $\pi$ -allyl complex *exo*-**221**, in contrast to the *endo* isomer suggested for allyl vinyl ether rearrangements. The TMS enol ether **185** is deprotected by acetate and attacks from the bound allyl from the *si* face to yield the ruthenium-amide complex **222**. Ligand substitution with MeCN reforms the active catalyst **210**. Based on our results with the ruthenium-catalyzed rearrangements of allyl vinyl carbonates, we can assume the reaction proceeds through practically identical mechanism however without the high degree of diastereocontrol exhibited by silyl enol ether nucleophile.

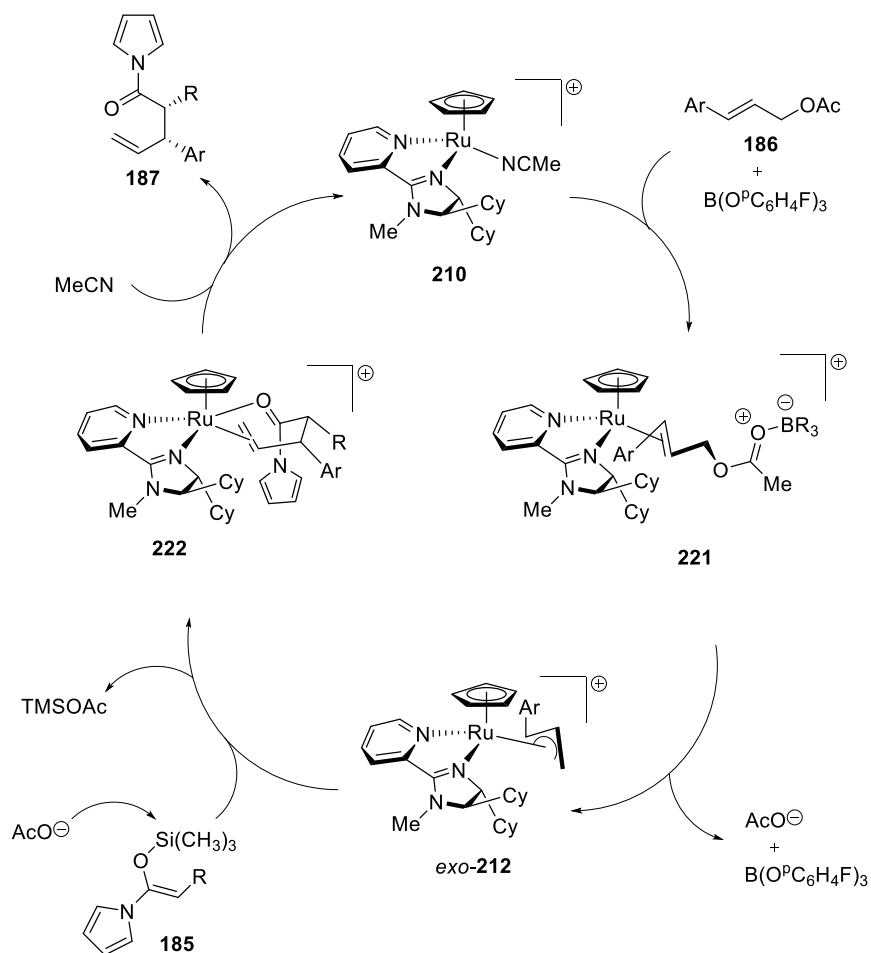


**Figure 30: Proposed Mechanism of Intermolecular Allylic Alkylation**

### 3.7 SUMMARY OF RUTHENIUM CATALYZED AAA REACTIONS

In summary, our group has developed a intermolecular, ruthenium(II) catalyzed asymmetric, allylic alkylation reaction. The reaction provides a complementary process to the ruthenium(II) catalyzed rearrangement of allyl vinyl ethers and carbonates. The AAA reaction proceeds with excellent regio- and enantioselectivity and moderate diastereoselectivity. The mechanism is virtually identical to that of carbonate rearrangements but distinct from that of ether rearrangement because of ligand dynamics. However, the AAA reaction has the greatest substrate scope and best potential for aliphatic variants.

The excellent results of the transformation warranted incorporation into the total synthesis of a natural product.

## 4.0 EFFORTS TOWARDS THE TOTAL SYNTHESIS OF ACTINORANONE

### 4.1 ACTINORANONE: A NEW, MESOTERPENOID NATURAL PRODUCT

We selected the potent, anticancer natural product actinoranone **223** as a target to assess the versatility of the ruthenium(II)-catalyzed asymmetric allylic alkylation (Figure 31). The stereocenter of the western, naphthalone portion **225** was set using our ruthenium chemistry and the penultimate, vinyltetrahydronaphthalone compound was isolated in 5 steps in 7.11% overall yield. It was our intent to introduce to second half *via* a diastereoselective alkylation of a chiral aldehyde (Figure 32). However, the eastern, terpenoid section **224** presented multiple problems and thus we were unable to achieve the complete natural product.

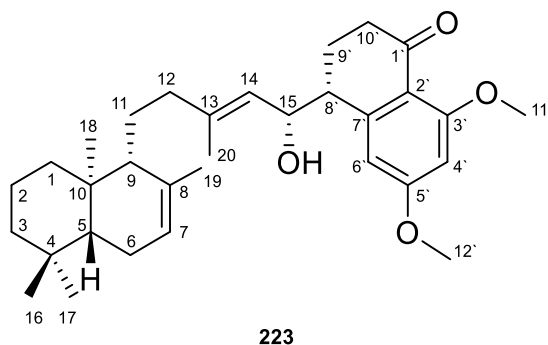


Figure 31: Proposed Structure of Actinoranone

#### 4.1.1 Actinoranone as a New Colorectal Cancer Therapeutic

Today, colorectal cancer is ranked among the most common cancers and unfortunately is highly susceptible towards metastasis.<sup>87</sup> Though early-stage colorectal cancer is often successfully treated with surgery, later-stage cases are plagued by reoccurrence.<sup>88</sup> Therefore, it is important to continue investigation into novel therapeutics to combat the disease. The meroterpenoid actinoranone,



isolated from the marine actinomycetes *Streptomyces marinus* strain CNQ-027 as a yellow oil, demonstrates remarkable 2  $\mu\text{g}/\text{mL}$  LD<sub>50</sub> cytotoxicity towards the HCT-116 human cancer carcinoma.<sup>89</sup> Such remarkable activity warrants further study. An effective, yet versatile, synthetic towards actinoranone and structural analogs will allow detailed study into the compounds mode of action and therapeutic potential.

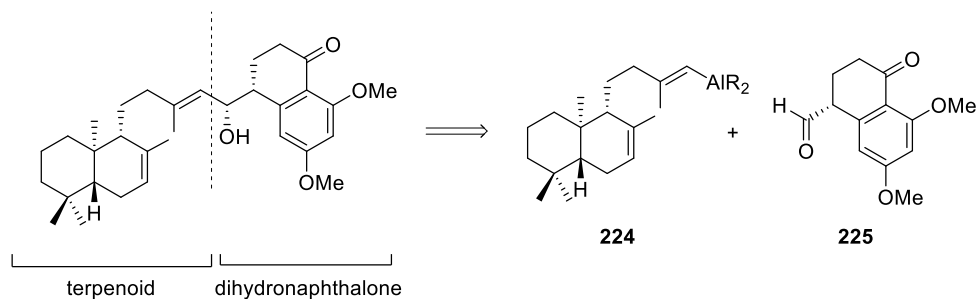


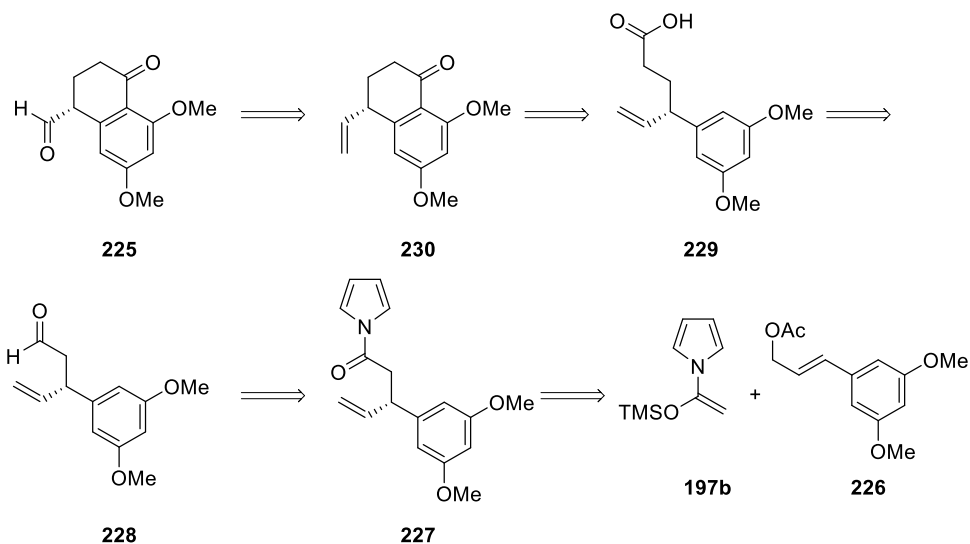
**Figure 32: Proposed Convergent Synthesis of Actinoranone**

## 4.2 SYNTHESIS OF THE WESTERN, NAPHTHALONE CORE

### 4.2.1 Retrosynthetic Analysis of Naphthalone Half

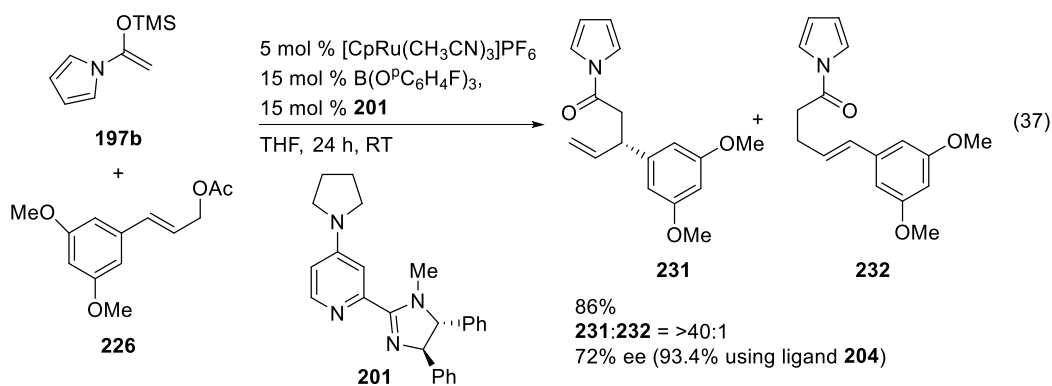
We envisioned setting the stereochemistry of the C1'-C12' naphthalone core using our ruthenium(II)-catalyzed asymmetric alkylation chemistry (Scheme 7). Subjecting **185b** and **226** to optimized AAA conditions would yield the amide **227**. Esterification and reduction would give aldehyde **228**. Subjecting the aldehyde to Wittig homologation and oxidation provides acid **229** and upon subjection to Friedel-Crafts acylation conditions the naphthalone **230** would be realized. Lastly, ozonolysis would cleave the vinyl substituent, revealing aldehyde coupling partner **431**.

## Scheme 7: Retrosynthesis of Tetrahydronaphthalone Half 225

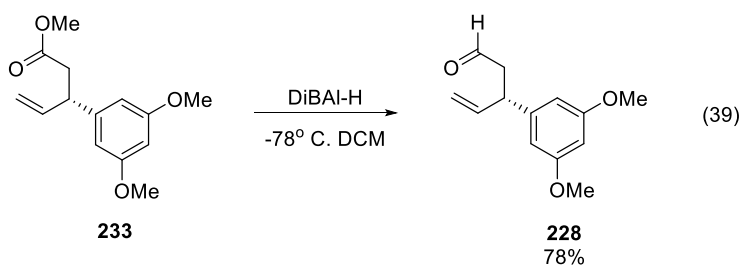
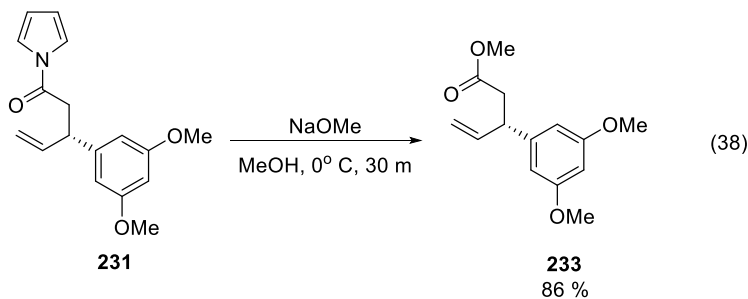


### 4.2.2 Application of Ruthenium(II) AAA Chemistry

The synthesis commenced using our ruthenium(II)-catalyzed AAA reaction of the acetate **226** and TMS enolate **197b**. Using the diphenyl **201** ligand, the desired amide **231** was produced in near-perfect regioselectivity for the branched product in a respectable 86% isolated yield (Eq 37). The selectivity is not surprising since electron-rich aromatic species routinely display strong regiochemical preference in our ruthenium chemistry. The easily-accessible ligand **201** translated to 72.0% ee; however, using cyclohexyl **204** improves the value to 93.4%.



The N-acyl pyrrole was converted to an aldehyde in a two-step process since direct addition of DiBAL-H to the amide results in a stable N,O acetal. Subjecting amide **231** to methoxide in methanol furnished the methyl ester **233** in 86% yield (Eq 38). Fortunately, the material is clean enough to be carried to the next stage without column purification. The ester was partially reduced using DiBAL-H providing the aldehyde **228** in 86% yield (Eq 39).

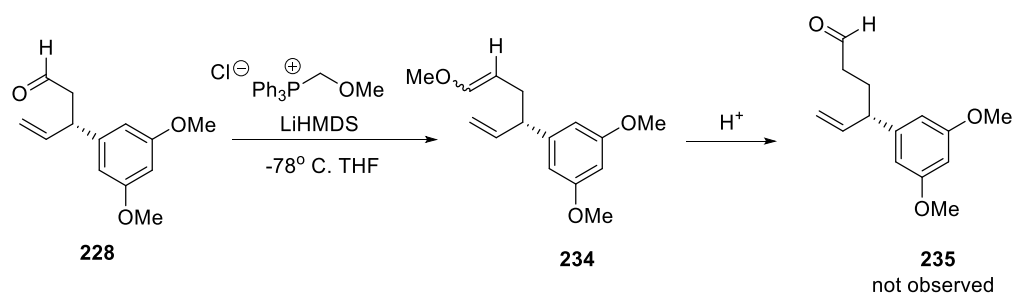


#### 4.2.3 Initial Attempt at a Wittig Homologation

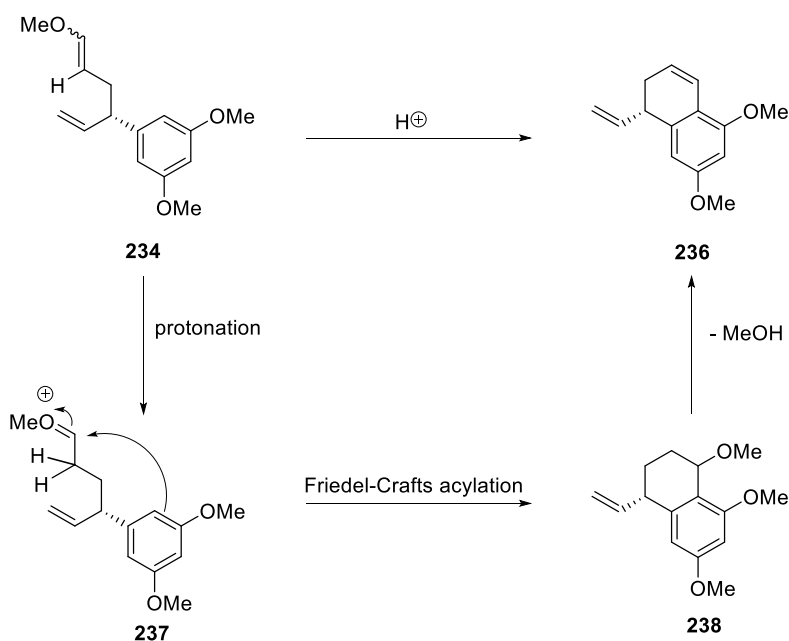
Our plan for the homologation of aldehyde **228** consisted of first converting the aldehyde to the homologated aldehyde **235** under Wittig conditions followed by mild oxidation to a carboxylic acid. The reaction of **228** with methoxymethyl(triphenylphosphonium) chloride provided the enol ether

**235**; however, standard deprotection procedures with dilute HCl did not yield expected aldehyde **235** (Scheme 8). We isolated the bicyclic compound **236** instead (Scheme 9). The undesired product results from a Friedel-Crafts reaction of the very electron-rich aromatic ring onto the intermediate oxocarbenium ion **238**. Subsequent elimination of MeOH from the cyclic alcohol **238** produced **236**. Regrettably, the natural product requires a carbonyl adjacent to the benzene ring and as such the loss of the oxygen functionality represented an unusable substrate as it would be difficult to chemically distinguish the unwanted vinyl group from the required vinyl substituent. Therefore, we sought a tandem homologation-oxidation procedure to eschew the formation of electrophilic intermediates.

### Scheme 8: Attempted Homologation of 228



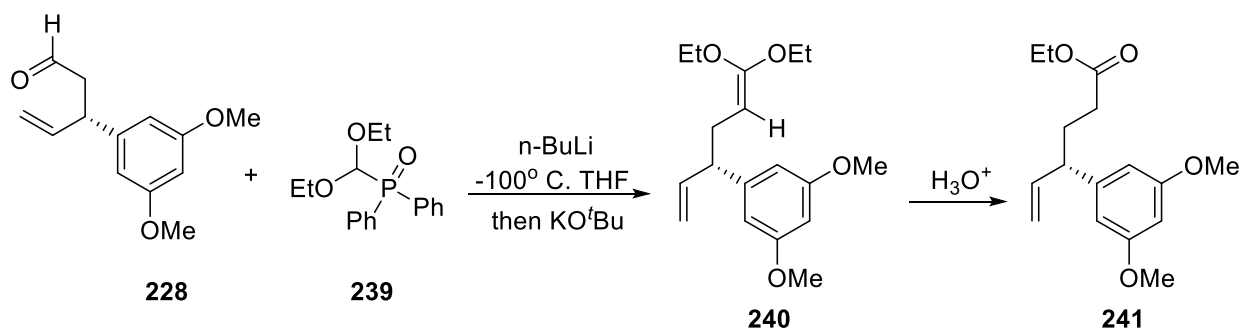
## Scheme 9: Mechanism of Dihydronaphthalene 236 Formation



### 4.2.4 Attempts at Homologation-Oxidation Wittig Approach

Alternative homologation-oxidation procedures are uncommon because in most cases the two-step, process is cheaper and more facile. However, several specialized Wittig-type procedures can afford access to a homologated product. Our first approach entailed simply increasing the oxidation state of the phosphonium reagent by incorporation of an additional alkoxy substituent (Scheme 10).<sup>90</sup> The reagent (diethoxymethyl)diphenylphosphine oxide **239** reacted with strong base to produce extremely reactive anion which adds to the aldehyde. Treatment of the resulting alkoxide with potassium *tert*-butoxide promoted elimination of diphenylphosphinate to generate an isolatable O,O ketene acetal **240**. Hydrolysis ultimately produced the ester **241**. Despite our best efforts, we were only able to obtain small quantities of **241**. The reaction is very sensitive to temperature and experimental difficulties with thermal regulation made the reaction problematic to perform using standard synthetic techniques.

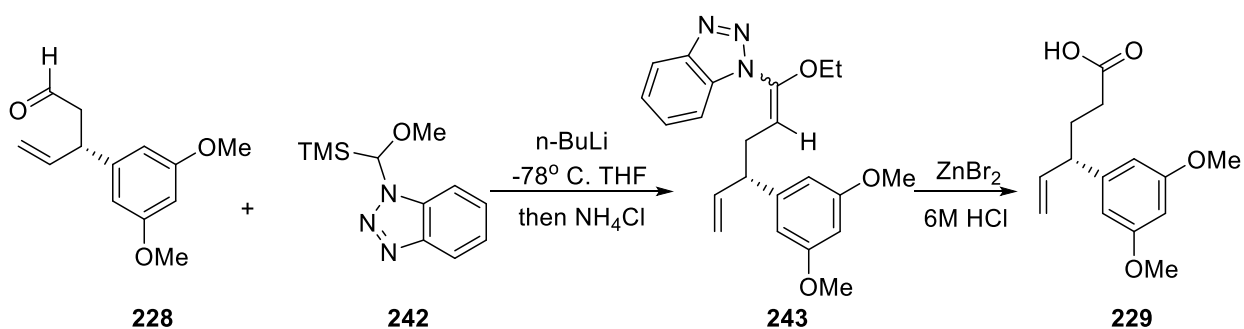
### Scheme 10: Wittig-Oxidation



### 4.2.5 Attempts at Peterson Olefination-Oxidation Approach

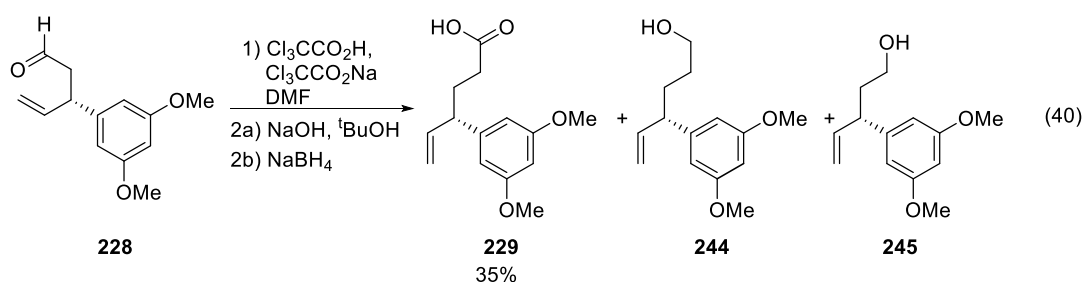
In similar fashion, we attempted a Peterson-type olefination approach (Scheme 11). The anion of benzotriazole (Bt) reagent **242** added to **234** to generate the N,O-ketene acetal **243**.<sup>91</sup> Treatment with zinc(II) bromide and acid affects hydrolysis to desired acid **229**. Surprisingly, the conditions also generate a small amount of the cyclized product **230**, owing to the large nucleophilicity of the aromatic ring. Despite simplified experimental parameters, the reaction is plagued by the stoichiometric formation of free benzotriazole. The amine was difficult to remove by column chromatography. Despite complicated isolate, we obtained a genuine sample of **229**.

### Scheme 11: Peterson Olefination-Oxidation

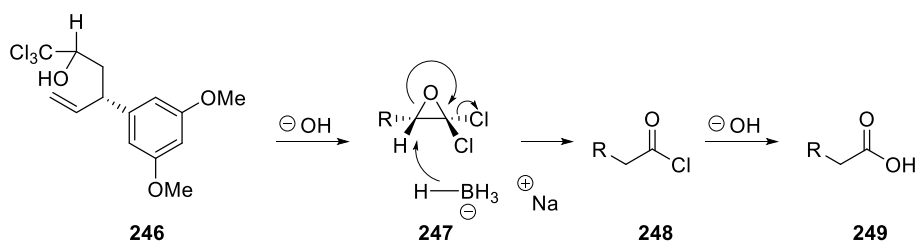


## 4.2.6 Homologation-Oxidation with a Jocic-type Reaction

We sought a different approach to the homologation through application of Jocic-type reactions (Eq 41).<sup>92-93</sup> In a first of a two-step procedure, aldehyde **228** is converted to trichloromethyl carbinol **246** by a Corey-Link reaction.<sup>94</sup> The crude intermediate was treated with base and borohydride in *tert*-butanol first yielding epoxide **247**. Nucleophilic attack by hydride results in acid chloride **248** which yields the desired homologated acid **249** after hydrolysis (Scheme 12). The procedure yielded the desired product in only 35% yield. Two other major products were isolated and proved to be inseparable by column chromatography. GC-MS analysis revealed the products to be **244** and **245**. Alcohol **245** resulted from reduction of aldehyde **228** formed from by reverse expulsion of trichlorocarbanion. The homologated alcohol forms from reduction of acid chloride **248** before hydrolysis can occur. Yields can be increased in future runs by using a selenium-mediated reduction.<sup>92</sup>

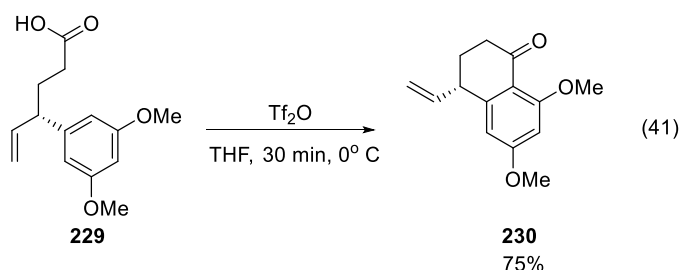


Scheme 12: Mechanism of Jocic-type Homologation



At the current juncture, we envisioned a Friedel-Craft acylation would efficiently provide the naphthalone **242**. The highly electron-rich aromatic ring had already exhibited remarkable nucleophilic

in our homologation attempts. Modern methods show that trifluoromethanesulfonic acid anhydride ( $\text{Tf}_2\text{O}$ ) can be used in place of  $\text{SOCl}_2$  and  $\text{AlCl}_3$  to promote the reaction.<sup>95</sup> Acid **229** cyclized to desired **230** quickly under  $\text{Tf}_2\text{O}$  conditions in 75% yield (Eq 41).



Ketone **242** represented the penultimate compound in the synthesis of the dihydronaphthalone core. Oxidative cleavage of the pendant vinyl substituent will reveal an aldehyde, upon which the diastereoselective nucleophilic addition of the terpenoid half will occur. However, the compound was stored as the vinyl compound to lessen the chance for oxidative decomposition. The desired aldehyde would be susceptible to enolization, and thus, racemization at the valuable chiral center. Overall, **230** was produced in 5 steps in 7.11% yield from cinnamyl acetate **226**. The ee of the final product was a modest 72% but substitution for the more selective cyclohexyl ligand **204** would raise the value to 93%. In addition, further optimization of the homologation process would contribute the greatest increase in the yield.

### 4.3 INITIAL EFFORTS TOWARDS THE SYNTHESIS OF TERPENOID HALF

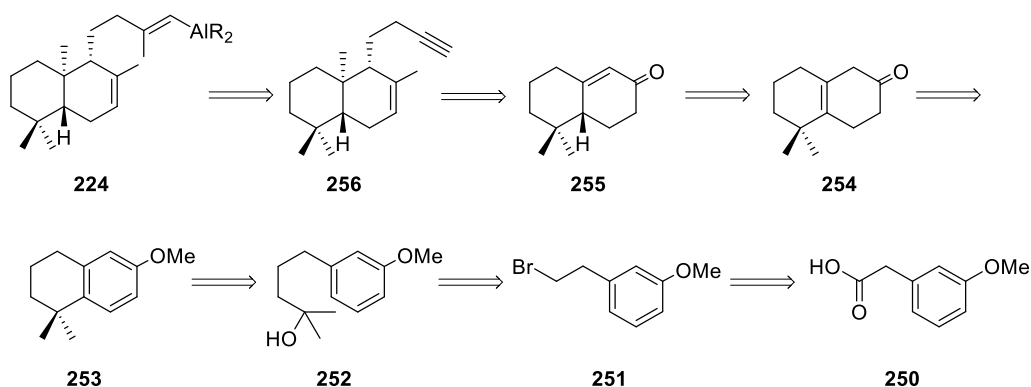
#### 4.3.1 First Retrosynthetic Analysis of Terpenoid Portion

As previously discussed, our intent was to realize the synthesis of actinoranone by a Felkin-Ahn addition of a vinyl organometallic reagent **236**, likely aluminum, into aldehyde **243** to yield the requisite allylic alcohol (Scheme 13).<sup>96-97</sup> The process begins with the reduction and bromination of commercially-available acid **263**. Grignard addition of the halide into dimethyloxirane would give the



tertiary alcohol **266**. Intramolecular, acid-mediated, Friedel-Crafts alkylation of **265** results in the naphthalene-type structure **266**. Subsequent reduction under Birch conditions yields  $\beta,\gamma$ -unsaturated ketone **267**. An asymmetric, iridium(I)-catalyzed isomerization would set the chirality of resulting enone **268**. Tandem conjugate-addition followed by enolate alkylation would yield the alkyne **269**. Finally, treatment of the terminal alkyne with tris(alkyl)aluminum or similar reagents would provide the organometallic **235**.

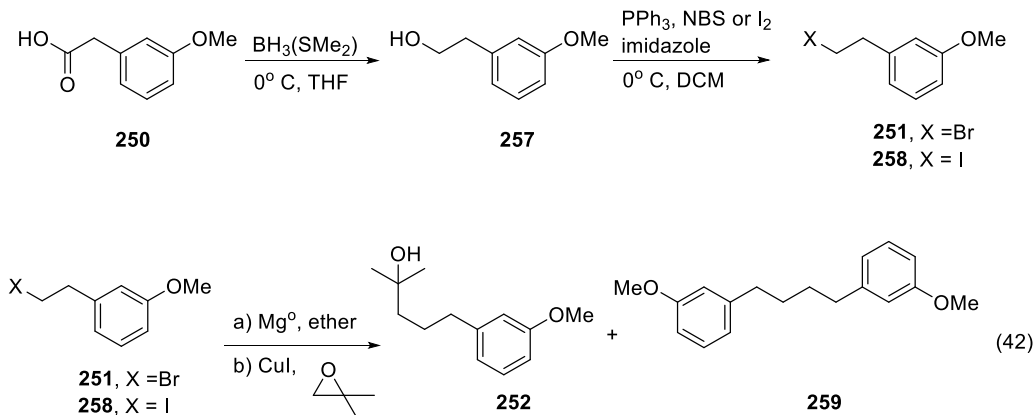
### Scheme 13: Retrosynthetic Analysis of Terpenoid Half 236



#### 4.3.2 First Synthetic Route: Synthesis of Tertiary Alcohol 252

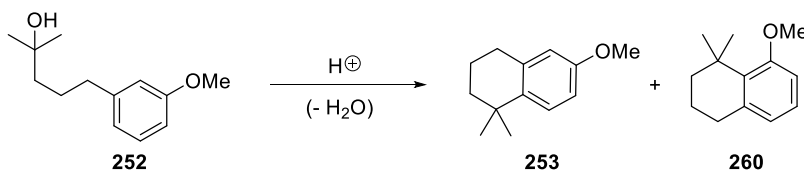
The organohalide **264** or **171** can be produced as the bromide or halide from the commercially available anisole derivative **263** (Scheme 14). Reduction by  $\text{BH}_3(\text{SMe}_2)$  yields alcohol in near quantitative yields.<sup>98</sup> Treatment with  $\text{PPh}_3$  and NBS or  $\text{I}_2$  furnishes the requisite organohalide.<sup>99</sup> The organobromide **251** was treated with magnesium and  $\text{CuI}$  to yield a nucleophilic organocuprate reagent which adds to dimethyloxirane (Eq 42).<sup>100</sup> Despite our best efforts, yields of **252** from the bromide were inconsistent despite reports of excellent (91%) yields.

### Scheme 14: Halogenation of Acid Precursor **250**



#### 4.3.3 Cyclization by Acid-catalyzed Friedel-Craft of a Tertiary Alcohol

Although the results for the epoxide addition were underwhelming, we decided to explore later synthetic steps. The tertiary alcohol **252** is an excellent substrate for a Friedel-Crafts alkylation to produce tetrahydronaphthalenes using  $\text{B}(\text{OTf})_3$  to initiate carbocation formation.<sup>101</sup> However, the cyclization can produce two regioisomers **253** and **260**.  $\text{B}(\text{OTf})_3$  affects the cyclization in 94% yield but only marginally prefers the **253** isomer over sterically demanding **260** in 1.5:1 ratio (Table 20, Entry 1). To maximize the steric differentiation, a bulky, polymeric acid catalyst can improve performance. Amberlyst® 15, a sulfonic acid-based resin, demonstrates activity in promoting Friedel-Crafts alkylations of tertiary alcohols.<sup>102</sup> Yet, exposure of alcohol **252** to the Amberlyst® conditions produced only moderate gains in regioselectivity increasing **253:260** to 2.5:1 (Table 20, Entry 2). The polymeric, polyphosphoric acid (PPA) also promotes tetrahydronaphthalene formation but is viscous and cumbersome to handle in the laboratory.<sup>100, 103</sup> Despite experimental difficulties, PPA drastically increased regioselectivity of the ring closing to 100:1 **253:260** in 70% yield (Table 20, Entry 3).

**Table 20: Cyclization of Tertiary Alcohol 252**

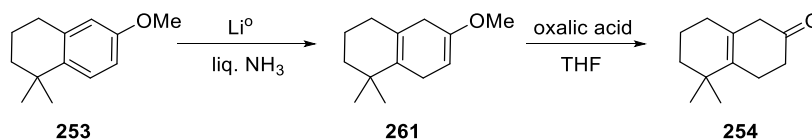
Entry	Acid	253:260 <sup>a</sup>	% yield
1	B(OTf) <sub>3</sub>	1.5:1	94
2	Amberlyst 15	2.5:1	N.D.
3	polyphosphoric acid (PPA)	100:1	70

<sup>a</sup> Determined by <sup>1</sup>H-NMR of the crude product mixture <sup>b</sup> N.D. = not determined

#### 4.3.4 Formation of Ketone 267 by a Birch Reduction

The tetrahydronaphthalene **266** was then reduced using Birch conditions (Scheme 15).<sup>104</sup> Our yields of ketone **254** were moderate and inconsistent, rarely exceeding 70% yield. Adding additional lithium metal or introducing the metal in portions failed to increase the reaction yield. Re-exposure of unreacted starting material was an undesired necessity.

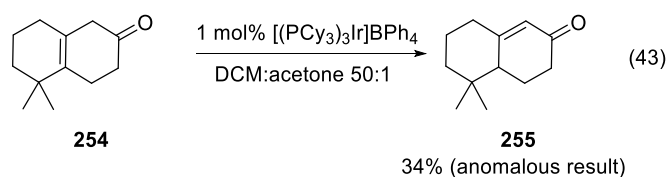
#### Scheme 15: Birch Reduction of Tetrahydronaphthalone 253



#### 4.3.5 Attempts to Use Iridium(I) Catalyzed Olefin Isomerization to Access Ketone

At the current point in the synthetic sequence, we endeavored to introduce asymmetry to the  $\beta,\gamma$ -unsaturated ketone **255**. Previous reports utilized a combination cinchona alkaloid-derived diamines and chiral  $\alpha$ -chloropropionic acid for the task.<sup>100</sup> In contrast, our intention was to set the chirality by means of iridium(I)-isomerization chemistry by substitution of tris(cyclohexyl)phosphine for an asymmetric bridged phosphine. Unfortunately, our basic, achiral conditions failed to adequately

provide useful results. The preliminary attempt at the isomerization of **254** resulted in a 34% yield of **255** using standard ICR conditions (Eq 43). Despite initial success, subsequent trails failed to replicate the initial yield of unsaturated ketone **255**. We varied reaction conditions such as phosphine loading and tested the effects of oxalic contamination from the Birch reaction workup to no avail. The likely explanation comes from the predisposition of the  $\beta,\gamma$ -unsaturated ketone **254** to rearrange to the thermodynamically stable **255** under ambient conditions. Our initial sample of **254** must have been exposed to excessive light or another undetermined factor which resulted in the false positive.



At the current juncture, the proposed route had become too cumbersome to adequately produce the material we needed. To begin, the results from the oxirane addition were erratic and the Birch reduction failed to completely reduce the aromatic ring translating to frustrating supply issues. However, we would have opted to improve the syntheses if we would have been able to successfully utilize iridium(I) isomerization techniques. Therefore, a new strategy was deemed necessary.

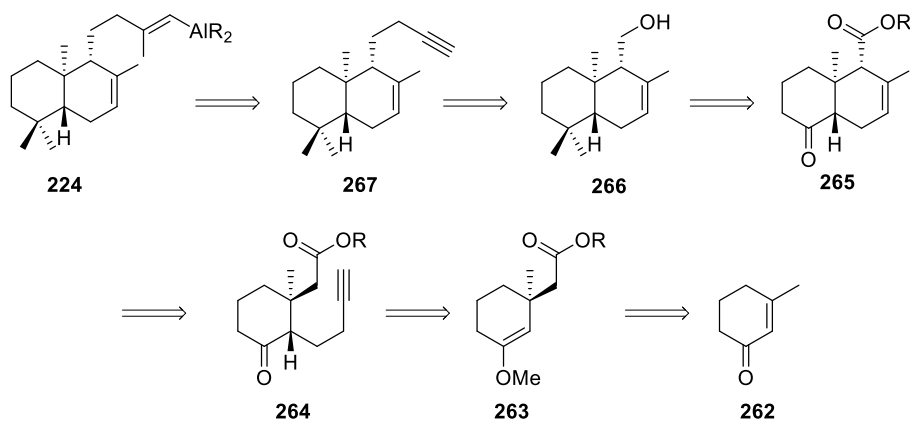
#### 4.4 SECOND SYNTHETIC APPROACH: DOUBLE ALKYLATION OF A SUBSTITUTED CYCLOHEXENONE

Upon reexamination of the terpenoid portion of actinoranone, we focused on the stereochemistry of the decalin system. The bicycle is a *trans*-decalin system which possesses greater stability than the *cis*-diastereomers. Therefore, if stereochemistry at the quaternary, bridgehead carbon of the decalin is established, the second can then be formed by allowing the system to reach thermodynamic equilibrium under acid or base-catalyzed conditions.

#### 4.4.1 Second Retrosynthetic Analysis of Naphthalone Half

The new synthetic sequence will begin with methylcyclohexenone **262** (Scheme 16). The requisite stereocenter will be set by an asymmetric Michael addition, followed by capping of the resultant enolate to give **263**.<sup>105-106</sup> Alkylation of the masked enolate gives disubstituted **264**. The decalin system is then constructed by the Au(I)-mediated cyclization of an enolate onto an alkyne producing **265**.<sup>107-109</sup> Reduction of the ester and a Rietz alkylation of the ketone furnish alcohol **266** and allow for any necessary equilibration to the desired decalin diastereomer.<sup>110</sup> Finally, the alcohol can be converted to an alkyne **267** to furnish the vinylaluminum **224**.

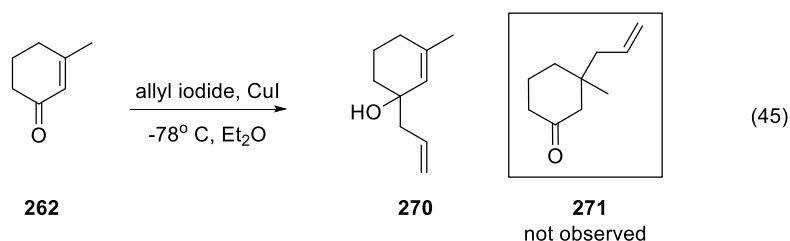
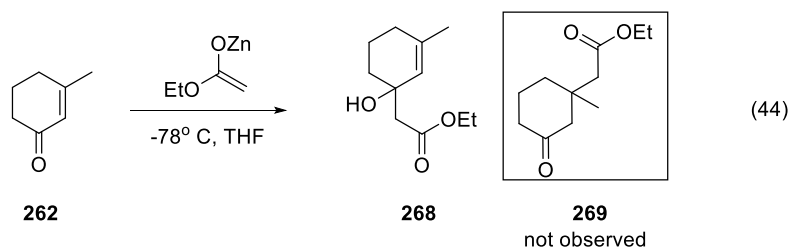
Scheme 16: Revised Retrosynthetic Analysis of Terpenoid Half **224**



#### 4.4.2 Initial Attempts at a Conjugate Addition

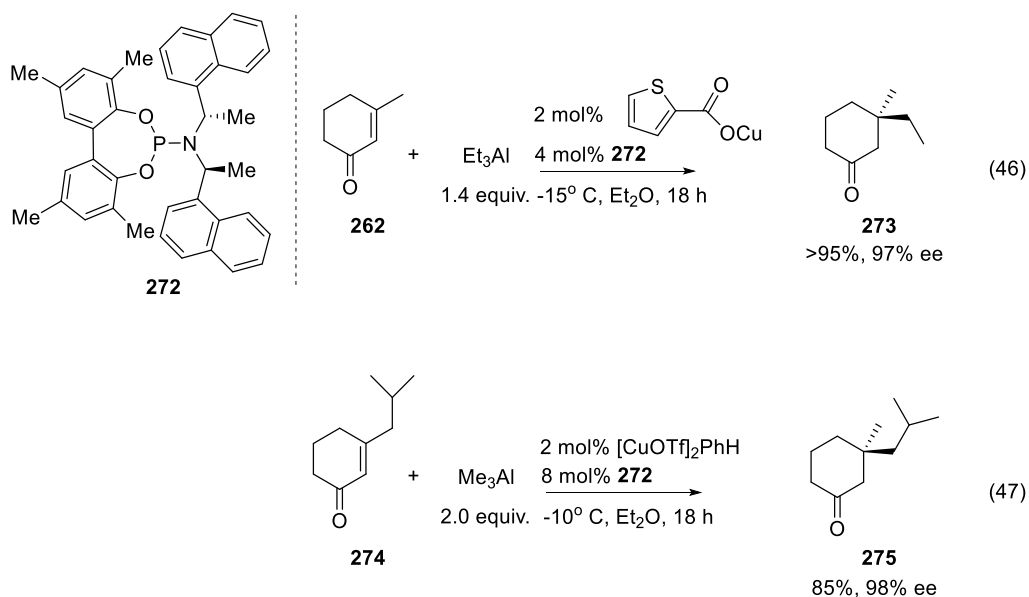
To start the new approach, methylcyclohexenone **262** was treated with zinc enolate of ethyl acetate. Unfortunately, the desired 1,4-alkylated product **269** was not detected but only the 1,2 product **268** (Eq 44). The steric hindrance from the methyl group must disrupt the requisite transition-state for the conjugate addition. Further tests demonstrate that traditional Gilman reagents derived from allyl iodide also demonstrate selectivity for the 1,2 product **270** over expected 1,4 conjugate addition

product **271** (Eq 45). Clearly, the methyl group presents a major steric obstacle to the synthetic plan. The problem may be avoided by reversing the order of substitution by adding the ester functionality first, followed by the methyl group.



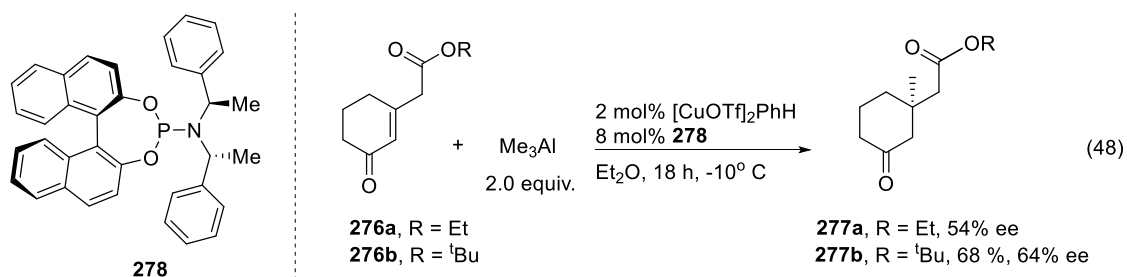
#### 4.4.3 Alternative Strategies to Sterically-Congested Conjugate Additions

There are many examples of asymmetric, 1,4-additions of simple alkyl groups to sterically-congested enones.<sup>105-106</sup> Copper(I)-complexes catalyze the conjugated addition of (tris)alkylaluminium to enones. The reaction effectiveness is highly dependent ligand and copper source. Of particular interest are phosphoramidate ligands which possess a strong record of asymmetric induction and easily-modified structure.<sup>111</sup> The absolute chemistry of the ultimate decalin system will depend on good enantioselectivity. For example, enone **262** can be successfully alkylated with  $\text{Et}_3\text{Al}$  catalyzed by thiophenecarboxylate(TC) copper(I) and phosphoramidate **272** to yield the cyclohexanone **273** (Eq 46)). The reaction still progresses as steric crowding is increased. The isobutyl-substituted **274** undergoes alkylation utilizing a benzene-copper(I) source and ligand **272** to yield the substituted **275** (Eq 47). Therefore, if the ester functionality is installed first, there is ample evidence to indicate the conjugate addition of the methyl group can be both regio- and enantioselectively.



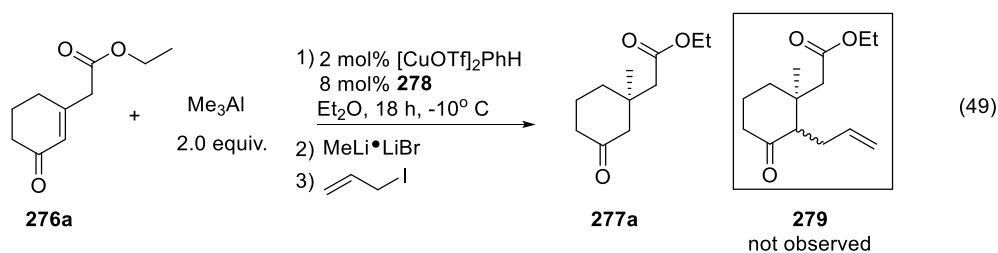
#### 4.4.4 Synthesis and Investigation of Keto Ester 288

The known keto-ester **276** was prepared by a two-step process by the addition of a cerium(III)-enolate of an acetate to cyclohexenone followed by a PCC-mediated rearrangement.<sup>112</sup> Our preliminary screenings indicated the copper(I) source,  $(\text{CuOTf})_2\text{PhH}$ , paired with phosphoramidate ligand **276** exhibited complete conversion in most cases (Eq 48). The ethyl ester **276a** produced methylated **277a** with 100% conversion however only moderate 54% ee. Increasing the sterics of the pendent ester could serve to help differentiate the transition states. Thus, the *tert*-butyl ester **276b** was found to improve enantioselectivity to 64% and while maintaining 100% conversion albeit with only 68% isolated yield of **277b**. Confident that the process could be further optimized as necessary, we decided to continue with the synthetic sequence to probe the enolate alkylation.



#### 4.4.5 Attempts at in situ Enolate Alkylation

The successful, asymmetric construction of the quaternary carbon led to investigation of possible routes to alkylation of the  $\alpha$ -carbon. The intention was to simply exploit the aluminum enolate **280** produced during the conjugate addition. However, the strong Al-O bond of intermediate aluminum enolate reduces the nucleophilicity of the enolate.<sup>113-114</sup> To overcome poor reactivity, a transmetalation to a more reactivity lithium enolate can effectively solve the problem.<sup>105</sup> However, the poor regioselectivity exhibited by strong alkyl lithium reagents rendered the approach ineffective (Eq 49). Thus, we concluded that a two-step process was necessary. The enolate would be covalently trapped, and isolated before exposing the substrate to alkylation conditions.



#### 4.4.6 Trapping and Isolation of Aluminum Enolate

There are two proven routes available for O-alkylation of an aluminum enolate. The aluminum enolate **280** undergoes acylation or silylation resulting in isolatable species **281** and **282** (Figure 33).<sup>105</sup> Acetic anhydride exposure results in acetate **281** and similarly, TMSOTf provides silyl ether **282**. Each compound has a different reactivity profile. The acetate **281** will be easier to isolate but will



require harsher deprotection conditions. Conversely, **282** will be sensitive towards isolation but will likely undergo facile activation. Both methods were analyzed in our study.

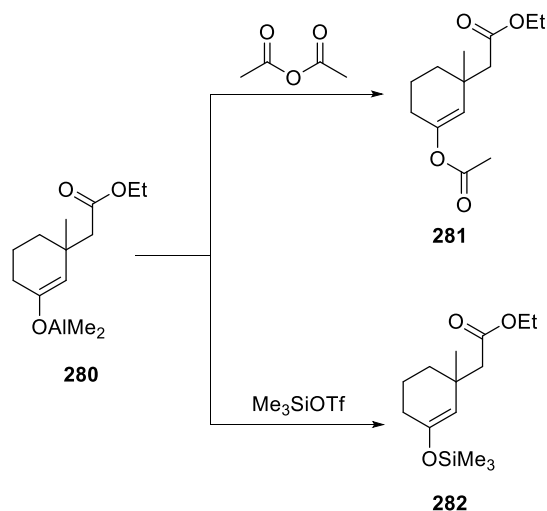


**Figure 33: Strategies for Trapping of Aluminum Enolate**

#### 4.4.7 Studies of Silyl Enol Ether **282**

Despite our concerns, introduction of TMSOTf in the conjugate addition to **276a** yielded the methylated, silyl enol ethers **282** in 70% yield (Eq 50).<sup>105</sup> Contrary to our predications, the silyl moiety proved unsuitable for the alkylation process. Treatment with MeLi led to decomposition which was not surprising given the multiple base-sensitive functionality (Table 21, Entry 1). Weaker nucleophiles LiCl and NaOAc were unable to promote desilylation (Table 21, Entries 2, 3). The common desilylation reagent TBAF successfully removed the TMS but the ensuing ammonium enolate would not undergo alkylation (Table 21, Entry 4). Now, we decided to focus on the enol acetate capping technique.

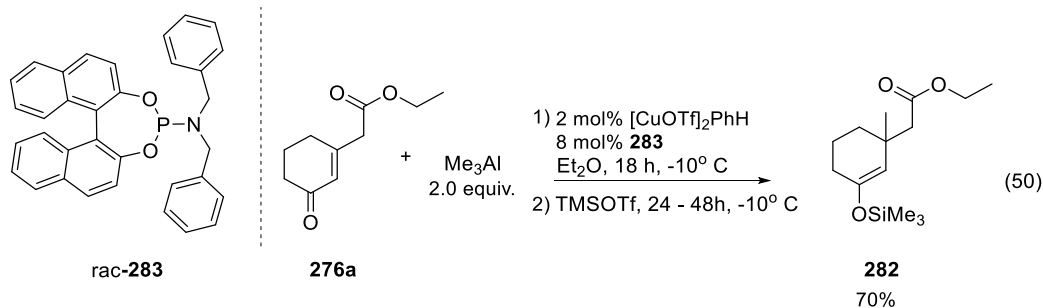
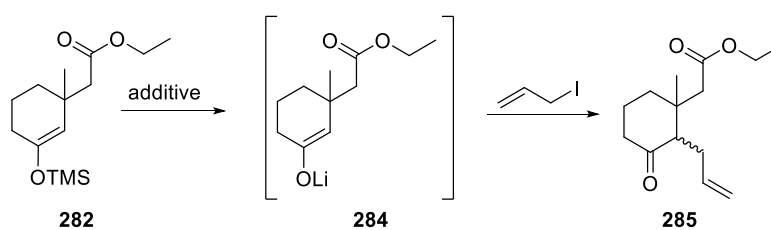


**Table 21: Attempts at Deprotection and Alkylation of Silyl Enol Ether 282**

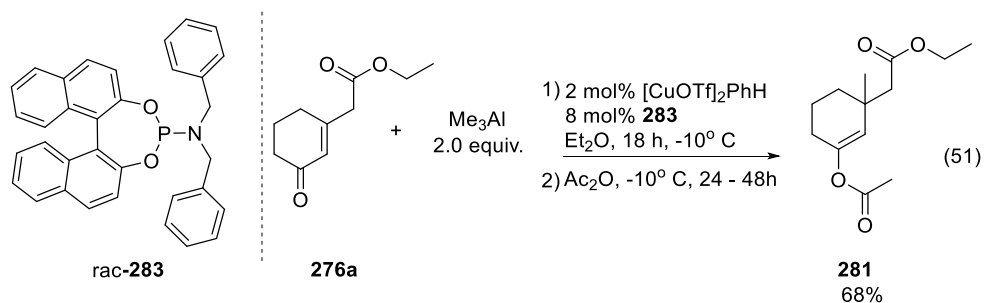


Entry	Reagent	Results
1	MeLi•LiBr	decomp
2	LiCl	no reaction
3	NaOAc	no reaction
4	TBAF	successful deprotection, no alkylation product observed

#### 4.4.8 Studies of Vinyl Acetate 281

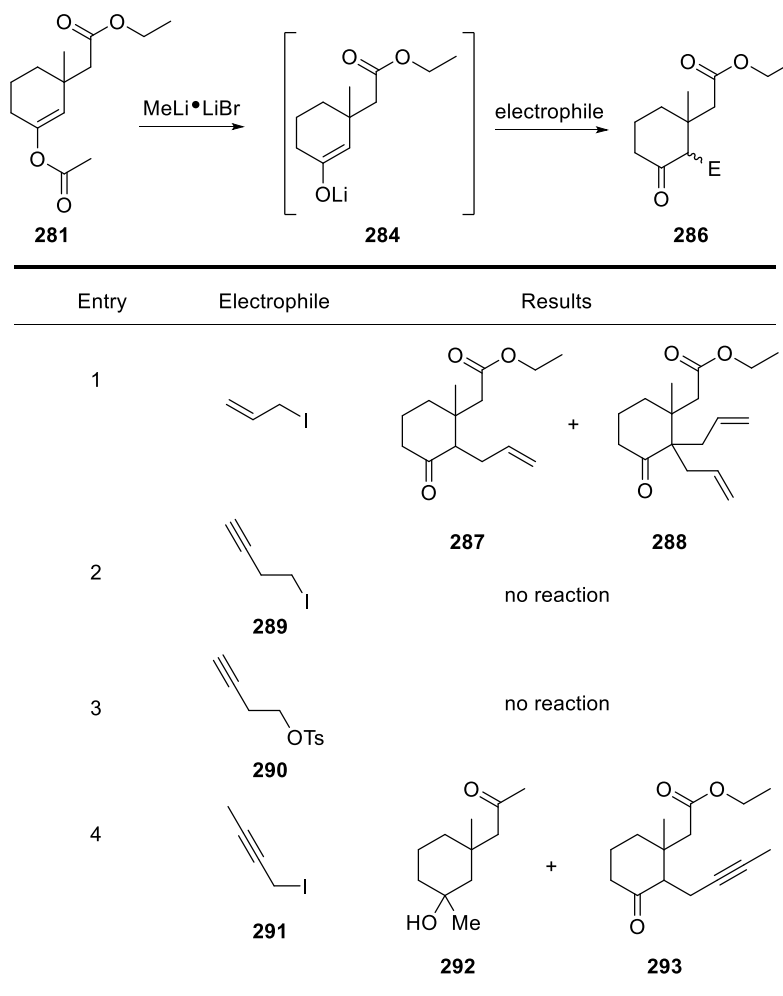
Fortunately, the racemic vinyl acetate **281** was accessed without incident from ketone **276a** in 68% yield (Eq 51). Traditionally, activation of enol acetates requires two equivalents of MeLi•LiBr to suppress regiochemical issues resulting from enolate equilibria and other side product formation.<sup>116</sup> One equivalent adds to the acetate to expose a reactive lithium enolate and the second converts the resultant acetone to a *tert*-butoxide. However, the reactive ester functionality in **281** raises an issue of chemoselectivity using excess alkyllithium. However, some examples indicate a signal equivalent of

MeLi suffices and that lithium *tert*-butoxide is sufficient to deprotect the enolate.<sup>117</sup> In either case, double alkylation remained the dominant minor product.



The enol acetate **281** was now to be alkylated using several typical electrophiles using a single equivalent of MeLi (Table 221). Exposure of **281** to allyl iodide successfully generated the desired alkylated product **287** and dialkylated **288** (Table 22, Entry 1). Encouraged by the successful result, the allyl iodide was exchanged for desired homopropargyl iodide **289** which ultimately produced no alkylated product (Table 22, Entry 2). Use of homopropargyl triflate **290** suffered the same results (Table 22, Entry 3). After some consideration, we reasoned that the homopropargyl substrates were instead undergoing an E2 process producing volatile but-1-en-3-yne. The terminal alkyne was necessary to the synthetic plan to ensure regioselectivity in the later gold(I)-mediated cyclization. An alternative halide, 1-iodo-2-butyne **291** reacted to produce some amount of the sought-after **293** but methylated product **292** dominated (Table 22, Entry 4).

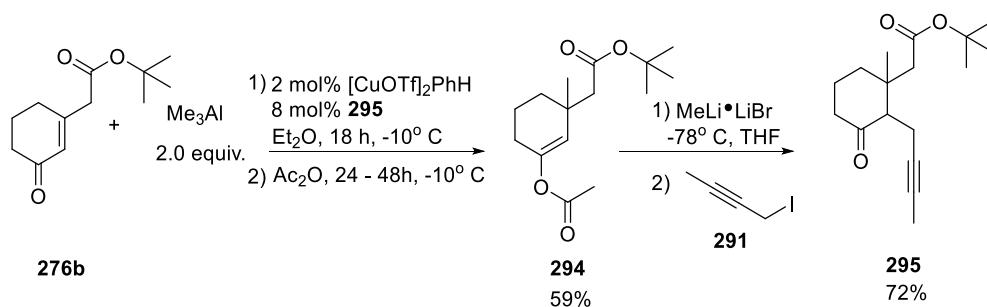
**Table 22: Deprotection and Alkylation of Acetate 281**



#### 4.4.8 Improving Alkylation Selectivity with Increased Sterics

Increasing the steric crowding of the ester functionality will subdue nucleophilic attack of the ester carbonyl. The racemic, *tert*-butyl enol acetate **294** was produced from **276b** in identical fashion as **281** in 59% yield. Pleasingly the reaction of **294** and 1-iodobut-2-yne **291** yielded the desired alkylated product **295** in 72% yield (Scheme 17). Despite the good outcome, the alkyne group was not in the ideal position required for the gold-catalyzed ring closing.

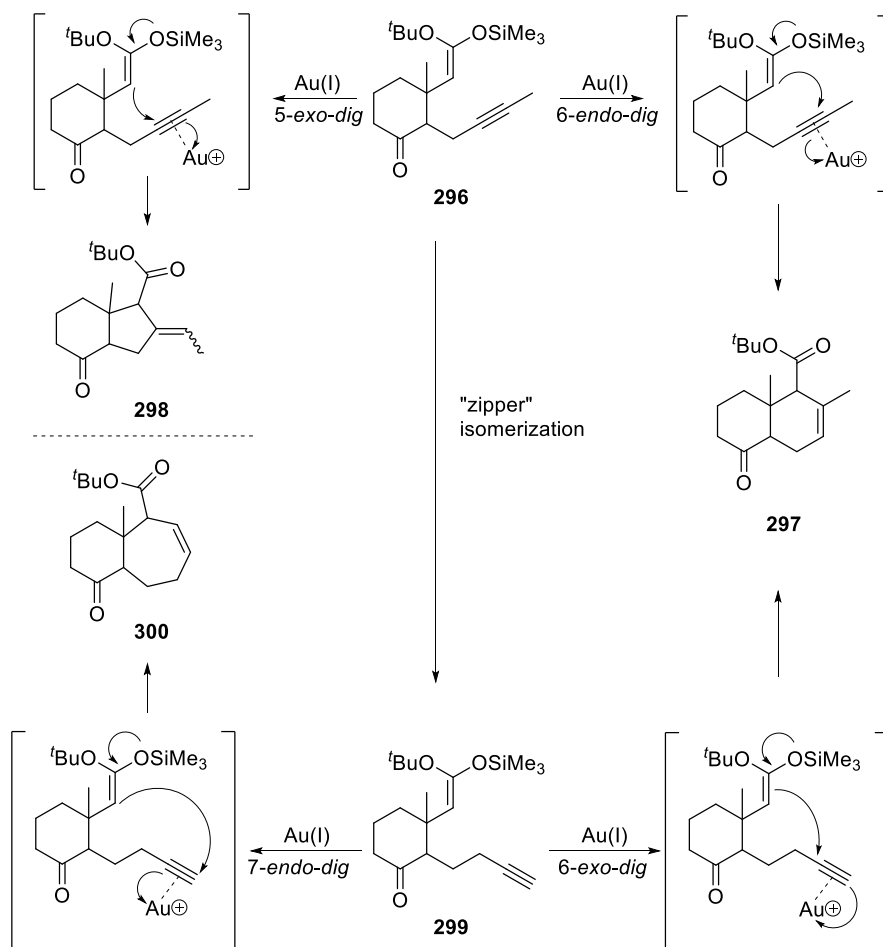
### Scheme 17: Double Alkylation of 276b via Acetate Trapping of Aluminum Enolate



#### 4.4.9 Planning the Au(I) Cyclization: Potential Regioselectivity Issues

The intention at the current stage of the project intended to convert keto ester **295** to silylated enolate **296**. Chemoselectivity between the ester and ketone could be limiting factor, however, the proposed order of the synthesis may be altered to alkylate the ketone before attempting the cyclization step. Once **296** is generated we intended to expose the silyl ether to Au(I) which activates the alkyne towards attack by the enolate carbon to form the decalin system (Scheme 18).<sup>108-109</sup> Unfortunately, the internal alkyne presents a competition between two favored cyclization pathways: a 5-*exo-dig* and a 6-*endo-dig*.<sup>108,</sup>  
<sup>118</sup> In this case, the 6-*endo-dig* produces the desired, thermodynamically-favored cyclohexyl structure **297**, but the 5-*exo-dig* forms faster resulting in the kinetically-favored cyclopentane **298**. Isomerization to the terminal alkyne would change the competition to be between 6-*exo-dig* and 7-*endo-dig* ring closing reaction. Both pathways are also favored by Baldwin's rules; however, there is a strong kinetic, and thermodynamic, preference for the 6-membered carbocycle **397** over the 7-membered **300**.

### Scheme 18: Gold(I) Catalyzed Cyclization of Alkynes 296 and 299



#### 4.4.10 Application of the Alkyne Zipper Reaction

To accomplish the alkyne isomerization, an alkyne “zipper” isomerization was attempted. The technique utilizes anionic, 1,3-diaminopropane which mediates a proton-transfer with internal alkynes to generate allenes, which in turn react to produce an alkyne (Figure 34). When a terminal alkyne is produced, rapid deprotonation of the acidic, alkynyl hydrogen renders the substrate and diamine unreactive. Unfortunately, exposure of the internal alkyne **308** to alkyne isomerization conditions was met with formation of many unidentifiable side reactions and no observed formation of **314** (Eq 52). Under the strongly basic condition, we assumed the amide base reacted with enolizable protons resulting in multiple, undesired aldol-type reaction pathways.

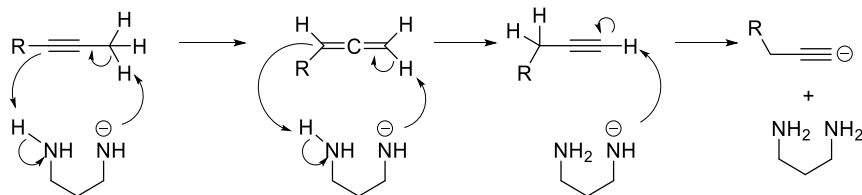
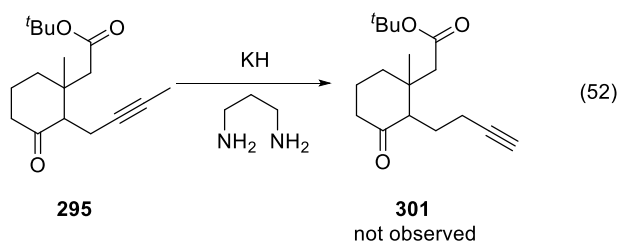


**Figure 34: Mechanism of Alkyne Zipper Isomerization**



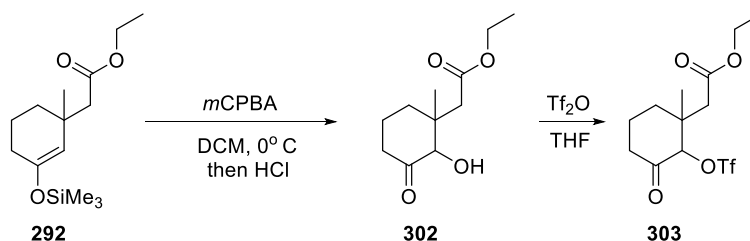
The unsuccessful isomerization attempt of **295** made us realize the current route was untenable. The iodide **291** remained a difficult substance to purify and handle. We were limited to isolating the substance as solutions in pentanes. Although many aspects of the current route were mediocre, we felt that ample study would resolve issues. Yet, the difficulty in procuring the necessary alkylating reagents imposed a need for an alternative strategy

#### 4.4.11 A Cross-Coupling Approach

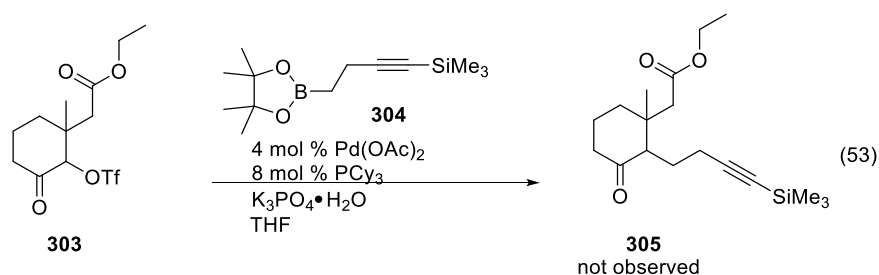
An alternative approach to installing the alkyne could be found using a transition-metal mediated alkylation. A Rubottom reaction would allow for the installation of an alcohol at the  $\alpha$ -carbon resulting in hydroxyketone **302**.<sup>119</sup> The hydroxyl group can be functionalized as a triflate to serve as a carbon source in a coupling reaction. A Suzuki-type coupling of a triflate and boric acid may promote the bond forming reaction. Thus, treatment of silyl ether **294** with *m*CPBA led to moderate yields of  $\alpha$ -hydroxy ketone **315** which was easily silylated under  $\text{TiF}_2\text{O}$  conditions to yield triflate **316** (Scheme 19).

Unfortunately, **316** is very sensitive and yields were erratic due to decomposition encountered during purification.

### Scheme 19: Synthesis of Suzuki Coupling Partner 303



The coupling partner, boroalkyne **304** was synthesized according to literature procedure.<sup>120-121</sup> Exposure of **303** to the borate under Suzuki conditions did not lead to the desired alkylated product **305** (Eq 53).<sup>122</sup> Interestingly, even the mild basic conditions are incompatible as evident by hydrolysis of both the borate and triflate functional groups. Confronted with multiple synthetic obstacles, we determined the Au(I)-catalyzed was not suitable for the construction of the decalin system.



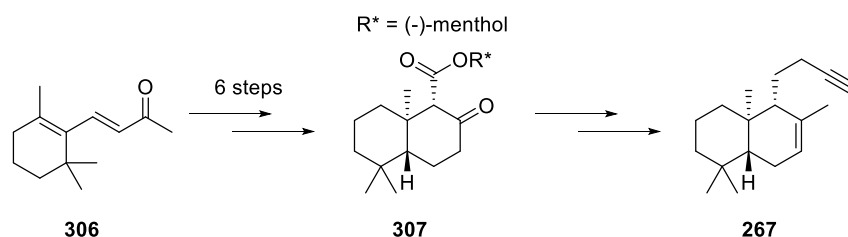
## 4.5 FUTURE EFFORTS

Our efforts towards the synthesis of the actinoranone decalin system were met with discouraging results. Exploring similar systems in the literature revealed that a *de nova* synthesis of an asymmetric decalin system are rare and often employ alternative strategies to access the desired stereocomplexity. One approach uses a racemic synthesis starting from  $\beta$ -ionone **306** followed by a chiral resolution



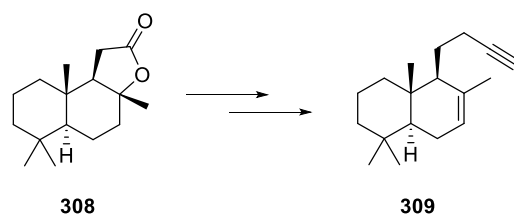
enabled by (-)-menthol to yield ketoester **307** (Scheme 20).<sup>123</sup> Our desired compound **267** could then be accessed by a few functional group conversions. Alternatively, one may employ a semi-synthetic method by exploiting the natural pool. Many projects have developed routes utilizing naturally occurring labdanes.<sup>124</sup> In particular, the natural (+)-scalerolide **308** possesses the correct relative configuration of stereogenic centers that would lead to the enantiomer of the desired decalin system **309** (Scheme 21).

### Scheme 20: Synthesis of **267** from $\beta$ -ionone



A racemic synthesis and resolution is highly uneconomical but would ultimately provide the stereochemistry encountered in the naturally-occurring substance and allow further biological testing to take place. Furthermore, we suspect the naphthalone portion of actinoranone is responsible for the biological activity and the terpenoid fragment serves to increase lipid permeability. Therefore, the overall effect of stereochemistry in the lipid fragment may even be negligible in the end. Regardless, either reaction scheme would allow optimization of the untested vinylaluminum-aldehyde coupling step to complete the final structure. However, from a synthetic point of view, both methods are relatively uninteresting. But the modular synthetic design provides a convenient way to introduce alternative terpenoid scaffolds and assess how the structural changes affect biological activity of the complete actinoranone system.

**Scheme 21: Synthesis of Enantiomeric 309 from (+)-Scalerolide**



## 5.0 CONCLUSION

In conclusion, our group has developed three ruthenium(II) catalyzed transformations resulting in enantioenriched products containing vicinal stereocenters. The iridium(I) catalyzed isomerization of di(allyl) ethers and carbonates allows access to allyl vinyl ethers and carbonates. The rearrangement of allyl vinyl carbonates proceeds with excellent regio- and enantioselectivities but poor diastereoselectivity and substrate scope. In contrast, the reaction of allyl vinyl ethers offers excellent diastereoselectivity resulting from an intramolecular transition state while maintaining respectable radiochemistry. Still, the transformation suffers from substrate scope limitations and poor results from aliphatic substrates. The intermolecular, ruthenium catalyzed asymmetric alkylations of allyl acetates with silyl enol ethers improves upon the earlier reactions. Overall, the reaction maintains excellent regio- and enantioselectivity, decent diastereoselectivity, and easier access to starting materials.

The AAA reaction was used to set the quintessential stereocenter of the potential cancer therapeutic, actinoranone. The penultimate, terpenoid half was synthesized in 7.11% yield in 6 major steps, leaving the vinyl group in place to prevent epimerization. In future work, the vinyl group will be cleaved to reveal an aldehyde coupling partner. In addition, the flexibility of the AAA methodology will allow the incorporation of a variety of substituents contributing to a potential library of analogs for medical screening. Despite successful synthesis of the dihydronaphthalone half, the synthesis of the terpenoid aliphatic portion was extremely difficult. Regardless of our best efforts, we were unable to form the required decalin system. However, examples of similar structures in chemical literature use racemic syntheses and asymmetric resolution or utilize the chiral pool. Hence, we are confident that future efforts in the Nelson laboratory will allow us to access to a tunable, reliable synthesis of actinoranone.

## SUPPORTING INFORMATION

### GENERAL INFORMATION:

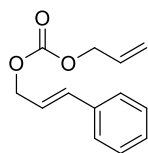
Unless otherwise indicated, all reactions were performed in dry glassware under an atmosphere of oxygen-free nitrogen using standard inert atmosphere techniques for the manipulation of both solvents and reagents. Anhydrous solvents were obtained by passage through successive alumina- and Q5-packed columns on a solvent purification system.  $[\text{CpRu}(\text{CH}_3\text{CN})_3]\text{PF}_6$  was synthesized according to the published procedure and was stored and weighed out in a nitrogen-filled glovebox. NMR spectra were recorded at the indicated magnetic field strengths with chemical shifts reported relative to residual  $\text{CHCl}_3$  (7.26 ppm) for  $^1\text{H}$  and  $\text{CDCl}_3$  (77.0 ppm) for  $^{13}\text{C}$  spectra. Analytical thin layer chromatography (TLC) was performed on 0.25 mm silica gel 60-F plates. Flash chromatography was performed over silica gel (230-240 mesh). Analytical gas chromatography (GC) was performed using a flame ionization detector and split mode capillary injection system using Varian Chirasil-Dex CB WCOT fused silica 25 m x 0.25 mm column (CP 7502). Analytical high-performance liquid chromatography (HPLC) was performed using a variable wavelength UV detector (deuterium lamp 190-600 nm) using a Chiracel OD-H column and HPLC-grade isopropanol and hexanes as the eluting solvents. Melting points were obtained on a Laboratory Devices Mel-Temp apparatus and are uncorrected.

### GENERAL PROCEDURE FOR THE FORMATION OF DI(ALLYL) CARBONATES

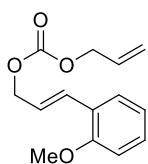
#### (GENERAL PROCEDURE A)

To a 0° C solution of alcohol A (1.0 equiv), and pyridine (2.5 equiv), in  $\text{Et}_2\text{O}$  (1.0 M), was added allyl chloroformate B (1.5 equiv) dropwise over 30 min. The resulting suspension was allowed to warm to ambient temperature, and stir overnight. The resulting suspension was filtered through celite, and washed with a saturated solution of  $\text{CuSO}_4$  (equal in volume to the reaction mixture). The organic

layer was dried over anhydrous MgSO<sub>4</sub>, solvent removed *in vacuo*, and the residue purified by column chromatography.

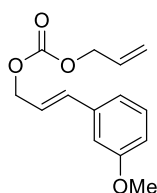


**Allyl cinnamyl carbonate (111):** General procedure A was followed employing cinnamyl alcohol (10.0 g, 74.5 mmol), pyridine (9.75 mL, 186.2 mmol) and allyl chloroformate (7.95 mL, 74.5 mmol) in Et<sub>2</sub>O. The crude product was purified by flash chromatography over silica gel (95:5 hexanes/EtOAc) to yield 14.8 g (91.1%) of the title compound as a colorless oil. <sup>1</sup>H NMR (300 MHz, CDCl<sub>3</sub>): δ 7.44-7.25 (m, 5H), 6.72 (d, *J* = 15.9 Hz, 1H), 6.33 (dt, *J* = 15.9, 6.6 Hz, 1H), 5.98 (app ddt, *J* = 17.1, 10.5, 5.7 Hz, 1H), 5.40 (dq, *J* = 17.1, 1.5 Hz, 1H), 5.30 (dq, *J* = 10.5, 1.2 Hz, 1H), 4.82 (dd, *J* = 6.6, 1.2 Hz, 2H), 4.67 (dt, *J* = 5.7, 1.2 Hz, 2H); <sup>13</sup>C NMR (75 MHz, CDCl<sub>3</sub>): δ 154.8, 135.9, 134.7, 131.5, 128.5, 128.1, 126.6, 122.3, 118.8, 68.4, 68.3; IR  $\nu_{\text{max}}^{\text{neat}}$  cm<sup>-1</sup>: 3059, 2950, 2887, 1746, 1650, 1449, 1256, 955; HRMS (EI) *m/z* calcd for C<sub>13</sub>H<sub>14</sub>O<sub>3</sub> (M)<sup>+</sup>: 218.0943; found: 218.0942.



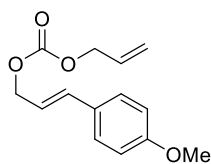
**(*E*)-Allyl 3-(2-methoxyphenyl)allyl carbonate (131b):** General procedure A was followed employing (*E*)-3-(2-methoxyphenyl)prop-2-en-1-ol (9.73 g, 59.3 mmol), pyridine (7.77 mL, 148.5 mmol) and allyl chloroformate (6.32 mL, 59.3 mmol) in Et<sub>2</sub>O. The crude product was purified by flash chromatography over silica gel (95:5 hexanes/EtOAc) to yield 12.0 g (81.6%) of the title compound as a colorless oil. <sup>1</sup>H NMR (300 MHz, CDCl<sub>3</sub>): δ 7.44 (dd, *J* = 7.5, 1.5 Hz, 1H), 7.27 (dt, *J* = 6.0, 1.5 Hz, 1H), 7.03 (d, *J* = 15.9 Hz, 1H), 6.94 (t, *J* = 7.5 Hz, 1H), 6.88 (d, *J* = 8.1 Hz, 1H), 6.34 (dt, *J* = 15.9, 6.3 Hz, 1H), 5.96 (app ddt, *J* = 16.2, 10.5, 5.7 Hz, 1H), 5.38 (dd, *J* = 17.1, 1.2 Hz, 2H), 5.28 (dd, *J* = 10.5, 1.2 Hz, 1H), 4.82 (dd, *J* = 6.6, 1.2 Hz, 2H), 4.66 (dd, *J* = 5.7, 1.2, 2H), 3.85 (s, 3H); <sup>13</sup>C NMR (75 MHz, CDCl<sub>3</sub>): δ 156.8, 154.7, 131.5, 129.8, 129.1,

127.1, 124.8, 122.8, 120.4, 118.7, 110.6, 68.9, 68.3, 55.2; IR  $\nu_{\max}^{\text{neat}}$   $\text{cm}^{-1}$ : 2938, 2838, 1747, 1598, 1462, 1249, 953; HRMS (EI)  $m/z$  calcd for  $\text{C}_{14}\text{H}_{16}\text{O}_4$  ( $\text{M}^+$ ): 248.1048; found: 248.1051.



**(E)-Allyl 3-(3-methoxyphenyl)allyl carbonate (131c):** General procedure A was followed employing (*E*)-3-(3-methoxyphenyl)prop-2-en-1-ol (1.96 g, 12.0 mmol), pyridine (2.89 mL, 35.9 mmol) and allyl chloroformate (1.90 mL, 17.9 mmol) in  $\text{Et}_2\text{O}$ .

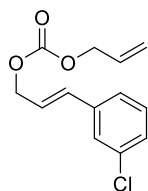
The crude product was purified by flash chromatography over silica gel (9:1 hexanes/ $\text{Et}_2\text{O}$ ) to yield 1.98 g (66.5%) of the title compound as a colorless oil.  $^1\text{H}$  NMR (400 MHz,  $\text{CDCl}_3$ ):  $\delta$  7.26 (t,  $J = 8.0$  Hz, 1H), 7.01 (d,  $J = 7.6$  Hz, 1H), 6.95 (d,  $J = 2.0$  Hz, 1H), 6.85 (ddd,  $J = 8.0, 2.4, 0.4$  Hz, 1H), 6.69 (d,  $J = 16.0$  Hz, 1H), 6.32 (dt,  $J = 16.0, 6.4$  Hz, 1H), 5.98 (ddt,  $J = 17.2, 10.4, 5.6$  Hz, 1H), 5.40 (dq,  $J = 17.2, 1.6$  Hz, 1H), 5.31 (dq,  $J = 8.0, 0.8$  Hz, 1H), 4.82 (dd,  $J = 6.4, 1.2$  Hz, 2H), 5.31 (dt,  $J = 6.0, 1.2$  Hz, 2H), 3.83 (s, 3H);  $^{13}\text{C}$  NMR (100 MHz,  $\text{CDCl}_3$ ):  $\delta$  160.0, 155.0, 137.7, 134.8, 131.7, 129.8, 122.9, 119.5, 119.1, 114.1, 112.1, 68.7, 68.5, 55.4; IR  $\nu_{\max}^{\text{neat}}$   $\text{cm}^{-1}$ : 3004, 3003, 2950, 2836, 1746, 1661, 1454, 1256, 1045, 957; HRMS (EI)  $m/z$  calcd for  $\text{C}_{14}\text{H}_{16}\text{O}_4$  ( $\text{M}^+$ ): 248.1048; found: 248.1051.



**(E)-Allyl 3-(4-methoxyphenyl)allyl carbonate (131d):** General procedure A was followed employing (*E*)-3-(4-methoxyphenyl)prop-2-en-1-ol (9.58 g, 58.4 mmol), pyridine (7.64 mL, 145.9 mmol) and allyl chloroformate (6.22 mL, 58.4 mmol) in  $\text{Et}_2\text{O}$ .

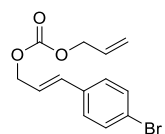
The crude product was purified by flash chromatography over silica gel (95:5 hexanes/ $\text{EtOAc}$ ) to yield 10.0 g (69.0%) of the title compound as a colorless oil.  $^1\text{H}$  NMR (300 MHz,  $\text{CDCl}_3$ ):  $\delta$  7.33 (d,  $J = 8.7$  Hz, 2H), 6.85 (d,  $J = 8.7$  Hz, 2H), 6.63 (d,  $J = 15.6$  Hz, 1H), 6.16 (dt,  $J = 15.9, 6.6$  Hz, 1H), 5.37 (dd,  $J = 17.1, 1.5$  Hz, 1H), 5.27 (dd,  $J = 10.5, 0.9$  Hz, 1H), 4.77 (d,  $J = 6.6$  Hz, 2H), 4.64 (d,  $J = 5.7$  Hz, 2H), 3.80 (s, 3H);  $^{13}\text{C}$  NMR (75 MHz,  $\text{CDCl}_3$ ):  $\delta$  159.5, 154.7, 134.5, 131.4,

128.6, 127.8, 119.9, 118.7, 113.8, 68.6, 68.3, 55.1; IR  $\nu_{\max}^{\text{neat}}$   $\text{cm}^{-1}$ : 3066, 3004, 2954, 1746, 1607, 1512, 1249, 1177, 1034, 952; HRMS (EI)  $m/z$  calcd for  $\text{C}_{14}\text{H}_{16}\text{O}_4$  ( $\text{M}$ )<sup>+</sup>: 248.1048; found: 248.1051.



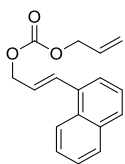
**(E)-Allyl 3-(3-chlorophenyl)allyl carbonate (131e):** General procedure A was followed employing (*E*)-3-(4-methoxyphenyl)prop-2-en-1-ol (2.11 g, 12.5 mmol), pyridine (3.03 mL, 37.56 mmol) and allyl chloroformate (2.00 mL, 18.8 mmol) in  $\text{Et}_2\text{O}$ .

The crude product was purified by flash chromatography over silica gel (9:1 hexanes/ $\text{Et}_2\text{O}$ ) to yield 2.03 g (64.4%) of the title compound as a colorless oil.  $^1\text{H}$  NMR (400 MHz,  $\text{CDCl}_3$ ):  $\delta$  7.40 (s, 1H), 7.27 (m, 3H), 6.66 (d,  $J = 16.0$  Hz, 1H), 6.33 (dt,  $J = 16.0, 6.0$  Hz, 1H), 5.98 (ddt,  $J = 17.2, 10.4, 5.6$  Hz, 1H), 5.41 (dq,  $J = 17.2, 1.2$  Hz, 1H), 5.31 (dq,  $J = 10.4, 1.2$  Hz, 1H), 4.82 (dd,  $J = 5.2, 1.2$  Hz, 2H), 4.67 (dt,  $J = 6.0, 1.2$  Hz, 2H);  $^{13}\text{C}$  NMR (100 MHz,  $\text{CDCl}_3$ ):  $\delta$  155.0, 138.1, 134.8, 133.3, 131.7, 130.0, 128.3, 126.8, 125.1, 124.2, 119.2, 68.8, 68.2; IR  $\nu_{\max}^{\text{neat}}$   $\text{cm}^{-1}$ : 3085, 2950, 1727, 1594, 1256, 1092, 960; HRMS (EI)  $m/z$  calcd for  $\text{C}_{13}\text{H}_{13}\text{ClO}_3$  ( $\text{M}$ )<sup>+</sup>: 252.0554; found: 252.0555



**(E)-Allyl 3-(4-bromophenyl)allyl carbonate (131f):** General procedure A was followed employing (*E*)-3-(4-bromophenyl)prop-2-en-1-ol (250 mg, 1.18 mmol),

pyridine (0.285 mL, 3.51 mmol) and allyl chloroformate (0.187 mL, 3.51 mmol) in  $\text{Et}_2\text{O}$ . The crude product was purified by flash chromatography over silica gel (9:1 hexanes/ $\text{Et}_2\text{O}$ ) to yield 251 mg (71.6%) of the title compound as a colorless oil.  $^1\text{H}$  NMR (400 MHz,  $\text{CDCl}_3$ ):  $\delta$  7.45 (d,  $J = 8.4$  Hz, 2H), 7.25 (d,  $J = 8.4$  Hz, 2H), 6.63 (d,  $J = 16.0$  Hz, 1H), 6.29 (dt,  $J = 16.0, 6.0$  Hz, 1H), 6.00 – 5.91 (m, 1H), 5.38 (dd,  $J = 17.2, 1.2$  Hz, 1H), 5.29 (d,  $J = 10.4$ , 1H), 4.79 (d,  $J = 6.4$ , 2H), 4.67 (d,  $J = 5.6$  Hz, 2H);  $^{13}\text{C}$  NMR (100 MHz,  $\text{CDCl}_3$ ):  $\delta$  155.1, 135.2, 133.7, 132.0, 131.8, 128.4, 123.5, 122.3, 119.3; IR  $\nu_{\max}^{\text{neat}}$   $\text{cm}^{-1}$ : 3085, 3026, 2949, 1746, 1650, 1588, 1487, 1386, 1257, 957.



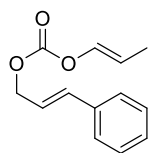
**(E)-Allyl 3-(naphthalen-1-yl)allyl carbonate (131g):** General procedure A was followed employing ((E)-3-(naphthalen-1-yl)prop-2-en-1-ol (0.455 g, 2.50 mmol), pyridine (0.590mL, 7.50 mmol) and allyl chloroformate (0.40 mL, 3.75 mmol) in Et<sub>2</sub>O.

The crude product was purified by flash chromatography over silica gel (9:1 hexanes/EtOAc) to yield 0.529 g (79.8%) of the title compound as a colorless oil. <sup>1</sup>H NMR (300 MHz, CDCl<sub>3</sub>): δ 8.06 (d, *J* = 9.0 Hz, 1H), 7.87-7.76 (m, 2H), 7.60 (d, *J* = 7.2 Hz, 1H), 7.55-7.43 (m, 4H), 6.34 (dt, *J* = 12.6, 6.3 Hz, 1H), 6.04-5.91 (m, 1H), 5.40 (dd, *J* = 17.1, 1.2 Hz, 1H), 5.29 (dd, *J* = 10.5, 0.9 Hz, 1H), 4.91 (dd, *J* = 6.6, 1.2 Hz, 2H), 4.68 (d, *J* = 6.9 Hz, 2H); <sup>13</sup>C NMR (75 MHz, CDCl<sub>3</sub>): δ 154.8, 133.6, 133.4, 131.9, 131.4, 130.9, 128.4, 128.4, 126.1, 125.7, 125.5, 125.4, 124.0, 123.6, 118.9, 68.5, 68.4; IR ν<sub>max</sub><sup>neat</sup> cm<sup>-1</sup>: 3058, 2950, 2886, 1745, 1450, 1253; (EI) *m/z* calcd for C<sub>17</sub>H<sub>16</sub>O<sub>3</sub> (M)<sup>+</sup>: 268.1099; found: 268.1094.

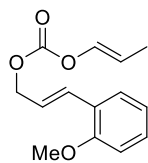


**GENERAL PROCEDURE FOR THE ISOMERIZATION OF DIALLYL  
CARBONATES (GENERAL PROCEDURE B)**

[Ir(COE)Cl]<sub>2</sub> (Ir dimer, 0.5 mol %, 0.01 eq Ir, or specified amount), PCy<sub>3</sub> (0.03 eq) and NaBPh<sub>4</sub> (0.02 eq) were combined in a flame dried flask in the glovebox, removed and combined with a mixture of CH<sub>2</sub>Cl<sub>2</sub>/acetone (25:1, 0.67 M final concentration of the target substrate). The resulting yellow/orange solution was then stirred for 5 min at ambient temperature. The desired diallyl carbonate (1.0 eq) was added to the reaction in a minimal amount of CH<sub>2</sub>Cl<sub>2</sub> (5% of the total calculated volume – a sufficient amount to solvate the starting material) and stirred for 24h. Upon completion by TLC, the mixture was concentrated under a stream of N<sub>2</sub>, pentanes (4x the reaction volume) added to precipitate the catalyst, the mixture subsequently filtered through a small plug of Florisil<sup>®</sup>, concentrated and the residue purified as indicated in the text.

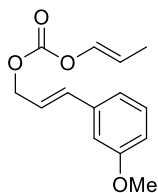


**Cinnamyl (*E*)-prop-1-enyl carbonate (112):** General procedure B was followed employing allyl cinnamyl carbonate (118) (1.5 g, 6.68 mmol), [Ir(COE)Cl]<sub>2</sub> (0.031 g, 0.033 mmol), PCy<sub>3</sub> (0.057 g, 0.200 mmol), and NaBPh<sub>4</sub> (0.047 g, 0.114 mmol). After 24 h the reaction mixture was filtered through a plug of Florisil<sup>®</sup> and concentrated. The crude product was purified by flash chromatography over silica gel (97:3 Hexanes/EtOAc) to yield 1.17 g (80.3%) of the title compound as a colorless oil. <sup>1</sup>H NMR (300 MHz, CDCl<sub>3</sub>): δ 7.41-7.25 (m, 5H), 6.88 (dq, *J* = 12.3, 1.8 Hz, 1H), 6.71 (d, *J* = 15.9 Hz, 1H), 6.30 (dt, *J* = 15.9, 6.3 Hz, 1H), 5.46 (app dq, *J* = 12.4, 6.9 Hz, 1H), 4.83 (dd, *J* = 1.2 Hz, 2H), 1.64 (dd, *J* = 6.9, 1.8 Hz, 3H); <sup>13</sup>C NMR (75 MHz, CDCl<sub>3</sub>): δ 152.7, 137.2, 135.1, 128.5, 128.2, 126.6, 121.9, 109.9, 68.6, 11.9; IR ν<sub>max</sub><sup>neat</sup> cm<sup>-1</sup>: 3084, 3029, 2923, 1753, 1680, 1449, 1385, 1256, 986; (EI) *m/z* calcd for C<sub>13</sub>H<sub>14</sub>O<sub>3</sub> (M)<sup>+</sup>: 218.0942; found: 218.0939.



**(E)-3-(2-Methoxyphenyl)allyl (E)-prop-1-enyl carbonate (132b):** General

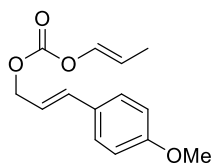
procedure B was followed employing (*E*)-allyl 3-(2-methoxyphenyl)allyl carbonate (**131c**) (2.0 g, 8.10 mmol),  $[\text{Ir}(\text{COE})\text{Cl}]_2$  (0.072 g, 0.081 mmol),  $\text{PCy}_3$  (0.136 g, 0.486 mmol), and  $\text{NaBPh}_4$  (0.063 g, 0.162 mmol). After 24 h the reaction mixture was filtered through a plug of Florisil<sup>®</sup> and concentrated. The crude product was purified by flash chromatography over silica gel (9:1 Hexanes/EtOAc) to yield 0.400 g (19.9%) of the title compound as a colorless oil. <sup>1</sup>H NMR (300 MHz,  $\text{CDCl}_3$ ):  $\delta$  7.42 (dd,  $J = 7.5, 1.5$  Hz, 1H), 7.26 (dt,  $J = 7.2, 1.5$  Hz, 1H), 7.02 (d,  $J = 16.2$  Hz, 1H), 6.95-6.85 (m, 3H), 6.33 (dt,  $J = 16.2, 6.9$  Hz, 1H), 5.45 (app dq,  $J = 12.3, 7.2$  Hz, 1H), 4.83 (dd,  $J = 6.9, 1.5$  Hz, 2H), 3.85 (s, 3H), 1.63 (dd,  $J = 6.9, 1.8$  Hz, 3H); <sup>13</sup>C NMR (75 MHz,  $\text{CDCl}_3$ ):  $\delta$  156.9, 152.7, 137.2, 130.2, 129.2, 127.1, 124.8, 122.4, 120.5, 110.7, 109.6, 69.2, 55.2, 11.9; IR  $\nu_{\text{max}}^{\text{neat}}$   $\text{cm}^{-1}$ : 3080, 2945, 2838, 1754, 1680, 1439, 1247, 974; (EI)  $m/z$  calcd for  $\text{C}_{14}\text{H}_{16}\text{O}_4$  ( $\text{M}$ )<sup>+</sup>: 248.1048; found: 248.1042



**(E)-3-(3-Methoxyphenyl)allyl (E)-prop-1-enyl carbonate (132c):** General procedure

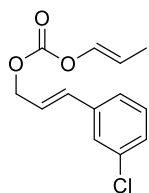
B was followed employing (*E*)-allyl 3-(3-methoxyphenyl)allyl carbonate (**131c**) (1.0 g, 4.03 mmol),  $[\text{Ir}(\text{COE})\text{Cl}]_2$  (0.018 g, 0.020 mmol),  $\text{PCy}_3$  (0.037 g, 0.131 mmol), and  $\text{NaBPh}_4$  (0.028 g, 0.081 mmol). After 24 h the reaction mixture was filtered through a plug of Florisil<sup>®</sup> and concentrated. The crude product was purified by flash chromatography over silica gel (9:1 Hexanes/EtOAc) to yield 0.428 g (43.8%) of the title compound as a colorless oil. <sup>1</sup>H NMR (400 MHz,  $\text{CDCl}_3$ ):  $\delta$  7.27 (t,  $J = 8.0$  Hz, 1H), 7.01 (d,  $J = 7.6$  Hz, 1H), 6.95 (t,  $J = 6.4$  Hz, 1H), 6.90 (dq,  $J = 12.0, 1.6$  Hz, 1H), 6.85 (dd,  $J = 8.4, 1.0$  Hz, 1H), 6.66 (d,  $J = 15.2$  Hz, 1H), 6.31 (dt,  $J = 16.0, 6.8$  Hz, 1H), 5.49 (dq,  $J = 14.4, 7.2$  Hz, 1H), 4.85 (dd,  $J = 6.4, 2.8$ , 2H), 3.84 (s, 3H), 1.66 (dd,  $J = 7.2, 1.6$  Hz); <sup>13</sup>C NMR (100 MHz,  $\text{CDCl}_3$ ):  $\delta$  160.0, 153.1, 137.6, 137.4, 135.3, 129.8, 122.5, 119.6, 114.25,

112.1, 110.3, 68.9, 55.4, 12.3 IR  $\nu_{\max}^{\text{neat}}$   $\text{cm}^{-1}$ : 2964, 2944, 2834, 1755, 1681, 1600, 1581, 1490, 1253, 1011, 970, 926, 760, 688; HRMS (EI)  $m/z$  calcd for  $\text{C}_{14}\text{H}_{16}\text{O}_4$  ( $\text{M}^+$ ): 248.1048; found: 248.1046.



**(E)-3-(4-Methoxyphenyl)allyl (E)-prop-1-enyl carbonate (132d):** General procedure B was followed employing (E)-allyl 3-(4-methoxyphenyl)allyl carbonate (**131d**) (1.0 g, 4.03 mmol),  $[\text{Ir}(\text{COE})\text{Cl}]_2$  (0.018 g, 0.020 mmol),  $\text{PCy}_3$  (0.034 g, 0.121

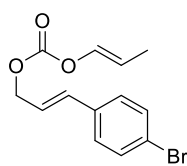
mmol), and  $\text{NaBPh}_4$  (0.028 g, 0.081 mmol). After 24 h the reaction mixture was filtered through a plug of Florisil<sup>®</sup> and concentrated. The crude product was purified by flash chromatography over silica gel (9:1 Hexanes/EtOAc) to yield 0.200 g (20.0%) of the title compound as a waxy solid.  $^1\text{H}$  NMR (300 MHz,  $\text{CDCl}_3$ ):  $\delta$  7.33 (d,  $J = 8.7$  Hz, 2H), 6.87 (d,  $J = 8.7$  Hz, 2H), 6.65 (d,  $J = 15.9$  Hz, 1H), 6.17 (dt,  $J = 15.9, 6.9$  Hz, 1H), 5.45 (app dq,  $J = 12.3, 7.2$  Hz, 1H), 4.80 (dd,  $J = 6.6, 0.9$  Hz, 2H), 3.81 (s, 3H), 1.63 (dd,  $J = 6.9, 1.5$  Hz, 3H);  $^{13}\text{C}$  NMR (75 MHz,  $\text{CDCl}_3$ ): 159.8, 152.8, 137.2, 135.1, 128.7, 128.0, 119.6, 114.0, 109.9, 69.0, 55.3, 12.0; IR  $\nu_{\max}^{\text{neat}}$   $\text{cm}^{-1}$ : 3004, 2938, 2838, 1754, 1607, 1512, 1455, 1247; (EI)  $m/z$  calcd for  $\text{C}_{14}\text{H}_{16}\text{O}_4$  ( $\text{M}^+$ ): 248.1048; found: 248.1036.



**(E)-3-(3-Chlorophenyl)allyl (E)-prop-1-en-1-yl carbonate (132e):** General procedure B was followed employing (E)-allyl 3-(3-chlorophenyl)allyl carbonate (**131e**)

(1.0 g, 3.96 mmol),  $[\text{Ir}(\text{COE})\text{Cl}]_2$  (0.018 g, 0.020 mmol),  $\text{PCy}_3$  (0.034 g, 0.11 mmol), and  $\text{NaBPh}_4$  (0.028 g, 0.080 mmol). After 24 h the reaction mixture was filtered through a plug of Florisil<sup>®</sup> and concentrated. The crude product was purified by flash chromatography over silica gel (9:1 Hexanes/EtOAc) to yield 0.501 g (50.0%) of the title compound as colorless oil.  $^1\text{H}$  NMR (400 MHz,  $\text{CDCl}_3$ ):  $\delta$  7.41 (s, 1H), 7.33 – 7.23 (m, 3H), 6.90 (dq,  $J = 12.4, 2.0$  Hz, 1H), 6.67 (d,  $J = 16.0$  Hz, 1H), 6.33 (dt,  $J = 16.0, 6.4$  Hz, 1H), 5.50 (dq,  $J = 14.0, 7.2$  Hz, 1H), 4.85 (dd,  $J = 6.4, 1.2$  Hz, 2H), 1.67 (dd,  $J = 7.2, 1.6$  Hz, 3H);  $^{13}\text{C}$  NMR (100 MHz,  $\text{CDCl}_3$ ):  $\delta$  153.0, 138.0, 137.3, 134.8, 133.1, 130.0,

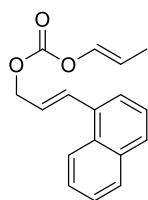
128.37, 126.8, 125.1, 123.8, 110.4, 68.4, 12.2; IR  $\nu_{\max}^{\text{neat}}$   $\text{cm}^{-1}$ : 3067, 2939, 1753, 1597, 1573, 1429, 1384, 1256, 926, 784, 691; HRMS (EI)  $m/z$  calcd for  $\text{C}_{13}\text{H}_{13}\text{O}_3\text{Cl}(\text{M})^+$ : 252.0556; found: 252.0553.



**(E)-3-(4-Bromophenyl)allyl (E)-prop-1-en-1-yl carbonate (132f):** General

procedure B was followed employing (*E*)-allyl 3-(4-bromophenyl)allyl carbonate

**(131f)** (0.710 g, 4.03 mmol),  $[\text{Ir}(\text{COE})\text{Cl}]_2$  (0.013 g, 0.0139 mmol),  $\text{PCy}_3$  (0.023 g, 0.083 mmol), and  $\text{NaBPh}_4$  (0.019 g, 0.057 mmol). After 24 h the reaction mixture was filtered through a plug of Florisil<sup>®</sup> and concentrated. The crude product was purified by flash chromatography over silica gel (9:1 Hexanes/EtOAc) to yield the title compound as a white solid.  $^1\text{H}$  NMR (400 MHz,  $\text{CDCl}_3$ ):  $\delta$  7.47 (d,  $J = 8.0$  Hz, 2H), 7.27 (d,  $J = 8.4$  Hz, 2H), 6.89 (dt,  $J = 12.4, 1.2$  Hz, 1H), 6.66 (d,  $J = 16.2$  Hz, 1H), 6.30 (dtd,  $J = 16.0, 6.4, 0.8$  Hz, 1H), 5.48 (m, 1H), 4.83 (d,  $J = 6.4$  Hz, 2H), 1.67 (d,  $J = 7.2$  Hz, 3H);  $^{13}\text{C}$  NMR (100 MHz,  $\text{CDCl}_3$ ):  $\delta$  152.8, 137.1, 134.8, 133.8, 131.8, 128.2, 122.8, 122.2, 110.2, 68.4, 12.1; IR  $\nu_{\max}^{\text{neat}}$   $\text{cm}^{-1}$ : 3083, 2942, 2918, 1744, 1681, 1487, 1265, 1072, 920, 806, 782; HRMS (EI)  $m/z$  calcd for  $\text{C}_{13}\text{H}_{13}\text{O}_3\text{Br}(\text{M})^+$ : 296.0041; found: 296.0048.



**(E)-3-(Naphthalen-1-yl)allyl (E)-prop-1-en-1-yl carbonate (132g):** General procedure

B was followed employing (*E*)-allyl 3-(naphthalen-1-yl)allyl carbonate **(131g)** (0.476 g,

1.77 mmol),  $[\text{Ir}(\text{COE})\text{Cl}]_2$  (0.008 g, 0.009 mmol),  $\text{PCy}_3$  (0.014 g, 0.053 mmol), and

$\text{NaBPh}_4$  (0.012 g, 0.035 mmol). After 24 h the reaction mixture was filtered through a plug of Florisil<sup>®</sup> and concentrated. The crude product was purified by flash chromatography over silica gel (98:2 hexanes/EtOAc) to yield 0.249 g (52.5%) of the title compound as a colorless oil.  $^1\text{H}$  NMR (300 MHz,  $\text{CDCl}_3$ ):  $\delta$  8.10 (d,  $J = 9.0$  Hz, 1H), 7.88-7.77 (m, 2H), 7.61 (d,  $J = 6.9$  Hz, 1H), 7.56-7.43 (m, 4H), 6.91 (dd,  $J = 12.0, 0.6$  Hz, 1H), 6.34 (dt,  $J = 15.6, 6.3$  Hz, 1H), 5.48 (app dq,  $J = 19.2, 7.2$  Hz,

1H), 4.95 (d,  $J = 6.9, 0.9$  Hz, 3H);  $^{13}\text{C}$  NMR (75 MHz,  $\text{CDCl}_3$ ): 152.8, 137.2, 133.5, 133.4, 132.8, 130.9, 128.5, 128.4, 126.1, 125.8, 125.4, 125.0, 124.0, 123.4, 109.9, 68.7, 11.9; (EI)  $m/z$  calcd for  $\text{C}_{17}\text{H}_{16}\text{O}_3$  (M) $^+$ : 268.1099; found: 268.1105.

## GENERAL PROCEDURE FOR THE FORMATION OF DI(ALLYL) ETHERS

### (GENERAL PROCEDURE C)

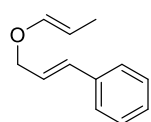
Sodium hydride (2.5 eq., 60% suspension in mineral oil) was added to a 0° C solution of alcohol A (1.0 equiv) in THF (0.5 M) and the reaction was stirred 30 min. Allylic bromide B (1.4 equiv) was added and the resulting suspension was warmed to ambient temperature and stirred overnight. A saturated solution of  $\text{NH}_4\text{Cl}$  (to double the reaction volume) was added slowly at 0° C to quench the reaction and the resulting mixture extracted with ether (3x initial volume of the reaction mixture). The combined organic extracts were dried over anhydrous  $\text{MgSO}_4$ , solvent removed *in vacuo*, and the residue purified.

## GENERAL PROCEDURE FOR THE ISOMERIZATION OF DI(ALLYL) ETHERS

### (GENERAL PROCEDURE D)

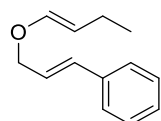
$[\text{Ir}(\text{C}_8\text{H}_{14})_2\text{Cl}]_2$  (0.5 mol %),  $\text{PCy}_3$  (3 mol %) and  $\text{NaBPh}_4$  (3 mol %) were combined in a flame dried flask in a nitrogen-filled glovebox. The flask was removed from the glovebox and a mixture of  $\text{CH}_2\text{Cl}_2$ /acetone (25:1, 0.67 M final concentration of the diallyl ether substrate) was added. The resulting yellow-orange solution was stirred for 5 min at ambient temperature. The diallyl ether (1.0 equiv) was added to the catalyst solution in a minimal amount of  $\text{CH}_2\text{Cl}_2$  ( $\leq 5\%$  of the total solvent volume) and the reaction was stirred for 10-60 min (until complete consumption of the starting material as monitored by TLC). The reaction mixture was concentrated under a stream of  $\text{N}_2$  then

pentanes (4x the reaction volume) were added and the resulting heterogeneous mixture was filtered through a Florisil® plug eluting with additional pentanes. The eluent was concentrated to afford the allyl vinyl ethers that were used in the subsequent reaction without further purification.



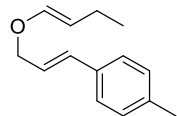
**[(E)-3-{{(E)-Prop-1-en-1-yl}oxy}prop-1-en-1-yl]benzene (111):** Characterization

materials match the data provided in the following publication: Geherty, M. E.; Dura, R. G.; Nelson, S. G. *J. Am. Chem. Soc.*, **2010**, *132*, 11875-11877.



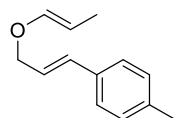
**[(E)-3-{{(E)-But-1-en-1-yl}oxy}prop-1-en-1-yl]benzene (148):** Characterization

materials match the data provided in the following publication: Geherty, M. E.; Dura, R. G.; Nelson, S. G. *J. Am. Chem. Soc.*, **2010**, *132*, 11875-11877.



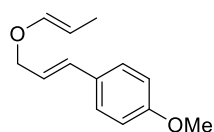
**1-[(E)-3-{{(E)-But-1-en-1-yl}oxy}prop-1-en-1-yl]-4-methylbenzene (160b):**

Characterization materials match the data provided in the following publication: Geherty, M. E.; Dura, R. G.; Nelson, S. G. *J. Am. Chem. Soc.*, **2010**, *132*, 11875-11877.



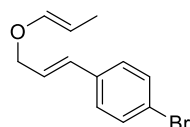
**1-Methoxy-4-[(E)-3-{{(E)-prop-1-en-1-yl}oxy}prop-1-en-1-yl]benzene (147):**

Characterization materials match the data provided in the following publication: Geherty, M. E.; Dura, R. G.; Nelson, S. G. *J. Am. Chem. Soc.*, **2010**, *132*, 11875-11877.



**1-Methoxy-2-[(E)-4-{{(E)-prop-1-en-1-yl}oxy}prop-1-en-1-yl]benzene**

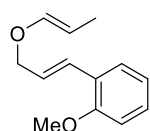
**(160d):** Characterization materials match the data provided in the following publication: Geherty, M. E.; Dura, R. G.; Nelson, S. G. *J. Am. Chem. Soc.*, **2010**, *132*, 11875-11877.



**1-Bromo-4-[(E)-3-[(E)-prop-1-en-1-yl]oxy}prop-1-en-1-yl]benzene (160e):**

Characterization materials match the data provided in the following publication:

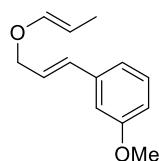
Geherty, M. E.; Dura, R. G.; Nelson, S. G. *J. Am. Chem. Soc.* **2010**, *132*, 11875-11877.



**1-Methoxy-2-[(E)-3-[(E)-prop-1-en-1-yl]oxy}prop-1-en-1-yl]benzene (160f):**

Characterization materials match the data provided in the following publication:

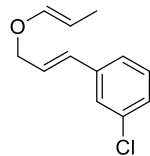
Geherty, M. E.; Dura, R. G.; Nelson, S. G. *J. Am. Chem. Soc.* **2010**, *132*, 11875-11877.



**1-Methoxy-3-[(E)-3-[(E)-prop-1-en-1-yl]oxy}prop-1-en-1-yl]benzene (160g):**

Characterization materials match the data provided in the following publication:

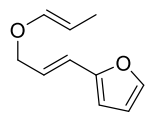
Geherty, M. E.; Dura, R. G.; Nelson, S. G. *J. Am. Chem. Soc.* **2010**, *132*, 11875-11877.



**1-Chloro-3-[(E)-3-[(E)-prop-1-en-1-yl]oxy}prop-1-en-1-yl]benzene (160h):**

Characterization materials match the data provided in the following publication:

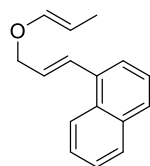
Geherty, M. E.; Dura, R. G.; Nelson, S. G. *J. Am. Chem. Soc.* **2010**, *132*, 11875-11877.



**2-[(E)-3-[(E)-Prop-1-en-1-yl]oxy}prop-1-en-1-yl]furan (160i):** Characterization

materials match the data provided in the following publication: Geherty, M. E.; Dura,

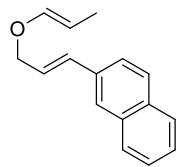
R. G.; Nelson, S. G. *J. Am. Chem. Soc.* **2010**, *132*, 11875-11877.



**1-[(E)-3-[(E)-Prop-1-en-1-yl]oxy}prop-1-en-1-yl]naphthalene (160j):**

Characterization materials match the data provided in the following publication:

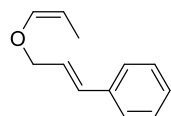
Geherty, M. E.; Dura, R. G.; Nelson, S. G. *J. Am. Chem. Soc.* **2010**, *132*, 11875-11877.



**2-[(E)-3-{{(E)-Prop-1-en-1-yl}oxy}prop-1-en-1-yl]naphthalene (160k):**

Characterization materials match the data provided in the following publication:

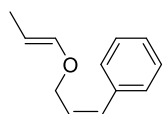
Geherty, M. E.; Dura, R. G.; Nelson, S. G. *J. Am. Chem. Soc.*, **2010**, *132*, 11875-11877.



**[(E)-3-{{(Z)-Prop-1-en-1-yl}oxy}prop-1-en-1-yl]benzene (163):** Characterization

materials match the data provided in the following publication: Wipf, P.; Waller, D.

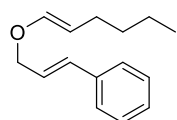
L.; Reeves, J. T. *J. Org. Chem.*, **2005**, *70*, 8096-8102



**[(Z)-3-{{(E)-Prop-1-en-1-yl}oxy}prop-1-en-1-yl]benzene (164):** Characterization

materials match the data provided in the following publication: Geherty, M. E.; Dura,

R. G.; Nelson, S. G. *J. Am. Chem. Soc.*, **2010**, *132*, 11875-11877.



**[(E)-3-{{(E)-Hex-1-en-1-yl}oxy}prop-1-en-1-yl]benzene (139):** [Ir(COE)Cl]<sub>2</sub> (Ir

dimer, 0.5 mol %, 0.01 eq Ir), PCy<sub>3</sub> (0.02 eq) and NaBPh<sub>4</sub> (0.02 eq) were combined

in a flame dried flask in the glovebox, removed and combined with a mixture of CH<sub>2</sub>Cl<sub>2</sub>/acetone (25:1,

0.67 M final concentration of the target substrate). The resulting yellow/orange solution was then

stirred for 5min at ambient temperature. (E)-[3-(allyloxy)prop-1-en-1-yl]cyclohexane (1.0 eq) was

added to the reaction mixture and stirred for 120 minute until completion as indicated by TLC analysis.

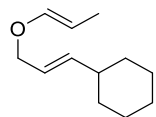
The mixture was concentrated and pentanes (4x the reaction volume) added to precipitate the catalyst,

the mixture subsequently filtered through a small plug of Florisil<sup>®</sup>, concentrated and the residue

purified. Characterization materials match the data provided in the following publication: Wipf, P.;

Waller, D. L.; Reeves, J. T. *J. Org. Chem.*, **2005**, *70*, 8096-8102

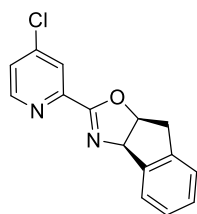




**[(E)-3-{(E)-Prop-1-en-1-yl}oxy}prop-1-en-1-yl]cyclohexane (165):** [Ir(COE)Cl]<sub>2</sub>

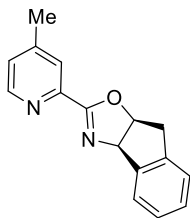
(Ir dimer, 0.5 mol %, 0.01 eq Ir), PCy<sub>3</sub> (0.04 eq) and NaBPh<sub>4</sub> (0.02 eq) were combined in a flame dried flask in the glovebox, removed and combined with a mixture of CH<sub>2</sub>Cl<sub>2</sub>/acetone (25:1, 0.67 M final concentration of the target substrate). The resulting yellow/orange solution was then stirred for 5 min at ambient temperature and then cooled to 0° C. (E)-[3-(allyloxy)prop-1-en-1-yl]cyclohexane (1.0 eq) was added to the reaction mixture and stirred for a few seconds. The mixture was concentrated and pentanes (4x the reaction volume) added to precipitate the catalyst, the mixture subsequently filtered through a small plug of Florisil<sup>®</sup>, concentrated and the residue purified. Characterization materials match the data provided in the following publication: Geherty, M. E.; Dura, R. G.; Nelson, S. G. *J. Am. Chem. Soc.*, **2010**, *132*, 11875-11877.

**General procedure for synthesis of pyridine oxazoline ligands (General Procedure E):** The amino alcohol (1 equiv), 2-cyanopyridine (1 equiv. 4.2 mmol), ZnCl<sub>2</sub> (5 mol %, 0.21 mmol) were dissolved in chlorobenzene (0.5 M solution). The reaction was refluxed at 130° C for 24 h under an inert atmosphere of N<sub>2</sub> at which time the heat was removed and the mixture was allowed to slowly cool to ambient temperature. The chlorobenzene was removed *in vacuo* and the crude material purified over silica gel (0-3% MeOH/CH<sub>2</sub>Cl<sub>2</sub>) to yield a solid. This solid was triturated with cold Et<sub>2</sub>O and filtered to provide the ligand as a white solid.



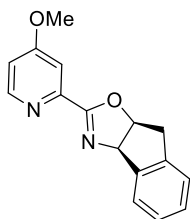
**(3aR,8aS)-2-(4-Chloropyridin-2-yl)-3a,8a-dihydro-8H-indeno[1,2-d]oxazole**

**(155):** Characterization materials match the data provided in the following publication: Geherty, M. E.; Dura, R. G.; Nelson, S. G. *J. Am. Chem. Soc.*, **2010**, *132*, 11875-11877.



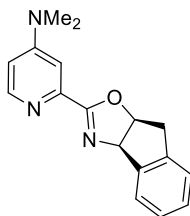
**(3aR,8aS)-2-(4-Methylpyridin-2-yl)-3a,8a-dihydro-8H-indeno[1,2-d]oxazole**

**(145):** Characterization materials match the data provided in the following publication: Geherty, M. E. PhD Dissertation, Pittsburgh, PA. 2012



**(3aR,8aS)-2-(4-Methoxypyridin-2-yl)-3a,8a-dihydro-8H-indeno[1,2-**

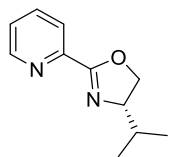
**d]oxazole (146):** Characterization materials match the data provided in the following publication: Geherty, M. E. PhD Dissertation, Pittsburgh, PA. 2012



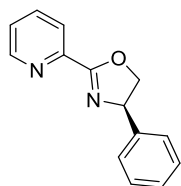
**2-((3aR,8aS)-8,8a-Dihydro-3aH-indeno[1,2-d]oxazol-2-yl)-N,N-**

**dimethylpyridin-4-amine (127):** (3aR, 8aS)-2-(4-chloropyridin-2-yl)-8,8a-dihydro-3aH-indeno[1,2-d]oxazole (0.200 g, 0.740 mmol) and 40% dimethyl amine in H<sub>2</sub>O solution (4 mL) were combined in a medium pressure reaction vessel. The reaction

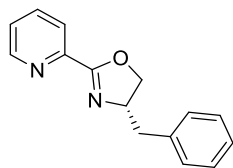
was sealed and heated at 110° C for 3 h. After, the reaction was allowed to cool. The solid precipitate was collected and subjected to purification on silica gel using 9:1 CH<sub>2</sub>Cl<sub>2</sub>/MeOH. [α]<sub>D</sub>+36 (c 0.94, CHCl<sub>3</sub>); <sup>1</sup>H NMR (400 MHz, CDCl<sub>3</sub>): δ 8.27(d, J = 6.0 Hz, 1H), 7.60 – 7.58 (m, 1H), 7.29 – 7.27 (m, 4H), 6.51 (dd, J = 6.0, 2.8 Hz, 1H), 5.78 (d, J = 8.0 Hz, 1H), 5.58 – 5.54 (m, 1H), 3.50 – 3.49 (m, 2H), 3.02 (s, 6H); <sup>13</sup>C NMR (100 MHz, CDCl<sub>3</sub>): δ 164.3, 154.7, 149.8, 147.0, 141.9, 140.1, 128.6, 127.5, 125.9, 125.5, 108.1, 107.0, 83.87, 77.2, 39.9, 39.4, 29.9; IR ν<sub>max</sub><sup>neat</sup> cm<sup>-1</sup>: 3031, 2922, 1601, 1511, 1378, 994;



**(S)-2-(Pyridin-2-yl)-4-isopropyl-4,5-dihydrooxazole (141):** Characterization materials match the data provided in the following publication: Chelucci, G.; Deiru, S. P.; Saba, A.; Valenti, R. *Tetrahedron: Asymm.* **1999**, 10, 1457-1464.



**(R)-2-(Pyridin-2-yl)-4-phenyl-4,5-dihydrooxazole (142):** Characterization materials match the data provided in the following publication: Chelucci, G.; Deiru, S. P.; Saba, A.; Valenti, R. *Tetrahedron: Asymm.* **1999**, 10, 1457-1464.

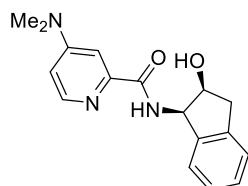


**(S)-4-Benzyl-2-(pyridin-2-yl)-4,5-dihydrooxazole (143):** Characterization materials match the data provided in the following publication: Chelucci, G.; Deiru, S. P.; Saba, A.; Valenti, R. *Tetrahedron: Asymm.* **1999**, 10, 1457-1464.

## GENERAL PROCEDURE FOR SYNTHESIS OF DIMETHYLAMINOPYRIDINE

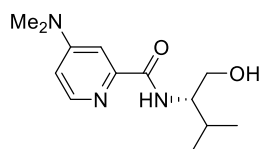
### AMIDE LIGANDS (GENERAL PROCEDURE F)

The 4-chloropyridine oxazoline compound is added to a medium pressure reaction vessel with 4 to 5 mL of 40% dimethylamine in H<sub>2</sub>O, sealed, and heated at 110° C for 36 h. After cooling, the resultant precipitant is collected, dried and purified by column chromatography (SiO<sub>2</sub>, 0-3% MeOH/DCM gradient) to afford the desired ligand.



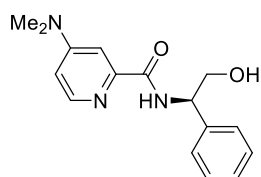
**(4-(Dimethylamino)-N-[(1R,2S)-2-hydroxy-2,3-dihydro-1H-inden-1-yl]picolinamide (130):** Characterization materials match the data provided in

the following publication: Geherty, M. E. PhD Dissertation, Pittsburgh, PA. 2012

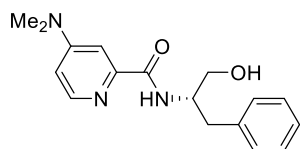


**(S)-4-(Dimethylamino)-N-(1-hydroxy-3-methylbutan-2-yl)picolinamide (156):** Characterization materials match the data provided in the following publication: Geherty, M. E. PhD Dissertation, Pittsburgh, PA.

2012



**(R)-4-(Dimethylamino)-N-(2-hydroxy-1-phenylethyl)picolinamide (157):** Characterization materials match the data provided in the following publication: Geherty, M. E. PhD Dissertation, Pittsburgh, PA. 2012



**(S)-4-(Dimethylamino)-N-(1-hydroxy-3-phenylpropan-2-yl)picolinamide (158):** Characterization materials match the data provided in the following publication: Geherty, M. E. PhD Dissertation, Pittsburgh,

PA. 2012

## GENERAL PROCEDURE FOR RUTHENIUM CATALYZED ASYMMETRIC CLAISEN REARRANGEMENTS OF ALLYL VINYL CARBONATES (GENERAL PROCEDURE E)

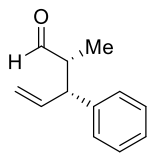
[CpRu(CH<sub>3</sub>CN)<sub>3</sub>]PF<sub>6</sub> (5 mol %) and ligand (5 mol %) were combined in a 2 dram vial under an inert atmosphere inside a glovebox. The required amount of THF (0.5 M final concentration of the desired substrate) was added to this vial and shaken occasionally over a 30 min period. While this mixture was being prepared, the other components were combined by placing the required allyl vinyl carbonate

(1 eq), B(OPh)<sub>3</sub> (5 mol %) and a stir bar into a PTFE capped 2 dram vial). After 30 min, the Ru-ligand mixture was added to the dry components in the 2 dram vial, sealed and removed from the glovebox. Immediately after removal from the glovebox, the mixture was then allowed to stir for the required amount of time (24-48 h). After this time the vessel was opened and concentrated under a stream of N<sub>2</sub>. Pentanes (4x the reaction volume) was added to this mixture to precipitate the Ru-catalyst complex followed by filtration through a plug of Florisil® and celite. The filtrate was concentrated and then analyzed by <sup>1</sup>H NMR.

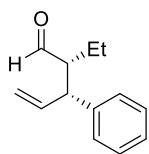
**GENERAL PROCEDURE FOR THE RUTHENIUM CATALYZED ASYMMETRIC  
CLAISEN REARRANGEMENT OF ALLYL VINYL ETHERS (GENERAL  
PROCEDURE F)**

[CpRu(CH<sub>3</sub>CN)<sub>3</sub>]PF<sub>6</sub> (5 mol %) and ligand (5 mol %) were combined in a 2 dram vial under an inert atmosphere inside a glovebox. The required amount of THF (0.5 M final concentration of the desired substrate) was added to this vial and shaken occasionally over a 30 min period. While this mixture was being prepared, the other components were combined by placing the required allyl vinyl ether (1 eq), 4 Å MS (w/w relative to the allyl vinyl ether employed), B(OPh)<sub>3</sub> (5 mol %) and a stir bar into a PTFE capped 2 dram vial (available from VWR). After 30 min, the Ru-ligand mixture was added to the dry components in the 2 dram vial, sealed and removed from the glovebox. Immediately after removal from the glovebox, CH<sub>3</sub>CN (20 mol %) was added to the vial via syringe. The mixture was then allowed to stir for the required amount of time (24-48 h). After this time the vessel was opened and concentrated under a stream of N<sub>2</sub>. Pentanes (4x the reaction volume) was added to this mixture

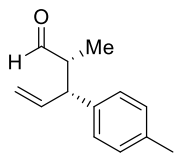
to precipitate the Ru-catalyst complex followed by filtration through a plug of Florisil® and celite. The filtrate was concentrated, analyzed by <sup>1</sup>H NMR, and purified by column chromatography.



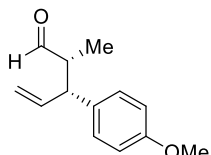
**(2R,3R)-2-Methyl-3-phenylpent-4-enal (114):** Characterization materials match the data provided in the following publication: Geherty, M. E.; Dura, R. G.; Nelson, S. G. *J. Am. Chem. Soc.*, **2010**, *132*, 11875-11877.



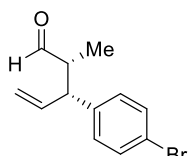
**(2R,3R)-2-Ethyl-3-phenylpent-4-enal (131b):** Characterization materials match the data provided in the following publication: Geherty, M. E. PhD Dissertation, Pittsburgh, PA. 2012



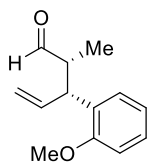
**(2R,3R)-2-Methyl-3-(p-tolyl)pent-4-enal (131c):** Characterization materials match the data provided in the following publication: Geherty, M. E. PhD Dissertation, Pittsburgh, PA. 2012



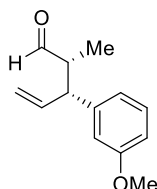
**(2R,3R)-3-(4-Methoxyphenyl)-2-methylpent-4-enal (161d):** Characterization materials match the data provided in the following publication: Geherty, M. E.; Dura, R. G.; Nelson, S. G. *J. Am. Chem. Soc.*, **2010**, *132*, 11875-11877



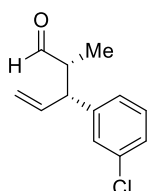
**(2R,3R)-3-(4-Bromophenyl)-2-methylpent-4-enal (161e):** Characterization materials match the data provided in the following publication: Geherty, M. E.; Dura, R. G.; Nelson, S. G. *J. Am. Chem. Soc.*, **2010**, *132*, 11875-11877.



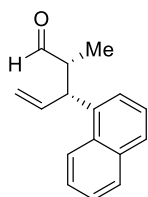
**(2R,3R)-3-(2-Methoxyphenyl)-2-methylpent-4-enal (161f):** Characterization materials match the data provided in the following publication: Geherty, M. E.; Dura, R. G.; Nelson, S. G. *J. Am. Chem. Soc.*, **2010**, *132*, 11875-11877.



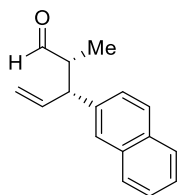
**(2R,3R)-3-(3-Methoxyphenyl)-2-methylpent-4-enal (161g):** Characterization materials match the data provided in the following publication: Geherty, M. E.; Dura, R. G.; Nelson, S. G. *J. Am. Chem. Soc.*, **2010**, *132*, 11875-11877



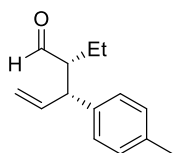
**(2R,3R)-3-(3-Chlorophenyl)-2-methylpent-4-enal (161h):** Characterization materials match the data provided in the following publication: Geherty, M. E.; Dura, R. G.; Nelson, S. G. *J. Am. Chem. Soc.*, **2010**, *132*, 11875-11877.



**(2R,3R)-2-Methyl-3-(naphthalen-1-yl)pent-4-enal (161i):** Characterization materials match the data provided in the following publication: Geherty, M. E.; Dura, R. G.; Nelson, S. G. *J. Am. Chem. Soc.*, **2010**, *132*, 11875-11877.



**(2R,3R)-2-Methyl-3-(naphthalen-2-yl)pent-4-enal (161j):** Characterization materials match the data provided in the following publication: Geherty, M. E.; Dura, R. G.; Nelson, S. G. *J. Am. Chem. Soc.*, **2010**, *132*, 11875-11877.

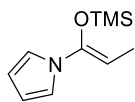


**(2R,3R)-2-Ethyl-3-(p-tolyl)pent-4-ena (151):** Characterization materials match the data provided in the following publication: Geherty, M. E. PhD Dissertation, Pittsburgh, PA. 201

## GENERAL PROCEDURE FOR THE SYNTHESIS OF PYRROLE SILYL ENOL

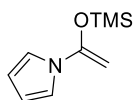
### ETHERS (GENERAL PROCEDURE G)

To a 0° C solution of diisopropylamine (1.0 equiv) in THF (1.6M relative to diisopropylamine) was added a solution of 1.6M *n*-BuLi in hexanes (1.1 equiv). The reaction was allowed to stir at 0° C for 10 min and then cooled to -78° C. Next, a 0.8 M solution of acylpyrrole (1.0 equiv) in THF was added dropwise to the reaction vessel over 5 min and the resulting solution was allowed to stir at -78° C for 30 min. TMSCl (1.1 equiv) was added dropwise over 5 min, and the reaction was allowed to stir an additional 20 min at -78 ° C. The dry ice/acetone bath was removed and the reaction was allowed to stir for an additional 1 h. Next, the reaction was diluted with pentane (4x the reaction volume), and the heterogenous mixture was filtered through a plug of celite and concentrated. The final product was purified *via* kugelrohr distillation.



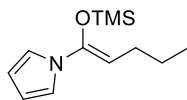
**(Z)-1-{1-[(Trimethylsilyl)oxy]prop-1-en-1-yl}-1H-pyrrole (185a):** Characterization materials match the data provided in the following publication: Evans, D. A.; Johnson,

D. S.; *Org. Lett.* **1999**, *1*, 595-598.



**1-{1-[(Trimethylsilyl)oxy]vinyl}-1H-pyrrole (185b):** Characterization materials match the data provided in the following publication: Frick, U.; Simchen, G. *Liebigs Ann.* 1987,

*10*, 839-845.



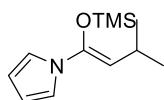
**(Z)-1-{1-[(Trimethylsilyl)oxy]pent-1-en-1-yl}-1H-pyrrole (185c):** General procedure G was followed employing 1.87 mL of diisopropylamine (13.2 mmol),

9.07 mL of 1.6 M *n*-BuLi (14.52 mmol), 2.0 g 1-(1*H*-pyrrol-1-yl)-1-Pentanone (13.2 mmol), 1.84 mL TMSCl (1.1 mmol) in 30 mL THF. The reaction was purified via kugelrohr distillation at 1 mm Hg.

The product distilled between 70 and 80° C (2.14 g, 73%) as a clear colorless oil. <sup>1</sup>H NMR (500 MHz,



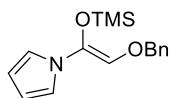
CDCl<sub>3</sub>):  $\delta$  6.86 (t,  $J$ = 2.0 Hz, 2H), 6.16 (t,  $J$ = 2.0 Hz, 2H), 4.68 (t,  $J$ = 7.5 Hz, 1H), 2.09 (q,  $J$ = 7.5 Hz, 2H), 1.43 (sextet,  $J$ = 7.5 Hz, 2H), 0.96 (t,  $J$ = 7.5 Hz, 3H), 0.15 (s, 9H); <sup>13</sup>C NMR (125 MHz, CDCl<sub>3</sub>):  $\delta$  143.0, 119.0, 108.8, 97.8, 27.4, 23.1, 13.8, -0.15; IR  $\nu_{\max}^{\text{neat}}$  cm<sup>-1</sup>: 2959, 2932, 2871, 1682, 1478, 1368, 1254, 1155, 1101, 1078, 1040, 960, 849, 737, 726; HRMS (EI)  $m/z$  calcd for C<sub>12</sub>H<sub>21</sub>NOSi (M + H)<sup>+</sup>: 224.1471; found: 224.1480.



**(Z)-1-{3-Methyl-1-[(trimethylsilyl)oxy]but-1-en-1-yl}-1H-pyrrole (185d):**

Characterization materials match the data provided in the following publication :

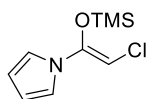
Evans, D. A.; Johnson, D. S.; *Org. Lett.* **1999**, *1*, 595-598.



**(Z)-1-{2-(Benzyloxy)-1-[(trimethylsilyl)oxy]vinyl}-1H-pyrrole (185e):**

Characterization materials match the data provided in the following publication:

Evans, D. A.; Scheidt, K. A.; Johnson, J. N.; Willis, M. C. *J. Am. Chem. Soc.* **2001**, *123*, 4480-4491.



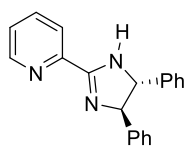
**(Z)-1-{2-Chloro-1-[(trimethylsilyl)oxy]vinyl}-1H-pyrrole (185f):** General

procedure G was followed employing 1.49 mL of diisopropylamine (10.5 mmol), 7.19 mL of 1.6 M *n*-BuLi (11.5 mmol), 1.5 g 2-chloro-1-(1H-pyrrol-1-yl)-Ethanone (10.5 mmol), 1.46 mL TMSCl in 30 mL THF. The reaction was purified via kugelrohr distillation at 1 mm Hg. The product distilled between 75 and 80° C (1.85 g, 82%) as a clear colorless oil. <sup>1</sup>H NMR (500 MHz, CDCl<sub>3</sub>):  $\delta$  6.85 (t,  $J$ = 2.0 Hz, 2H), 6.23 (t,  $J$ = 2.0 Hz, 2H), 5.53 (s, 1H), 0.27 (s, 9H); <sup>13</sup>C NMR (125 MHz, CDCl<sub>3</sub>):  $\delta$  145.3, 118.9, 110.1, 89.0, 0.06; IR  $\nu_{\max}^{\text{neat}}$  cm<sup>-1</sup>: 3108, 2961, 2900, 1723, 1655, 1562, 1475, 1353, 1258, 1134, 1078, 961, 887, 789, 728; HRMS (EI)  $m/z$  calcd for C<sub>9</sub>H<sub>14</sub>ClNOSi (M + H)<sup>+</sup>: 216.0611; found: 216.0619.

## GENERAL PROCEDURE FOR THE SYNTHESIS OF IMIDAZOLYLPYRIDINE

### LIGANDS (GENERAL PROCEDURE H)

To a solution of picolinaldehyde (1.0 equiv) in CH<sub>2</sub>Cl<sub>2</sub> (0.10 M relative to picolinaldehyde) was added the diamine (1.05 equiv). The reaction was allowed to stir for 30 min before *N*-bromosuccinimide (1.05 equiv) was added as a solid. The resulting solution was stirred overnight. The reaction was quenched with 10% NaOH/H<sub>2</sub>O solution of equivalent volume. Organics were extracted with CH<sub>2</sub>Cl<sub>2</sub> (3x the reaction volume), dried with MgSO<sub>4</sub>, and concentrated in vacuo. The crude product was then subjected to methylation conditions without purification. A solution of the crude product in THF (0.10 M) was cooled to -78° C. To this was added 1.3 equiv. NaHMDS (1.0 M in THF). After stirring for 30 min, iodomethane (1.1 equiv) was added. The reaction flask was then allowed to warm to room temperature and stir for 2 h. Next, the reaction was quenched with an equivalent volume of H<sub>2</sub>O and the organics were extracted with CH<sub>2</sub>Cl<sub>2</sub> (3x the reaction volume). The extract was dried with MgSO<sub>4</sub> and concentrated in vacuo. The product mixture was purified by column chromatography.

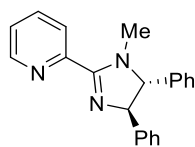


**2-[(4*R*,5*R*)-4,5-Diphenyl-4,5-dihydro-1H-imidazol-2-yl]pyridine (198):**

Characterization materials match the data provided in the following publication:

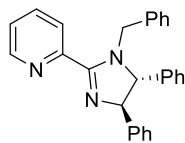
Bastero, A.; Claver, C.; Ruiz, A.; Castillon, S.; Daura, E.; Bo, C.; Zangrando, E. *Chem.*

*Eur. J.* **2004**, *10*, 3747-3760.



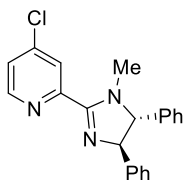
**2-[(4*R*,5*R*)-1-Methyl-4,5-diphenyl-4,5-dihydro-1H-imidazol-2-yl]pyridine (196):** Characterization materials match the data provided in the following

publication: Bastero, A.; Claver, C.; Ruiz, A.; Castillon, S.; Daura, E.; Bo, C.; Zangrando, E. *Chem. Eur. J.* **2004**, *10*, 3747-3760.



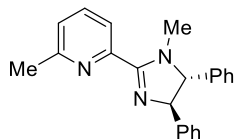
**2-[(4*R*,5*R*)-1-Benzyl-4,5-diphenyl-4,5-dihydro-1H-imidazol-2-yl]pyridine (197):** Characterization materials match the data provided in the following publication: Bastero, A.; Claver, C.; Ruiz, A.; Castillon, S.; Daura, E.; Bo, C.;

Zangrando, E. *Chem. Eur. J.* **2004**, *10*, 3747-3760.



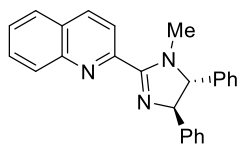
**4-Chloro-2-[(4*R*,5*R*)-1-methyl-4,5-diphenyl-4,5-dihydro-1H-imidazol-2-yl]pyridine (195a):** General procedure G was followed employing 222.8 mg of 4-chloropicolinaldehyde (1.57 mmol), 350.8 mg (1*R*,2*R*)-diphenylethylenediamine

(1.65 mmol), 294.1 mg *N*-bromosuccinimide (1.65 mmol), in 15 mL CH<sub>2</sub>Cl<sub>2</sub>. After workup, 590.3 mg (1.74 mmol) crude product was recovered. Then the crude product was subjected to methylation employing 2.30 mL of NaHMDS (1.0M in THF, 2.26 mmol) and 121 μL iodomethane (1.91 mmol) in 18 mL THF. The reaction mixture was purified by column chromatography (SiO<sub>2</sub>, 0-2% MeOH/CH<sub>2</sub>Cl<sub>2</sub> gradient) to afford 440.0 mg (72%) of the title compound as a pale brown oil:  $[\alpha]_D^{19} +0.369$  (*c* 2.22, CHCl<sub>3</sub>); <sup>1</sup>H NMR (500 MHz, CDCl<sub>3</sub>): δ 8.59 (dd, *J*= 5.0, 0.5 Hz, 1H), 8.19 (d, *J*= 1.5 Hz, 1H), 7.41-7.33 (m, 11H), 4.99 (d, *J* = 10.5 Hz, 1H), 4.38 (d, *J* = 10.5 Hz, 1H), 3.01 (s, 3H); <sup>13</sup>C NMR (125 MHz, CDCl<sub>3</sub>): δ 163.2, 152.0, 149.3, 144.8, 143.1, 140.7, 128.9, 128.5, 127.9, 127.3, 127.2, 126.9, 125.3, 124.9, 79.0, 77.5, 34.3; IR  $\nu_{\max}^{\text{neat}}$  cm<sup>-1</sup>: 3059, 3028, 2855, 1575, 1550, 1491, 1407, 1343, 1277, 1075, 972, 834; HRMS (EI) *m/z* calcd for C<sub>21</sub>H<sub>18</sub>ClN<sub>3</sub> (M + H)<sup>+</sup>: 348.1268; found: 348.1250.



**2-Methyl-6-[(4*R*,5*R*)-1-methyl-4,5-diphenyl-4,5-dihydro-1*H*-imidazol-2-yl]pyridine (199):** General procedure G was followed employing 163 mg of 6-

methylpicolinaldehyde (1.34 mmol), 300 mg (1*R*,2*R*)-diphenylethylenediamine (1.41 mmol), 252 mg *N*-bromosuccinimide (1.41 mmol), in 13 mL CH<sub>2</sub>Cl<sub>2</sub>. After workup, 429 mg (1.37 mmol) crude product was recovered. The crude product was then subjected to methylation conditions employing 1.78 mL of NaHMDS (1.0M in THF, 1.78 mmol) and 94 μL iodomethane (1.51 mmol) in 13 mL THF. The reaction mixture was purified by column chromatography (SiO<sub>2</sub>, 5% MeOH/CH<sub>2</sub>Cl<sub>2</sub>) to afford 256 mg (57%) of the title compound as a pale brown oil:  $[\alpha]_{\text{D}}^{19} +0.209$  (*c* 4.12, CHCl<sub>3</sub>); <sup>1</sup>H NMR (500 MHz, CDCl<sub>3</sub>): δ 7.93 (d, *J* = 7.5 Hz, 1H), 7.69 (t, *J* = 8.0 Hz, 1H), 7.42-7.22 (m, 11H), 5.00 (d, *J* = 10.5 Hz, 1H), 4.39 (d, *J* = 10.5 Hz, 1H), 3.00 (s, 3H), 2.64 (s, 3H); <sup>13</sup>C NMR (125 MHz, CDCl<sub>3</sub>): δ 164.3, 157.5, 149.8, 143.3, 140.8, 136.8, 128.8, 128.4, 127.9, 127.4, 127.1, 126.9, 124.2, 122.0, 34.2, 24.5; IR  $\nu_{\text{max}}^{\text{neat}}$  cm<sup>-1</sup>: 3060, 2922, 1591, 1569, 1453, 1388, 1302, 1277, 1222, 1156, 1080, 913, 808, 752; HRMS (EI) *m/z* calcd for C<sub>22</sub>H<sub>21</sub>N<sub>3</sub> (M + H)<sup>+</sup>: 328.1814; found: 328.1813.



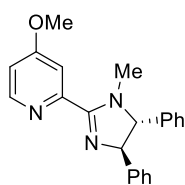
**2-[(4*R*,5*R*)-1-Methyl-4,5-diphenyl-4,5-dihydro-1*H*-imidazol-2-**

**yl]quinoline (200):** General procedure G was followed employing 106 mg of quinoline-2-carbaldehyde (0.67 mmol), 150 mg (1*R*,2*R*)-

diphenylethylenediamine (0.71 mmol), 125 mg *N*-bromosuccinimide (0.70 mmol), in 7 mL CH<sub>2</sub>Cl<sub>2</sub>. After workup, 104 mg (0.30 mmol) crude product was recovered. The crude product was then subjected to methylation conditions employing 0.39 mL of NaHMDS (1.0M in THF, 0.39 mmol) and 24 μL iodomethane (0.33 mmol) in 3 mL THF. The reaction mixture was purified by column chromatography (SiO<sub>2</sub>, 5% MeOH/CH<sub>2</sub>Cl<sub>2</sub>) to afford 94 mg (86%) of the title compound as a pale

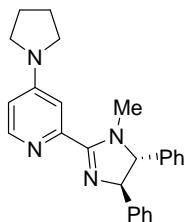
brown oil:  $[\alpha]_{\text{D}}^{19} -1.86$  (*c* 2.01, CHCl<sub>3</sub>); <sup>1</sup>H NMR (500 MHz, CDCl<sub>3</sub>): δ 8.27 (dd, *J* = 14.5, 9.0 Hz, 2H),

8.20 (d,  $J = 8.5$  Hz, 1H), 7.88 (d,  $J = 8.5$  Hz, 1H), 7.77 (ddd,  $J = 8.5, 7.0, 1.5$  Hz, 1H), 7.61 (ddd,  $J = 8.0, 1.0$  Hz, 1H), 7.44-7.28 (m, 10H), 5.06 (d,  $J = 10.5$  Hz, 1H), 4.44 (d,  $J = 10.5$  Hz, 1H), 3.20 (s, 3H);  $^{13}\text{C}$  NMR (125 MHz,  $\text{CDCl}_3$ ):  $\delta$  164.0, 150.5, 147.0, 143.3, 140.9, 136.4, 129.9, 129.7, 128.8, 128.5, 128.2, 127.9, 127.6, 127.4, 127.2, 127.1, 122.1, 79.2, 77.4, 34.6; IR  $\nu_{\text{max}}^{\text{neat}} \text{cm}^{-1}$ : 3059, 3028, 2926, 1600, 1555, 1491, 1392, 1277, 1067, 839, 755; HRMS (EI)  $m/z$  calcd for  $\text{C}_{25}\text{H}_{21}\text{N}_3$  ( $\text{M} + \text{H}$ ) $^+$ : 364.1814; found: 364.1808.



**4-Methoxy-2-[(4*R*,5*R*)-1-methyl-4,5-diphenyl-4,5-dihydro-1H-imidazol-2-yl]pyridine (201):** General procedure G was followed employing 355 mg of 4-methoxypicolinaldehyde (2.59 mmol), 577 mg (1*R*,2*R*)-diphenylethylenediamine

(2.59 mmol), 461 mg *N*-bromosuccinimide (2.59 mmol), in 26 mL  $\text{CH}_2\text{Cl}_2$ . After workup, 861 mg (2.61 mmol) crude product was recovered. The crude product was then subjected to methylation conditions employing 3.40 mL of NaHMDS (1.0M in THF, 3.40 mmol) and 42  $\mu\text{L}$  iodomethane (0.67mmol) in 6 mL THF. The reaction mixture was purified by column chromatography ( $\text{SiO}_2$ , 0-2% MeOH/ $\text{CH}_2\text{Cl}_2$  gradient) to afford 836 mg (72%) of the title compound as a pale brown oil:  $[\alpha]_{\text{D}}^{22} +0.995$  ( $c$  2.21,  $\text{CHCl}_3$ );  $^1\text{H}$  NMR (500 MHz,  $\text{CDCl}_3$ ):  $\delta$  8.50 (d,  $J = 5.5$  Hz, 1H), 7.68 (d,  $J = 2.5$  Hz, 1H), 7.40-7.26 (m, 10H), 6.91 (dd,  $J = 6.0, 2.5$  Hz, 1H), 4.99 (d,  $J = 10.5$  Hz, 1H), 4.39 (d,  $J = 10.5$  Hz, 1H), 3.93 (s, 3H), 3.01 (s, 3H);  $^{13}\text{C}$  NMR (125 MHz,  $\text{CDCl}_3$ ):  $\delta$  166.2, 164.3, 151.8, 149.8, 143.0, 140.6, 128.8, 126.9, 111.9, 110.2, 78.8, 76.9, 55.5, 34.3; IR  $\nu_{\text{max}}^{\text{neat}} \text{cm}^{-1}$ : 3060, 2939, 1593, 1562, 1474, 1435, 1376, 1304, 1280, 1190, 1070, 977, 866, 756; HRMS (EI)  $m/z$  calcd for  $\text{C}_{22}\text{H}_{21}\text{N}_3\text{O}$  ( $\text{M} + \text{H}$ ) $^+$ : 344.1763; found: 344.1765.

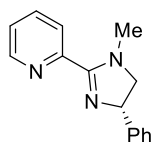


**2-[(4*R*,5*R*)-1-Methyl-4,5-diphenyl-4,5-dihydro-1*H*-imidazol-2-yl]-4-(pyrrolidin-1-yl)pyridine (202):** Compound **195a**, 440.0 mg (1.27 mmol) was added

to a medium pressure reaction vessel along with 4.2 mL pyrrolidine (neat, 50.6 mmol). The vessel was sealed and heated to 90°C for 24 h. At this time the reaction

vessel was removed from the oil bath and allowed to cool to ambient temperature and then concentrated in vacuo. The crude reaction mixture was purified by column chromatography (SiO<sub>2</sub>, 2-10% MeOH/CH<sub>2</sub>Cl<sub>2</sub> gradient) to afford 256.4 mg (53%) of the title compound as an off-white solid:

decomposition 62-65°C;  $[\alpha]_{\text{D}}^{19}$  -1.57 (*c* 1.08, CHCl<sub>3</sub>); <sup>1</sup>H NMR (500 MHz, CDCl<sub>3</sub>): δ 8.28 (d, *J* = 5.5 Hz, 1H), 7.38-7.26 (m, 10H), 7.19 (br s, 1H), 6.44 (dd, *J* = 6.0, 2.5 Hz, 1H), 4.99 (d, *J* = 10.0 Hz, 1H), 4.36 (d, *J* = 10.0 Hz, 1H), 3.40 (d, *J* = 2.0 Hz, 4H), 2.98 (s, 3H), 2.04 (p, *J* = 7.0 Hz, 4.0 Hz, 4H); <sup>13</sup>C NMR (125 MHz, CDCl<sub>3</sub>): δ 152.2, 148.7, 128.7, 128.4, 127.9, 127.3, 127.2, 126.9, 107.7, 78.7, 47.1, 34.2, 25.3; IR  $\nu_{\text{max}}^{\text{neat}}$  cm<sup>-1</sup>: 3029, 2969, 2855, 1600, 1538, 1495, 1455, 1346, 1275, 1219, 1157, 1082, 1007, 813, 753; HRMS (EI) *m/z* calcd for C<sub>25</sub>H<sub>26</sub>N<sub>4</sub>(M + H)<sup>+</sup>: 383.2236; found: 383.2248.

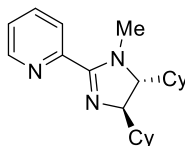


**(S)-2-(1-Methyl-4-phenyl-4,5-dihydro-1*H*-imidazole-2-yl)pyridine (203):**

Characterization materials match the data provided in the following publication:

Malkov, A. V.; Stewart-Kiddon, A. J. P.; McGeoch, G. D.; Ramírez-López, P.;

Kocovsky, P.; *Org. Biomol. Chem.*, **2012**, *10*, 4864-4877

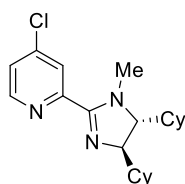


**2-[(4*R*,5*R*)-4,5-Dicyclohexyl-1-methyl-4,5-dihydro-1*H*-imidazole-2-yl]pyridine**

**(204):** General procedure G was followed employing 83 μL picolinaldehyde (0.87 mmol), 186 mg (1*R*,2*R*)-dicyclohexylethylenediamine (0.83 mmol), and 155.2 mg *N*-

bromosuccinimide (0.87 mmol) in 9 mL of CH<sub>2</sub>Cl<sub>2</sub>. After workup, 233.0 mg (0.75 mmol) of the crude

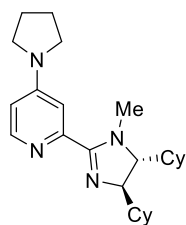
product was recovered. Then the crude product was subjected to methylation employing 0.97 mL NaHMDS (1.0M in THF, 0.974 mmol) and 51.3  $\mu$ L iodomethane (0.82 mmol) in 7 mL of THF. The reaction mixture was purified by column chromatography (SiO<sub>2</sub>, 5-10% MeOH/CH<sub>2</sub>Cl<sub>2</sub> gradient then 10% MeOH/2% Et<sub>3</sub>N/8% CH<sub>2</sub>Cl<sub>2</sub>) to afford 202.0 mg (83%) the title product, an orange/brown viscous oil;  $[\alpha]_D^{18} +11.29$  (*c* 1.15, CHCl<sub>3</sub>); <sup>1</sup>H NMR (500 MHz, CDCl<sub>3</sub>):  $\delta$  8.64 (dd, *J*= 4.5, 0.5 Hz, 1H), 7.99 (d, *J*= 7.0 Hz, 1H), 7.75 (dt, *J*= 7.5, 1.5 Hz, 1H), 7.32 (ddd, *J*= 7.5, 5.0, 1.0 Hz, 1H), 3.69 (t, *J*= 5.0 Hz, 1H), 3.14 (t, *J*= 4.0 Hz, 1H), 3.04 (s, 3H), 1.79-1.60 (m, 11H), 1.28-0.99 (m, 11H); <sup>13</sup>C NMR (125 MHz, CDCl<sub>3</sub>):  $\delta$  162.7, 148.7, 136.7, 125.3, 124.6, 71.2, 43.4, 41.2, 34.7, 28.6, 28.5, 27.2, 26.6, 26.5, 26.4, 26.3, 26.2; IR  $\nu_{\max}^{\text{neat}} \text{ cm}^{-1}$ : 2923, 2851, 1589, 1563, 1448, 1397, 1318, 1259, 1069, 1044, 799, 748; HRMS (EI) *m/z* calcd for C<sub>21</sub>H<sub>31</sub>N<sub>3</sub> (M + H)<sup>+</sup>: 326.2596; found: 326.2588.



**4-Chloro-2-[(4*R*,5*R*)-4,5-dicyclohexyl-1-methyl-4,5-dihydro-1*H*-imidazol-2-yl]pyridine (195b):** General procedure G was followed employing 146.7 mg 4-

chloropicolinaldehyde (1.00 mmol), 213 mg (1*R*,2*R*)-dicyclohexylethylenediamine (0.95 mmol), and 178.0 mg *N*-bromosuccinimide (1.00 mmol) in 10 mL of CH<sub>2</sub>Cl<sub>2</sub>. After workup, 319.0 mg (0.924 mmol) of the crude product was recovered. Then the crude product was subjected to methylation employing 1.20 mL NaHMDS (1.0 M in THF, 1.20 mmol) and 63.3  $\mu$ L iodomethane (1.02 mmol) in 10 mL of THF. The reaction mixture was purified by column chromatography (SiO<sub>2</sub>, 3-10% MeOH/ CH<sub>2</sub>Cl<sub>2</sub> gradient) to afford 203.0 mg (61%) of the title compound as a viscous, orange oil;  $[\alpha]_D^{19} +10.6$  (*c* 0.870, CHCl<sub>3</sub>); <sup>1</sup>H NMR (500 MHz, CDCl<sub>3</sub>):  $\delta$  8.52 (d, *J*= 5.0 Hz, 1H), 8.17 (br s, 1H), 7.35 (dd, *J*= 3.5, 1.5 Hz, 1H), 3.73 (br s, 1H), 3.24 (br s, 1H), 3.09 (s, 3H), 1.79-1.70 (m, 5H), 1.67-1.56 (m, 6H), 1.28-0.95 (m, 11H); <sup>13</sup>C NMR (125 MHz, CDCl<sub>3</sub>):  $\delta$  161.2, 149.6, 145.1, 126.1, 125.5, 71.3, 43.1, 40.7, 34.5, 28.3, 28.2, 28.1, 26.4, 26.3, 26.2, 26.1, 26.0; IR  $\nu_{\max}^{\text{neat}} \text{ cm}^{-1}$ : 2924, 2851,

1574, 1550, 1447, 1409, 1315, 1262, 1070, 981, 893, 843, 752 ; HRMS (EI)  $m/z$  calcd for  $C_{21}H_{30}ClN_3$  ( $M + H$ )<sup>+</sup>: 360.2210; found: 360.2207.



**2-[(4*R*,5*R*)-4,5-Dicyclohexyl-1-methyl-4,5-dihydro-1*H*-imidazol-2-yl]-4-(pyrrolidin-1-yl)pyridine (205):** Compound **195b**, 203.0 mg (0.57 mmol) was added to a medium pressure reaction vessel along with 1.86 mL neat pyrrolidine (22.6 mmol). The vessel was sealed and heated to 90°C for 24 h. At this time the

reaction vessel was removed from the oil bath and allowed to cool to ambient temperature and then concentrated in vacuo. The crude reaction mixture was purified by column chromatography (SiO<sub>2</sub>, 5-8% MeOH/CH<sub>2</sub>Cl<sub>2</sub> gradient) to afford 229.0 mg of the unmethylated HCl salt. The HCl salt was reexposed to the methylation procedure employing 187 mg of the salt (0.45 mmol), 1.12 mL NaHMDS (1.0 M in THF, 1.12 mmol), and 30.7 μL iodomethane (0.49 mmol) in 6 mL THF. The crude reaction mixture was purified by column chromatography (SiO<sub>2</sub>, 5-10% MeOH/ CH<sub>2</sub>Cl<sub>2</sub> gradient then 10% MeOH/1% Et<sub>3</sub>N/9% CH<sub>2</sub>Cl<sub>2</sub>) to afford 157 mg (89%) of the title compound

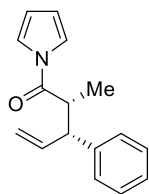
as a pale yellow oil:  $[\alpha]_D^{19} +7.07$  ( $c$  0.990, CHCl<sub>3</sub>); <sup>1</sup>H NMR (500 MHz, CDCl<sub>3</sub>): δ 8.18 (d,  $J$ = 6.0 Hz, 1H), 6.90 (br s, 1H), 6.31 (d,  $J$ = 5.5 Hz, 1H), 3.61 (t,  $J$ = 4.5 Hz, 1H), 3.30 (br s, 4H), 3.01 (br s, 1H), 2.94 (s, 3H), 1.96 (t,  $J$ = 6.0 Hz, 4H), 1.72-1.52 (m, 11H), 1.24-0.98 (m, 11H); <sup>13</sup>C NMR (125 MHz, CDCl<sub>3</sub>): δ 164.0, 151.9, 150.8, 148.6, 107.5, 107.0, 71.5, 70.5, 46.9, 43.4, 41.2, 34.4, 28.6, 28.4, 28.3, 27.2, 26.7, 26.6, 26.4, 26.4, 26.3, 26.2, 25.2; IR  $\nu_{max}^{neat}$  cm<sup>-1</sup>: 2922, 2850, 1600, 1539, 1484, 1460, 1388, 1349, 1315, 1262, 1181, 1073, 1006, 811, 750; HRMS (EI)  $m/z$  calcd for  $C_{25}H_{38}N_4$  ( $M + H$ )<sup>+</sup>: 395.3175; found: 395.3201.



## GENERAL PROCEDURE FOR THE RUTHENIUM CATALYZED ASYMMETRIC ENOLATE ALLYLIC ALKYLATIONS (GENERAL PROCEDURE I)

[CpRu(CH<sub>3</sub>CN)<sub>3</sub>]PF<sub>6</sub> (5 mol %) and ligand (5 mol %) were combined in a 2 dram vial inside a nitrogen-filled glovebox. THF (0.5 M final concentration of the allylic acetate substrate) was added and the reaction mixture was periodically shaken over 15 min. The resulting solution was then added to another 2 dram vial containing the allylic acetate (1 equiv), pyrrole silyl enol ether (1.05 equiv), B(O<sup>*i*</sup>C<sub>6</sub>H<sub>4</sub>F)<sub>3</sub> (15 mol %) and a Teflon-coated stir bar. The vial was sealed with a threaded cap containing a rubber septum inlet. The vial was removed from the glovebox, and the mixture was stirred at ambient temperature for 16 h. After this time, the vial was opened and the reaction mixture was concentrated under a stream of N<sub>2</sub>. Pentanes (4x the reaction volume) were added and the resulting heterogeneous mixture was filtered through a Florisil<sup>®</sup> plug eluting with additional pentanes. The filtrate was concentrated and the resulting mixture of the *anti/syn* [3,3] products and [1,3] regioisomer was analyzed by <sup>1</sup>H NMR and chiral stationary phase GC. The amide product was purified by column chromatography.

**Enantiomer ratio determination:** Enantiomer ratios of the branched products were determined by chiral stationary phase GLC (Varian Chirasil-Dex CB WCOT Fused Silica CP 7502 column, 25 m x 0.25 mm) or analytical high-performance liquid chromatography (HPLC) using a variable wavelength UV detector (deuterium lamp, 190-600 nm), a Chiracel OD-H column and HPLC-grade isopropanol and hexanes as the eluting solvents. Authentic samples of racemic *syn* and *anti* diastereomers of the products were used for comparison.



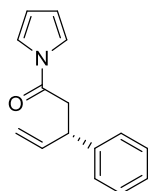
**(2R,3R)-2-Methyl-3-phenyl-1-(1H-pyrrol-1-yl)pent-4-en-1-one (187a):** General

Procedure I was followed employing 75 mg (0.43 mmol) cinnamyl acetate, 87.3 mg (0.45 mmol) (*Z*)-1-(1-((trimethylsilyl)oxy)prop-1-en-1-yl)-1H-pyrrole, 6.9 mg (0.021 mmol) ligand **204**, 9.2 mg (0.021 mmol) [CpRu(CH<sub>3</sub>CN)<sub>3</sub>]PF<sub>6</sub>, 21.9 mg (0.064 mmol) B(O<sup>*i*</sup>C<sub>6</sub>H<sub>4</sub>F)<sub>3</sub>, and 0.80 mL THF. The reaction mixture was stirred for 16 h at which time it was concentrated under a stream of N<sub>2</sub>, filtered through a plug of Florisil<sup>®</sup> and concentrated. The crude product was purified by column chromatography (SiO<sub>2</sub>, 3% Et<sub>2</sub>O/hexanes) to yield 90 mg (89%) as a mixture of diastereomers. Separating the stereoisomers of **187a** by GLC (flow rate 1.5 mL/min, method: 105 °C for 10 min, ramp @ 0.2 °C/min to 155 °C, hold for 5 min; T<sub>r</sub> (min) = 116.5 [(2*S*,3*S*)- **187a**<sub>anti</sub>], 117.2 [(2*R*,3*R*)- **187a**<sub>anti</sub>], 134.3 (**187a**<sub>syn1</sub>), 135.4 (**187a**<sub>syn2</sub>), (ratio = 2.1:129.5:1:20.9)) provided the enantiomer ratio (2*S*,3*S*)- **187a**<sub>anti</sub>:(2*R*,3*R*)- **187a**<sub>anti</sub> = 1.5:98.4 (97% ee), and (**187a**<sub>syn1</sub>):(**187a**<sub>syn2</sub>) = 4.5:95.4 (91% ee).

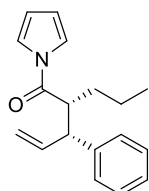
*Anti* diastereomer (white crystalline solid): mp 49-51 °C; [α]<sub>D</sub><sup>23</sup> +6.67 (*c* 2.34, CHCl<sub>3</sub>); <sup>1</sup>H NMR (500 MHz, CDCl<sub>3</sub>): δ 7.26-7.20 (m, 6H), 7.16-7.12 (m, 1H), 6.22 (dd, *J* = 2.0 Hz, 2H), 6.00 (dt, *J* = 16.5, 9.5, Hz, 1H), 5.19 (m, 2H), 3.76 (t, *J* = 10.0 Hz, 1H), 3.51 (dq, *J* = 10.0, 7.0 Hz, 1H), 1.38 (d, *J* = 6.5 Hz, 3H); <sup>13</sup>C NMR (125 MHz, CDCl<sub>3</sub>): δ 173.1, 142.0, 138.3, 128.6, 127.4, 126.7, 118.9, 117.3, 113.0, 53.3, 43.2, 16.8; IR ν<sub>max</sub><sup>neat</sup> cm<sup>-1</sup>: 3150, 3027, 1708, 1637, 1491, 1301, 1096, 915, 433; HRMS (EI) *m/z* calcd for C<sub>16</sub>H<sub>17</sub>NO (M + H)<sup>+</sup>: 240.1388; found: 240.1404.

*Syn* diastereomer (pale yellow oil): [α]<sub>D</sub><sup>23</sup> +7.57 (*c* 1.06, CHCl<sub>3</sub>); <sup>1</sup>H NMR (500 MHz, CDCl<sub>3</sub>): δ 7.37-7.32 (m, 4H), 7.26-7.22 (m, 3H), 6.32 (app t, *J* = 2.0 Hz, 2H), 5.97 (ddd, *J* = 18.0, 10.0, 8.0 Hz, 1H), 5.02 (dt, *J* = 17.0, 1.0 Hz, 1H), 4.97 (d, *J* = 10.0 Hz, 1H), 3.72 (t, *J* = 10.0 Hz, 1H), 3.46 (dq, *J* = 10.5, 7.0 Hz, 1H), 1.08 (d, *J* = 7.0 Hz, 3H); <sup>13</sup>C NMR (125 MHz, CDCl<sub>3</sub>): δ 173.5, 140.8, 138.9, 128.8, 128.3,

127.0, 119.0, 116.2, 113.3, 53.1, 43.3, 17.0; IR  $\nu_{\max}^{\text{neat}}$   $\text{cm}^{-1}$ : 3027, 2930, 1711, 1600, 1467, 914, 742; HRMS (EI)  $m/z$  calcd for  $\text{C}_{16}\text{H}_{17}\text{NO}$  ( $\text{M} + \text{H}$ )<sup>+</sup>: 240.1388; found: 240.1373.



**(S)-3-Phenyl-1-(1H-pyrrol-1-yl)pent-4-en-1-one (187b):** General Procedure I was followed employing 75 mg (0.43 mmol) cinnamyl acetate, 81 mg (0.45 mmol) 1-(1-((trimethylsilyl)oxy)vinyl)-1H-pyrrole, 6.9 mg (0.021 mmol) ligand **204**, 9.2 mg (0.021 mmol)  $[\text{CpRu}(\text{CH}_3\text{CN})_3]\text{PF}_6$ , 21.9 mg (0.064 mmol)  $\text{B}(\text{O}^i\text{C}_6\text{H}_4\text{F})_3$ , 0.80 mL THF. The reaction mixture was stirred for 16 h at which time it was concentrated under a stream of  $\text{N}_2$  filtered through a plug of Florisil<sup>®</sup> and concentrated. The crude product was purified via column chromatography ( $\text{SiO}_2$ , 3%  $\text{Et}_2\text{O}$ /hexanes) to yield 78 mg (82%) of the product as a colorless oil. Separating the stereoisomers of **187b** by GLC (flow rate 1.5 mL/min, method: 105 °C for 10 min, ramp @ 0.3 °C/min to 175 °C, hold for 5 min;  $T_r$  (min) = 120.4 [(3*S*-(**187b**)], 120.9 [3*R*-(**187b**)], (ratio = 1:37.4)) provided an ee of 95%.  $[\alpha]_{\text{D}}^{23} +0.940$  ( $c$  0.830,  $\text{CHCl}_3$ );  $^1\text{H}$  NMR (500 MHz,  $\text{CDCl}_3$ ):  $\delta$  7.33-7.29 (m, 4H), 7.27-7.21 (m, 3H), 6.28 (app t,  $J = 2.0$  Hz, 2H), 6.06 (ddd,  $J = 24.0, 10.5, 7.0$  Hz, 1H), 5.10 (m, 2H), 4.10 (dd,  $J = 14.5, 7.0$  Hz, 1H), 3.24 (dq,  $J = 16.0, 7.5$  Hz, 2H);  $^{13}\text{C}$  NMR (125 MHz,  $\text{CDCl}_3$ ):  $\delta$  168.6, 142.3, 139.9, 128.7, 127.6, 126.9, 119.0, 115.3, 113.2, 44.8, 40.3; IR  $\nu_{\max}^{\text{neat}}$   $\text{cm}^{-1}$ : 3148, 3028, 2921, 1717, 1638, 1600, 1468, 1338, 1275, 1073, 922, 740; HRMS (EI)  $m/z$  calcd for  $\text{C}_{15}\text{H}_{15}\text{NO}$  ( $\text{M} + \text{H}$ )<sup>+</sup> 226.1232; found: 226.1224.



**(2*R*,3*R*)-3-Phenyl-2-propyl-1-(1H-pyrrol-1-yl)pent-4-en-1-one (187c):** General Procedure I was followed employing 75 mg (0.43 mmol) cinnamyl acetate, 100 mg (0.45 mmol) (*Z*)-1-(1-((trimethylsilyl)oxy)pent-1-en-1-yl)-1H-pyrrole (**187c**), 6.9 mg (0.021 mmol) ligand **204**, 9.2 mg (0.021 mmol)  $[\text{CpRu}(\text{CH}_3\text{CN})_3]\text{PF}_6$ , 146 mg (0.43 mmol)  $\text{B}(\text{O}^i\text{C}_6\text{H}_4\text{F})_3$ , 0.80

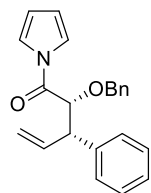
mL THF. The reaction mixture was stirred for 16 h at which time it was concentrated under a stream of N<sub>2</sub>, filtered through a plug of Florisil<sup>®</sup> and concentrated. The crude product was purified via column chromatography (SiO<sub>2</sub>, 3% Et<sub>2</sub>O/hexanes) to yield 93 mg (82%) of the product as a mixture of diastereomers.

*Anti* diastereomer (white crystalline solid): mp 81-83 °C;  $[\alpha]_{\text{D}}^{22} +6.40$  (*c* 4.56, CHCl<sub>3</sub>); <sup>1</sup>H NMR (500 MHz, CDCl<sub>3</sub>): δ 7.20-7.15 (m, 5H), 7.10 (m, 1H), 6.16 (app t, *J* = 2.0 Hz, 2H), 6.02 (ddd, *J* = 17.0, 9.5 Hz, 1H), 5.17 (m, 2H), 3.71 (t, *J* = 9.5 Hz, 1H), 3.41 (dt, *J* = 10.0, 4.0 Hz, 1H), 3.14 (dt, *J* = 10.0, 4.0 Hz, 1H), 1.83-1.74 (m, 2H), 1.34-1.18 (m, 2H), 0.88 (t, *J* = 7.0 Hz, 3H); <sup>13</sup>C NMR (125 MHz, CDCl<sub>3</sub>): δ 173.0, 141.8, 138.5, 128.6, 127.5, 126.7, 119.0, 117.2, 112.9, 53.3, 49.3, 33.7, 20.4, 14.1; IR  $\nu_{\text{max}}^{\text{neat}} \text{cm}^{-1}$ : 3148, 3029, 2927, 1694, 1638, 1468, 1345, 1274, 1110, 1048, 924, 758; HRMS (EI) *m/z* calcd for C<sub>18</sub>H<sub>21</sub>NO (M + H)<sup>+</sup>: 268.1701; found: 268.1720.

*Syn* diastereomer (pale yellow oil):  $[\alpha]_{\text{D}}^{22} +1.67$  (*c* 1.28, CHCl<sub>3</sub>); <sup>1</sup>H NMR (500 MHz, CDCl<sub>3</sub>): δ 7.38 (br s, 2H), 7.34 (t, *J* = 7.5 Hz, 2H), 7.23 (dd, *J* = 10.0, 8.5 Hz, 3H), 6.31 (app t, *J* = 2.0 Hz, 2H), 5.93 (ddd, *J* = 19.0, 10.5, 8.3 Hz, 1H), 5.00 (d, *J* = 17.0 Hz, 1H), 4.92 (d, *J* = 10.0 Hz, 1H), 3.68 (t, *J* = 9.0 Hz, 1H), 3.42 (dt, *J* = 10.0, 3.5 Hz, 1H), 1.70-1.63 (m, 1H), 1.34-1.28 (m, 1H), 1.25-1.20 (m, 1H), 1.20-1.17 (m, 1H), 0.74 (t, *J* = 7.0 Hz, 3H); <sup>13</sup>C NMR (125 MHz, CDCl<sub>3</sub>): δ 173.3, 141.2, 138.5, 128.8, 128.0, 126.9, 119.0, 116.4, 113.3, 53.4, 49.3, 33.7, 20.5, 14.0; IR  $\nu_{\text{max}}^{\text{neat}} \text{cm}^{-1}$ : 3150, 3027, 2924, 1709, 1466, 1371, 1114, 1073, 742; HRMS (EI) *m/z* calcd for C<sub>18</sub>H<sub>21</sub>NO (M + H)<sup>+</sup>: 268.1701; found: 268.1720.

The compound was derivatized to the methyl ester for ee determination. General procedure: To a solution of acyl pyrrole (1.0 equiv) in MeOH (0.1M) was added NaOMe (10.0 equiv). The reaction was allowed to stir at rt for 24 h, and then quenched with saturated ammonium chloride. The reaction was extracted 3 times with Et<sub>2</sub>O, dried over MgSO<sub>4</sub>, and concentrated. Separating the stereoisomers

of **187c** by GLC (flow rate 2.0 mL/min, method: 80 °C for 10 min, ramp @ 0.4 °C/min to 160 °C, hold for 5 min;  $T_r$  (min) = 60.0 [(2*R*,3*R*)- **187c**<sub>anti</sub>], 60.7 [(2*S*,3*S*)- **187c**<sub>anti</sub>], 81.2 (**187c**<sub>syn1</sub>), 82.4 (**187c**<sub>syn2</sub>), (ratio = 374:7.4:1:65.9)) provided the enantiomer ratio (2*R*,3*R*)- **187c**<sub>anti</sub>:(2*S*,3*S*)- **187c**<sub>anti</sub> = 98.0:1.9 (96% ee), and (**187c**<sub>syn1</sub>):(**187c**<sub>syn2</sub>) = 1.5:98.5 (97% ee).



**(2*R*,3*S*)-2-(Benzyloxy)-3-phenyl-1-(1*H*-pyrrol-1-yl)pent-4-en-1-one (187f):**

General Procedure I was followed employing 100 mg (0.57 mmol) cinnamyl acetate, 171 mg (0.59 mmol) (*Z*)-1-(2-(benzyloxy)-1-((trimethylsilyl)oxy)vinyl)-1*H*-pyrrole, 9.2 mg (0.028 mmol) ligand **204**, 12.3 mg (0.028 mmol) [CpRu(CH<sub>3</sub>CN)<sub>3</sub>]PF<sub>6</sub>, 29 mg (0.085 mmol) B(O<sup>*i*</sup>C<sub>6</sub>H<sub>4</sub>F)<sub>3</sub>, 1.0 mL THF. The reaction mixture was stirred for 16 h at which time it was concentrated under a stream of N<sub>2</sub>, filtered through a plug of Florisil<sup>®</sup> and concentrated. The crude product was purified via column chromatography (SiO<sub>2</sub>, 5% Et<sub>2</sub>O/hexanes) to yield 141 mg (75%) of the product as a mixture of diastereomers.

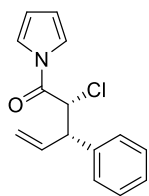
*Anti* diastereomer (white solid): mp 77-79 °C;  $[\alpha]_D^{22} +5.00$  (*c* 0.280, CHCl<sub>3</sub>); <sup>1</sup>H NMR (500 MHz, CDCl<sub>3</sub>): δ 7.37 (br s, 2H), 7.32-7.16 (m, 10H), 6.30-6.23 (m, 3H), 5.20 (d, *J* = 10.5 Hz, 1H), 5.08 (d, *J* = 17.0 Hz, 1H), 4.70 (m, 2H), 4.41 (d, *J* = 11.5 Hz, 1H), 3.90 (t, *J* = 7.0 Hz, 1H); <sup>13</sup>C NMR (125 MHz, CDCl<sub>3</sub>): δ 168.7, 139.2, 136.3, 136.1, 128.6, 128.4, 128.3, 128.1, 128.0, 127.3, 119.5, 117.9, 113.2, 83.3, 72.5, 53.4; IR  $\nu_{\max}^{\text{neat}}$  cm<sup>-1</sup>: 3083, 3029, 2859, 1715, 1688, 1466, 1329, 1289, 1096, 1019, 926, 739; HRMS (EI) *m/z* calcd for C<sub>22</sub>H<sub>21</sub>NO<sub>2</sub> (M + H)<sup>+</sup>: 332.1651; found: 332.1640.

*Syn* diastereomer (yellow oil):  $[\alpha]_D^{18} +2.50$  (*c* 0.08, CHCl<sub>3</sub>); <sup>1</sup>H NMR (500 MHz, CDCl<sub>3</sub>): δ 7.48 (t, *J* = 2.5 Hz, 2H), 7.33-7.28 (m, 3H), 7.23-7.20 (m, 5H), 6.97 (m, 2H), 6.28 (t, *J* = 2.5 Hz, 2H), 5.95 (ddd, *J* = 9.0, 10, 17 Hz, 1H), 4.98 (m, 2H), 4.63 (d, *J* = 9.0 Hz, 1H), 4.57 (d, *J* = 9.0 Hz, 1H), 4.23 (d, *J* = 9.0,

1H), 3.89 (t,  $J=9$  Hz, 1H);  $^{13}\text{C}$  NMR (125 MHz,  $\text{CDCl}_3$ ):  $\delta$ 169.4, 139.6, 136.3, 135.6, 128.5, 128.3, 127.9, 127.1, 119.5, 118.0, 113.3, 83.7, 72.4, 54.2; IR  $\nu_{\text{max}}^{\text{neat}}$   $\text{cm}^{-1}$ : 2956, 2926, 2867, 1712, 1602, 1505, 1468, 1409, 1344, 1255, 1088, 926, 820.0, 745; HRMS (EI)  $m/z$  calcd for  $\text{C}_{18}\text{H}_{21}\text{NO}$  ( $\text{M} + \text{Na}$ ) $^+$ : 354.1470; found: 254.1467.

The benzyl ether protecting group was removed for ee determination. General Procedure: To a  $-78$  °C solution of compound **187f** (1.0 equiv) in  $\text{CH}_2\text{Cl}_2$  (0.1M) was added a 1.0M solution of  $\text{BCl}_3$  in  $\text{CH}_2\text{Cl}_2$  dropwise. The reaction was allowed to stir at  $-78$  °C for 3 h at which time it was quenched with an equal volume of MeOH. The reaction was allowed to warm to rt and then concentrated in vacuo.

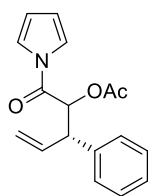
Separating the stereoisomers of **187f** by GLC (flow rate 1.0 mL/min, method: 105 °C for 10 min, ramp @ 0.7 °C/min to 200 °C, hold for 5 min;  $T_r$  (min) = 99.3 (**187f**<sub>syn1</sub>), 99.9 (**187f**<sub>syn2</sub>) 100.9 [(2*S*,3*S*)-**187f**<sub>anti</sub>], , 101.5 [(2*R*,3*R*)-**187f**<sub>anti</sub>], (ratio = 1:17:2:104)) provided the enantiomer ratio (2*S*,3*S*)-**187f**<sub>anti</sub>:(2*R*,3*R*)-**187f**<sub>anti</sub> = 1.9:98.1 (96% ee), and (**187f**<sub>syn1</sub>):(**187f**<sub>syn2</sub>) = 5.6:94.4 (89% ee).



**(2*R*,3*S*)-2-Chloro-3-phenyl-1-(1H-pyrrol-1-yl)pent-4-en-1-one (187f):** General

Procedure I was followed employing 100 mg (0.57 mmol) cinnamyl acetate, 128 mg (0.59 mmol) (*Z*)-1-(2-chloro-1-((trimethylsilyl)oxy)vinyl)-1H-pyrrole **187f**, 9.2 mg (0.028 mmol) ligand **204**, 12.3 mg (0.028 mmol)  $[\text{CpRu}(\text{CH}_3\text{CN})_3]\text{PF}_6$ , 29 mg (0.085 mmol)  $\text{B}(\text{O}^i\text{C}_6\text{H}_4\text{F})_3$ , 1.0 mL THF. The reaction mixture was stirred for 16 h at which time it was concentrated under a stream of  $\text{N}_2$  filtered through a plug of Florisil<sup>®</sup> and concentrated. The crude product was purified via column chromatography ( $\text{SiO}_2$ , 3%  $\text{Et}_2\text{O}$ /hexanes) to yield 56 mg (38%) of the product as an inseparable mixture of diastereomers. In addition, 16mg (10%) of the OAc substituted product was collected eluting with 10%  $\text{Et}_2\text{O}$ /hexanes. Separating the stereoisomers of **187f** by GLC (flow rate 1.5 mL/min,

method: 105 °C for 10 min, ramp @ 0.3 °C/min to 175 °C, hold for 5 min;  $T_r$  (min) = 140.6 [(2*S*,3*S*)-**187f**<sub>anti</sub>], 141.2 [(2*R*,3*R*)-**187f**<sub>anti</sub>], (ratio = 66.1:1)) provided an ee of 97%. The *syn* stereoisomers could not be separated. Diastereomer ratio(*anti:syn*) = 1.0: 0.80 (pale yellow oil);  $[\alpha]_D^{23} +4.17$  ( $c$  5.72, CHCl<sub>3</sub>); <sup>1</sup>H NMR (500 MHz, CDCl<sub>3</sub>):  $\delta$  7.43-7.23 (m, 9H), 6.40 (t,  $J$ = 2.5 Hz, 2H), 6.29 (t,  $J$ = 2.0 Hz, 1.5H), 6.23 (ddd,  $J$  = 18.5, 10.5, 2.0 Hz, 0.8H), 6.01 (ddd,  $J$ = 17.5, 11.0, 6.5 Hz, 1H), 5.32 (d,  $J$ = 10.0 Hz, 0.8H), 5.25 (dt,  $J$ = 17.0, 10.0 Hz, 0.8H), 5.18 (d,  $J$ = 1.0 Hz, 1H), 5.15 (d,  $J$ = 6.5 Hz, 1H), 5.12 (d,  $J$ = 10.0 Hz, 0.8H), 5.09 (d,  $J$ = 10.5 Hz, 1H), 4.21 (dd,  $J$ = 17.5, 7.5 Hz, 1.8H); <sup>13</sup>C NMR (125 MHz, CDCl<sub>3</sub>):  $\delta$  164.5, 165.1, 138.9, 138.6, 136.2, 135.8, 128.9, 128.8, 128.5, 128.1, 127.6, 127.6, 119.4, 119.3, 119.1, 118.9, 114.2, 113.9, 57.4, 57.1, 53.1, 52.8; IR  $\nu_{\max}^{\text{neat}}$  cm<sup>-1</sup>: 3150, 3063, 3029, 1638, 1600, 1547, 1411, 1364, 1318, 1265, 1233, 1076, 988, 860, 742; HRMS (EI)  $m/z$  calcd for C<sub>15</sub>H<sub>14</sub>ClNO (M + H)<sup>+</sup>: 260.0842; found: 260.0825.



**(3*S*)-1-Oxo-3-phenyl-1-(1*H*-pyrrol-1-yl)pent-4-en-2-yl acetate (**187f**):** Separating

the stereoisomers of **187f** by GLC (flow rate 1.5 mL/min, method: 105 °C for 10 min,

ramp @ 0.2 °C/min to 155 °C, hold for 5 min;  $T_r$  (min) = 172.7 [(2*R*,3*S*)-**187f**<sub>syn</sub>], 174.1

[(2*S*,3*R*)-**187f**<sub>syn</sub>], 176.3 (**187f**<sub>anti1</sub>), 178.9 (**187f**<sub>anti2</sub>), (ratio = 1.1:112.6:79.9:1)) provided the enantiomer

ratio (2*R*,3*S*)-**187f**<sub>syn</sub>:(2*S*,3*R*)-**187f**<sub>syn</sub> = 1.0:99.0 (98% ee), and (**187f**<sub>syn1</sub>): (**187f**<sub>syn2</sub>) = 1.5:98.7 (97%

ee). *Anti* diastereomer: *Syn* diastereomer = 1.0: 0.80 (pale yellow oil);  $[\alpha]_D^{23} +3.31$  ( $c$  1.16, CHCl<sub>3</sub>); <sup>1</sup>H

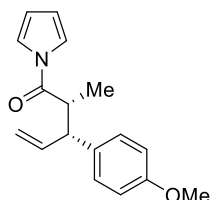
NMR (500 MHz, CDCl<sub>3</sub>):  $\delta$  7.38-7.20 (m, 13H), 6.33 (app t,  $J$ = 2.5 Hz, 1.4H), 6.25 (app t,  $J$ = 2.5 Hz,

2H), 6.17 (ddd,  $J$  = 17.0, 10.0, 8.5 Hz, 1.3H), 5.99 (ddd,  $J$ = 17.0, 10.0, 8.5 Hz, 0.8H), 5.94 (m, 0.8H),

5.92 (s, 1H), 5.22 (d,  $J$ = 10.0 Hz, 1.1H), 5.12 (m, 2.8H), 4.02 (m, 1.8H), 2.16 (s, 3H), 1.96 (s, 2H); <sup>13</sup>C

NMR (125 MHz, CDCl<sub>3</sub>):  $\delta$  170.2, 170.0, 166.5, 166.1, 138.3, 138.1, 135.0, 134.6, 128.8, 128.6, 128.4,

128.1, 127.6, 127.5, 119.2, 119.1, 118.7, 118.6, 113.9, 113.7, 74.1, 73.9, 51.9, 51.7, 20.6, 20.3; IR  $\nu_{\max}^{\text{neat}}$   $\text{cm}^{-1}$ : 3150, 3030, 2923, 1722, 1640, 1601, 1470, 1415, 1373, 1323, 1294, 1234, 1123, 1073, 926, 817, 744; HRMS (EI)  $m/z$  calcd for  $\text{C}_{15}\text{H}_{14}\text{ClNO}$  ( $\text{M} + \text{Na}$ ) $^{+}$ : 306.1106; found: 306.1124.



**(2R,3R)-3-(4-Methoxyphenyl)-2-methyl-1-(1H-pyrrol-1-yl)pent-4-en-1-one**

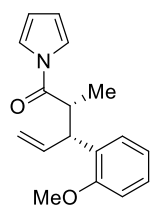
**(187g):** General Procedure I was followed employing 100 mg (0.49 mmol) (E)-3-(4-methoxyphenyl)allyl acetate, 99 mg (0.51 mmol) (Z)-1-(1-((trimethylsilyl)oxy)prop-1-en-1-yl)-1H-pyrrole, 7.9 mg (0.024 mmol) ligand **204**, 10.5 mg (0.024 mmol)  $[\text{CpRu}(\text{CH}_3\text{CN})_3]\text{PF}_6$ , 25 mg (0.073 mmol)  $\text{B}(\text{O}^i\text{C}_6\text{H}_4\text{F})_3$ , 1.0 mL THF. The reaction mixture was stirred for 16 h at which time it was concentrated under a stream of  $\text{N}_2$ , filtered through a plug of Florisil<sup>®</sup> and concentrated. The crude product was purified via column chromatography ( $\text{SiO}_2$ , 5%  $\text{Et}_2\text{O}$ /hexanes) to yield 103 mg (79%) of the product as a mixture of diastereomers. *Anti* diastereomer (white crystalline solid): mp 56-59 °C;  $[\alpha]_{\text{D}}^{22} +0.291$  ( $c$  1.10,  $\text{CHCl}_3$ );  $^1\text{H}$  NMR (500 MHz,  $\text{CDCl}_3$ ):  $\delta$  7.22 (br s, 2H), 7.11 (d,  $J=9$  Hz, 2H), 6.76 (d,  $J=8.5$  Hz, 2H), 6.22 (app t,  $J=2.0$  Hz, 2H), 5.97 (ddd,  $J=18.0, 16.5, 9.0$  Hz, 1H), 5.15 (m, 2H), 3.73 (s, 3H), 3.71 (m, 1H), 3.46 (dq,  $J=9.5, 7.0$  Hz, 1H), 1.36 (d,  $J=7.0$  Hz, 3H);  $^{13}\text{C}$  NMR (125 MHz,  $\text{CDCl}_3$ ):  $\delta$  173.1, 158.2, 138.5, 134.2, 128.4, 118.9, 116.9, 114.0, 113.0, 55.1, 52.4, 43.4, 16.9; IR  $\nu_{\max}^{\text{neat}}$   $\text{cm}^{-1}$ : 3149, 3074, 2935, 2836, 1714, 1636, 1491, 1467, 1366, 1273, 1125, 1072, 995, 896, 742; HRMS (EI)  $m/z$  calcd for  $\text{C}_{17}\text{H}_{19}\text{NO}_2$  ( $\text{M} + \text{H}$ ) $^{+}$ : 270.1494; found: 270.1501.

*Syn diastereomer* (clear colorless oil):  $[\alpha]_{\text{D}}^{22} +9.74$  ( $c$  0.310,  $\text{CHCl}_3$ );  $^1\text{H}$  NMR (500 MHz,  $\text{CDCl}_3$ ):  $\delta$  7.38 (br s, 2H), 7.14 (d,  $J=8.5$  Hz, 2H), 6.89 (d,  $J=8.5$  Hz, 2H), 6.32 (app t,  $J=2.5$  Hz, 2H), 5.96 (ddd,  $J=17.5, 10.5, 8.0$  Hz, 1H), 4.98 (m, 2H), 3.81 (s, 3H), 3.68 (t,  $J=8.0$  Hz, 1H), 3.41 (dq,  $J=10.0, 3.5$  Hz, 1H), 1.08 (d,  $J=7.0$  Hz, 3H);  $^{13}\text{C}$  NMR (125 MHz,  $\text{CDCl}_3$ ):  $\delta$  173.6, 158.5, 139.1, 132.8, 129.2,



119.0, 115.8, 114.2, 113.3, 55.3, 52.2, 43.4, 16.9; IR  $\nu_{\max}^{\text{neat}}$   $\text{cm}^{-1}$ : 2930, 2360, 1709, 1492, 1466, 1371, 1274, 1120, 1073, 914, 743; HRMS (EI)  $m/z$  calcd for  $\text{C}_{17}\text{H}_{19}\text{NO}_2$  ( $\text{M} + \text{H}$ )<sup>+</sup>: 270.1494; found: 270.1479.

The compound was derivatized to the methyl ester for ee determination. General procedure: To a solution of acyl pyrrole (1.0 equiv) in MeOH (0.1M) was added NaOMe(10.0 equiv). The reaction was allowed to stir at rt for 24 h, and then quenched with saturated ammonium chloride. The reaction was extracted 3 times with Et<sub>2</sub>O, dried over MgSO<sub>4</sub>, and concentrated. Separating the stereoisomers of **187g** by GLC (flow rate 2.0 mL/min, method: 80 °C for 10 min, ramp @ 0.4 °C/min to 160 °C, hold for 5 min; T<sub>r</sub> (min) = 112.9 [(2*S*,3*S*)- **187g**<sub>anti</sub>], 113.9 [(2*R*,3*R*)- **187g**<sub>anti</sub>], 123.4 (**187g**<sub>syn1</sub>), 123.7 (**187g**<sub>syn2</sub>), (ratio = 2.2:66.8:1:16.6)) provided the enantiomer ratio (2*S*,3*S*)- **187g**<sub>anti</sub>:(2*R*,3*R*)- **187g**<sub>anti</sub> = 3.2:96.8 (94% ee), and (**187g**<sub>syn1</sub>): (**187g**<sub>syn2</sub>) = 5.6:94.3 (89% ee).

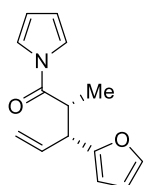


**(2*R*,3*R*)-3-(2-Methoxyphenyl)-2-methyl-1-(1H-pyrrol-1-yl)pent-4-en-1-one**

**(187h)**: General Procedure I was followed employing 100 mg (0.49 mmol) (E)-3-(2-methoxyphenyl)allyl acetate, 99 mg (0.51 mmol) (Z)-1-(1-((trimethylsilyl)oxy)prop-1-en-1-yl)-1H-pyrrole, 7.9 mg (0.024 mmol) ligand **204**, 10.5 mg (0.024 mmol) [CpRu(CH<sub>3</sub>CN)<sub>3</sub>]PF<sub>6</sub>, 25 mg (0.073 mmol) B(O<sup>*t*</sup>C<sub>6</sub>H<sub>4</sub>F)<sub>3</sub>, 1.0 mL THF. The reaction mixture was stirred for 16 h at which time it was concentrated under a stream of N<sub>2</sub>, filtered through a plug of Florisil<sup>®</sup> and concentrated. The crude product was purified via column chromatography (SiO<sub>2</sub>, 5% Et<sub>2</sub>O/hexanes) to yield 104 mg (80%) of the product as a mixture of diastereomers. Separating the stereoisomers of **187h** by GLC (flow rate 1.5 mL/min, method: 105 °C for 10 min, ramp @ 0.2 °C/min to 155 °C, hold for 5 min; T<sub>r</sub> (min) = 170.9 [(2*S*,3*S*)- **187h**<sub>anti</sub>], 172.4 [(2*R*,3*R*)- **187h**<sub>anti</sub>], 186.4 (**187h**<sub>syn1</sub>), 187.9 (**187h**<sub>syn2</sub>), (ratio = 1:84.2:19.0:1.5)) provided the enantiomer ratio (2*S*,3*S*)- **187h**<sub>anti</sub>:(2*R*,3*R*)- **187h**<sub>anti</sub> = 1.2:98.8 (98% ee), and (**187h**<sub>syn1</sub>): (**187h**<sub>syn2</sub>) = 92.7:7.3 (85% ee).

*Anti* diastereomer (white crystalline solid): mp 50-52 °C;  $[\alpha]_{\text{D}}^{22} +7.83$  ( $c$  2.84, CHCl<sub>3</sub>); <sup>1</sup>H NMR (500 MHz, CDCl<sub>3</sub>): δ 7.36 (dd,  $J$ = 2.0 Hz, 2H), 7.17-7.14 (m, 2H), 6.86 (app t,  $J$ = 7.0, 7.0 Hz, 1H), 6.82 (d,  $J$  = 8.0 Hz, 1H), 6.24 (t,  $J$ = 2.0 Hz, 2H), 6.21 (m, 1H), 5.10 (m, 2H), 4.03 (t,  $J$ = 9.0 Hz, 1H), 3.87 (s, 3H), 3.81 (ddd,  $J$ = 7.0 Hz, 1H), 1.25 (d,  $J$ = 7.0 Hz, 3H); <sup>13</sup>C NMR (125 MHz, CDCl<sub>3</sub>): δ 173.3, 156.5, 136.4, 129.9, 129.2, 127.8, 120.7, 119.1, 117.6, 112.6, 110.8, 55.2, 49.1, 41.1, 15.0; IR  $\nu_{\text{max}}^{\text{neat}}$  cm<sup>-1</sup>: 3151, 3004, 2905, 2835, 1701, 1611, 1513, 1469, 1376, 1278, 1179, 835, 743 ; HRMS (EI)  $m/z$  calcd for C<sub>17</sub>H<sub>19</sub>NO<sub>2</sub> (M + Na)<sup>+</sup>: 292.1313; found: 292.1310.

*Syn diastereomer* (clear colorless oil):  $[\alpha]_{\text{D}}^{22} +5.74$  ( $c$  0.380, CHCl<sub>3</sub>); <sup>1</sup>H NMR (500 MHz, CDCl<sub>3</sub>): δ 7.38 (br s, 2H), 7.23 (dt,  $J$ = 8.0, 1.5 Hz, 1H), 7.16 (dd,  $J$  = 7.5, 1.5 Hz, 1H), 6.93 (dt,  $J$  = 7.5, 1.0 Hz, 1H), 6.89 (d,  $J$  = 8.5 Hz, 1H), 6.30 (app t,  $J$ = 2.0 Hz, 2H), 6.10 (ddd,  $J$ = 18.5, 10.0, 8.0 Hz, 1H), 5.04 (dt,  $J$  = 17.0, 1.0 Hz, 1H), 4.94 (dd,  $J$ = 10.0, 0.5 Hz, 1H), 4.04 (t,  $J$ = 9.0 Hz, 1H), 3.85 (s, 3H), 3.75 (dq,  $J$ = 9.5, 7.0 Hz, 1H), 1.08 (d,  $J$ = 6.5 Hz, 3H); <sup>13</sup>C NMR (125 MHz, CDCl<sub>3</sub>): δ 173.9, 157.2, 138.0, 129.7, 129.0, 128.0, 120.8, 119.1, 116.2, 113.0, 111.0, 55.4, 48.9, 41.5, 16.5; IR  $\nu_{\text{max}}^{\text{neat}}$  cm<sup>-1</sup>: 2930, 2835, 1711, 1637, 1511, 1466, 1408, 1320, 1269, 1178, 1115, 1073, 993, 828, 742; HRMS (EI)  $m/z$  calcd for C<sub>17</sub>H<sub>19</sub>NO<sub>2</sub> (M + H)<sup>+</sup>: 270.1494; found: 270.1531.



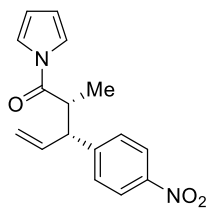
**(2R,3R)-3-(Furan-2-yl)-2-methyl-1-(1H-pyrrol-1-yl)pent-4-en-1-one (187i):**

General Procedure I was followed employing 100 mg (0.60 mmol) (E)-3-(furan-2-yl)allyl acetate, 123 mg (0.63 mmol) (Z)-1-(1-((trimethylsilyl)oxy)prop-1-en-1-yl)-1H-pyrrole, 9.8 mg (0.030 mmol) ligand **204**, 13.1 mg (0.030 mmol) [CpRu(CH<sub>3</sub>CN)<sub>3</sub>]PF<sub>6</sub>, 31 mg (0.090 mmol) B(O<sup>*i*</sup>C<sub>6</sub>H<sub>4</sub>F)<sub>3</sub>, 1.2 mL THF. The reaction mixture was stirred for 16 h at which time it was concentrated under a stream of N<sub>2</sub> filtered through a plug of Florisil<sup>®</sup> and concentrated. The crude

product was purified via column chromatography (SiO<sub>2</sub>, 3% Et<sub>2</sub>O/hexanes) to yield 136 mg (99%) of the product as a mixture of diastereomers. Separating the stereoisomers of **187i** by GLC (flow rate 2.0 mL/min, method: 80 °C for 10 min, ramp @ 0.4 °C/min to 160 °C, hold for 5 min; T<sub>r</sub> (min) = 105.3 [(2*S*,3*S*)- **187i**<sub>anti</sub>], 106.0 [(2*R*,3*R*)- **187i**<sub>anti</sub>], 108.0 (**187i**<sub>syn1</sub>), 109.2 (**187i**<sub>syn2</sub>), (ratio = 1.1:43.1:1:28.9)) provided the enantiomer ratio (2*S*,3*S*)- **187i**<sub>anti</sub>:(2*R*,3*R*)- **187i**<sub>anti</sub> = 2.4:97.5 (95% ee), and (**187i**<sub>syn1</sub>): (**187i**<sub>syn2</sub>) = 3.3:96.7 (93% ee)

*Anti* diastereomer (off white, waxy solid): mp 26-28 °C; [ $\alpha$ ]<sub>D</sub><sup>22</sup> +3.24 (*c* 4.64, CHCl<sub>3</sub>); <sup>1</sup>H NMR (500 MHz, CDCl<sub>3</sub>):  $\delta$  7.31 (br s, 2H), 7.25 (m, 1H), 6.27 (app t, *J* = 2.5 Hz, 2H), 6.21 (dd, *J* = 3.0, 2.0 Hz, 1H), 6.01 (d, *J* = 3.5 Hz, 1H), 5.92 (ddd, *J* = 17.0, 10.0, 9.5 Hz, 1H), 5.24 (dd, *J* = 10.0, 1.0 Hz, 1H), 5.18 (d, *J* = 17.0 Hz, 1H), 3.88 (t, *J* = 9.0 Hz, 1H), 3.57 (dq, *J* = 8.5, 7.0 Hz, 1H), 1.29 (d, *J* = 7.0 Hz, 3H); <sup>13</sup>C NMR (100 MHz, CDCl<sub>3</sub>):  $\delta$  172.9, 154.6, 141.5, 134.7, 119.1, 118.7, 113.1, 110.2, 106.0, 46.7, 41.5, 15.4; IR  $\nu_{\max}^{\text{neat}}$  cm<sup>-1</sup>: 3149, 2980, 1714, 1503, 1468, 1364, 1321, 1272, 1096, 994, 734; HRMS (EI) *m/z* calcd for C<sub>14</sub>H<sub>15</sub>NO<sub>2</sub> (M + H)<sup>+</sup>: 230.1181; found: 230.1183.

*Syn* diastereomer (light yellow oil): [ $\alpha$ ]<sub>D</sub><sup>22</sup> +3.03 (*c* 1.79, CHCl<sub>3</sub>); <sup>1</sup>H NMR (500 MHz, CDCl<sub>3</sub>):  $\delta$  7.37 (dd, *J* = 2.0, 1.0 Hz, 1H), 7.35 (br s, 2H), 6.32 (m, 3H), 6.15 (d, *J* = 3.0 Hz, 1H), 5.95 (ddd, *J* = 18.5, 10.5, 8.0 Hz, 1H), 5.08 (dt, *J* = 17.0, 1.0 Hz, 1H), 5.04 (d, *J* = 10.0 Hz, 1H), 3.85 (t, *J* = 9.0 Hz, 1H), 3.56 (dq, *J* = 9.5, 6.5 Hz, 1H), 1.16 (t, *J* = 7.0 Hz, 3H); <sup>13</sup>C NMR (125 MHz, CDCl<sub>3</sub>):  $\delta$  172.9, 153.8, 141.8, 135.9, 119.1, 117.4, 113.3, 110.2, 107.3, 46.5, 42.1, 16.8; IR  $\nu_{\max}^{\text{neat}}$  cm<sup>-1</sup>: 2978, 2929, 1712, 1639, 1503, 1467, 1409, 1318, 1274, 1148, 1073, 1010, 994, 909, 806, 737; HRMS (EI) *m/z* calcd for C<sub>14</sub>H<sub>15</sub>NO<sub>2</sub> (M + H)<sup>+</sup>: 230.1181; found: 230.1183.



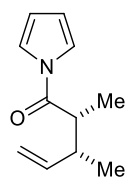
**(2*R*,3*R*)-2-Methyl-3-(4-nitrophenyl)-1-(1*H*-pyrrol-1-yl)pent-4-en-1-one**

**(187h):** General Procedure I was followed employing 100 mg (0.45 mmol) (*E*)-3-(4-nitrophenyl)allyl acetate, 93 mg (0.48 mmol) (*Z*)-1-(1-((trimethylsilyl)oxy)prop-1-en-1-yl)-1*H*-pyrrole, 7.4 mg (0.023 mmol) ligand **204**, 9.8 mg (0.023 mmol) [CpRu(CH<sub>3</sub>CN)<sub>3</sub>]PF<sub>6</sub>, 23 mg (0.068 mmol) B(O<sup>*i*</sup>C<sub>6</sub>H<sub>4</sub>F)<sub>3</sub>, 0.90 mL THF. The reaction mixture was stirred for 16 h at which time it was concentrated under a stream of N<sub>2</sub>, filtered through a plug of Florisil<sup>®</sup> and concentrated. The crude product was purified via column chromatography (SiO<sub>2</sub>, 6% Et<sub>2</sub>O/hexanes) to yield 112 mg (88%) of the product as a mixture of diastereomers. Separating the enantiomers by chiral HPLC [Daicel Chiralpak OD-H column, flow rate 1.0 ml/min, 1% *i*PrOH, 99% hexane; T<sub>r</sub> (min) = 13.3 [(2*S*,3*S*)-**187h**<sub>anti</sub>], 14.3 [(2*R*,3*R*)- **187h**<sub>anti</sub>], 15.9 (**187h**<sub>syn1</sub>), 17.0 (**187h**<sub>syn2</sub>), (ratio = 1:30.4:6.7:220.9)] provided the enantiomer ratio (2*S*,3*S*)- **187h**<sub>anti</sub>:(2*R*,3*R*)- **187h**<sub>anti</sub> = 3.2:96.8 (94% ee), and (**187h**<sub>syn1</sub>): (**187h**<sub>syn2</sub>) = 2.9:97.1 (94% ee)

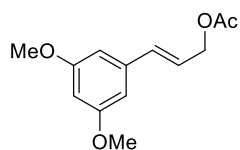
*Anti* diastereomer (off white solid): mp 93-95 °C; [α]<sub>D</sub><sup>22</sup> +8.71 (*c* 1.84, CHCl<sub>3</sub>); <sup>1</sup>H NMR (500 MHz, CDCl<sub>3</sub>): δ 8.09 (d, *J* = 8.5 Hz, 2H), 7.36 (d, *J* = 9.0 Hz, 2H), 7.18 (m, 2H), 6.24 (dd, *J* = 2.5 Hz, 2H), 5.94 (m, 1H), 5.23 (m, 2H), 3.86 (t, *J* = 10.0 Hz, 1H), 3.50 (dq, *J* = 10.0, 7.0 Hz, 1H), 1.42 (d, *J* = 7.0 Hz, 3H); <sup>13</sup>C NMR (125 MHz, CDCl<sub>3</sub>): δ 172.4, 149.8, 146.7, 137.0, 128.4, 123.9, 118.8, 118.7, 113.6, 53.1, 43.1, 17.3; IR ν<sub>max</sub><sup>neat</sup> cm<sup>-1</sup>: 3148, 3078, 2927, 1709, 1638, 1598, 1467, 1408, 1298, 1235, 1094, 994, 919, 893, 822, 743, 704; HRMS (EI) *m/z* calcd for C<sub>16</sub>H<sub>16</sub>N<sub>2</sub>O<sub>3</sub> (M + H)<sup>+</sup>: 285.1239; found: 285.1211.

*Syn* diastereomer (clear, colorless oil): [α]<sub>D</sub><sup>22</sup> +2.63 (*c* 0.950, CHCl<sub>3</sub>); <sup>1</sup>H NMR (500 MHz, CDCl<sub>3</sub>): δ 8.22 (d, *J* = 9.0 Hz, 2H), 7.41 (d, *J* = 8.5 Hz, 2H), 7.36 (br s, 2H), 6.35 (app t, *J* = 2.0 Hz, 2H), 5.96 (ddd, *J* = 18.0, 10.5, 7.5 Hz, 1H), 5.07 (m, 2H), 3.90 (t, *J* = 9.5 Hz, 1H), 3.50 (dq, *J* = 10.0, 7.0 Hz, 1H), 1.10 (t, *J* = 7.0 Hz, 3H); <sup>13</sup>C NMR (100 MHz, CDCl<sub>3</sub>): δ 172.5, 148.5, 147.1, 137.3, 129.2, 124.0, 119.0,

117.8, 113.7, 52.7, 43.0, 16.9; IR  $\nu_{\max}^{\text{neat}}$   $\text{cm}^{-1}$ : 2927, 1711, 1602, 1519, 1467, 1409, 1346, 1322, 1273, 1113, 1073, 914, 852, 740, 702; HRMS (EI)  $m/z$  calcd for  $\text{C}_{16}\text{H}_{16}\text{N}_2\text{O}_3$  ( $\text{M} + \text{H}$ )<sup>+</sup>: 285.1239; found: 285.1241.



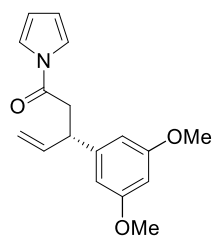
**(2R,3R)-2,3-Dimethyl-1-(1H-pyrrol-1-yl)pent-4-en-1-one (207):** General Procedure I was followed employing 50 mg (0.44 mmol) (E)-but-2-en-1-yl acetate, 90 mg (0.46 mmol) (Z)-1-(1-((trimethylsilyl)oxy)prop-1-en-1-yl)-1H-pyrrole, 8.7 mg (0.022 mmol) ligand **204**, 9.5 mg (0.022 mmol)  $[\text{CpRu}(\text{CH}_3\text{CN})_3]\text{PF}_6$ , 23 mg (0.066 mmol)  $\text{B}(\text{O}^i\text{C}_6\text{H}_4\text{F})_3$ , 0.8 mL THF. The reaction mixture was stirred for 16 h at which time it was concentrated under a stream of  $\text{N}_2$ , filtered through a plug of Florisil<sup>®</sup> and concentrated. The crude product was purified via column chromatography ( $\text{SiO}_2$ , 1%  $\text{Et}_2\text{O}$ /hexanes) to yield 29 mg (37%) of the product as an inseparable mixture of diastereomers and regioisomers. The mixture of products was saponified to the carboxylic acid (to a solution of 11 mg compound **207** (0.061 mmol) in 0.60 mL THF was added a solution of 0.60 mL of 1.0M NaOH. The solution was allowed to stir over night. The THF was evaporated and the aqueous layer was basified with the addition of an equal volume of saturated sodium bicarbonate. The aqueous layer was extracted 3x  $\text{CH}_2\text{Cl}_2$  and discarded. The aqueous layer was then acidified to  $\text{pH} = 1$  with 1M HCl and extracted 3x  $\text{CH}_2\text{Cl}_2$ , dried over  $\text{MgSO}_4$  and concentrated) which matched literature data. For *Anti* product see: Metz, P.; Hungerhoff, B. *J. Org. Chem.* **1997**, *62*, 4442-4448, for *Syn* product see: Rye, C. E.; Barker, D. *J. Org. Chem.* **2011**, *76*, 6636-6648, and for linear product see: Deyo, D. T.; Aebi, J. D.; Rich, D. H. *Synthesis* **1988**, *8*, 608-610.



**(E)-3-(3,5-Dimethoxyphenyl)allyl acetate (226):** (E)-3-(3,5-

dimethoxyphenyl)-2-propen-1-ol, 6.61 g (34.0 mmol) was added to a solution of pyridine (102 mmol) in diethyl ether (0.5 M relative to the alcohol) at 0°C. To

this solution was added acetyl chloride (55.1 mmol) drop-wise. The reaction was allowed to warm to room temperature and stirred for 16 h. The reaction was quenched with an equivalent volume of H<sub>2</sub>O and extracted with diethyl ether (3x the reaction volume). The resultant organics were washed with saturated CuSO<sub>4</sub> (1x equivalent volume), dried over MgSO<sub>4</sub> and concentrated in vacuo. The product mixture was purified by column chromatography (SiO<sub>2</sub> 5% EtOAc:hexanes) to afford 7.10 g (88.0%) as a colorless crystalline solid: mp 31.2-32.4 °C; <sup>1</sup>H NMR (500 MHz, CDCl<sub>3</sub>): δ 6.58 (d, J = 16.0, 1H), 6.54 (s, 2H), 6.39 (s, 1H), 6.27 (apt dt, J = 6.5, 15, 1H), 4.72 (d, J = 6.5, 2H), 3.79 (s, 6H), 2.10 (s, 3H); <sup>13</sup>C NMR (125 MHz, CDCl<sub>3</sub>): δ 170.8, 160.9, 138.2, 134.1, 123.7, 104.7, 100.4, 64.9, 55.4, 21.0; IR  $\nu_{\text{max}}^{\text{neat}}$  cm<sup>-1</sup>: 3002, 2940, 2839, 1738, 1592, 1458, 1427, 1347, 1299, 1240, 1205, 1153, 1064, 1025, 965, 682; HRMS (TOF AP<sup>+</sup>)  $m/z$  for C<sub>13</sub>H<sub>17</sub>O<sub>4</sub> (M + H)<sup>+</sup>: 237.1127; found: 237.1126.

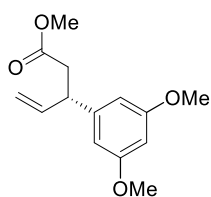


**(3S)-3-(3,5-Dimethoxyphenyl)-1-(1H-pyrrol-1-yl)pent-4-en-1-one (231):**

General procedure i was followed employing 1.00 g (4.24 mmol) (E)-3-(3,5-dimethoxyphenyl)allyl acetate, 1.00 g (5.48 mmol) 1-(1-[(trimethylsilyl)oxy]vinyl)-1H-pyrrole, 82 mg (0.211 mmol) ligand **201**, 92 mg (0.211 mmol)

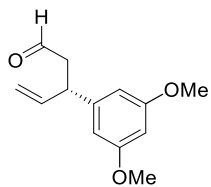
[CpRu(CH<sub>3</sub>CN)<sub>3</sub>PF<sub>6</sub>, 230 mg (0.633 mmol) (4-FPh)<sub>3</sub>B, 6.3 mL THF (0.67M). The reaction mixture was stirred for 16 h at which time it was dissolved onto SiO<sub>2</sub> and dried overnight in *vacuo*. The product was purified by column chromatography (SiO<sub>2</sub>, 5% EtOAc/Hexanes) to yield 1.04 g (85.7%) as a white crystalline solid. [α]<sub>D</sub> +8.37 (*c* 0.023, CHCl<sub>3</sub>); mp 72.9-74.3 °C; <sup>1</sup>H NMR (400 MHz, CDCl<sub>3</sub>): δ 7.30 (b s, 2H), 6.41 (d, J = 2.4, 2H), 6.34 (apt t, J = 2.4, 1H), 6.28 (apt t, J = 2.4, 1H), 6.03 (ddd, J =

6.8, 10.8, 16.0, 1H), 5.13 (d, J = 1.2, 1H), 5.10 (apt dt, J = 1.2, 7.6, 1H), 4.03 (q, J = 6.8, 1H), 3.78 (s, 6H), 3.21 (ddd, J = 7.6, 16.0, 27.2, 1H); <sup>13</sup>C NMR (100 MHz, CDCl<sub>3</sub>): δ 168.6, 161.0, 144.8, 139.5, 119.0, 115.5, 113.2, 105.8, 98.5, 55.3, 45.0, 40.1; IR ν<sub>max</sub><sup>neat</sup> cm<sup>-1</sup>: 3159, 3074, 2937, 2837, 1717, 1596, 1469, 1287, 1261, 1205, 1155, 1069, 923, 834, 744; HRMS (TOF MSES+) *m/z* for C<sub>17</sub>H<sub>20</sub>NO<sub>3</sub> (M + H)<sup>+</sup>: 286.1443; found 286.1439.



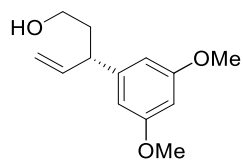
**(S)-Methyl-3-(3,5-dimethoxyphenyl)pen-4-enonate (233):** (3*S*)-(3,5-

dimethoxyphenyl)-1-(1H-pyrrol-1-yl)pent-4-en-1-one, 510 mg (1.78 mmol) in MeOH (0.1 M relative to the acyl pyrrole) at room temperature was added sodium methoxide (17.8 mmol as a 25% wt/wt solution in MeOH). The reaction was monitored by TLC for consumption of starting material. The reaction was quenched with an equivalent volume of H<sub>2</sub>O and extracted with Et<sub>2</sub>O (3x equivalent volume), dried over MgSO<sub>4</sub>, and concentrated in vacuo. The product was purified by column chromatography (SiO<sub>2</sub> 5% EtOAc/Hexanes) to afford 385 mg (86.5%) as a colorless oil. [α]<sub>D</sub> -3.90 (c 0.049 CHCl<sub>3</sub>); <sup>1</sup>H NMR (400 MHz, CDCl<sub>3</sub>): δ 6.37 (d, J = 2.4, 2H), 6.32 (t, J = 2.4, 1H), 5.95 (ddd, J = 7.2, 10.4, 17.2, 1H), 5.10 (apt dt, J = 1.2, 10.4, 1H), 5.06 (m, 1H), 3.87 (q, J = 7.2, 15.2, 1H), 3.77 (s, 6H), 3.64 (s, 3H), 2.71 (dddd, J = 2.1, 15.6, 22.4, 23.6, 2H); <sup>13</sup>C NMR (100 MHz, CDCl<sub>3</sub>): δ 172.5, 161.2, 145.1, 140.0, 115.2, 106.0, 105.8, 98.7, 55.5, 51.8, 45.9, 40.2; IR ν<sub>max</sub><sup>neat</sup> cm<sup>-1</sup>: 3081, 3001, 2953, 2838, 1737, 1596, 1461, 1431, 1357, 1205, 1067, 922, 835; HRMS (TOF MSES+) *m/z* for C<sub>14</sub>H<sub>19</sub>O<sub>4</sub> (M + H)<sup>+</sup>: 251.1283; found 251.1285.



**(S)-3-(3,5-Dimethoxyphenyl)pent-4-enal (228):** (S)-methyl 3-(3,5-dimethoxyphenyl)pen-4-enonate, 536 mg (2.14 mmol) in DCM (0.3 M relative to the ester) at -78° C was subjected to DiBALH (3.21 mmol as a 1.0 M solution in

DCM) drop-wise. The reaction was stirred at  $-78^{\circ}\text{C}$  for 2 h and subsequently quenched with MeOH (3.2 mL) followed by saturated sodium potassium tartrate solution. The reaction mixture was allowed to warm to room temperature and stir for 16 h. The resulting clear solution was extracted with DCM (3x equivalent volume), dried over  $\text{MgSO}_4$ , and concentrated in vacuo. The product mixture was purified by column chromatography (5% EtOAC/Hexanes) to afford 370 mg (77.8%) as a colorless oil.  $[\alpha]_{\text{D}} -1.27$  ( $c$  0.078  $\text{CHCl}_3$ );  $^1\text{H NMR}$  (400 MHz,  $\text{CDCl}_3$ ):  $\delta$  9.72 (t,  $J = 2.0$ , 1H), 6.37 (d,  $J = 2.4$ , 2H), 6.33 (t,  $J = 2.0$ , 2H), 5.96 (ddd,  $J = 6.8, 10.4, 17.2$ , 1H), 5.29 (s, 6H), 5.12 (apt dt,  $J = 1.2, 8.0$ , 1H), 5.08 (apt dt,  $J = 1.2, 14.4$ , 1H), 3.88 (q,  $J = 7.2, 14.4$ , 1H), 3.78 (s, 6H), 2.81 (m, 2H);  $^{13}\text{C NMR}$  (100 MHz,  $\text{CDCl}_3$ ):  $\delta$  201.2, 161.0, 144.6, 139.7, 115.2, 105.7, 98.4, 53.4, 48.3, 43.6; IR  $\nu_{\text{max}}^{\text{neat}} \text{cm}^{-1}$ : 3080, 3001, 2938, 2838, 2756, 1721, 1595, 1459, 1429, 1347, 1292, 1204, 1152, 1062, 923, 835, 737, 697; HRMS (TOF MSES+)  $m/z$  for  $\text{C}_{13}\text{H}_{17}\text{O}_3$  ( $\text{M} + \text{H}$ ) $^+$ : 222.1178; found 221.1183.

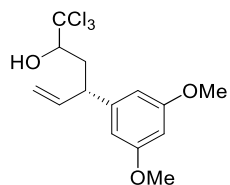


**(S)-3-(3,5-Dimethoxyphenyl)pent-4-en-1-ol (245):** (*S*)-methyl 3-(3,5-dimethoxyphenyl)pen-4-enonate, 308 mg (1.22 mmol) in DCM (0.3 M relative to the ester) at  $-78^{\circ}\text{C}$  was subjected to DiBALH (3.05 mmol as a 1.0 M solution

in DCM) drop-wise. The reaction was stirred at  $-78^{\circ}\text{C}$  for 2 h and subsequently quenched with MeOH (3.1 mL) followed by saturated sodium potassium tartrate solution. The reaction mixture was allowed to warm to room temperature and stir for 16 h. The resulting clear solution was extracted with DCM (3x equivalent volume), dried over  $\text{MgSO}_4$ , and concentrated in vacuo. The product mixture was purified by column chromatography (5% EtOAC/Hexanes) to afford 231 mg (84.8%) as a colorless oil. Separating the stereoisomers of **245** by GC (flow rate 2.0 mL/min, method: 120  $^{\circ}\text{C}$  for 10 min, ramp @ 0.1  $^{\circ}\text{C}/\text{min}$  to 160  $^{\circ}\text{C}$  hold for 15 min;  $T_{\text{r}}$  (min) = 136.8 (3R-**245**), 138.0 (3S-**245**), (ratio = 1:6.1)) provided an ee of 72%.  $[\alpha]_{\text{D}} +22.27$  ( $c$  0.043  $\text{CHCl}_3$ );  $^1\text{H NMR}$  (500 MHz,  $\text{CDCl}_3$ ):  $\delta$  6.37(d,  $J$



= 2.0, 2H), 6.32 (dd, J= 2.0, 1H), 5.95 (ddd, J = 8.0, 10.5, 17.5, 1H), 5.10 (apt dt, J = 1.0, 17.0, 1H), 5.05 (d, J = 10, 1H), 3.78 (s, 6H), 3.63 (m, 2H), 3.40 (dd, J = 8.0, 15.0, 1H), 1.96 (m, 2H);  $^{13}\text{C}$  NMR (100 MHz,  $\text{CDCl}_3$ ):  $\delta$  160.9, 146.2, 141.4, 114.5, 105.7, 98.1, 61.0, 60.9, 55.3, 46.6, 37.8; IR  $\nu_{\text{max}}^{\text{neat}}$   $\text{cm}^{-1}$ : 3369, 3000, 2938, 2838, 1597, 1463, 1430, 1346, 1292, 1205, 1155, 1059, 995, 835, 717, 695; HRMS (ESI)  $m/z$  for  $\text{C}_{13}\text{H}_{19}\text{O}_3$  ( $\text{M} + \text{H}$ ) $^+$ : 223.1329; found 223.1314.

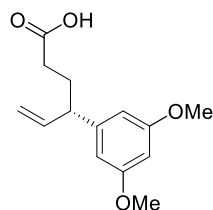


**(4S)-1,1,1-Trichloro-4-(3,5-dimethoxyphenyl)hex-5-en-2-ol (246):** To a

solution of (*S*)-3-(3,5-Dimethoxyphenyl)pent-4-enal (1.40 g, 6.36 mmol) in DMF (8.5 mL) was added trichloroacetic acid (1.56 g, 9.54 mmol), followed by sodium

trichloroacetate (1.77 g, 9.54 mmol). Vigorous evolution of  $\text{CO}_2$  was observed and the reaction is allowed to stir overnight. Ether was added to double the volume and the reaction washed with 3x 10 mL sat.  $\text{NaHCO}_3$ . The organic layer was dried over an.  $\text{MgSO}_4$ , concentrated by rotary evaporator and

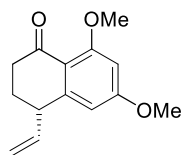
columned in 5% EtOAc in hexanes to yield a 1.10 g (51.0%) of a colorless oil as a mix of diastereomers.  $^1\text{H}$  NMR (500 MHz,  $\text{CDCl}_3$ ):  $\delta$  6.42 – 6.40 (2H), 6.38 – 6.33 (1H), 6.04 – 5.88 (1H), 5.25 – 5.06 (2H), 4.15 (ddd, J = 15.3, 5.3, 2 Hz, 0.5H), 3.79 – 3.76 (6.5 H), 3.63 – 3.60 (1H), 2.75 – 2.73 (1H), 2.47 – 2.38 (1H), 2.08 – 1.97 (1H), 1.55 (s, 1H)  $^{13}\text{C}$  NMR (125 MHz,  $\text{CDCl}_3$ ):  $\delta$  161.3, 161.2, 146.4, 144.6, 141.6, 140.0, 116.7, 114.5, 106.3, 105.7, 104.4, 104.3, 98.8, 98.5, 81.1, 80.7, 55.5, 55.5, 46.6, 46.3, 37.4, 36.5; IR  $\nu_{\text{max}}^{\text{neat}}$   $\text{cm}^{-1}$ : 3458, 3001, 2938, 2828, 1597, 1462, 1430, 1346, 1293, 1205, 1155, 1094, 1063, 924, 809, 629. HRMS (ESI)  $m/z$  for  $\text{C}_{13}\text{H}_{17}\text{O}_3$  ( $\text{M} + \text{H}$ ) $^+$ : 339.03160; found 339.03034.



**(S)-4-(3,5-Dimethoxyphenyl)hex-5-enoic acid (229):** To a solution of 975 mg

(2.87 mmol) **246** in *tert*-butyl alcohol (0.1 M relative to the carbinol) at 30 °C was subjected to freshly powdered  $\text{NaOH}$  (9.4 mmol).. After 10 minutes,  $\text{NaBH}_4$  (4.5

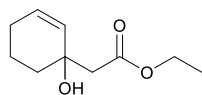
mmol) was added to the slurry and the temperature increased to 55° C. After 18 h the solvent was removed by rotary evaporator and the slurry was dissolved in 15 mL Et<sub>2</sub>O and 15 ml H<sub>2</sub>O. The pH of the mixture was adjusted to 1 using 1 M HCl and extracted with 5 x 20 mL. dried with an. MgSO<sub>4</sub>, and then concentrated by rotary evaporator. The crude material was purified by flash chromatography 1:4 EtOAc: hexanes to furnish 250 mg of the homologated acid as a colorless oil (34.6%). [ $\alpha$ ]<sub>D</sub> +11.01 (*c* 0.051 CHCl<sub>3</sub>); <sup>1</sup>H NMR (500 MHz, CDCl<sub>3</sub>)  $\delta$  10.18 (s, 1H), 6.35 (d, J = 2.5, 2H), 6.32 (t, J = 2.5, 1H), 5.91 (ddd, J = 7.5, 10.0, 17.0, 1H), 5.09 (apt dt, J = 1.0, 14.5, 1H), 5.07 (apt dt, J = 1.0, 7.5, 1H), 3.78 (s, 6H), 3.22 (q, J = 7.5, 2H), 2.33 (m, 2H), 2.03 (m, 2H); <sup>13</sup>C NMR (125 MHz, CDCl<sub>3</sub>) 178.3, 160.9, 145.7, 140.8, 115.0, 105.7, 98.3 55.3, 49.2, 31.7, 29.8; IR  $\nu_{\max}^{\text{neat}}$  cm<sup>-1</sup>: 3229, 2082, 3000, 2936, 2838, 1708, 1596, 1461, 1429, 1292, 1204, 1155, 1063, 920, 834; HRMS (ESI)  $m/z$  for C<sub>14</sub>H<sub>19</sub>O<sub>4</sub> (M + H)<sup>+</sup>: 251.1278; found 251. 1268.



**(S)-6,8-Dimethoxy-4-vinyl-3,4-dihydronaphthalen-1(2H)-one (230):** To a

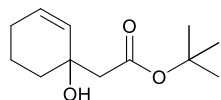
solution of (*S*)-4-(3,5-dimethoxyphenyl)hex-5-enoic acid, 250 mg (1.0 mmol) in nitromethane (0.5 M relative to the acid) at room temperature was added triflic anhydride (0.20 mL, 1.2 mmol). The reaction was complete after 60 min. The mixture was quenched with saturated NaHCO<sub>3</sub> solution (equivalent volume) and the organics were extracted with EtOAc (3x equivalent volume), dried over MgSO<sub>4</sub>, and concentrated en vacuo. The crude product mixture was purified by column chromatography (25% EtOAc/Hexanes) to afford 175 mg (75%) of a pale yellow solid. [ $\alpha$ ]<sub>D</sub> +59.34 (*c* 0.052 CHCl<sub>3</sub>); mp 74.0-75.7 °C; <sup>1</sup>H NMR (500 MHz, CDCl<sub>3</sub>)  $\delta$  6.38 (d, J = 2.0, 1H), 6.36 (d, J = 2.0, 1H), 5.93 (ddd, J = 7.5, 10.5, 17.5), 5.19 (d, J = 10, 1H), 5.02 (dd, J = 1.5, 17.0, 1H), 3.89 (s, 3H), 3.85 (s, 3H), 3.56 (dd, J = 5.5, 6.5, 1H) 2.61 (dddd, J = 5.0, 9.5, 14.5, 77.0, 2H), 2.18 (m, 1H), 1.98 (m, 1H); <sup>13</sup>C NMR (125 MHz, CDCl<sub>3</sub>)  $\delta$  196.2, 164.2, 162.8, 150.1, 140.2, 117.2,

116.3, 105.3, 97.7, 56.2, 55.6, 44.8, 37.7, 28.6; IR  $\nu_{\max}^{\text{neat}}$   $\text{cm}^{-1}$ : 3066, 3004, 2939, 2834, 1670, 1596, 1570, 1455, 1419, 1324, 1253, 1201, 1160; HRMS (ESI)  $m/z$  for  $\text{C}_{14}\text{H}_{17}\text{O}_3$  ( $\text{M} + \text{H}$ )<sup>+</sup>: 233.11722; found 233.11642.



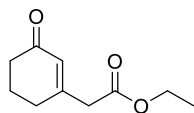
**Ethyl 2-(1-hydroxycyclohex-2-en-1-yl)acetate:** Characterization materials match

the data provided in the following publications: Liu, H.; Zhu, B; *Can. J. Chem.* 1991, 69, 2008-2013; Eidman, K. F.; MacDougall, B. S.; *J. Org. Chem.* 2006, 71, 9513-9516.



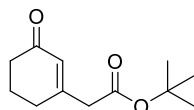
**tert-Butyl 2-(1-hydroxycyclohex-2-en-1-yl)acetate:** To a stirred solution of

lithium hexamethyldisilazide (10.8 mmol) in THF (0.2 M relative to the tert-butyl acetate) at  $-78$  °C was added *tert*-butyl acetate (2.80 mL, 20.8 mmol) and the reaction was stirred for 2 h. To this solution was added anhydrous  $\text{CeCl}_3$  (5.13 g, 20.8 mmol) as a solid and the resulting suspension was stirred for an additional 2 h at  $-78$  °C. Cyclohexenone (1.07 mL, 10.4 mmol) was then added to the reaction and stirring continued at  $-78$  °C for 2 h. The reaction was quenched with 10% acetic acid solution (250 mL) and extracted with EtOAc (3x equivalent volume). The resultant organics were sequentially washed with saturated sodium bicarbonate solution (equivalent volume) and brine (equivalent volume), dried over  $\text{MgSO}_4$ , and concentrated in vacuo. The crude reaction mixture was purified by column chromatography ( $\text{SiO}_2$ , 10% EtOAc/Hex) to afford the product (2.201 g, quantitative yield) as a yellow oil.  $^1\text{H}$  NMR (500 MHz,  $\text{CDCl}_3$ )  $\delta$  5.81 (apt dt,  $J = 3.5, 10.0$ , 1H), 5.65 (d,  $J = 10.5$ , 1H), 3.82 (b s, 1H), 2.46 (dd,  $J = 15.0, 26.5$ , 2H), 2.04 (m, 1H), 1.94 (m, 1H), 1.81 (m, 2H), 1.61 (m, 2H), 1.48 (s, 9H);  $^{13}\text{C}$  NMR (125 MHz,  $\text{CDCl}_3$ )  $\delta$  172.1, 131.1, 130.1, 81.6, 68.3, 46.4, 35.7, 28.1, 25.0, 18.9; IR  $\nu_{\max}^{\text{neat}}$   $\text{cm}^{-1}$ : 3498, 2978, 2936, 2872, 1710, 1456, 1393, 1369, 1255, 1151, 1070, 998, 953, 735; HRMS (ESI)  $m/z$  for  $\text{C}_{12}\text{H}_{20}\text{O}_3\text{Na}$  ( $\text{M} + \text{Na}$ )<sup>+</sup>: 235.1305; found 235.1307.



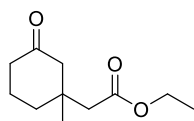
**Ethyl 2-(3-oxocyclohex-1-en-1-yl)acetate (276a):** Characterization materials

match the data provided in the following publications: Liu, H.; Zhu, B; *Can. J. Chem.* 1991, *69*, 2008-2013; Eidman, K. F.; MacDougall, B. S.; *J. Org. Chem.* 2006, *71*, 9513-9516.



**tert-Butyl 2-(3-oxocyclohex-1-en-1-yl)acetate (276b):** Pyridinium

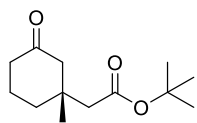
chlorochromate (4.61 g, 21.4 mmol) was added to a solution of *tert*-Butyl 2-(1-hydroxycyclohex-2-en-1-yl)acetate (1.81 g, 8.54 mmol) in DCM (0.2 M relative to the alcohol) and reacted for 5 h. The reaction mixture was diluted with Et<sub>2</sub>O and the resultant solution was plugged through Florisil. The column was washed with Et<sub>2</sub>O (3x 50 mL) and the combined organics were concentrated in vacuo. The crude reaction mixture was purified by column chromatography (SiO<sub>2</sub> 10% EtOAc/Hexanes) to afford the product 1.270 g (70.4%) as a yellow oil. <sup>1</sup>H NMR (500 MHz, CDCl<sub>3</sub>) δ 5.93 (s, 1H), 3.14 (s, 2H), 2.39 (t, J = 7, 4H), 2.02 (dd, J = 6.5, 13.0, 2H), 1.49 (s, 9H); <sup>13</sup>C NMR (125 MHz, CDCl<sub>3</sub>) δ 199.7, 168.8, 158.1, 128.8, 81.9, 45.0, 37.4, 29.9, 28.2, 22.9; IR ν<sub>max</sub><sup>neat</sup> cm<sup>-1</sup>: 2978, 2930, 2865, 1730, 1674, 1456, 1370, 1153, 973.12, 888; HRMS (TOF AP+) *m/z* for C<sub>12</sub>H<sub>18</sub>O<sub>3</sub> (M + H)<sup>+</sup>: 211.1334; found 211.1335.



**Ethyl 2-(1-methyl-3-oxocyclohexyl)acetate (277a):** In a glovebox, a flask was

charged with CuOTf<sub>2</sub>•PhH (11.1 mg, 0.022 mmol) and (3,5-dioxa-4-phosphacyclohepta[2,1-a;3,4-a']dinaphthalene-4-yl)bis(1-phenylmethyl)amine (45.0 mg, 0.088 mmol). The flask was pumped out of the inert atmosphere and Et<sub>2</sub>O was added to the solids and the mixture was stirred at room temperature for 30 min, resulting in a cloudy suspension. To this was added ethyl 2-(3-oxocyclohex-1-en-1-yl)acetate (200 mg, 1.10 mmol) and the reaction was cooled to -10 °C. After 30 min, Me<sub>3</sub>Al (1.10 mL of a 2.0 M solution in heptanes, 2.20 mmol) was added and the resultant

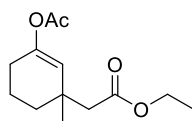
yellow solution was allowed to stir for 16h. The reaction was carefully quenched with MeOH (2 mL) and then saturated ammonium chloride solution (equivalent volume) and extracted with Et<sub>2</sub>O (3x equivalent volume), dried over MgSO<sub>4</sub>, and concentrated in vacuo. The reaction mixture was purified by column chromatography (SiO<sub>2</sub> 10% EtOAc/Hexanes) to yield the product (177 mg, 80.8%) as a colorless oil. <sup>1</sup>H NMR (500 MHz, CDCl<sub>3</sub>) δ 4.13 (q, J = 7.0, 2H), 2.42 (d, J = 13.5, 1H), 2.31 (m, 2H), 2.27 (d, J = 3.5, 2H), 2.20 (apt dt, J = 2.0, 14.0, 1H), 1.91 (m, 2H), 1.81 (m 1H), 1.66 (m, 1H), 1.26 (t, J = 7.0, 3H), 1.06 (s, 3H); <sup>13</sup>C NMR (125 MHz, CDCl<sub>3</sub>) δ 211.0, 171.1, 60.3, 53.3, 46.1, 40.8, 38.2, 35.7, 25.2, 21.9, 14.3; IR ν<sub>max</sub><sup>neat</sup> cm<sup>-1</sup>: 2961, 2931, 2880, 1730, 1710, 1458, 1370, 1228, 1180, 1146, 1034; HRMS (ESI) *m/z* for C<sub>11</sub>H<sub>19</sub>O<sub>3</sub> (M + H)<sup>+</sup>: 199.13287; found 199.13344.



***tert*-Butyl (*R*)-2-(1-methyl-3-oxocyclohexyl)acetate (**277b**):** In a glovebox, a

flask was charged with CuOTf<sub>2</sub>•PhH (4.8 mg, 0.01 mmol) and (*S*)-(+)-(3,5-dioxo-4-phospha-cyclohepta[2,1-*a*;3,4-*a'*]dinaphthalene-4-yl)bis[(1*R*)-1-phenylethyl]amine (20.7 mg, 0.04 mmol). The flask was pumped out of the inert atmosphere and Et<sub>2</sub>O (1 mL, 0.4 M relative to acetate) was added to the solids and the mixture was stirred at room temperature for 30 min, resulting in a cloudy suspension. To this was added *tert*-butyl 2-(3-oxocyclohex-1-en-1-yl)acetate (100 mg, 0.48 mmol) and the reaction was cooled to -10 °C. After 30 min, Me<sub>3</sub>Al (0.48 mL of a 2.0 M solution in heptanes, 0.96 mmol) was added and the resultant yellow solution was allowed to stir for 16h. The reaction was carefully quenched with MeOH (2 mL) and then saturated ammonium chloride solution (equivalent volume) and extracted with Et<sub>2</sub>O (3x equivalent volume), dried over MgSO<sub>4</sub>, and concentrated in vacuo. The reaction mixture was purified by column chromatography (SiO<sub>2</sub> 10% EtOAc/Hexanes) to yield the product (73.5 mg, 68%) as a colorless oil. Separating the stereoisomers of **277b** by GC flow rate 0.6 mL/min, method: 105 °C for 10 min, ramp @ 0.7 °C/min to 160 °C

hold for 5 min;  $T_r$  (min) = 62.095 (*R*-**277b**), 63.006 (*S*-**277b**), (ratio = 4.56:1)) provided an ee of 64%.  $^1\text{H}$  NMR (500 MHz,  $\text{CDCl}_3$ )  $\delta$  2.40 (d,  $J$  = 13.5, 1H), 2.29 (m, 2H), 2.19 (m, 1H), 2.18 (dd,  $J$  = 14.0, 20.0, 2H), 1.87 (m, 3H), 1.65 (m, 1H), 1.45 (s, 9H), 1.06 (s, 3H);  $^{13}\text{C}$  NMR (125 MHz,  $\text{CDCl}_3$ )  $\delta$  211.2, 170.6, 80.6, 53.4, 47.2, 40.8, 38.3, 35.7, 28.1, 25.3, 21.9; IR  $\nu_{\text{max}}^{\text{neat}}$   $\text{cm}^{-1}$ : 2967, 2942, 2876, 1716, 1457, 1367, 1333, 1252, 1142, 1109, 958, 842; HRMS (ESI)  $m/z$  for  $\text{C}_{13}\text{H}_{23}\text{O}_3$  ( $\text{M} + \text{H}$ ) $^+$ : 227.16417; found 227.16442.

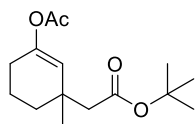


**Ethyl-2-(3-acetoxy-1-methylcyclohex-2-en-1-yl)acetate (281):** In a glovebox, a

flask was charged with  $\text{CuOTf}_2 \cdot \text{PhH}$  (80.5 mg, 0.16 mmol) and (3,5-dioxa-4-phospha-cyclohepta[2,1-a;3,4-a']dinaphthalene-4-yl)bis(1-phenylmethyl)amine (321 mg, 0.63 mmol).

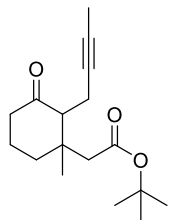
The flask was pumped out of the inert atmosphere and  $\text{Et}_2\text{O}$  was added to the solids and the mixture was stirred at room temperature for 30 min, resulting in a cloudy suspension. To this was added ethyl 2-(3-oxocyclohex-1-en-1-yl)acetate (1.430 g, 7.84 mmol) and the reaction was cooled to  $-10\text{ }^\circ\text{C}$ . After 30 min,  $\text{Me}_3\text{Al}$  (7.84 mL of a 2.0 M solution in heptanes, 15.68 mmol) was added and the resultant yellow solution was allowed to stir for 16h. Acetic anhydride (3.0 mL, 31.4 mmol) was added and the reaction was warmed to room temperature and stirred for 72 h. The reaction mixture was quenched by carefully pouring over and equal volume of saturated ammonium chloride and ice solution. The organics were extracted with  $\text{Et}_2\text{O}$  (3x equal volume), dried over  $\text{MgSO}_4$ , and concentrated in vacuo. The crude reaction mixture was purified by column chromatography ( $\text{SiO}_2$  5%  $\text{EtOAc}$ /Hexanes) to afford 1.282 g (68%) of the product as a yellow oil.  $^1\text{H}$  NMR (500 MHz,  $\text{CDCl}_3$ )  $\delta$  5.31 (s, 1H), 4.12 (q,  $J$  = 7.0, 2H), 2.32 (s, 2H), 2.12 (m, 2H), 2.10 (s, 3H), 1.76 (m 2H), 1.66 (m, 1H), 1.47 (m, 1H), 1.25 (t,  $J$  = 7.0, 2H), 1.15 (s, 3H);  $^{13}\text{C}$  NMR (125 MHz,  $\text{CDCl}_3$ )  $\delta$  171.5, 169.1, 148.1, 121.8, 60.1, 46.6, 34.5,

27.1, 26.7, 21.1, 19.2, 14.3, 14.1; IR  $\nu_{\max}^{\text{neat}}$   $\text{cm}^{-1}$ : 2939, 2884, 1756, 1732, 1456, 1366, 1218, 1135, 1115, 1053, 1088, 1035; HRMS (TOF AP+)  $m/z$  for  $\text{C}_{13}\text{H}_{21}\text{O}_4$  ( $\text{M} + \text{H}$ ) $^+$ : 241.1440; found 241.1434.

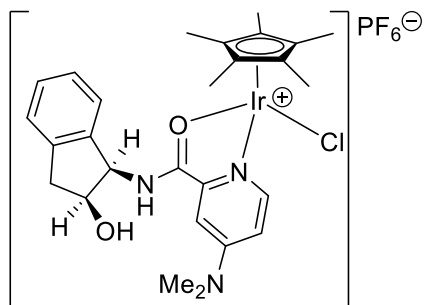


**tert-Butyl 2-(3-acetoxy-1-methylcyclohex-2-en-1-yl)acetate (294):** In a

glovebox, a flask was charged with  $\text{Cu}(\text{OTf})_2 \cdot \text{PhH}$  (10.1 mg, 0.02 mmol) and (3,5-dioxa-4-phospha-cyclohepta[2,1-a;3,4-a']dinaphthalene-4-yl)bis(1-phenylmethyl)amine (38.9 mg, 0.08 mmol). The flask was pumped out of the inert atmosphere and  $\text{Et}_2\text{O}$  was added to the solids and the mixture was stirred at room temperature for 30 min, resulting in a cloudy suspension. To this was added ethyl 2-(3-oxocyclohex-1-en-1-yl)acetate (200 mg, 0.95 mmol) and the reaction was cooled to  $-10$  °C. After 30 min,  $\text{Me}_3\text{Al}$  (0.95 mL of a 2.0 M solution in heptanes, 1.90 mmol) was added and the resultant yellow solution was allowed to stir for 16h. Acetic anhydride (0.36 mL, 3.80 mmol) was added and the reaction was warmed to room temperature and stirred for 72 h. The reaction mixture was quenched by carefully pouring over an equal volume of saturated ammonium chloride and ice solution. The organics were extracted with  $\text{Et}_2\text{O}$  (3x equal volume), dried over  $\text{MgSO}_4$ , and concentrated in vacuo. The crude reaction mixture was purified by column chromatography ( $\text{SiO}_2$  5%  $\text{EtOAc}$ /Hexanes) to afford 164.9 g (59.6%) of the product as a pale yellow oil.  $^1\text{H}$  NMR (500 MHz,  $\text{CDCl}_3$ )  $\delta$  5.30 (s, 1H), 2.22 (s, 2H), 2.11 (m, 1H), 2.09 (s, 3H), 1.75 (apt dq,  $J = 6.5, 12.0$ , 2H), 1.66 (m, 1H), 1.56 (d,  $J = 1.0$ , 1H), 1.47 (m, 1H), 1.44 (s, 9H), 1.14 (s, 2H);  $^{13}\text{C}$  NMR (125 MHz,  $\text{CDCl}_3$ )  $\delta$  171.0, 169.2, 147.8, 122.1, 80.3, 47.8, 34.5, 34.5, 28.1, 27.1, 26.7, 21.1, 19.2; IR  $\nu_{\max}^{\text{neat}}$   $\text{cm}^{-1}$ : 2969, 2937, 2872, 1757, 1726, 1457, 1367, 1219, 1135, 1087, 1053, 1010, 961, 903, 841, 760; HRMS (ESI)  $m/z$  for  $\text{C}_{15}\text{H}_{24}\text{O}_4\text{Na}$  ( $\text{M} + \text{Na}$ ) $^+$ : 291.1567; found 291.1566.



**tert-Butyl 2-(2-(but-2-yn-1-yl)-1-methyl-3-oxocyclohexyl)acetate (295):** To a solution of *tert*-butyl 2-(3-acetoxy-1-methylcyclohex-2-en-1-yl)acetate, 300 mg (1.12 mmol) in THF (2.0 M relative to the vinyl acetate) at  $-78\text{ }^{\circ}\text{C}$  was added  $\text{MeLi}\bullet\text{LiBr}$  (0.82 mL of a 1.5 M solution in THF, 1.23 mmol). After 30 min, 1-iodobut-2-yne (221.4 mg, 1.23 mmol) was added to the reaction and then protected from light by with aluminum foil. The reaction was then allowed to warm to room temperature and stir for 16 h. The reaction was quenched with saturated ammonium chloride (equivalent volume) and the organics extracted with EtOAc (3x equivalent volume), dried over  $\text{MgSO}_4$ , and concentrated in vacuo. The crude reaction mixture was purified by column chromatography ( $\text{SiO}_2$ , 5% EtOAc/Hexanes) to yield the product, 243 mg (72%) as a yellow oil. Separating the stereoisomers of **295** by GC (flow rate 0.6 mL/min, method:  $105\text{ }^{\circ}\text{C}$  for 10 min, ramp @  $0.7\text{ }^{\circ}\text{C}/\text{min}$  to  $200\text{ }^{\circ}\text{C}$  hold for 5 min;  $T_r$  (min) = 102.717, 103.192, 109.051, 109.640 (ratio = 1.0:1.0:1.4:1.4));  $^1\text{H}$  NMR (500 MHz,  $\text{CDCl}_3$ )  $\delta$  2.53 (apt dtd,  $J = 2.5, 5.0, 16.5$ , 1H), 2.48 (2,  $J = 13.0$ , 1H), 2.38 (m, 1H), 2.28 (m, 1H), 2.24 (d,  $J = 2.5$ , 1H), 2.22 (s, 2H), 2.15 (m, 1H), 1.85 (apt dt,  $J = 4.0, 13.5$ , 1H), 1.77 (t,  $J = 2.5$ , 3H), 1.73 (m, 1H), 1.59 (m, 1H), 1.46 (s, 9H), 0.97 (s, 3H);  $^{13}\text{C}$  NMR (125 MHz,  $\text{CDCl}_3$ )  $\delta$  210.2, 170.5, 80.7, 52.8, 49.5, 49.0, 38.9, 35.9, 29.7, 28.2, 23.4, 18.8, 3.47; IR  $\nu_{\text{max}}^{\text{neat}}\text{ cm}^{-1}$ : 2965, 2925, ote, 2360, 1716, 1456, 1368, 1255, 1152; HRMS (ESI)  $m/z$  for  $\text{C}_{17}\text{H}_{26}\text{O}_3\text{Na}$  ( $\text{M} + \text{Na}$ ) $^+$ : 301.1774; found 301.1776.



**[Cp\*Ir(126)Cl]PF<sub>6</sub>.** 50.0 mg (0.0627 mmol)  $[\text{Cp}^*\text{IrCl}_2]_2$ , 37.2 mg ligand **126** (0.125 mmol), and 20.4 mg (0.125 mmol)  $\text{NH}_4\text{PF}_6$  were combined in a flame-dried, 25 mL flask. MeOH (11 mL) was added and the reaction was allowed to stir at RT for 4 h. The resulting homogeneous yellow solution was evaporated to



dryness and taken up in  $\text{CH}_2\text{Cl}_2$  and filtered. The  $\text{CH}_2\text{Cl}_2$  was reduced to *ca.* 1 ml and hexanes were added resulting in the precipitation of yellow solid which was collected by filtration in air and dried *in vacuo*. Crystals suitable for X-ray diffraction were grown from a saturated solution of acetone/hexanes. 82 mg (81%).

## APPENDIX A: CRYSTAL DATA FOR [CP\*IR(126)CL]PF<sub>6</sub>

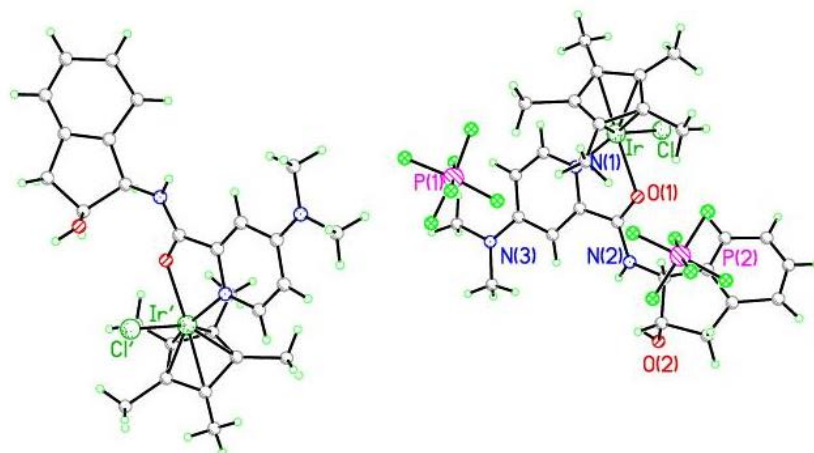


**Table 23: Crystal data and structure refinement for [Cp\*Ir(126)Cl]PF<sub>6</sub>**

Identification code [Cp\*Ir(126)Cl]PF<sub>6</sub>

Empirical formula C<sub>27</sub> H<sub>34</sub> Cl F<sub>6</sub> Ir N<sub>3</sub> O<sub>2</sub> P

Formula weight 805.19

Temperature 203(2) K

Wavelength 0.71073 Å

Crystal system Monoclinic

Space group C 2

Unit cell dimensions  $a = 23.140(4)$  Å  $\beta = 90^\circ$ .

$b = 8.1492(15)$  Å  $\beta = 103.423(4)^\circ$ .

$c = 37.534(7)$  Å  $\beta = 90^\circ$ .

Volume 6885(2) Å<sup>3</sup>

Z 8

Density (calculated) 1.554 Mg/m<sup>3</sup>

Absorption coefficient 4.062 mm<sup>-1</sup>

F(000) 3168

Crystal size 0.21 x 0.12 x 0.08 mm<sup>3</sup>

Theta range for data collection 1.67 to 25.00°.

Index ranges -27<=h<=26, -9<=k<=9, 0<=l<=44

Reflections collected 12153

Independent reflections 12153 [R(int) = 0.0000]

Completeness to theta = 25.00° 100.0 %

Absorption correction Semi-empirical from equivalents

Max. and min. transmission 0.7371 and 0.4826

Refinement method Full-matrix least-squares on F<sup>2</sup>

Data / restraints / parameters 12153 / 427 / 685

Goodness-of-fit on F<sup>2</sup> 0.907

Final R indices [I>2sigma(I)] R1 = 0.0739, wR2 = 0.1562

R indices (all data) R1 = 0.1058, wR2 = 0.1717

Absolute structure parameter 0.073(15)

Largest diff. peak and hole 3.803 and -1.865 e.Å<sup>-3</sup>

**Table 24: Atomic coordinates ( $\times 10^4$ ) and equivalent isotropic displacement parameters ( $\text{\AA}^2 \times 10^3$ ) for  $[\text{Cp}^*\text{Ir}(\text{126Cl})\text{PF}_6]$ .**

$U(\text{eq})$  is defined as one third of the trace of the orthogonalized  $U^{ij}$  tensor.

---

	x	y	z	$U(\text{eq})$
Ir	5167(1)	14826(1)	1254(1)	35(1)
Cl	4912(2)	16300(6)	683(1)	52(1)
O(1)	5519(5)	12991(13)	943(3)	38(3)
O(2)	5702(6)	8498(18)	136(5)	89(6)
N(1)	4443(5)	13270(17)	1050(4)	37(4)
N(2)	5301(5)	10828(14)	565(3)	32(3)
N(3)	3201(6)	9450(18)	796(4)	50(4)
C(1)	5230(7)	14800(30)	1825(4)	44(4)
C(2)	5738(8)	14250(20)	1780(5)	51(5)
C(3)	6001(7)	15560(20)	1608(5)	45(5)
C(4)	5592(7)	16910(20)	1571(5)	38(4)
C(5)	5091(7)	16460(20)	1688(4)	34(4)
C(6)	4777(8)	13900(30)	2016(5)	60(6)
C(7)	6025(11)	12540(20)	1876(7)	87(8)
C(8)	6574(7)	15360(20)	1488(5)	64(6)
C(9)	5697(9)	18450(20)	1415(6)	59(5)
C(10)	4577(8)	17560(30)	1690(5)	60(6)

---

C(11) 3909(7)13340(20) 1139(4)35(4)  
C(12) 3515(7)12160(20) 1071(5)49(5)  
C(13) 3599(7)10696(18) 870(4) 31(4)  
C(14) 4160(6)10617(18) 770(4) 35(4)  
C(15) 4537(6)11892(18) 860(4) 25(3)  
C(16) 5162(7)11950(20) 790(5) 42(4)  
C(17) 5958(6)10691(18) 555(4) 29(4)  
C(18) 6180(6)11820(20) 313(5) 38(4)  
C(19) 6008(7)13420(20) 185(5) 45(5)  
C(20) 6321(8)14190(30) -39(5)62(6)  
C(21) 6761(10) 13430(30) -136(5) 66(6)  
C(22) 6954(8)11860(20) -25(5)48(5)  
C(23) 6624(7)10970(20) 199(5) 42(5)  
C(24) 6735(7)9300(20) 349(5) 38(4)  
C(25) 6127(8)8990(20) 463(7) 62(6)  
C(26) 3346(11) 7910(20) 646(7) 81(8)  
C(27) 2586(8)9630(40) 879(5) 78(6)  
P(1) 5641(3)9320(7)2749(2)76(2)  
F(1) 5429(9)7569(19) 2619(5)146(7)  
F(2) 6207(6)8542(19) 3004(5)110(5)  
F(3) 5792(8)11091(19) 2894(6)139(7)  
F(4) 5049(7)10180(30) 2509(4)153(7)  
F(5) 5930(10) 9430(20) 2428(5)174(9)  
F(6) 5322(9)9110(20) 3073(5)144(7)

P(2) 7589(2)10584(6) 1558(2)51(1)  
F(7) 7807(8)12313(19) 1669(5)138(7)  
F(8) 7006(5)11380(20) 1314(4)104(5)  
F(9) 7337(6)8852(18) 1456(6)126(7)  
F(10) 8187(5)9930(30) 1781(4)126(5)  
F(11) 7847(6)10627(19) 1205(4)112(5)  
F(12) 7295(10) 10440(20) 1897(5)167(9)  
Cl' 3394(3)-1041(8) 3604(2)74(2)  
Ir' 3036(1)180(1) 3008(1)44(1)  
C(1') 3014(7)70(20) 2443(4)42(4)  
N(1') 3740(7)1820(20) 3167(4)45(4)  
N(2') 2950(7)3870(20) 3755(4)60(5)  
O(1') 2704(5)1976(17) 3324(3)51(3)  
O(2') 2847(8)1409(19) 4205(4)96(5)  
C(2') 2444(9)550(30)2495(5)61(6)  
N(3') 5039(6)5400(20) 3512(5)68(5)  
C(3') 2219(8)-640(20) 2673(5)48(5)  
C(4') 2597(10) -1980(30) 2743(6)55(6)  
C(5') 3130(8)-1630(30) 2607(6)54(6)  
C(6') 3384(11) 900(30)2207(6)100(10)  
C(7') 2137(8)2170(20) 2380(6)63(6)  
C(8') 1632(9)-610(30) 2817(6)92(8)  
C(9') 2518(13) -3630(20) 2935(6)103(9)  
C(10')3602(10) -2780(30) 2593(6)75(7)

C(11')3072(9)2960(20) 3483(5)48(5)  
C(12')3667(7)3090(20) 3396(4)39(5)  
C(13')4082(7)4290(20) 3504(5)54(5)  
C(14')4633(9)4260(30) 3399(6)66(6)  
C(15')4695(10) 2960(20) 3173(6)66(6)  
C(16')4264(8)1800(30) 3071(6)60(6)  
C(17')2378(7)3750(20) 3846(5)38(4)  
C(18')2286(8)4890(30) 4128(5)66(5)  
C(19')2472(10) 6670(30) 4161(6)71(6)  
C(20')2354(12) 7530(30) 4459(8)90(8)  
C(21')2083(13) 6750(40) 4721(8)104(10)  
C(22')1996(9)5140(30) 4690(6)71(6)  
C(23')2030(7)4240(30) 4400(6)62(6)  
C(24')1966(10) 2460(30) 4317(7)76(7)  
C(25')2275(11) 2060(20) 4023(6)64(6)  
C(26')5593(9)5340(30) 3401(5)78(6)  
C(27')4961(9)6780(30) 3736(8)102(10)

---

—

**Table 25: Bond lengths [Å] and angles [°] for [Cp\*Ir(126)Cl]PF<sub>6</sub>.**

---

Ir-N(1)	2.098(12)
Ir-C(1)	2.114(15)
Ir-C(5)	2.144(16)
Ir-C(2)	2.159(18)
Ir-C(3)	2.158(16)
Ir-O(1)	2.169(10)
Ir-C(4)	2.175(16)
Ir-Cl	2.408(5)
O(1)-C(16)	1.23(2)
O(2)-C(25)	1.44(3)
O(2)-H(2A)	0.8300
N(1)-C(11)	1.353(19)
N(1)-C(15)	1.375(18)
N(2)-C(16)	1.34(2)
N(2)-C(17)	1.534(17)
N(2)-H(2B)	0.8700
N(3)-C(13)	1.355(19)
N(3)-C(26)	1.44(2)
N(3)-C(27)	1.53(2)
C(1)-C(2)	1.31(2)
C(1)-C(5)	1.46(3)
C(1)-C(6)	1.58(2)



C(2)-C(3) 1.45(2)  
C(2)-C(7) 1.54(3)  
C(3)-C(4) 1.44(2)  
C(3)-C(8) 1.50(2)  
C(4)-C(5) 1.38(2)  
C(4)-C(9) 1.43(2)  
C(5)-C(10) 1.49(2)  
C(6)-H(6A) 0.9700  
C(6)-H(6B) 0.9700  
C(6)-H(6C) 0.9700  
C(7)-H(7A) 0.9700  
C(7)-H(7B) 0.9700  
C(7)-H(7C) 0.9700  
C(8)-H(8A) 0.9700  
C(8)-H(8B) 0.9700  
C(8)-H(8C) 0.9700  
C(9)-H(9A) 0.9700  
C(9)-H(9B) 0.9700  
C(9)-H(9C) 0.9700  
C(10)-H(10D) 0.9700  
C(10)-H(10E) 0.9700  
C(10)-H(10F) 0.9700  
C(11)-C(12) 1.31(2)  
C(11)-H(11A) 0.9400

C(12)-C(13) 1.45(2)  
C(12)-H(12A) 0.9400  
C(13)-C(14) 1.43(2)  
C(14)-C(15) 1.349(19)  
C(14)-H(14A) 0.9400  
C(15)-C(16) 1.53(2)  
C(17)-C(18) 1.47(2)  
C(17)-C(25) 1.50(2)  
C(17)-H(17B) 0.9900  
C(18)-C(23) 1.38(2)  
C(18)-C(19) 1.42(2)  
C(19)-C(20) 1.38(2)  
C(19)-H(19B) 0.9400  
C(20)-C(21) 1.31(3)  
C(20)-H(20B) 0.9400  
C(21)-C(22) 1.39(3)  
C(21)-H(21B) 0.9400  
C(22)-C(23) 1.45(2)  
C(22)-H(22B) 0.9400  
C(23)-C(24) 1.47(2)  
C(24)-C(25) 1.58(2)  
C(24)-H(24C) 0.9800  
C(24)-H(24D) 0.9800  
C(25)-H(25B) 0.9900

C(26)-H(26D) 0.9700  
C(26)-H(26E) 0.9700  
C(26)-H(26F) 0.9700  
C(27)-H(27D) 0.9700  
C(27)-H(27E) 0.9700  
C(27)-H(27F) 0.9700  
P(1)-F(5) 1.510(15)  
P(1)-F(1) 1.550(17)  
P(1)-F(3) 1.554(16)  
P(1)-F(2) 1.567(15)  
P(1)-F(6) 1.573(16)  
P(1)-F(4) 1.612(15)  
P(2)-F(7) 1.522(16)  
P(2)-F(10) 1.538(14)  
P(2)-F(9) 1.541(15)  
P(2)-F(11) 1.574(14)  
P(2)-F(12) 1.583(15)  
P(2)-F(8) 1.582(13)  
Cl'-Ir' 2.411(5)  
Ir'-N(1') 2.085(15)  
Ir'-C(2') 2.110(19)  
Ir'-C(1') 2.113(15)  
Ir'-C(3') 2.122(17)  
Ir'-O(1') 2.133(12)

Ir'-C(4') 2.16(2)  
Ir'-C(5') 2.16(2)  
C(1')-C(2') 1.43(2)  
C(1')-C(6') 1.53(3)  
C(1')-C(5') 1.52(3)  
N(1')-C(16') 1.34(2)  
N(1')-C(12') 1.38(2)  
N(2')-C(11') 1.34(2)  
N(2')-C(17') 1.45(2)  
N(2')-H(2'B) 0.8700  
O(1')-C(11') 1.22(2)  
O(2')-C(25') 1.44(3)  
O(2')-H(2'A) 0.8300  
C(2')-C(3') 1.35(2)  
C(2')-C(7') 1.51(3)  
N(3')-C(14') 1.32(2)  
N(3')-C(26') 1.44(2)  
N(3')-C(27') 1.44(3)  
C(3')-C(4') 1.38(3)  
C(3')-C(8') 1.57(3)  
C(4')-C(5') 1.47(3)  
C(4')-C(9') 1.56(3)  
C(5')-C(10') 1.45(2)  
C(6')-H(6'A) 0.9700

C(6')-H(6'B) 0.9700  
C(6')-H(6'C) 0.9700  
C(7')-H(7'A) 0.9700  
C(7')-H(7'B) 0.9700  
C(7')-H(7'C) 0.9700  
C(8')-H(8'A) 0.9700  
C(8')-H(8'B) 0.9700  
C(8')-H(8'C) 0.9700  
C(9')-H(9'A) 0.9700  
C(9')-H(9'B) 0.9700  
C(9')-H(9'C) 0.9700  
C(10')-H(10A) 0.9700  
C(10')-H(10B) 0.9700  
C(10')-H(10C) 0.9700  
C(11')-C(12') 1.49(2)  
C(12')-C(13') 1.37(2)  
C(13')-C(14') 1.42(3)  
C(13')-H(13A) 0.9400  
C(14')-C(15') 1.39(3)  
C(15')-C(16') 1.36(3)  
C(15')-H(15A) 0.9400  
C(16')-H(16A) 0.9400  
C(17')-C(18') 1.46(3)  
C(17')-C(25') 1.58(2)

C(17')-H(17A) 0.9900  
C(18')-C(23') 1.40(3)  
C(18')-C(19') 1.51(3)  
C(19')-C(20') 1.40(3)  
C(19')-H(19A) 0.9400  
C(20')-C(21') 1.43(4)  
C(20')-H(20A) 0.9400  
C(21')-C(22') 1.33(4)  
C(21')-H(21A) 0.9400  
C(22')-C(23') 1.33(3)  
C(22')-H(22A) 0.9400  
C(23')-C(24') 1.48(3)  
C(24')-C(25') 1.48(3)  
C(24')-H(24A) 0.9800  
C(24')-H(24B) 0.9800  
C(25')-H(25A) 0.9900  
C(26')-H(26A) 0.9700  
C(26')-H(26B) 0.9700  
C(26')-H(26C) 0.9700  
C(27')-H(27A) 0.9700  
C(27')-H(27B) 0.9700  
C(27')-H(27C) 0.9700  
N(1)-Ir-C(1) 103.0(6)  
N(1)-Ir-C(5) 117.0(6)

C(1)-Ir-C(5) 40.1(7)  
N(1)-Ir-C(2) 117.9(6)  
C(1)-Ir-C(2) 35.6(6)  
C(5)-Ir-C(2) 65.3(6)  
N(1)-Ir-C(3) 156.2(6)  
C(1)-Ir-C(3) 62.4(6)  
C(5)-Ir-C(3) 65.2(6)  
C(2)-Ir-C(3) 39.3(6)  
N(1)-Ir-O(1) 75.8(4)  
C(1)-Ir-O(1) 126.4(6)  
C(5)-Ir-O(1) 160.9(5)  
C(2)-Ir-O(1) 96.6(6)  
C(3)-Ir-O(1) 97.3(5)  
N(1)-Ir-C(4) 153.3(6)  
C(1)-Ir-C(4) 62.4(7)  
C(5)-Ir-C(4) 37.3(6)  
C(2)-Ir-C(4) 64.4(7)  
C(3)-Ir-C(4) 38.9(6)  
O(1)-Ir-C(4) 130.9(5)  
N(1)-Ir-Cl 88.2(4)  
C(1)-Ir-Cl 148.4(6)  
C(5)-Ir-Cl 108.6(5)  
C(2)-Ir-Cl 153.5(5)  
C(3)-Ir-Cl 114.2(5)

O(1)-Ir-Cl 84.8(3)  
C(4)-Ir-Cl 94.8(5)  
C(16)-O(1)-Ir 115.5(10)  
C(25)-O(2)-H(2A) 109.5  
C(11)-N(1)-C(15) 115.1(13)  
C(11)-N(1)-Ir 125.7(11)  
C(15)-N(1)-Ir 118.2(9)  
C(16)-N(2)-C(17) 116.8(13)  
C(16)-N(2)-H(2B) 121.6  
C(17)-N(2)-H(2B) 121.6  
C(13)-N(3)-C(26) 121.5(13)  
C(13)-N(3)-C(27) 120.5(16)  
C(26)-N(3)-C(27) 118.0(16)  
C(2)-C(1)-C(5) 114.0(16)  
C(2)-C(1)-C(6) 127.5(19)  
C(5)-C(1)-C(6) 118.4(15)  
C(2)-C(1)-Ir 74.0(11)  
C(5)-C(1)-Ir 71.1(9)  
C(6)-C(1)-Ir 124.5(12)  
C(1)-C(2)-C(3) 106.6(15)  
C(1)-C(2)-C(7) 129(2)  
C(3)-C(2)-C(7) 124.3(17)  
C(1)-C(2)-Ir 70.4(10)  
C(3)-C(2)-Ir 70.3(10)



C(7)-C(2)-Ir 123.3(14)  
C(4)-C(3)-C(2) 105.8(13)  
C(4)-C(3)-C(8) 131.1(17)  
C(2)-C(3)-C(8) 123.0(15)  
C(4)-C(3)-Ir 71.2(9)  
C(2)-C(3)-Ir 70.4(10)  
C(8)-C(3)-Ir 120.8(12)  
C(5)-C(4)-C(9) 126.7(17)  
C(5)-C(4)-C(3) 110.4(15)  
C(9)-C(4)-C(3) 122.8(15)  
C(5)-C(4)-Ir 70.2(9)  
C(9)-C(4)-Ir 124.1(13)  
C(3)-C(4)-Ir 69.9(9)  
C(4)-C(5)-C(1) 103.0(14)  
C(4)-C(5)-C(10) 125.0(17)  
C(1)-C(5)-C(10) 131.8(16)  
C(4)-C(5)-Ir 72.6(9)  
C(1)-C(5)-Ir 68.9(9)  
C(10)-C(5)-Ir 125.7(12)  
C(1)-C(6)-H(6A) 109.5  
C(1)-C(6)-H(6B) 109.5  
H(6A)-C(6)-H(6B) 109.5  
C(1)-C(6)-H(6C) 109.5  
H(6A)-C(6)-H(6C) 109.5

H(6B)-C(6)-H(6C) 109.5  
C(2)-C(7)-H(7A) 109.5  
C(2)-C(7)-H(7B) 109.5  
H(7A)-C(7)-H(7B) 109.5  
C(2)-C(7)-H(7C) 109.5  
H(7A)-C(7)-H(7C) 109.5  
H(7B)-C(7)-H(7C) 109.5  
C(3)-C(8)-H(8A) 109.5  
C(3)-C(8)-H(8B) 109.5  
H(8A)-C(8)-H(8B) 109.5  
C(3)-C(8)-H(8C) 109.5  
H(8A)-C(8)-H(8C) 109.5  
H(8B)-C(8)-H(8C) 109.5  
C(4)-C(9)-H(9A) 109.5  
C(4)-C(9)-H(9B) 109.5  
H(9A)-C(9)-H(9B) 109.5  
C(4)-C(9)-H(9C) 109.5  
H(9A)-C(9)-H(9C) 109.5  
H(9B)-C(9)-H(9C) 109.5  
C(5)-C(10)-H(10D) 109.5  
C(5)-C(10)-H(10E) 109.5  
H(10D)-C(10)-H(10E) 109.5  
C(5)-C(10)-H(10F) 109.5  
H(10D)-C(10)-H(10F) 109.5

H(10E)-C(10)-H(10F) 109.5  
C(12)-C(11)-N(1) 123.8(16)  
C(12)-C(11)-H(11A) 118.1  
N(1)-C(11)-H(11A) 118.1  
C(11)-C(12)-C(13) 122.4(15)  
C(11)-C(12)-H(12A) 118.8  
C(13)-C(12)-H(12A) 118.8  
N(3)-C(13)-C(14) 121.8(14)  
N(3)-C(13)-C(12) 123.8(14)  
C(14)-C(13)-C(12) 114.3(14)  
C(15)-C(14)-C(13) 118.3(14)  
C(15)-C(14)-H(14A) 120.9  
C(13)-C(14)-H(14A) 120.9  
C(14)-C(15)-N(1) 126.0(13)  
C(14)-C(15)-C(16) 124.4(14)  
N(1)-C(15)-C(16) 109.4(13)  
O(1)-C(16)-N(2) 122.3(15)  
O(1)-C(16)-C(15) 120.2(15)  
N(2)-C(16)-C(15) 117.5(15)  
C(18)-C(17)-C(25) 106.8(12)  
C(18)-C(17)-N(2) 117.6(12)  
C(25)-C(17)-N(2) 112.7(12)  
C(18)-C(17)-H(17B) 106.3  
C(25)-C(17)-H(17B) 106.3

N(2)-C(17)-H(17B) 106.3  
C(23)-C(18)-C(19) 121.5(16)  
C(23)-C(18)-C(17) 105.9(14)  
C(19)-C(18)-C(17) 132.5(14)  
C(20)-C(19)-C(18) 118.5(17)  
C(20)-C(19)-H(19B) 120.8  
C(18)-C(19)-H(19B) 120.8  
C(21)-C(20)-C(19) 120.7(19)  
C(21)-C(20)-H(20B) 119.6  
C(19)-C(20)-H(20B) 119.6  
C(20)-C(21)-C(22) 124(2)  
C(20)-C(21)-H(21B) 117.8  
C(22)-C(21)-H(21B) 117.8  
C(21)-C(22)-C(23) 117.1(18)  
C(21)-C(22)-H(22B) 121.4  
C(23)-C(22)-H(22B) 121.4  
C(18)-C(23)-C(22) 117.5(16)  
C(18)-C(23)-C(24) 114.6(15)  
C(22)-C(23)-C(24) 127.7(16)  
C(23)-C(24)-C(25) 99.7(14)  
C(23)-C(24)-H(24C) 111.8  
C(25)-C(24)-H(24C) 111.8  
C(23)-C(24)-H(24D) 111.8  
C(25)-C(24)-H(24D) 111.8

H(24C)-C(24)-H(24D) 109.6  
O(2)-C(25)-C(17) 106.7(17)  
O(2)-C(25)-C(24) 106.8(16)  
C(17)-C(25)-C(24) 101.8(13)  
O(2)-C(25)-H(25B) 113.5  
C(17)-C(25)-H(25B) 113.5  
C(24)-C(25)-H(25B) 113.5  
N(3)-C(26)-H(26D) 109.5  
N(3)-C(26)-H(26E) 109.5  
H(26D)-C(26)-H(26E) 109.5  
N(3)-C(26)-H(26F) 109.5  
H(26D)-C(26)-H(26F) 109.5  
H(26E)-C(26)-H(26F) 109.5  
N(3)-C(27)-H(27D) 109.5  
N(3)-C(27)-H(27E) 109.5  
H(27D)-C(27)-H(27E) 109.5  
N(3)-C(27)-H(27F) 109.5  
H(27D)-C(27)-H(27F) 109.5  
H(27E)-C(27)-H(27F) 109.5  
F(5)-P(1)-F(1) 88.4(12)  
F(5)-P(1)-F(3) 96.9(12)  
F(1)-P(1)-F(3) 173.8(12)  
F(5)-P(1)-F(2) 92.9(11)  
F(1)-P(1)-F(2) 88.7(9)

F(3)-P(1)-F(2) 94.2(11)  
F(5)-P(1)-F(6) 176.6(13)  
F(1)-P(1)-F(6) 88.3(11)  
F(3)-P(1)-F(6) 86.4(10)  
F(2)-P(1)-F(6) 87.6(10)  
F(5)-P(1)-F(4) 90.4(11)  
F(1)-P(1)-F(4) 93.4(12)  
F(3)-P(1)-F(4) 83.4(11)  
F(2)-P(1)-F(4) 176.2(10)  
F(6)-P(1)-F(4) 89.3(10)  
F(7)-P(2)-F(10) 88.4(11)  
F(7)-P(2)-F(9) 176.6(12)  
F(10)-P(2)-F(9) 93.3(10)  
F(7)-P(2)-F(11) 92.5(10)  
F(10)-P(2)-F(11) 89.8(8)  
F(9)-P(2)-F(11) 90.5(10)  
F(7)-P(2)-F(12) 91.5(11)  
F(10)-P(2)-F(12) 92.0(10)  
F(9)-P(2)-F(12) 85.4(11)  
F(11)-P(2)-F(12) 175.7(11)  
F(7)-P(2)-F(8) 87.8(9)  
F(10)-P(2)-F(8) 174.8(11)  
F(9)-P(2)-F(8) 90.7(9)  
F(11)-P(2)-F(8) 86.8(8)

F(12)-P(2)-F(8) 91.6(10)  
N(1')-Ir'-C(2') 118.0(7)  
N(1')-Ir'-C(1') 98.5(6)  
C(2')-Ir'-C(1') 39.6(6)  
N(1')-Ir'-C(3') 154.4(6)  
C(2')-Ir'-C(3') 37.2(7)  
C(1')-Ir'-C(3') 65.2(7)  
N(1')-Ir'-O(1') 76.1(5)  
C(2')-Ir'-O(1') 99.7(7)  
C(1')-Ir'-O(1') 131.1(6)  
C(3')-Ir'-O(1') 99.2(6)  
N(1')-Ir'-C(4') 155.2(7)  
C(2')-Ir'-C(4') 63.8(8)  
C(1')-Ir'-C(4') 66.7(8)  
C(3')-Ir'-C(4') 37.8(7)  
O(1')-Ir'-C(4') 128.7(7)  
N(1')-Ir'-C(5') 116.0(7)  
C(2')-Ir'-C(5') 67.0(8)  
C(1')-Ir'-C(5') 41.6(8)  
C(3')-Ir'-C(5') 65.8(7)  
O(1')-Ir'-C(5') 164.8(6)  
C(4')-Ir'-C(5') 39.8(7)  
N(1')-Ir'-Cl' 85.5(4)  
C(2')-Ir'-Cl' 156.3(6)

C(1')-Ir'-Cl' 146.8(5)  
C(3')-Ir'-Cl' 119.2(5)  
O(1')-Ir'-Cl' 81.9(4)  
C(4')-Ir'-Cl' 96.6(6)  
C(5')-Ir'-Cl' 107.3(6)  
C(2')-C(1')-C(6') 128.2(18)  
C(2')-C(1')-C(5') 105.9(15)  
C(6')-C(1')-C(5') 124.8(16)  
C(2')-C(1')-Ir' 70.1(10)  
C(6')-C(1')-Ir' 132.8(14)  
C(5')-C(1')-Ir' 70.7(10)  
C(16')-N(1')-C(12') 115.2(16)  
C(16')-N(1')-Ir' 127.5(14)  
C(12')-N(1')-Ir' 117.2(11)  
C(11')-N(2')-C(17') 120.5(16)  
C(11')-N(2')-H(2'B) 119.8  
C(17')-N(2')-H(2'B) 119.8  
C(11')-O(1')-Ir' 115.1(11)  
C(25')-O(2')-H(2'A) 109.5  
C(3')-C(2')-C(1') 110.3(18)  
C(3')-C(2')-C(7') 124.1(18)  
C(1')-C(2')-C(7') 125.6(19)  
C(3')-C(2')-Ir' 71.9(12)  
C(1')-C(2')-Ir' 70.3(10)



C(7')-C(2')-Ir' 123.2(14)  
C(14')-N(3')-C(26') 119.8(19)  
C(14')-N(3')-C(27') 124.1(16)  
C(26')-N(3')-C(27') 116.2(18)  
C(2')-C(3')-C(4') 111.2(18)  
C(2')-C(3')-C(8') 128.5(18)  
C(4')-C(3')-C(8') 120.3(18)  
C(2')-C(3')-Ir' 70.9(12)  
C(4')-C(3')-Ir' 72.4(11)  
C(8')-C(3')-Ir' 120.8(13)  
C(3')-C(4')-C(5') 109.0(18)  
C(3')-C(4')-C(9') 129(2)  
C(5')-C(4')-C(9') 122(2)  
C(3')-C(4')-Ir' 69.8(11)  
C(5')-C(4')-Ir' 70.0(12)  
C(9')-C(4')-Ir' 125.9(15)  
C(10')-C(5')-C(4') 126.0(19)  
C(10')-C(5')-C(1') 129.9(17)  
C(4')-C(5')-C(1') 103.6(16)  
C(10')-C(5')-Ir' 131.9(16)  
C(4')-C(5')-Ir' 70.1(11)  
C(1')-C(5')-Ir' 67.7(10)  
C(1')-C(6')-H(6'A) 109.5  
C(1')-C(6')-H(6'B) 109.5

H(6'A)-C(6')-H(6'B)109.5  
C(1')-C(6')-H(6'C) 109.5  
H(6'A)-C(6')-H(6'C)109.5  
H(6'B)-C(6')-H(6'C)109.5  
C(2')-C(7')-H(7'A) 109.5  
C(2')-C(7')-H(7'B) 109.5  
H(7'A)-C(7')-H(7'B)109.5  
C(2')-C(7')-H(7'C) 109.5  
H(7'A)-C(7')-H(7'C)109.5  
H(7'B)-C(7')-H(7'C)109.5  
C(3')-C(8')-H(8'A) 109.5  
C(3')-C(8')-H(8'B) 109.5  
H(8'A)-C(8')-H(8'B)109.5  
C(3')-C(8')-H(8'C) 109.5  
H(8'A)-C(8')-H(8'C)109.5  
H(8'B)-C(8')-H(8'C)109.5  
C(4')-C(9')-H(9'A) 109.5  
C(4')-C(9')-H(9'B) 109.5  
H(9'A)-C(9')-H(9'B)109.5  
C(4')-C(9')-H(9'C) 109.5  
H(9'A)-C(9')-H(9'C)109.5  
H(9'B)-C(9')-H(9'C)109.5  
C(5')-C(10')-H(10A)109.5  
C(5')-C(10')-H(10B)109.5

H(10A)-C(10')-H(10B) 109.5  
C(5')-C(10')-H(10C) 109.5  
H(10A)-C(10')-H(10C) 109.5  
H(10B)-C(10')-H(10C) 109.5  
O(1')-C(11')-N(2') 119.5(18)  
O(1')-C(11')-C(12') 120.8(17)  
N(2')-C(11')-C(12') 119.6(18)  
C(13')-C(12')-N(1') 122.9(14)  
C(13')-C(12')-C(11') 127.3(17)  
N(1')-C(12')-C(11') 109.7(16)  
C(12')-C(13')-C(14') 121.4(17)  
C(12')-C(13')-H(13A) 119.3  
C(14')-C(13')-H(13A) 119.3  
N(3')-C(14')-C(15') 124.7(19)  
N(3')-C(14')-C(13') 121.2(19)  
C(15')-C(14')-C(13') 114.1(18)  
C(16')-C(15')-C(14') 122(2)  
C(16')-C(15')-H(15A) 119.0  
C(14')-C(15')-H(15A) 119.0  
N(1')-C(16')-C(15') 124(2)  
N(1')-C(16')-H(16A) 117.9  
C(15')-C(16')-H(16A) 117.9  
N(2')-C(17')-C(18') 115.2(15)  
N(2')-C(17')-C(25') 113.3(16)

C(18')-C(17')-C(25') 101.0(15)  
N(2')-C(17')-H(17A) 109.0  
C(18')-C(17')-H(17A) 109.0  
C(25')-C(17')-H(17A) 109.0  
C(23')-C(18')-C(17') 116.4(19)  
C(23')-C(18')-C(19') 117.9(18)  
C(17')-C(18')-C(19') 125.7(17)  
C(20')-C(19')-C(18') 116(2)  
C(20')-C(19')-H(19A) 121.9  
C(18')-C(19')-H(19A) 121.9  
C(19')-C(20')-C(21') 122(2)  
C(19')-C(20')-H(20A) 119.1  
C(21')-C(20')-H(20A) 119.1  
C(22')-C(21')-C(20') 117(2)  
C(22')-C(21')-H(21A) 121.4  
C(20')-C(21')-H(21A) 121.4  
C(23')-C(22')-C(21') 126(2)  
C(23')-C(22')-H(22A) 117.1  
C(21')-C(22')-H(22A) 117.1  
C(22')-C(23')-C(18') 120(2)  
C(22')-C(23')-C(24') 134(2)  
C(18')-C(23')-C(24') 104.9(17)  
C(23')-C(24')-C(25') 109.3(18)  
C(23')-C(24')-H(24A) 109.8

C(25')-C(24')-H(24A) 109.8  
C(23')-C(24')-H(24B) 109.8  
C(25')-C(24')-H(24B) 109.8  
H(24A)-C(24')-H(24B) 108.3  
O(2')-C(25')-C(24') 106.1(19)  
O(2')-C(25')-C(17') 108.0(16)  
C(24')-C(25')-C(17') 105.4(17)  
O(2')-C(25')-H(25A) 112.3  
C(24')-C(25')-H(25A) 112.3  
C(17')-C(25')-H(25A) 112.3  
N(3')-C(26')-H(26A) 109.5  
N(3')-C(26')-H(26B) 109.5  
H(26A)-C(26')-H(26B) 109.5  
N(3')-C(26')-H(26C) 109.5  
H(26A)-C(26')-H(26C) 109.5  
H(26B)-C(26')-H(26C) 109.5  
N(3')-C(27')-H(27A) 109.5  
N(3')-C(27')-H(27B) 109.5  
H(27A)-C(27')-H(27B) 109.5  
N(3')-C(27')-H(27C) 109.5  
H(27A)-C(27')-H(27C) 109.5  
H(27B)-C(27')-H(27C) 109.5

---

Symmetry transformations used to generate equivalent atoms:

**Table 26: Anisotropic displacement parameters ( $\text{\AA}^2 \times 10^3$ ) for Bond lengths [ $\text{\AA}$ ] and angles [ $^\circ$ ] for  $[\text{Cp}^*\text{Ir}(\text{126})\text{Cl}]\text{PF}_6$ .**

The anisotropic displacement factor exponent takes the form:  $-2\pi^2 [h^2 a^{*2} U^{11} + \dots + 2 h k a^* b^* U^{12}]$

---

	$U^{11}$	$U^{22}$	$U^{33}$	$U^{23}$	$U^{13}$	$U^{12}$
Ir	28(1)	25(1)	54(1)	-5(1)	14(1)	-3(1)
Cl	44(3)	49(3)	63(3)	6(2)	11(2)	-2(2)
O(1)	30(6)	34(6)	54(8)	-15(6)	16(6)	-4(5)
O(2)	31(8)	76(10)	166(16)	-63(11)	34(9)	-20(8)
N(1)	9(6)	31(8)	72(11)	-15(7)	13(6)	3(6)
N(2)	20(6)	23(6)	57(9)	-24(6)	16(6)	-10(5)
N(3)	25(7)	42(10)	90(11)	-2(8)	30(7)	-13(6)
C(2)	46(11)	29(9)	65(13)	-15(8)	-11(9)	4(8)
C(3)	28(9)	39(10)	70(12)	-28(9)	13(8)	12(8)
C(4)	30(9)	34(9)	51(11)	-13(8)	11(8)	-17(8)
C(6)	39(11)	71(13)	82(15)	6(11)	39(10)	-12(10)
C(7)	110(20)	33(11)	130(20)	13(13)	36(17)	5(12)
C(8)	39(10)	40(11)	116(16)	-11(11)	22(10)	-5(9)
C(9)	67(13)	35(10)	84(15)	4(10)	35(11)	14(10)
C(10)	30(10)	80(15)	60(13)	-33(12)	-11(9)	14(10)
C(12)	27(9)	50(11)	82(15)	-12(10)	34(10)	4(9)
C(14)	16(7)	19(8)	72(12)	-3(8)	16(7)	-9(6)

C(15) 19(8) 23(8) 35(9) -5(7) 10(7) 4(6)  
 C(16) 33(10) 39(10) 56(12) 10(9) 13(9) 17(9)  
 C(17) 13(7) 36(9) 42(9) 2(7) 15(7) 6(6)  
 C(18) 11(8) 44(10) 62(12) -13(9) 13(8) -3(7)  
 C(19) 27(9) 33(9) 73(13) 15(9) 3(9) 11(8)  
 C(20) 42(11) 71(14) 84(14) 23(11) 34(11) 0(10)  
 C(21) 83(16) 62(14) 56(13) -13(11) 23(12) -40(12)  
 C(23) 12(8) 58(11) 56(12) -3(9) 7(8) -11(8)  
 C(24) 22(8) 50(10) 49(11) 0(8) 20(8) 4(7)  
 C(25) 41(12) 35(9) 130(20) -9(11) 64(13) 3(9)  
 C(26) 104(19) 37(11) 120(20) -27(12) 69(16) -34(12)  
 P(1) 71(4) 55(4) 104(5) 8(3) 27(4) 22(3)  
 F(1) 174(18) 68(10) 170(17) -15(11) -14(13) -9(11)  
 F(2) 56(9) 95(11) 173(15) -1(10) 13(9) 23(8)  
 F(3) 115(14) 76(10) 250(20) -54(12) 83(15) -30(10)  
 F(4) 147(14) 163(17) 156(13) 61(15) 50(11) 108(16)  
 F(5) 260(20) 133(18) 196(17) 50(14) 176(17) 39(16)  
 F(6) 191(18) 117(14) 159(15) 31(11) 113(14) 27(12)  
 P(2) 37(3) 39(3) 83(4) 2(3) 24(3) 5(2)  
 F(7) 159(17) 80(11) 140(14) 1(10) -36(12) -8(11)  
 F(8) 45(8) 137(14) 122(12) -1(10) 2(8) 44(9)  
 F(9) 62(10) 77(10) 240(20) 2(11) 35(11) -45(8)  
 F(10) 52(7) 158(15) 152(12) -13(15) -5(7) 15(13)  
 F(11) 107(11) 109(12) 141(12) 32(10) 72(9) 43(9)

F(12) 280(20) 113(16)162(15) 54(13) 158(16) 78(16)  
 Cl' 87(4) 77(4) 53(3) 10(3) 10(3) 8(3)  
 Ir' 48(1) 36(1) 51(1) -4(1) 13(1) -1(1)  
 N(1') 45(9) 64(11) 27(8) -17(8)8(7) -7(8)  
 N(2') 58(11) 68(11) 53(10) -11(9)13(8) -28(9)  
 O(1') 18(6) 74(9) 64(9) -24(8)16(6) -2(6)  
 O(2') 100(13) 69(10) 115(14) 23(10) 19(11) 8(10)  
 N(3') 36(9) 65(13) 111(14) -24(11) 35(9) -10(9)  
 C(3') 52(11) 34(10) 51(11) 1(8) -3(9) -9(8)  
 C(4') 65(14) 40(11) 59(13) 4(10) 12(11) -10(11)  
 C(5') 41(11) 49(12) 81(15) 2(11) 32(10) 2(9)  
 C(6') 110(20) 110(20)75(16) 21(15) 25(15) 53(18)  
 C(7') 30(10) 41(11) 110(18) 2(11) -4(10) 24(9)  
 C(8') 72(15) 100(20)111(19) -26(16) 34(13) -22(14)  
 C(9') 170(30) 31(11) 100(20) 17(12) 24(18) -18(14)  
 C(10')115(19) 59(13) 68(14) 2(11) 57(14) 52(14)  
 C(11')53(12) 51(12) 37(11) -10(9)2(9) 13(10)  
 C(12')17(8) 71(13) 33(10) 31(9) 16(7) 16(9)  
 C(13')36(10) 47(12) 84(14) -27(10) 23(9) -5(8)  
 C(14')44(12) 70(15) 85(15) -16(12) 15(11) -20(10)  
 C(15')64(14) 49(12) 96(17) -11(12) 41(13) -1(11)  
 C(16')35(11) 48(12) 105(17) 3(12) 35(11) -5(9)  
 C(18')68(12) 73(13) 66(12) -3(13)31(10) -2(14)  
 C(19')78(16) 51(13) 90(17) -13(12) 36(13) 1(12)



C(20')110(20) 42(12) 120(20) -19(14) 23(18) 7(13)

C(21')130(20) 100(20)100(20) -20(17) 63(18) 46(19)

C(23')24(9) 84(15) 83(14) -41(12) 26(9) -26(9)

C(24')59(14) 90(17) 92(18) -26(14) 43(13) -19(13)

C(25')89(17) 28(10) 71(15) -9(10)10(13) -30(11)

C(27')48(14) 80(18) 190(30) -37(19) 53(17) -38(13)

---

**Table 27: Hydrogen coordinates ( $\times 10^4$ ) and isotropic displacement parameters ( $\text{\AA}^2 \times 10^3$ ) for  $[\text{Cp}^*\text{Ir}(\text{126Cl})\text{PF}_6]$ .**

---

x	y	z	U(eq)	
H(2A)	5361	8648	165	134
H(2B)	5031	10202431	38	
H(6A)	4903	140422279	90	
H(6B)	4767	127411957	90	
H(6C)	4384	143681928	90	
H(7A)	6280	125732121	131	
H(7B)	6258	122571701	131	
H(7C)	5716	117291867	131	
H(8A)	6901	157701679	96	
H(8B)	6553	159811265	96	
H(8C)	6639	142111444	96	
H(9A)	5905	191791607	88	
H(9B)	5321	189421293	88	
H(9C)	5937	182801237	88	
H(10D)	4649	181641919	91	
H(10E)	4219	169091664	91	
H(10F)	4527	183311487	91	
H(11A)	3815	142871256	42	

---

H(12A)3166 122611156 59  
H(14A)4262 9700 646 42  
H(17B)6189 10922806 35  
H(19B)5688 13956251 55  
H(20B)6218 15258-12275  
H(21B)6959 13997-29179  
H(22B)7283 11386-93 58  
H(24C)7075 9271 560 46  
H(24D) 6797 8521 163 46  
H(25B)6162 8199 668 74  
H(26D) 3745 7968 607 121  
H(26E)3066 7705 415 121  
H(26F)3323 7031 816 121  
H(27D) 2556 10688990 117  
H(27E)2531 8766 1046 117  
H(27F)2283 9536 653 117  
H(2'B) 3218 4541 3877 72  
H(2'A) 2802 504 4297 144  
H(6'A) 3244 557 1955 150  
H(6'B) 3798 599 2294 150  
H(6'C) 3345 2086 2223 150  
H(7'A) 1899 2079 2131 95  
H(7'B) 2434 3022 2391 95  
H(7'C) 1883 2445 2543 95

H(8'A) 1302 -9842625 138  
H(8'B) 1556 498 2888 138  
H(8'C) 1677 -1331 3028 138  
H(9'A) 2319 -4419 2753 154  
H(9'B) 2282 -3454 3114 154  
H(9'C) 2905 -4058 3057 154  
H(10A)3498 -3402 2367 112  
H(10B)3656 -3524 2800 112  
H(10C)3968 -2183 2603 112  
H(13A)4001 5158 3651 65  
H(15A)5045 2867 3088 79  
H(16A)4338 929 2923 72  
H(17A)2062 3922 3622 45  
H(19A)2657 7170 3991 85  
H(20A)2456 8644 4488 108  
H(21A)1971 7356 4908 125  
H(22A)1902 4591 4889 85  
H(24A)1544 2177 4237 91  
H(24B)2137 1821 4537 91  
H(25A)2046 1281 3841 77  
H(26A)5586 4425 3234 116  
H(26B)5916 5189 3615 116  
H(26C)5650 6353 3279 116  
H(27A)4561 6763 3775 153

H(27B) 5024 7789 3615 153

H(27C) 5246 6704 3970 153

---

## BIBLIOGRAPHY

1. Martín Castro, A. M., Claisen Rearrangement over the Past Nine Decades. *Chem. Rev.* **2004**, *104*, 2939-3002.
2. Hiersemann, M.; Abraham, L., Catalysis of the Claisen Rearrangement of Aliphatic Allyl Vinyl Ethers. *Eur. J. Org. Chem.* **2002**, 1461-1471.
3. Borgulya, J.; Madeja, R.; Fahrni, P.; Hansen, H.-J.; Schmid, H.; Barner, R., Umlagerung von Allyl-aryläthern und Allyl-cyclohexadienonen mittels Bortrichlorid. *Helv. Chim. Acta* **1973**, *56*, 14-75.
4. Bryusova, L. Y.; Ioffe, M. L., The Synthesis of Eugenol. *Zh. Obshch. Khim.* **1941**, *11*, 722-728.
5. Bates, D. K.; Jones, M. C., Acid Catalysis of the Claisen Rearrangement 2. Formation of the Benzofurobenzopyran and Benzofuro[3,2-b]benzofuran Kkeletons from 1,4-Bis(aryloxy)-2-butyne. *J. Org. Chem.* **1978**, *43*, 3856-3861.
6. Takai, K.; Mori, I.; Oshima, K.; Nozaki, H., Aliphatic Claisen Rearrangement Promoted by Organoaluminium Compounds. *Tetrahedron Lett.* **1981**, *22*, 3985-3988.
7. Takai, K.; Mori, c.; Oshima, K.; Nozaki, H., Aliphatic Claisen Rearrangement Promoted by Organoaluminium Reagents. *Bull. Chem. Soc. Jpn.* **1984**, *57*, 446-451.
8. Ito, H.; Sato, A.; Taguchi, T., Enantioselective Aromatic Claisen Rearrangement. *Tetrahedron Lett.* **1997**, *38*, 4815-4818.
9. Corey, E. J.; Lee, D. H., Highly Enantioselective and Diastereoselective Ireland-Claisen Rearrangement of Achiral Allylic Esters. *J. Am. Chem. Soc.* **1991**, *113*, 4026-4028.

10. Maruoka, K.; Banno, H.; Yamamoto, H., Enantioselective Activation of Ethers by Chiral Organoaluminum Reagents: Application to Asymmetric Claisen Rearrangement. *Tetrahedron: Asymm.* **1991**, *2*, 647-666.
11. Maruoka, K.; Banno, H.; Yamamoto, H., Asymmetric Claisen rearrangement catalyzed by chiral organoaluminum reagent. *J. Am. Chem. Soc.* **1990**, *112* (21), 7791-7793.
12. Yoon, T. P.; MacMillan, D. W. C., Enantioselective Claisen Rearrangements: Development of a First Generation Asymmetric Acyl-Claisen Reaction. *J. Am. Chem. Soc.* **2001**, *123*, 2911-2912.
13. Takanami, T.; Hayashi, M.; Suda, K., Metalloporphyrin Cr(TPP)Cl-catalyzed Claisen Rearrangement of Simple Aliphatic Allyl Vinyl Ethers and its Unique Stereoselectivity. *Tetrahedron Lett.* **2005**, *46*, 2893-2896.
14. Sreedhar, B.; Swapna, V.; Sridhar, C., Bismuth(III) Triflate: Novel and Efficient Catalyst for Claisen and Fries Rearrangements of Allyl Ethers and Phenyl Esters. *Synth. Commun.* **2004**, *34*, 1433-1440.
15. Trost, B. M.; Toste, F. D., Asymmetric O- and C-Alkylation of Phenols. *J. Am. Chem. Soc.* **1998**, *120*, 815-816.
16. Trost, B. M.; Schroeder, G. M., Cyclic 1,2-Diketones as Building Blocks for Asymmetric Synthesis of Cycloalkenones. *J. Am. Chem. Soc.* **2000**, *122*, 3785-3786.
17. Hiersemann, M.; Abraham, L., The Cu(OTf)<sub>2</sub>- and Yb(OTf)<sub>3</sub>-Catalyzed Claisen Rearrangement of 2-Alkoxy carbonyl-Substituted Allyl Vinyl Ethers. *Org. Lett.* **2001**, *3*, 49-52.
18. Abraham, L.; Czerwonka, R.; Hiersemann, M., The Catalytic Enantioselective Claisen Rearrangement of an Allyl Vinyl Ether. *Angew. Chem. Int. Ed.* **2001**, *40*, 4700-4703.

19. Abraham, L.; Körner, M.; Hiersemann, M., Highly Enantioselective Catalytic Asymmetric Claisen Rearrangement of 2-Alkoxy-carbonyl-substituted Allyl Vinyl Ethers. *Tetrahedron Lett.* **2004**, *45*, 3647-3650.
20. Uyeda, C.; Jacobsen, E. N., Enantioselective Claisen Rearrangements with a Hydrogen-Bond Donor Catalyst. *J. Am. Chem. Soc.* **2008**, *130*, 9228-9229.
21. Overman, L. E.; Knoll, F. M., Palladium(II)-catalyzed Rearrangement of Allylic Acetates. *Tetrahedron Lett.* **1979**, *20*, 321-324.
22. Le Nôtre, J.; Brissieux, L.; Sémeril, D.; Bruneau, C.; Dixneuf, P. H., Tandem Isomerization/Claisen Transformation of Allyl Homoallyl and Diallyl Ethers Into  $\gamma,\delta$ -Unsaturated Aldehydes with a New Three Component Catalyst  $\text{Ru}_3(\text{CO})_{12}$ /Imidazolium salt/ $\text{Cs}_2\text{CO}_3$ . *Chem. Commun.* **2002**, 1772-1773.
23. Tamaru, Y.; Kagotani, M.; Yoshida, Z., The Regioselective S $\rightarrow$ C and S $\rightarrow$ N Allylic Rearrangement of S-Allylthioimidate. *Tetrahedron Lett.* **1981**, *22*, 4245-4248.
24. Oehlschlager, C.; Mishra, P.; Dhimi, S., Metal-catalyzed Rearrangements of Allylic Esters. *Can. J. Chem.* **1984**, *62*, 791-797.
25. Overman, L. E.; Knoll, F. M., Catalyzed Sigmatropic Rearrangements. 5. Palladium(II) Chloride Catalyzed Cope Rearrangements of Acyclic 1,5-dienes. *J. Am. Chem. Soc.* **1980**, *102*, 865-867.
26. Overman, L. E.; Jacobsen, E. J., Chair Topology of the Palladium Dichloride Catalyzed Cope Rearrangement of Acyclic 1,5-dienes. *J. Am. Chem. Soc.* **1982**, *104*, 7225-7231.
27. Overman, L. E., Mercury(II)- and Palladium(II)-Catalyzed [3,3]-Sigmatropic Rearrangements. *Angew. Chem. Int. Ed. Engl.* **1984**, *23*, 579-586.



28. van der Baan, J. L.; Bickelhaupt, F., Palladium(II)-catalyzed Claisen Rearrangement of allyl vinyl ethers. *Tetrahedron Lett.* **1986**, *27*, 6267-6270.
29. Sugiura, M.; Nakai, T., Stereochemical Feature of Palladium(II)-Catalyzed Claisen Rearrangement. *Chem. Lett.* **1995**, *24*, 697-698.
30. Calter, M.; Hollis, T. K.; Overman, L. E.; Ziller, J.; Zipp, G. G., First Enantioselective Catalyst for the Rearrangement of Allylic Imidates to Allylic Amides. *J. Org. Chem.* **1997**, *62*, 1449-1456.
31. Hollis, T. K.; Overman, L. E., Cyclopalladated Ferrocenyl Amines as Enantioselective Catalysts for the Rearrangement of Allylic Imidates to Allylic Amides. *Tetrahedron Lett.* **1997**, *38*, 8837-8840.
32. Donde, Y.; Overman, L. E., High Enantioselection in the Rearrangement of Allylic Imidates with Ferrocenyl Oxazoline Catalysts. *J. Am. Chem. Soc.* **1999**, *121*, 2933-2934.
33. Anderson, C. E.; Overman, L. E., Catalytic Asymmetric Rearrangement of Allylic Trichloroacetimidates. A Practical Method for Preparing Allylic Amines and Congeners of High Enantiomeric Purity. *J. Am. Chem. Soc.* **2003**, *125*, 12412-12413.
34. Schenck, T. G.; Bosnich, B., Homogeneous Catalysis. Transition-metal-catalyzed Claisen Rearrangements. *J. Am. Chem. Soc.* **1985**, *107*, 2058-2066.
35. Tsuji, J.; Takahashi, H.; Morikawa, M., Organic Syntheses by Means of Noble Metal Compounds XVII. Reaction of  $\pi$ -Allylpalladium Chloride with Nucleophiles. *Tetrahedron Lett.* **1965**, *6*, 4387-4388.
36. Trost, B. M.; Fullerton, T. J., New Synthetic Reactions. Allylic Alkylation. *J. Am. Chem. Soc.* **1973**, *95*, 292-294.

37. Shimizu, I.; Yamada, T.; Tsuji, J., Palladium-catalyzed Rearrangement of Allylic Esters of Acetoacetic Acid to Give  $\gamma,\delta$ -Unsaturated Methyl Ketones. *Tetrahedron Lett.* **1980**, *21*, 3199-3202.
38. Trost, B. M.; Xu, J.; Schmidt, T., Palladium-Catalyzed Decarboxylative Asymmetric Allylic Alkylation of Enol Carbonates. *J. Am. Chem. Soc.* **2009**, *131*, 18343-18357.
39. Lu, Z.; Ma, S., Metal-catalyzed Enantioselective Allylation in Asymmetric Synthesis. *Angew. Chem. Int. Ed. Engl.* **2008**, *47*, 258-297.
40. Belda, O.; Moberg, C., Molybdenum-Catalyzed Asymmetric Allylic Alkylations. *Acc. Chem. Res.* **2004**, *37*, 159-167.
41. Trost, B. M.; Lautens, M., Chemoselectivity and Stereocontrol in Molybdenum-catalyzed Allylic Alkylations. *J. Am. Chem. Soc.* **1987**, *109*, 1469-1478.
42. Lehmann, J.; Lloyd-Jones, G. C., Regiocontrol and Stereoselectivity in Tungsten-Bipyridine Catalysed Allylic Alkylation. *Tetrahedron* **1995**, *5*, 8863-8874.
43. Evans, P. A.; Nelson, J. D., Regioselective Rhodium-catalyzed Allylic Alkylation with a Modified Wilkinson's Catalyst. *Tetrahedron Lett.* **1998**, *39*, 1725-1728.
44. Kazmaier, U.; Stolz, D., Regio- and Stereoselective Rhodium-catalyzed Allylic Alkylations of Chelated Enolates. *Angew. Chem. Int. Ed. Engl.* **2006**, *45*, 3072-2075.
45. Tosatti, P.; Nelson, A.; Marsden, S. P., Recent Advances and Applications of Iridium-catalysed Asymmetric Allylic Substitution. *Org. Biomol. Chem.* **2012**, *10*, 3147-3163.
46. Takeuchi, R.; Ue, N.; Tanabe, K.; Yamashita, K.; Shiga, N., Iridium Complex-Catalyzed Allylic Amination of Allylic Esters. *J. Am. Chem. Soc.* **2001**, *123*, 9525-9534.

47. Lipowsky, G.; Miller, N.; Helmchen, G., Regio- and Enantioselective Iridium-catalyzed Allylic Alkylation with *in situ* Activated P,C-chelate Complexes. *Angew. Chem. Int. Ed. Engl.* **2004**, *43*, 4595-4597.
48. Ohmura, T.; Hartwig, J. F., Regio- and Enantioselective Allylic Amination of Achiral Allylic Esters Catalyzed by an Iridium–Phosphoramidite Complex. *J. Am. Chem. Soc.* **2002**, *124*, 15164-15165.
49. Zhang, S.-W.; Mitsudo, T.-a.; Kondo, T.; Watanabe, Y., Ruthenium Complex-catalyzed Allylic Alkylation of Carbonucleophiles with Allylic Carbonates. *J. Organomet. Chem.* **1993**, *450*, 197-207.
50. Zhang, S. W.; Mitsudo, T. A.; Kondo, T.; Watanabe, Y., Syntheses of Cyclohexanone Derivatives by the Ruthenium Complex-catalysed Reactions of Allylic Compounds with  $\beta$ -Keto Esters. *J. Organomet. Chem.* **1995**, *485*, 55-62.
51. Trost, B. M.; Fraisse, P. L.; Ball, Z. T., A Stereospecific Ruthenium-Catalyzed Allylic Alkylation. *Angew. Chem. Int. Ed.* **2002**, *41*, 1059-1061.
52. Mbaye, M. D.; Demerseman, B.; Renaud, J. L.; Toupet, L.; Bruneau, C., [Cp\*( $\eta^2$ -bipy)(MeCN)Ru<sup>II</sup>][PF<sub>6</sub>] Catalysts for Regioselective Allylic Substitution and Characterization of Dicationic [Cp\*( $\eta^2$ -bipy)( $\eta^3$ -allyl)Ru<sup>IV</sup>][PF<sub>6</sub>]<sub>2</sub> Intermediates. *Angew. Chem. Int. Ed. Engl.* **2003**, *42*, 5066-5068.
53. Burger, E. C.; Tunge, J. A., Ruthenium-Catalyzed Decarboxylative Allylation of Nonstabilized Ketone Enolates. *Org. Lett.* **2004**, *6*, 2603-2605.
54. Wang, C.; Tunge, J. A., Ruthenium-Catalyzed Decarboxylative Insertion of Electrophiles. *Org. Lett.* **2005**, *7*, 2137-2139.

55. Mbaye, M. D.; Renaud, J. L.; Demerseman, B.; Bruneau, C., First Enantioselective Allylic Etherification with Phenols Catalyzed by Chiral Ruthenium Bisoxazoline Complexes. *Chem. Commun.* **2004**, 1870-1871.
56. Austeri, M.; Linder, D.; Lacour, J., Enantioselective and Regioselective Ruthenium-catalyzed Decarboxylative Etherification of Allyl Aryl Carbonates. *Chem. Eur. J.* **2008**, *14*, 5737-5741.
57. Constant, S.; Tortoioli, S.; Muller, J.; Lacour, J., An Enantioselective CpRu-catalyzed Carroll Rearrangement. *Angew. Chem. Int. Ed. Engl.* **2007**, *46*, 2082-2085.
58. Linder, D.; Buron, F.; Constant, S.; Lacour, J., Enantioselective CpRu-Catalyzed Carroll Rearrangement - Ligand and Metal Source Importance. *Eur. J. Org. Chem.* **2008**, 5778-5785.
59. Hermatschweiler, R.; Fernández, I.; Pregosin, P. S.; Watson, E. J.; Albinati, A.; Rizzato, S.; Veiros, L. F.; Calhorda, M. J., X-ray, <sup>13</sup>C NMR, and DFT Studies on a Ruthenium(IV) Allyl Complex. Explanation for the Observed Control of Regioselectivity in Allylic Alkylation Chemistry. *Organometallics* **2005**, *24*, 1809-1812.
60. Fernández, I.; Hermatschweiler, R.; Pregosin, P. S.; Albinati, A.; Rizzato, S., Synthesis, X-ray Studies, and Catalytic Allylic Amination Reactions with Ruthenium(IV) Allyl Carbonate Complexes. *Organometallics* **2006**, *25*, 323-330.
61. Ziegler, F. E., The Thermal, Aliphatic Claisen Rearrangement. *Chem. Rev.* **1988**, *88*, 1423-1452.
62. Kim, H.; Lee, C., A Mild and Efficient Method for the Stereoselective Formation of C-O Bonds: Palladium-Catalyzed Allylic Etherification Using Zinc(II) Alkoxides. *Org. Lett.* **2002**, *4*, 4369-4371.
63. Nugent, W., MIB: An Advantageous Alternative to DAIB for the Addition of Organozinc Reagents to Aldehydes. *Chem. Commun.* **1999**, 1369-1370.

64. Prosser, T. J., The Rearrangement of Allyl Ethers to Propenyl Ethers. *J. Am. Chem. Soc.* **1961**, *83*, 1701-1704.
65. Vyglazov, O. G.; Chuiko, V. A.; Izotova, L. V., Conversions of Allyl Ethers in a Superbasic Medium. *Russ. J. Gen. Chem.* **2003**, *73*, 933-939.
66. Suzuki, H.; Koyama, Y.; Moro-Oka, Y.; Ikawa, T., Novel Preparation of Silyl Enol Ethers from Allyl Alcohols. *Tetrahedron Lett.* **1979**, *20*, 1415-1418.
67. Wille, A.; Tomm, S.; Frauenrath, H., A Highly Z-Selective Isomerization (Double-Bond Migration) Procedure for Allyl Acetals and Allyl Ethers Mediated by Nickel Complexes. *Synthesis* **1998**, 305-308.
68. Ohmura, T.; Yamamoto, Y.; Miyaura, N., Stereoselective Synthesis of Silyl Enol Ethers via the Iridium-Catalyzed Isomerization of Allyl Silyl Ethers. *Organometallics* **1999**, *18*, 413-416.
69. Reuter, J. M.; Salomon, R. G., Ruthenium(II) Catalyzed Rearrangement of Diallyl Ethers. A Synthesis of  $\gamma,\delta$ -Unsaturated Aldehydes and Ketones. *J. Org. Chem.* **1977**, *42*, 3360-3364.
70. Higashino, T.; Sakaguchi, S.; Ishii, Y., Rearrangement of Allyl Homoallyl Ethers to  $\gamma,\delta$ -Unsaturated Carbonyl Compounds Catalyzed by Iridium Complexes. *Org. Lett.* **2000**, *2*, 4193-4195.
71. Wang, K. Development and Synthesis Applications of Olefin Isomerization-Claisen Rearrangement Reactions. Ph.D. Dissertation, The University of Pittsburgh, Pittsburgh, PA, November 2007.
72. Nelson, S. G.; Bungard, C. J.; Wang, K., Catalyzed Olefin Isomerization Leading to Highly Stereoselective Claisen Rearrangements of Aliphatic Allyl Vinyl Ethers. *J. Am. Chem. Soc.* **2003**, *125*, 13000-13001.

73. Nelson, S. G.; Wang, K., Asymmetric Claisen Rearrangements Enabled by Catalytic Asymmetric Di(allyl) Ether Synthesis. *J. Am. Chem. Soc.* **2006**, *128*, 4232-4233.
74. List, B.; Doehring, A.; Hechavarria Fonseca, M. T.; Job, A.; Rios Torres, R., A Practical, Efficient, and Atom Economic Alternative to the Wittig and Horner–Wadsworth–Emmons Reactions for the Synthesis of (E)- $\alpha,\beta$ -Unsaturated Esters from Aldehydes. *Tetrahedron* **2006**, *62*, 476-482.
75. Geherty, M. E. Catalytic Asymmetric Claisen Rearrangements. The Development of Ru(II)-Catalyzed Formal [3,3] Sigmatropic Rearrangements and Related Enolate Allylation Reactions. Ph.D. Dissertation, The University of Pittsburgh, Pittsburgh, PA, University of Pittsburgh, Pittsburgh, PA.
76. Geherty, M. E.; Dura, R. D.; Nelson, S. G., Catalytic Asymmetric Claisen Rearrangement of Unactivated Allyl Vinyl Ethers. *J. Am. Chem. Soc.* **2010**, *132*, 11875-11877.
77. Brancatelli, G.; Drommi, D.; Femino, G.; Saporita, M.; Bottari, G.; Faraone, F., Basicity and Bulkiness Effects of 1,8-Diaminonaphthalene, 8-Aminoquinoline and Their Alkylated Derivatives on the Different Efficiencies of  $\eta^5$ -C<sub>5</sub>H<sub>5</sub> and  $\eta^5$ -C<sub>5</sub>Me<sub>5</sub> Ruthenium Precatalysts in Allylic Etherification Reactions. *New J. Chem.* **2010**, *34*, 2853-2860.
78. Tanaka, S.; Saburi, H.; Ishibashi, Y.; Kitamura, M., CpRu<sup>II</sup>PF<sub>6</sub>/Quinaldic Acid-Catalyzed Chemoselective Allyl Ether Cleavage. A Simple and Practical Method for Hydroxyl Deprotection. *Org. Lett.* **2004**, *6*, 1873-1875.
79. Mikami, K.; Terada, M.; Nakai, T., Catalytic Asymmetric Glyoxylate-ene Reaction: A Practical Access to  $\alpha$ -Hydroxy Esters in High Enantiomeric Purities. *J. Am. Chem. Soc.* **1990**, *112*, 3949-3954.

- 80.Chandra, B.; Fu, D.; Nelson, S. G., Catalytic Asymmetric Synthesis of Complex Polypropionates: Lewis Base Catalyzed Aldol Equivalents in the Synthesis of Erythronolide B. *Angew. Chem. Int. Ed. Engl.* **2010**, *49*, 2591-2594.
- 81.Mao, B.; Ji, Y.; Fananas-Mastral, M.; Caroli, G.; Meetsma, A.; Feringa, B. L., Highly Enantioselective Synthesis of 3-Substituted  $\gamma$ -Butenolides by Palladium-catalyzed Kinetic Resolution of Unsymmetrical Allyl Acetates. *Angew. Chem. Int. Ed. Engl.* **2012**, *51*, 3168-3173.
- 82.Fujioka, H.; Murai, K.; Kubo, O.; Ohba, Y.; Kita, Y., One-pot Synthesis of Imidazolines from Aldehydes: Detailed Study About Solvents and Substrates. *Tetrahedron* **2007**, *63*, 638-643.
- 83.Brown, H. C.; Kanner, B., Preparation and Reactions of 2,6-Di-*t*-butylpyridine and Related Hindered Bases. A Case of Steric Hindrance toward the Proton<sup>1,2</sup>. *J. Am. Chem. Soc.* **1966**, *88*, 986-992.
- 84.Denmark, S. E.; Lee, W., Investigations on Transition-State Geometry in the Lewis Acid-(Mukaiyama) and Fluoride-Promoted Aldol Reactions. *J. Org. Chem.* **1994**, *59*, 707-709.
- 85.Heathcock, C. H.; Davidsen, S. K.; Hug, K. T.; Flippin, L. A., Acyclic Stereoselection. 36. Simple Diastereoselection in the Lewis Acid Mediated Reactions of Enol Silanes with Aldehydes. *J. Org. Chem.* **1986**, *51*, 3027-3037.
- 86.Lee, J. M.; Helquist, P.; Wiest, O., Diastereoselectivity in Lewis-Acid-Catalyzed Mukaiyama Aldol Reactions: A DFT Study. *J. Am. Chem. Soc.* **2012**, *134*, 14973-14981.
- 87.Jemal, A.; Siegel, R.; Ward, E.; Hao, Y.; Xu, J.; Murray, T.; Thun, M. J., Cancer Statistics. 2008. *CA Cancer J. Clin.* **2008**, *58*, 71-96.

88. Chung, K. Y.; Saltz, L. B., Adjuvant Therapy of Colon Cancer: Current Status and Future Directions. *Cancer J.* **2007**, *13*, 197-197
89. Nam, S.-J.; Kauffman, C. A.; Paul, L. A.; Jensen, P. R.; Fenical, W., Actinoranone, a Cytotoxic Meroterpenoid of Unprecedented Structure from a Marine Adapted Streptomyces sp. *Org. Lett.* **2013**, *15*, 5400-5403.
90. van Schaik, T. A. M.; Henzen, A. V.; van der Gen, A., A Horner-Wittig Solution to the Synthesis of Ketene, O,O-Acetals. *Tetrahedron Lett.* **1983**, *24*, 1303-1306.
91. Katritzky, A. R.; Toader, D.; Xie, L., Efficient Transformations of Aldehydes and Ketones into One-Carbon Homologated Carboxylic Acids. *Synthesis* **1996**, 1425-1427.
92. Li, Z.; Gupta, M. K.; Snowden, T. S., One-Carbon Homologation of Primary Alcohols and the Reductive Homologation of Aldehydes Involving a Jovic-Type Reaction. *Eur. J. Org. Chem.* **2015**, 7009-7019.
93. Cafiero, L. R.; Snowden, T. S., General and Practical Conversion of Aldehydes to Homologated Carboxylic Acids. *Org. Lett.* **2008**, *10*, 3853-3856.
94. Corey, E. J.; Link, J. O.; Shao, Y., Two Effective Procedures for the Synthesis of Trichloromethyl Ketones, useful Precursors of Chiral  $\alpha$ -Amino and  $\alpha$ -Hydroxy Acids. *Tetrahedron Lett.* **1992**, *33*, 3435-3438.
95. Khodaei, M. M.; Alizadeh, A.; Nazari, E., Tf<sub>2</sub>O as a Rapid and Efficient Promoter for the Dehydrative Friedel–Crafts Acylation of Aromatic Compounds with Carboxylic Acids. *Tetrahedron Lett.* **2007**, *48*, 4199-4202.



96. Lipshutz, B. H.; Butler, T.; Lower, A., Controlling Regiochemistry in Negishi Carboaluminations. Fine Tuning the Ligand on Zirconium. *J. Am. Chem. Soc.* **2006**, *128*, 15396-15398.
97. Okukado, N.; Negishi, E.-i., One-step Conversion of Terminal Acetylenes into Terminally Functionalized (E)-3-Methyl-2-alkenes *via* Zirconium-catalyzed Carboalumination. A Simple and Selective Route to Terpenoids. *Tetrahedron Lett.* **1978**, *19*, 2357-2360.
98. Parker, K. A.; Fokas, D., The Radical Cyclization Approach to Morphine. Models for Highly Oxygenated Ring-III Synthons. *J. Org. Chem.* **1994**, *59*, 3933-3938.
99. Tallman, K. A.; Roschek, B.; Porter, N. A., Factors Influencing the Autoxidation of Fatty Acids: Effect of Olefin Geometry of the Nonconjugated Diene. *J. Am. Chem. Soc.* **2004**, *126*, 9240-9247.
100. Lee, J. H.; Deng, L., Asymmetric Approach Toward Chiral Cyclohex-2-enones from Anisoles *via* an Enantioselective Isomerization by a New Chiral Diamine Catalyst. *J. Am. Chem. Soc.* **2012**, *134*, 18209-18212.
101. Nammalwar, B.; Bunce, R. A., Friedel–Crafts Cyclization of Tertiary Alcohols Using Bismuth(III) Triflate. *Tetrahedron Lett.* **2013**, *54*, 4330-4332.
102. Bunce, R. A.; Cox, A. N., Tetrahydronaphthalene Derivatives by Amberlyst® 15-Promoted Friedel-Crafts Cyclizations. *Org. Prep. Proced. Int.* **2010**, *42*, 83-93.
103. Parlow, J. J., Syntheses of Tetrahydronaphthalenes. Part II. *Tetrahedron* **1994**, *50*, 3297-3314.
104. Braude, E. A.; Webb, A. A.; Sultanbawa, M. U. S., Studies in the Vitamin D Field. Part III: Approaches to Derivatives of 5-Hydroxy-2-methylcyclohexanone. *J. Chem. Soc.* **1958**, 3328-3336.

105. Vuagnoux-d'Augustin, M.; Alexakis, A., Copper-catalyzed Asymmetric Conjugate Addition of Trialkylaluminium Reagents to Trisubstituted Enones: Construction of Chiral Quaternary Centers. *Chem. Eur. J.* **2007**, *13*, 9647-9662.
106. Alexakis, A.; Bäckvall, J. E.; Krause, N.; Pàmies, O.; Diéguez, M., Enantioselective Copper-Catalyzed Conjugate Addition and Allylic Substitution Reactions. *Chem. Rev.* **2008**, *108*, 2796-2823.
107. Liu, Y.; Xu, W.; Wang, X., Gold(I)-Catalyzed Tandem Cyclization Approach to Tetracyclic Indolines. *Org. Lett.* **2010**, *12*, 1448-1451.
108. Barabé, F.; Bétournay, G.; Bellavance, G.; Barriault, L., Gold-catalyzed Synthesis of Carbon-Bridged Medium-Sized Rings. *Org. Lett.* **2009**, *11*, 4236-4238.
109. Staben, S. T.; Kennedy-Smith, J. J.; Huang, D.; Corkey, B. K.; Lalonde, R. L.; Toste, F. D., Gold(I)-catalyzed Cyclizations of Silyl Enol Ethers: Application to the Synthesis of (+)-Lycoplidine A. *Angew. Chem. Int. Ed. Engl.* **2006**, *45*, 5991-5994.
110. Reetz, M. T.; Westermann, J.; Kyung, S.-H., Direct Geminal Dimethylation of Ketones and Exhaustive Methylation of Carboxylic Acid Chlorides Using Dichlorodimethyltitanium. *Chem. Ber.* **1985**, *118*, 1050-1057.
111. Teichert, J. F.; Feringa, B. L., Phosphoramidites: Privileged Ligands in Asymmetric Catalysis. *Angew. Chem. Int. Ed. Engl.* **2010**, *49*, 2486-2528.
112. Liu, H.-J.; Zhu, B.-Y., Efficient Addition of Cerium(III) Enolate of Ethyl Acetate to Ketones: Application to the Synthesis of  $\beta$ -Ethoxycarbonylmethyl- $\alpha,\beta$ -unsaturated ketones. *Can. J. Chem.* **1991**, *69*, 2002-2007.

113. Jarugumilli, G. K.; Zhu, C.; Cook, S. P., Re-Evaluating the Nucleophilicity of Zinc Enolates in Alkylation Reactions. *Eur. J. Org. Chem.* **2012**, 1712-1715.
114. Tran, N. D.; Albicker, M.; Schneider, L.; Cramer, N., Enantioselective Assembly of the Benzo[d]xanthene Tetracyclic Core of Anti-influenza Active Natural Products. *Org. Biomol. Chem.* **2010**, *8*, 1781-1784.
115. Tsuda, T.; Satomi, H.; Hayashi, T.; Saegusa, T., Alkylation and silylation of the aluminum enolates generated by Hydroalumination of  $\alpha,\beta$ -Unsaturated Carbonyl Compounds. *J. Org. Chem.* **1987**, *52*, 439-443.
116. House, H. O.; Gall, M.; Olmstead, H. D., Chemistry of Carbanions. XIX. Alkylation of Enolates from Unsymmetrical Ketones. *J. Org. Chem.* **1971**, *36*, 2361-2371.
117. Duhamel, P.; Cahard, D.; Poirier, J.-M., Unprecedented Route to Enolates from Silyl Enol Ethers and Enol Acetates: Reaction with Hard and Soft Electrophiles. *J. Chem. Soc., Perkin Trans. 1* **1993**, 2509-2511.
118. Baldwin, J. E., Rules for Ring Closure. *J. Chem. Soc., Chem. Commun.* **1976**, 734-736.
119. Rubottom, G. M.; Vazquez, M. A.; Pelegrina, D. R., Peracid Oxidation of Trimethylsilyl Enol Ethers: A Facile  $\alpha$ -Hydroxylation Procedure. *Tetrahedron Lett.* **1974**, *15*, 4319-4322.
120. Clary, J. W.; Rettenmaier, T. J.; Snelling, R.; Bryks, W.; Banwell, J.; Wipke, W. T.; Singaram, B., Hydride as a Leaving Group in the Reaction of Pinacolborane with Halides under Ambient Grignard and Barbier Conditions. One-Pot Synthesis of Alkyl, Aryl, Heteroaryl, Vinyl, and Allyl Pinacolboronic Esters. *J. Org. Chem.* **2011**, *76*, 9602-9610.

121. Ito, H.; Kubota, K., Copper(I)-Catalyzed Boryl Substitution of Unactivated Alkyl Halides. *Org. Lett.* **2012**, *14*, 890-893.
122. Netherton, M. R.; Dai, C.; Neuschütz, K.; Fu, G. C., Room-Temperature Alkyl-Alkyl Suzuki Cross-Coupling of Alkyl Bromides that Possess  $\beta$ -Hydrogens. *J. Am. Chem. Soc.* **2001**, *123*, 10099-10100.
123. Pollini, G. P.; Bianchi, A.; Casolari, A.; De Risi, C.; Zanirato, V.; Bertolasi, V., An Efficient Approach to Chiral Nonracemic *trans*- and *cis*-Decalin Scaffolds for Drimane and Labdane Synthesis. *Tetrahedron: Asymm.* **2004**, *15*, 3223-3231.
124. Frija, L. M.; Frade, R. F.; Afonso, C. A., Isolation, Chemical, and Biotransformation Routes of Labdane-type Diterpenes. *Chem. Rev.* **2011**, *111*, 4418-4452.